Vol. 143, November 1, 1982
Complete in one issue

ISSN 0003-2670

ANALYTICA CHIMICA ACTA

International journal devoted to all branches of analytical chemistry

ELSEVIER SCIENTIFIC PUBLISHING COMPANY

ANALYTICA CHIMICA ACTA

International journal devoted to all branches of analytical chemistry
Revue internationale consacrée à tous les domaines de la chimie analytique
Internationale Zeitschrift für alle Gebiete der analytischen Chemie

PUBLICATION SCHEDULE FOR 1982

	J	F	M	A	M	J	J	A	S	O	N	D
Analytica Chimica Acta	134	135/1	135/2	136	137	138	139	140/1 140/2	141	142	143	144

Scope. *Analytica Chimica Acta* publishes original papers, short communications, and reviews dealing with every aspect of modern chemical analysis, both fundamental and applied.

Submission of Papers. Manuscripts (three copies) should be submitted as designated below for rapid and efficient handling:

Papers from the Americas to: Professor Harry L. Pardue, Department of Chemistry, Purdue University, West Lafayette, IN 47907, U.S.A.

Papers from all other countries to: Dr. A. M. G. Macdonald, Department of Chemistry, The University, P.O. Box 363, Birmingham B15 2TT, England. Papers dealing particularly with computer techniques to: Professor J. T. Clerc, Universität Bern, Pharmazeutisches Institut, Sahlistrasse 10, CH-3012 Bern, Switzerland.

Submission of an article is understood to imply that the article is original and unpublished and is not being considered for publication elsewhere. Upon acceptance of an article by the journal, authors resident in the U.S.A. will be asked to transfer the copyright of the article to the publisher. This transfer will ensure the widest dissemination of information under the U.S. Copyright Law.

Information for Authors. Papers in English, French and German are published. There are no page charges. Manuscripts should conform in layout and style to the papers published in this Volume. Authors should consult Vol. 132, p. 239 for detailed information. Reprints of this information are available from the Editors or from: Elsevier Editorial Services Ltd., Mayfield House, 256 Banbury Road, Oxford OX2 7DH (Great Britain).

Reprints. Fifty reprints will be supplied free of charge. Additional reprints (minimum 100) can be ordered. An order form containing price quotations will be sent to the authors together with the proofs of their article.

Advertisements. Advertisement rates are available from the publisher.

Subscriptions. Subscriptions should be sent to: Elsevier Scientific Publishing Company, P.O. Box 211, 1000 AE Amsterdam, The Netherlands.

Publication. *Analytica Chimica Acta* appears in 11 volumes in 1982. The subscription for 1982 (Vols. 134–144) is Dfl. 1815.00 plus Dfl. 220.00 (postage) (total approx. U.S. $814.00). Journals are sent automatically by airmail to the U.S.A. and Canada at no extra cost and to Japan, Australia and New Zealand for a small additional postal charge. All earlier volumes (Vols. 1–133) except Vols. 23 and 28 are available at Dfl. 182.00 (U.S. $72.80), plus Dfl. 14.00 (U.S. $5.60) postage and handling, per volume.

Claims for issues not received should be made within three months of publication of the issue, otherwise they cannot be honoured free of charge.

Customers in the U.S.A. and Canada who wish to obtain additional bibliographic information on this and other Elsevier journals should contact Elsevier Science Publishing Company Inc., Journal Information Center, 52 Vanderbilt Avenue, New York, NY 10017. Tel: (212) 867-9040.

ANALYTICA CHIMICA ACTA
VOL. 143 (1982)

ANALYTICA CHIMICA ACTA

International journal devoted to all branches of analytical chemistry

ELSEVIER SCIENTIFIC PUBLISHING COMPANY

Anal. Chim. Acta, Vol. 143 (1982)

Analytica Chimica Acta, 143 (1982) 1
Elsevier Scientific Publishing Company, Amsterdam — Printed in The Netherlands

Guest Editorial

COST EFFECTIVENESS?

The development of very sophisticated and very large apparatus is one of the main trends in analytical research. It is pertinent to ask whether or not all decisions to develop or to buy such equipment have a rational basis. Too often, the lasting impression is that these large instruments are more of a status symbol than a scientific necessity.

This general trend presents some problems to analytical chemists. The first is that an evaluation of the economics (a utility analysis or a cost-benefit analysis) of new costly apparatus would be welcome. Unhappily, most analysts have no idea how to go about this. Even the calculation of total costs is very difficult, because no one teaches chemists about commercial systems analysis. The computation of benefit or utility offers insurmountable problems at present. What is the true benefit of having an apparatus which is twice as precise or has a detection limit which is lower by a factor of ten? The economics of analytical chemistry are not considered to be a glamorous research object. Nevertheless, such studies are necessary and I hope that analytical journals will try to stimulate publication of articles on cost-benefit analysis of analytical instrumentation and research.

The second and related problem is the amount of information generated. The emphasis of our research is too often on finding ways of producing more data in a shorter time. No doubt this is important, but we clearly lag behind in the development of methods for digesting all these data and for extracting from it action-orientated information. It is, for instance, a well known fact that only a small fraction of the clinical chemical data produced in clinical laboratories really contributes to the diagnosis. In the same way, we may wonder what fraction of the data generated by some networks for environmental control are put to use. The economic crisis which now affects research laboratories all over the World will perhaps have the good effect of providing the necessary stimulus to pay more attention to a cost-benefit analysis of such data-producing organisations. One way of increasing benefits without greatly increasing costs is to extract the maximum amount of information from the data. This is one of the aims of the science of chemometrics, a relatively new branch of the analytical sciences, which will undoubtedly repay manifoldly both its study and its application.

D. L. Massart

Analytica Chimica Acta, 143 (1982) 3—34
Elsevier Scientific Publishing Company, Amsterdam — Printed in The Netherlands

Review

PRECONCENTRATION METHODS FOR THE ANALYSIS OF WATER BY X-RAY SPECTROMETRIC TECHNIQUES

R. VAN GRIEKEN

Department of Chemistry, University of Antwerp (U.I.A.), B-2610 Wilrijk (Belgium)

(Received 2nd July 1982)

SUMMARY

All published procedures for multi-element preconcentration of trace elements, prior to x-ray fluorescence analysis of water, are reviewed and critically evaluated. Most preconcentration methods applied to the determination of single elements in water are also listed.

X-ray spectrometry (x.r.s.) is a well established analytical technique. Its underlying spectroscopic principles are well understood, as are its possible pitfalls. The technique offers the advantages of a truly multi-element character, acceptable speed and economy, and ease of automation. Recent instrumental advances include the upgrading of the classical wavelength-dispersive instrument with respect to elemental range, reliability and automation; and about ten years ago, the advent of the non-dispersive or so-called energy-dispersive detection mode with a semi-conductor detector, and of particle-induced x-ray emission (p.i.x.e.) with a nuclear accelerator as excitation source. Each of the x.r.s. modes has its characteristic advantages, and fervent supporters as well, and each can advantageously be applied on a routine basis for many analytical problems. Yet, direct x.r.s. has the distinct disadvantage that its sensitivity is often not sufficient to yield the low level of determination that is desirable in many modern analytical problems. The combination of x.r.s. with a preconcentration step extends the application range significantly, e.g., in the fields of environmental research and monitoring. Not surprisingly, much effort has already been devoted to designing and studying suitable preconcentration techniques that are attractive for x.r.s. of aqueous samples.

Preconcentration, defined by IUPAC [1] as "an operation (process) as a result of which the ratio of the concentration or the amount of micro-components (trace constituents) and macrocomponents (matrix) increases", not only improves the analytical detection limit; it also reduces matrix effects, and so enhances the accuracy of the results and facilitates calibration. Further, preconcentration allows the sample volume taken to be increased and so improves the representative nature of the results. However,

preconcentration increases the time required for analyses, complicates the analyses, and may involve risks of contamination and losses of trace elements or of certain species.

In principle, any preconcentration and separation method developed for any analytical technique could be used in combination with x.r.s. However, x.r.s. operates best on solid samples, gives optimal sensitivity (especially in the energy-dispersive mode) and accuracy for thin homogeneous targets, and offers sufficient spectral resolution for assessing several elements simultaneously. Thus multi-element preconcentration leading to solid thin targets will be ideal for x.r.s. Conversely, preconcentration techniques developed for x.r.s. can be combined with other techniques, e.g., with neutron activation if the sodium, chlorine, bromine and other elements leading to tedious spectral interferences are not significantly collected, with emission spectrometry and spark-source mass spectrometry if the resulting sample is a solid conductor without an excess of major ions, and with flame atomic absorption and inductively-coupled plasma emission spectroscopy if the preconcentrated elements can easily be eluted into a small volume. In view of the present developments in multi-element analysis, the latter group of techniques will probably become of increasing importance.

Direct analysis of whole or filtered water is almost invariably done on a few millilitres placed in a cup with a thin Mylar or polyethylene bottom in a non-evacuated x.r.s. setup. Reported detection limits for energy-dispersive x-ray spectrometry (e.d.x.r.s.) with 30-min counting include, for example, 100 mg l^{-1} for K, 10 mg l^{-1} for Ti, 1 mg l^{-1} for Fe, 0.3 mg l^{-1} for Zn and 0.1 mg l^{-1} for Sr when tube excitation and a secondary target are used [2], and 10 mg l^{-1} or more for these elements when radioactive sources are used for excitation [3, 4]. The correction for x-ray absorption in the Mylar film has been investigated in detail in this context [5]. Special cells for operation in vacuum have been proposed [6]. Typical detection limits in the ppm range are certainly not satisfactory for many environmental water applications and necessitate a preconcentration step.

Several studies have been aimed at x.r.s. of the particulate matter in water and the environmental or geochemical applications thereof, by means of wavelength-dispersive x-ray spectrometry (w.d.x.r.s.) [7—9] or e.d.x.r.s. [10—12] and also p.i.x.e. [13—16]. In general, a simple filtration through a thin membrane, like a 0.45-μm pore-size Millipore or, preferably, a Nuclepore membrane, is quite satisfactory for collecting the particulate matter in a suitable form for measurement. The only problems are then those pertaining to corrections for x-ray absorption and particle size effects.

Necessarily much less obvious is the choice of the preconcentration method to be used for the dissolved ions in water: the literature abounds with alternative procedures. Based on a thorough computer search through the analytical and environmental literature since 1967, as many as possible articles on preconcentration for x.r.s. of water were collected together; more than 170 relevant articles were obtained and studied. Table 1 gives a

TABLE 1

Number of publications pertaining to preconcentration of dissolved elements in water for x-ray spectrometry

Multi-element determinations: 120		Single-element determinations: 43	
General	5	U	7
Physical preconcentration (evaporation, freeze-drying, ...)	23	Cl, Br and I	9
		S^{2-} and SO_4^{2-}	5
Ion-exchange resins	48[a]	Se	3
Coprecipitation	36	Cr	2
Extraction	6	P, K, Fe, Ni, As, Mo, Ba, Hg	1 each
Immobilization after chelation	7		
Electrodeposition	5		

[a]Of which 21 are on ion-exchange filters.

classification of this literature on preconcentration for x.r.s. applied to water. It is the purpose of the present review to describe the published work nearly completely and make this large literature easy to survey. Further, the merits and drawbacks of the various preconcentration procedures for x.r.s. are compared. Industrial or various other samples are sometimes dissolved for subsequent x.r.s. measurements: the literature on the treatment of such aqueous solutions, not comparable or related to environmental waters, will not be considered here.

Very few studies have been dedicated to comparing experimentally some of the proposed preconcentration procedures with respect to sensitivity, precision, linearity, inter-element effects and the influence of humic substances [17—20]. The results reported are certainly not conclusive enough about which method is preferable. Of course, it must be borne in mind that no method of preconcentration will be a panacea because the choice will be influenced by the types of water that have to be examined, the elements of interest, the number of samples, the required accuracy, precision and sensitivity, the available equipment, etc.

EVAPORATION

Perhaps the most obvious and straightforward method for preconcentrating ions from solution is evaporation of the solvent. Yet, in no other method have the inherent problems with respect to x.r.s. been so grossly underestimated. Evaporation collects quantitatively all non-volatile elements irrespective of their speciation in water (which is usually not true for other preconcentration methods), it requires little attention or manpower, and the risks of contamination are minimal. The obvious drawbacks are, however, at least as numerous: the evaporation step is time-consuming; samples with high salinity or hardness cannot be preconcentrated efficiently and analysed sensitively; incomplete recovery of the evaporation residue from the con-

tainer can lead to errors unless an internal standard is included; and pelletizing or some other target preparation is required prior to the x.r.s. step. There are possibly more important inconveniences. For example, the variability of the residue from variable types of water implies variable matrix effects unless sophisticated matrix correction procedures are applied or unless a diluter is used at the expense of lowering the detection limits. Further, the formation of finite crystals, even from very dilute solutions can lead to large and unknown x-ray absorption effects, and the occurrence of fractional crystallization resulting in microscopically inhomogeneous residues may result in very problematic matrix corrections.

Of course, several ways of removing the water matrix physically are available. Straightforward evaporation of a large water sample, pelletizing the evaporation residue and measuring versus doped calcium carbonate matrix standards was proposed by Haberer [21]. Meier et al. [22] and Cornil and Ledent [23] mixed the evaporation residue with an organic binder to reduce matrix effects. Freeze-drying of, for example, 80 ml of waste water on 1.2 g of cellulose followed by grinding and pelletizing of the residue for e.d.x.r.s. led to 0.1 mg l^{-1} detection limits for many elements [24]. The variable absorption correction for the residues were then calculated via the Compton-scattered x-ray tube line. Van Dyck [25] added to a 250-ml water aliquot a spike of yttrium as an internal standard and, if no substantial residue was expected, 100 mg of graphite, then freeze-dried, pelletized and measured by secondary-target e.d.x.r.s. Calculating the x-ray attenuation effect for every energy via the coherent and incoherent scatter peaks ratio and the fluorescent peaks, Van Dyck obtained typical detection limits of 5 $\mu g\ l^{-1}$, and accuracies around 10% for very variable and complex samples like sewage water and sludge. The so-called "vapor filtration" procedure [26] offers an interesting alternative approach, at least for similar samples with low salinity. The cellophane bottom of a container is permeable to water vapor but not to water or dissolved material. The bottom surface is exposed to vacuum, the water vapor is pumped away and all the dissolved solids are left behind on or in the membrane. In combination with p.i.x.e., typical detection limits of 0.1–3 $\mu g\ l^{-1}$ have been claimed [27].

In general, the more advantageous detection limits of p.i.x.e. and its predominant use in nuclear physics laboratories where chemical manipulations are often unpopular, have resulted frequently in a combination of p.i.x.e. with a simple water pretreatment step consisting of pipetting one drop or at most 1 ml of water onto a thin Formvar or Mylar carrier and evaporating [13, 14, 28–31]. The reported detection limits are then usually around 10 $\mu g\ l^{-1}$, or lower if the sample is concentrated by partial evaporation at 50–60°C prior to spotting [32]. The absorption-enhancing effect in the finite residue crystals, that may plague such an approach, may be reduced by nebulizing the liquid onto the substrate [33, 34]. A more convincing alternative is the previous addition of homogenizers such as liposomes, i.e., synthetic phospholipid bilayer vesicles [35]. Such vesicles are capable of

entrapping ions and small molecules and interfere with the crystallization in very small areas. Robaye et al. [35] observed that, in the absence of a homogenizer, 20 μg of salts dissolved in a droplet covering an 8-mm diameter area before drying, may give rise to a crystal with a superficial density of 10 mg cm^{-2}.

Another approach that partially circumvents such problems and allows larger samples to be evaporated and so better detection limits to be reached in x.r.s., consists of impregnating a filter paper with the sample solution. In combination with w.d.x.r.s., this method was first described by Pfeiffer and Zemany [36] and has since been used by several authors, e.g., Felten et al. [37]. The sensitivity can be improved further by applying the ring oven technique, e.g., as recommended by Ackermann et al. [38]. Johnson and Nagel [39] proposed spotting within a controlled area which was obtained by applying a hydrophobic wax ring on the filter paper. After further optimization of the various parameters of such a simple spotting procedure for e.d.x.r.s. of water, the following procedure was proposed [40]: 1.5 ml of water sample was spotted on a Whatman-41 cellulose filter paper provided with a wax ring of 3-cm diameter, and the water was evaporated by passing an unheated air stream from underneath. The detection limits were found to be below 100 μg l^{-1} for most elements and often below 50 μg l^{-1} when the optimal secondary fluorescence was used. Accuracy and precision were usually in the 15—20% range, but were somewhat better when an internal standard was added to the solution prior to the spotting. The hydrophobic wax ring reduces the spreading of the solution in the filter and any differential chromatographic effects, and so increases the sensitivity and reduces errors arising from heterogeneous analyte distribution within an exciting beam of non-uniform intensity.

Other approaches that give a more homogeneously distributed deposit on a filter paper include the nebulization technique [33, 34, 41] and the multidrop technique [42] in which, e.g., 220 μl is deposited in 10—15 μl drops, just enough to wet the entire surface. For subsequent p.i.x.e., Kivits et al. [43] recommended wetting a filter paper fixed on a rotating table (18 000 rpm) with 50 μl of a water sample diluted (1:1) with ethanol as a surface reactant, and air drying.

In general, it seems that physical preconcentration methods are quite suitable for simple screening of waters, when extreme sensitivity, accuracy and versatility are not required, and when the trace metal speciation is complex or variable. In fact, physical preconcentration is the only practical possibility when sewage, waste waters or similar samples, are to be analyzed.

ION EXCHANGERS

As in other analytical techniques, materials with ion-exchange properties have extensively been used for preconcentration in x.r.s., in both the batch and the column mode. The effect of the ion-exchange resin particle size on the

results obtained by x.r.s. was studied [44], and particle sizes below 50 μm were recommended.

Ordinary cation and anion exchangers are of limited use for concentrating trace elements from natural water because of their inability to exclude major ions selectively. Still, for samples with a limited alkali and alkaline earth ion content, conventionally available cation- and anion-exchange resins can be applied. Cesareo et al. [45] reported on such preconcentration for radioisotope x.r.s. Murata and Noguchi [46] used a cation exchanger to determine several ions in acidified waste water, by w.d.x.r.s., down to 10 $\mu g\ l^{-1}$, with a 3% standard deviation at the 1 mg l^{-1} level. They added 1.5 g of epoxy resin binder to 6 g of cation exchanger and allowed the mixture to harden into a pellet. Up to 1000 mg l^{-1} Na^+, 200 mg l^{-1} Mg^{2+} and 100 mg l^{-1} Ca^{2+} could be tolerated; above this level, the transition metal uptake was strongly depressed. Indeed, as these resins operate on an ion-association basis, they are not very selective and the abundant alkali and alkaline ions can compete well with transition metals.

In cases where the alkali ions are not of interest, chelating ion-exchange resins are more promising. The most popular one is undoubtedly Dowex A1, or Chelex-100 (BioRad Laboratories), with iminodiacetate functional groups (Fig. 1). Generally, it offers very high distribution ratios for transition metal ions and for Hg^{2+} and Pb^{2+}, but not for alkali ions, and its chemistry can be accurately predicted by analogy with EDTA. Florkowski et al. [47] studied the potential of Chelex-100 resin preconcentrations in the analysis of ground water and rain water, and found that 9000 mg l^{-1} Na^+ and 200 mg l^{-1} Ca^{2+}

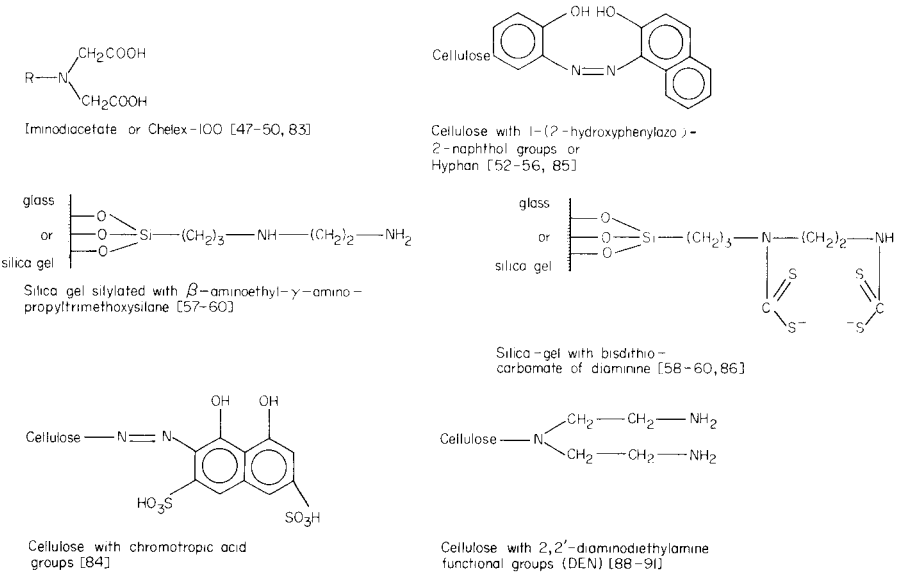

Fig. 1. Functional groups of ion exchangers and of ion-exchange/chelating filters useful for preconcentration in x.r.s.

could be tolerated under their experimental conditions. Clanet and coworkers [48—50] used a Chelex-100 column in a Makrolon cartridge which was pelletized for x.r.s. measurement after the collection of trace metals; they noted that an abundance of alkaline earth ions in the water sample necessitates either recycling of the water sample over the column or previous dilution.

For more versatile preconcentrations, the ion-exchange substrate should not show any affinity for alkali and alkaline earth ions and be selective towards transition metals. Leyden et al. [51] used 100 mg of polyamine—polyurea resin columns prepared from tetraethylenepentamine and toluene diisocyanate, to preconcentrate nickel, copper and zinc quantitatively from 4 l of seawater of natural pH (in spite of the 16 g l^{-1} Na^+, 1300 mg l^{-1} Mg^{2+} and 500 mg l^{-1} Ca^{2+} normally present in sea water) and to determine these trace metals by w.d.x.r.s. down to 0.1—0.3 μg l^{-1} concentrations. Burba and Lieser [52] immobilized 1-(2-hydroxyphenylazo)-2-naphthol or Hyphan (see Fig. 1) on cellulose powder by diazotization of *o*-aminophenolcellulose and subsequent coupling with β-naphthol. Later papers described the x.r.s.-determination of Fe, Zn, Pb and especially Cu and U in freshwater, seawater and mineral water with this ion exchanger [52—56] which has a capacity of 0.5 mmol g^{-1} and is now commercially available (Riedel de Haën). The detection limits were typically just below 1 μg l^{-1} for e.d.x.r.s. or w.d.x.r.s., but some weak influence of Ca^{2+} cannot be excluded.

Considerable research has been dedicated to finding simple methods of immobilizing ion-collecting functional groups in a very versatile way. Leyden and coworkers [57—60] have intensively studied and used the silylation reaction to immobilize chelating or coordinating functional groups onto controlled pore glass beads or silica gel. After homogenization and pelletizing, such material is a suitable matrix for x.r.s. determinations. They used *N*-β-aminoethyl-γ-aminopropyltrimethoxysilane (Dow-Corning Z-6020 reagent) and γ-aminopropyltrimethoxysilane (Dow-Corning XZ-2024 reagent) to immobilize diamine functional groups, and also prepared the dithiocarbamate derivatives thereof (see Fig. 1) to preconcentrate cations and anions efficiently. Capacities of 0.5—0.9 meq g^{-1} were obtained, and after solutions had been passed at 50 ml min^{-1} through a 100-mg column, Mn, Fe, Co, Ni, Cu at 1 μg l^{-1} concentrations could be determined directly by x.r.s. on the pelletized column without interference from Ca or Mg. Hirayama and Unohara [61] worked along similar lines and treated similar silylated silica with either monochloroacetate or salicylaldehyde to produce acetate or Schiff base functional groups; they obtained enrichment factors of 500, and x.r.s. detection limits around 10 μg l^{-1}.

In general, ion exchangers will recover hydrated ions, charged complexes and ions complexed by labile ligands, but the recovery depends on the distribution ratio of the ion on the resin, the stability constants of the complexes in the solution, the exchange kinetics and the presence of other competing ions. More specifically, it is not always obvious that trace transi-

tion metals bound to stable complexes and naturally occurring organic material or adsorbed on colloids, will be collected efficiently by ion-exchange resins. In this context, the use of Chelex-100 for trace metal preconcentration from natural water has been criticized by Florence and Batley [62], who measured very low recoveries from sea water of, e.g., zinc in its natural speciation, although freshly added radioactive ionic spikes were recovered fully. This was confirmed by Abdullah et al. [63] who found that metals in colloidal form or adsorbed on particulates which could be separated from the sample by centrifugation were not retained by Chelex-100, while only the dissolved and electro-reducible species of Cu, Zn, Cd and Pb correspond to the fraction taken up by the resin. This problem is not particular to the ion-exchange process, but also plagues most other preconcentration methods.

All the preconcentration procedures based on ion-exchange resins share some drawbacks. First, the sensitivity is not optimal because the preconcentration factor (ratio of original to final sample weight) is typically around 5000 only (e.g. 100 mg of ion exchanger per 500 ml of water); moreover, a diluting binder may be necessary for pelleting. Secondly, after column preconcentration, the ion exchanger should be homogenized and pelletized prior to x.r.s. Thirdly, in thick targets of ion-exchanger beads, absorption and particle-size effects can be considerable.

The use of ion-exchange filters could remedy these problems.

ION-COLLECTING FILTERS

Ion-collecting filters offer a very elegant way of preconcentration if quantitative recovery can be accomplished by a single filtration step at natural pH. In fact, ion-collecting filters are more attractive for combination with x.r.s. than with any other analytical technique. The loaded filter is ideally a thin homogeneous target of low Z number that can be presented directly to the x.r.s. machine, without any preparation. Thin targets offer optimal accuracy and sensitivity, because the absorption-enhancement corrections remain small and the background of exciting radiation scatter is limited. Ideally, particulate and dissolved trace metals could thus be determined in tapwater, for example, by simply plugging a filter holder with both a common filter and an ion-collecting membrane onto the tap, running a certain volume of water through, and subjecting both loaded filters to x.r.s. Preconcentration based on paper tape loaded with ion-exchange resin could also be highly automated, as in the "Sample Collection and Preparation Module" with automated e.d.x.r.s., proposed by Carlton and Russ [64]. Naturally, much effort has been devoted to preconcentration by ion-collecting filters for x.r.s., but, surprisingly, almost all research has been focussed on the ion-collecting membrane types that are least interesting for environmental samples of waters.

Grubb and Zemany [65] first proposed the use of ion-exchange membranes for x.r.s. Campbell and coworkers published well-known pioneering work on

ion-exchange resin-loaded papers for x.r.s. [66] and later reviewed their applications [67, 68]. They used Reeve-Angel cation-exchange papers SA-2, and found satisfactory recoveries for a dozen cations at pH 2 after seven successive filtrations but warned about the effects of abundant alkali and alkaline ions. They also reported good collections of anions on Reeve-Angel anion-exchange papers SB-2 with quaternary ammonium groups. The detection limits were just below 1 μg for w.d.x.r.s.

Up to 1977, practically all published work on ion-collecting filters for water research [69—80] was devoted to the use of the commercially available SA-2 filters with sulfonic acid functional groups, containing approximately 50% Amberlite IR-120 resin and 50% cellulose, and having an exchange capacity of 2 meq g^{-1}. Several of these articles reported only preliminary experiments; others essentially confirmed the original results of Campbell et al. [66], and, depending on the sample volume (typically only 10—100 ml), the number of passes (6—10), the excitation mode and measurement time and the filtration procedure used, the reported detection limits were typically between 10 and 400 μg l^{-1}. In spite of some rather optimistic preliminary conclusions, most of these authors were well aware of the severe restrictions of SA-2 filters: they have an exchange capacity of only 0.25 meq/filter and a significant affinity for the alkali and alkaline earth ions. Therefore, the collection of transition metal ions is not quantitative for large sample volumes of natural water in which alkali and particularly alkaline earth ions are usually abundant: the applicable sample volume is thus severely limited, and then the preconcentration factor is too low to yield environmentally relevant detection limits. This was confirmed in recent intercomparison studies [17—19]. Moreover, passing the sample several times over the filter is inconvenient, and adding acid to adjust the pH to 2 implies a risk of contamination. Clearly SA-2 filters are not ideal for direct x.r.s. of waters.

Nor did Ulrich and Hopke [79] find the SB-2 anion-exchange filters to be satisfactory for trace metal collection from natural waters, after a complexation step at pH 12 with 0.01—0.02 mM cyanide or with 0.02 mM BPPM-S [2-(3′-sulfobenzoyl)-pyridine-2-pyridylhydrazone]. The authors had expected that such a step would minimize the problems of determining naturally occurring complexed ions, but at alkaline pH, large concentrations of calcium and magnesium form a gel that prevents filtration.

Kingston and Pella [81] were successful in indirectly using SA-2 filters for the determination of Ni, Mn, Zn, Cu and Pb in sea water, at the 2—4 μg l^{-1} level with a standard deviation of only 0.2 μg l^{-1} by e.d.x.r.s. The sea water was first processed for the separation of the trace elements from Na, K, Ca and Mg, on a Chelex-100 column, and the eluate was evaporated, heated to sublime ammonium salts, taken up in acid, and only then passed through SA-2 filters.

Lochmüller et al. [82] briefly studied MC-3142 ion-exchange membranes (Ionic Chemical Co.) that are characterized by a slow metal uptake. Exposure

of the membrane to a changing concentration in a stream should therefore lead to a collection that represents an average concentration. Further, P-81 filters (Whatman) with phosphate groups and WA-2 papers (Reeve-Angel) with carboxylic functional groups have been mentioned but not studied in much detail [78]. It is not likely that any of these materials is vastly superior to SA-2 filters; clearly, more selective filters, with no affinity for alkali or alkaline earth ions, are required.

Van Grieken et al. [83] therefore evaluated the commercially available Acropor CH filters (Gelman Co.) with Chelex-100 or iminodiacetate groups that were expected to show a much less pronounced affinity for alkali and alkaline earth ions and to collect at natural pH levels. It appeared that filtering 200 ml of water through a pair of Chelex-100 filters, under a 2—3 bar pressure at pH 7—8 in not less than 20 min, provided an efficient collection of many trace metals (up to the 0.07 meq capacity per filter pair), with x.r.s. detection limits at the 1 $\mu g\ l^{-1}$ level and a precision around 10%. Again, however, the still significant affinity for alkaline earth ions restricted the applicability. With calcium-rich water, for example, only small volumes could be preconcentrated and the detection limits were accordingly worse. Thus the long-term objective of applying resin-loaded filters for continuous on-line collection of ions from drinking water and other near neutral aqueous solutions could not be attained. Although longer filtration times (e.g., 10 h) favor the chelation process relative to simple cation exchange and reduce the alkaline earth interference, Chelex-100 filters are not promising either.

Cellulose-powder films with immobilized chromotropic acid functional groups (see Fig. 1) allow fast collections at pH 4—6.5 with a 0.01 meq capacity, but they suffer even more from Na^+ and Ca^{2+} interferences; 5 ppm calcium reduces the transition metal uptake to 40% only [84].

Hyphan filters are prepared by immobilizing 1-(2-hydroxyphenylazo)-2-naphthol on short-fibred cellulose powder and pelletizing 0.1 g of the product, which has a 0.05 meq exchange capacity, into thin layers. These are much more suitable: after acetate addition, high recoveries of trace metals are possible from 3 l of fresh water and 0.5 M NaCl solutions, at a flow rate up to 18 ml min^{-1} cm^{-2} at pH 7, and the detection limits for e.d.x.r.s. are typically around 1 $\mu g\ l^{-1}$ [52—54]. The influence of alkali and alkaline earth ions, although small, is not negligible; preconcentrations from sea water require thicker filters, smaller sample volumes and lower filtration rates. When, however, the trace transition metals were first preconcentrated in small Hyphan columns, eluted by dilute hydrochloric acid and then bound on 100 mg of Hyphan that was prepared as a thin layer for e.d.x.r.s., sea water and 20% NaCl solutions could be analysed [85].

Gendre et al. [86] silylated a silica-gel filter with *N*-β-aminoethylaminopropyltrimethoxysilane and then treated the resulting diamine with carbon disulphide to obtain the dithiocarbamate (Fig. 1) modified filters. Up to 20 μg of transition metals could be taken up from 50 ml of water at pH 5—6 after 10 cycles at 10 ml cm^{-2} min^{-1} but the influence of major ions was not studied.

Disam et al. [87] followed a different and very novel approach: they filtered 0.1—6 l of aqueous samples through a freshly prepared homogeneous metal sulfide layer (e.g., 450 μg of zinc sulfide) and sufficiently enriched numerous elements that form insoluble sulfides, to obtain w.d.x.r.s. detection limits of about 0.2 $\mu g\ l^{-1}$ for surface waters. Only Fe^{3+}, HPO_4^{2-} and strong chelating agents interfered seriously.

An ideal complexing molecule for preconcentrating filters should fulfil the following requirements: (1) no affinity for alkali and alkaline earth ions, (2) high stability constants for heavy metal ions, (3) formation of a stable molecular structure, (4) easy immobilization onto cellulose, for example. Theoretical considerations indicated that 2,2′-diaminodiethylamine, often called diethylenetriamine (DEN), would satisfy these requirements very well. A considerable amount of work to optimize the synthesis of cellulose-DEN filters (see Fig. 1) led to the following recipe [88]. Ten dried Whatman-41 cellulose filters are pre-swelled by soaking for 30—60 min in 200 ml of dry *N,N*-dimethylformamide (DMF; distilled with 10 ml of benzene per 100 ml of DMF); then 6 ml of $POCl_3$ is added and the mixture is heated to 90°C for at least 15 min. The filters are washed successively with DMF, water, 50% (w/v) NaOH, water, 5% (v/v) acetic acid and water. The chlorine functional group is then replaced by heating the filters in an excess of purified DEN at 130°C for at least 2 h. The average transition metal uptake capacity of the resulting filters is 3.6 $\mu eq\ cm^{-2}$ or 37 μeq/filter.

Many parameters that might influence the trace cation uptake by the DEN filters were subsequently studied [89]. At a filtration rate below 1.5 ml $min^{-1}\ cm^{-2}$ and at a pH above 6, recoveries of 90—100% are obtained for Cr^{3+}, Fe^{3+}, Co^{2+}, Ni^{2+}, Zn^{2+}, Ag^{+}, Cd^{2+}, Eu^{3+}, Hg^{2+}, Pb^{2+} and UO_2^{2+}. For sample volumes up to 100 ml cm^{-2}, there is no elution of the collected cations. The possible influence of foreign substances was checked by adding salts of Na^{+}, K^{+}, Mg^{2+}, Ca^{2+}, NH_4^{+}, NO_3^{-}, Cl^{-}, I^{-}, HCO_3^{-}, SO_4^{2-}, $H_2PO_4^{-}$ and also glycine and humic material to numerous multi-element transition metal solutions. While the collection of Mn^{2+} was depressed by several agents, the uptake of the other cations was only influenced by NH_4^{+} and amino acids (above 5000 mg l^{-1}), which compete with the nitrogen donors in the DEN filters, and not by 350 g l^{-1} NaCl or 30 g l^{-1} $CaCl_2$. Anions can also be preconcentrated by DEN filters [90], at least from diluted solutions, at a filtration rate below 0.7 ml $min^{-1}\ cm^{-2}$ and at pH 4.5, up to a total load of at least 1.5 $\mu eq\ cm^{-2}$. It appeared, however, that the anion collection mechanism is based purely on electrostatic attraction, and so is not selective: ionic strengths above 0.01 M NaCl strongly depress the collection efficiency. This limits the applicability of DEN filters for anion preconcentrations to diluted samples only. The combination of the DEN filter with conventional secondary-fluorescer e.d.x.r.s. has been evaluated [91]. A perfectly linear relation was noted between the x-ray response and the metal concentration in solution up to the ca. 20 μeq capacity of a 10-cm^2 DEN filter. Practical detection limits were around 0.5 $\mu g\ l^{-1}$ and often lower. Accuracy and precision were

both around 10% for higher concentration levels. The major drawback of the DEN filters is that they are not commercially available while their synthesis is not trivial and requires some precautions.

PRECIPITATION AND COPRECIPITATION

Many precipitation procedures have been devised over the years for preconcentration in various analytical techniques. Although they may be less attractive for those techniques that require liquid samples, most can be combined very advantageously with x.r.s., particularly if they lead to a homogeneous surface load on a thin filter. In analytical chemistry, much effort has been devoted to finding specific precipitation reagents. However, for a technique with a high inherent selectivity, like x.r.s., selective precipitation is usually not necessary and non-specific multi-element reagents are more attractive. The simplicity of the procedure, the completeness of the precipitation and the inherent capacities available will be the most important features.

In an effort to measure on infinitely thin precipitate layers only, Smiricz [92] first evaporated a 24-l water sample, dissolved the residue, precipitated and measured the sulfides insoluble at pH 2, separated off the iron, and precipitated and measured the sulfides insoluble at pH 8. This tedious procedure gave detection limits around 1 $\mu g\ l^{-1}$. A preliminary investigation of the preconcentration of a few elements from water as sulfides was also carried out by Ellgren [93].

More common in water analysis is direct precipitation with an organic reagent, and direct measurements on the filtered precipitate. Most popular, and undoubtedly also extremely attractive as reagents for precipitation, are the dithiocarbamates, in view of the low aqueous solubility of their metal chelates. The pioneering work of Luke [94] established the conditions for the determination of many trace metal ions by hydroxide precipitation and by coprecipitation with sodium diethyldithiocarbamate (NaDDTC, see Fig. 2). Luke's well-known "coprex" technique involves adding DDTC and a spike of a suitable metal ion as a coprecipitating agent and as an internal standard, adjusting the pH and filtering off for x.r.s. measurements.

Watanabe et al. [95], Florkowski et al. [3] and Holynska and Bisiniek [96] studied the precipitation of several elements, including mercury, in waters by NaDDTC. They found that Na^+, Ca^{2+} and Mg^{2+} did not interfere, while some interelement effects occurred for the transition metals; the detection limits for w.d.x.r.s. and radioisotope e.d.x.r.s. were 0.05—3 $\mu g\ l^{-1}$ and 5—10 $\mu g\ l^{-1}$, respectively. Moriyama et al. [97] reported that Cr, Mn, Fe, Co, Ni, Cu, Zn, Cd, Hg, Pb, etc., could be determined in water as carbamates or hydroxides after precipitation with NaDDTC at pH 9, with detection limits of 0.01—0.3 $\mu g\ l^{-1}$. For waste water, Sasuga et al. [98] recommended precipitation with DDTC at pH 4.2 and ultrasonic treatment to collect Co, Ni, Cu, Zn, Cd and Pb quantitatively and uniformly on a

filter paper, with an 8% precision at the 0.1 ppm level and detection limits of 2—40 and 1—5 $\mu g\ l^{-1}$ for w.d.x.r.s. and e.d.x.r.s., respectively. Tanoue et al. [99] developed an automated device for DDTC preconcentration and x.r.s. measurement of waste water. Other Japanese articles are available on this topic (see, e.g., [100]).

To lower the x.r.s. detection limits, the "coprex" preconcentration method has been combined with a "microdot" filtration procedure, in which the DDTC/hydroxide precipitate is collected within a filtration area with a diameter of 100 mil, and measured in a separate sample-positioning setup where the sample is focussed visually relative to a collimator with a 50-mil aperture [101]. Others evaporated 500 ml of sea water down to 100 ml prior to DDTC precipitation, in order to boost the sensitivity [102], or first preconcentrated 10 l of water on a cation-exchange resin, precipitated with NaDDTC and measured [103]. Knöchel and Prange [104] found that DDTC can collect many elements quantitatively in a homogeneous precipitate for direct x.r.s. measurements, or for subsequent elution by chloroform onto a special quartz support which is directly suitable for e.d.x.r.s. in the highly sensitive total reflection mode (see below).

Leyden et al. [19] observed, however, that the recovery with DDTC decreases for lower concentrations and is certainly not quantitative at or below 10 $\mu g\ l^{-1}$. In this respect, ammoniumpyrrolidinedithiocarbamate (APDC, see Fig. 2) seems generally preferable as a coprecipitating agent.

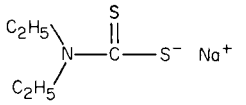

Na DDTC

[94, 104, 109–111]

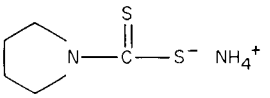

APDC

[79, 105–108, 111]

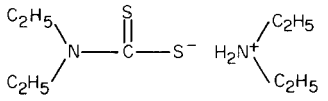

DDDC

[112, 113]

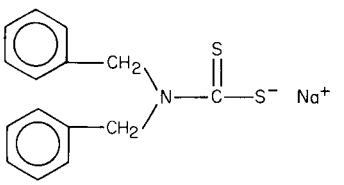

DBDTC

[114, 115]

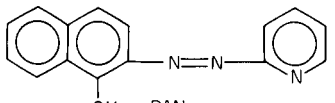

PAN

[95, 118–120]

Fig. 2. Reagents useful for (co)precipitation prior to x.r.s.

In general, the type of dithiocarbamate substituent influences the solubility of the chelates and their sensitivity to hydrolysis rather more than the selectivity of the complex formation which favours the transition metals in all cases. Ulrich and Hopke [79], comparing several x.r.s. preconcentration methods, concluded that APDC at pH 4 was the best non-specific precipitating agent, superior to DDTC for Zn and Pb; they found adequate recoveries for Fe, Ni, Cu, Zn, Se, Pb, Hg, Cd, Ti, Cr, Th and Tl, independent of the alkaline ion concentration level. Elder et al. [105] had earlier precipitated at pH 2 with a fresh APDC solution and obtained quantitative recoveries for Cu, Hg and Pb, though not for Fe and Zn; but they noted a strong depression of zinc recoveries in natural water. In the analysis of polluted rivers by radioisotope-induced e.d.x.r.s., Meier and Unger [106] reported a standard deviation of 3% at the 125 $\mu g\ l^{-1}$ level and of 15% at the 15 $\mu g\ l^{-1}$ level and detection limits around 6 $\mu g\ l^{-1}$, for both DDTC and APDC precipitations.

Several authors have tried to improve the precipitation characteristics by adding a carrier, as in the "coprex" technique [94]. In precipitation, the use of carriers, or of a coprecipitation technique, is especially important when, in exceedingly dilute solutions, the solubility is not low enough to prevent complete precipitation, or when the particle size of the precipitate is very small so that it passes through the filters, or when a supersaturated solution can exist. Pradzynski and coworkers [107, 108] used APDC and a Fe^{3+}-carrier, and reported e.d.x.r.s. detection limits of 1 $\mu g\ l^{-1}$ for V, Cr, Mn, Cu, Zn, As, Se, Hg and Pb, but they did not check the influence of abundant ions or humic material. Tanoue et al. [109] used cobalt as a carrier for the DDTC coprecipitation of Zn, Cu, Fe, Mn and Cr in waste water of pH 6, and copper for the coprecipitation of cadmium at pH 4. Brüggerhoff et al. [110] added molybdenum, prior to DDTC precipitation, to act as a carrier and an internal standard in analysis of solutions by p.i.x.e., but Ulrich and Hopke [79] argued that additions of molybdenum do not increase the recoveries with APDC from surface and drinking water, probably because of the relatively high iron concentration that is already naturally present. After precipitating metals in water with DDTC (for Pb, Fe, Cu, Zn, Mn, Cd, Cr^{3+} and Sb) or APDC (for As^{3+}), Takemoto et al. [111] added some dibenzylidene-*D*-sorbitol solution in dimethylsulfoxide to coagulate the chelate better before the filtration and w.d.x.r.s. step.

Other dithiocarbamates have been recommended as well. Scheubeck and coworkers [112, 113] advocated the use of a certain quantity of diethylammonium-*N*,*N'*-diethyldithiocarbamate (DDDC, see Fig. 2) and a particular metal carrier, after a particular pretreatment step, all depending on the water type: recoveries above 80% were noted for 500–2000 $\mu g\ l^{-1}$ metal ion spikes. Lindner et al. [114] and later Watanabe and Kose [115] have recommended the use of dibenzyldithiocarbamate (DBDTC, see Fig. 2) mainly because its very low solubility in water eliminates the need for a metal carrier. In a very recent study, where seven preconcentration procedures for x.r.s. [58, 66, 95, 105, 114, 116, 138] were compared for sensitivity,

precision, detection limit, linear range and interferences by concomitant ions and salts, Leyden et al. [20] recommended the latter DBDTC precipitation technique as being the most valuable. They investigated the trace elements Cr, Mn, Fe, Co, Ni, Cu, Zn, As, Se, Sb, Hg, Tl, Ag, Cd and Pb, and found nearly quantitative recoveries (except for Cr and As) in a variety of field-sampled waters; the e.d.x.r.s. detection limits were 1—5 $\mu g\ l^{-1}$ for 100-ml water samples.

Various other multi-element coprecipitating agents have been proposed, each with specific advantages and drawbacks relative to the dithiocarbamates. Panayappan et al. [116] reported that a combination of polyvinylpyrrolidine and thionalide as precipitating agents for x.r.s. can provide particularly rapid and quantitative preconcentrations, not influenced by Ca, Mg and alkali metal ions. A combination of 1,10-phenanthroline and tetraphenylboron also appears to collect most transition metal ions quickly and quantitatively at pH 5 without interferences from Ca and Mg, and to allow e.d.x.r.s. detection limits of 0.1 μg, e.g., in 50-ml water samples [117].

1-(2-Pyridylazo)-2-naphthol (PAN, see Fig. 2) is another chelating agent which forms strong insoluble chelates with many transition metal ions: PAN is very soluble in hot water and ethanol, but not in cold water. Püschel [118] introduced the use of PAN for preconcentration purposes and Watanabe et al. [95] applied it in combination with w.d.x.r.s. Cocrystallizations with PAN have been found to be very convenient and efficient [119]. Addition of 20 mg of PAN to a neutral 2-l water sample at 70°C, and filtration after cooling leads to nearly quantitative recoveries of at least 15 cations, independent of the sample salinity and, up to the 100-μeq capacity of 20 mg of PAN, of the ion concentration. Enrichment factors as high as 10^5 can be obtained routinely; counting statistics would then allow e.d.x.r.s. detection limits of 0.03 $\mu g\ l^{-1}$ but the PAN blank levels lead to realistic limits around 0.5 $\mu g\ l^{-1}$. A precision of 5—10% can be achieved at the 10 $\mu g\ l^{-1}$ level. Some disturbance by high contents of humic material and, e.g., sulfide has been noted [120]. For waters with a relatively constant composition like seawater, however, this method is quite attractive.

Although there is an extensive literature on coprecipitation with hydrated iron oxide, this method has seldom been used in x.r.s. work. Yet, Bruninx and coworkers [121, 122] claimed that 2—10 mg l^{-1} Fe^{3+} could quickly collect even non-ionic forms of dissolved transition metals efficiently without interference from Ca, Mg, etc., while the Fe—K_α x-ray can be used as an internal standard; they showed experimentally than Zn^{2+} and Pb^{2+} could be measured by w.d.x.r.s. in polluted river water. In a recent study, it was found that hydrated iron oxide can indeed scavenge Ni^{2+}, Cu^{2+}, Zn^{2+} and Pb^{2+} from seawater adjusted to pH 9 [123]. The collection is not significantly influenced by the major components. It depends on the concentrations of both the iron carrier and the transition metal, fortunately in a very predictable way. Indeed, the ratio of the resulting trace metal concentration in the precipitate to the remaining concentration in solution is constant, and

the logarithms of these ratios are equal to 4.1 ± 0.1 for Mn^{2+}, 5.1 ± 0.1 for Co^{2+}, 4.9 ± 0.1 for Ni^{2+}, 5.7 ± 0.1 for Cu^{2+}, 6.5 ± 0.1 for Zn^{2+}, 4.5 ± 0.1 for Cd^{2+} and >7 for Pb^{2+} and rare earth ions, at pH 9. This observation allows a convenient compromise to be achieved between a minimal amount of iron, hence high enrichment factor and low detection limit on the one hand, and a high collection yield, hence optimal precision and accuracy on the other hand, and to make corrections for inadequate coprecipitation. In routine practice in this laboratory, the use of 10 mg l^{-1} Fe in 200-ml samples of pH 9 is preferred; collection yields are above 90% at 10 μg l^{-1} metal concentrations (except for Mn^{2+} and Cd^{2+}), the e.d.x.r.s. precision is around 5%, and detection limits are around 0.4 μg l^{-1} for a 3000-s counting time. The environmental applicability of this approach is still under investigation.

Other multi-element coprecipitation agents that have been considered for x.r.s. are 8-quinolinol (oxine) [124] (which is less attractive because of incomplete transition metal collections from polluted waters and because it also precipitates Mg^{2+}, which can lead to variable enrichment factors), alizarin blue, phenylfluorone, cupferron, fluorides, tellurium, etc. [125].

Dithiols are promising as more selective precipitants. For example, Watanabe and Ueda [126] studied the use of 6-aniline-1,3,5-triazine-2,4-dithiol either alone or in combination with benzyldimethyltetradecylammonium chloride for enrichments of Cu, Cd and Pb; they determined these three elements in hot-spring waters at levels from several to several ten μg l^{-1} by w.d.x.r.s.

In general, although the literature abounds with precipitation enrichment procedures, many of which are truly attractive for combination with x.r.s., a common failure of most publications is the lack of thorough and systematic checking of the performance of these procedures for waters containing abundant alkaline earth and alkali ions, examination of complications caused by humic material, and the effects of variable speciation of the trace metals. Although acidification to a low pH as required in some procedures (e.g., APDC precipitation) might overcome some of these problems, at the cost of a higher contamination risk, and although u.v. irradiation prior to preconcentration might often be helpful [127], serious checking of the procedures, prior to their routine application in environmental problems, should be regarded as mandatory.

LIQUID–LIQUID EXTRACTION

Solvent extraction is undoubtedly the most popular routine preconcentration method, e.g., in atomic absorption spectrometry. Many monographs and reviews on this technique are available, and an excellent general survey by Bächmann [128] refers to much of the work. Extraction procedures are usually simple and rapid, and they may be automated fairly easily. Yet they are not commonly applied in x.r.s., mainly because subsequent evaporation is necessary and because the preconcentration coefficients are usually quite low.

Marcie [129] added to 250-ml water samples 5 ml of pH 5 buffer, and 5 ml of a 2% APDC solution, extracted the transition metals after equilibration for 5 min into three 5-ml portions of chloroform, and carefully evaporated these on a filter paper carrier. The capacity was 300 μeq of divalent transition metals. Similarly, Iwasaki et al. [130] extracted microgram quantities of various metals with DDTC from solutions buffered at pH 5—6 into chloroform or with cupferron into chloroform from hydrochloric acid solutions, and dropped the extract on a filter paper. Kuroha and Shibuya [131] extracted with DDTC from pH 5—9 medium into carbon tetrachloride, added polystyrene and an internal standard to the extract, and dried it under i.r. radiation on a Mylar foil to obtain a very thin film for w.d.x.r.s. They achieved detection limits down to 0.03-1 μg for 15 elements, with a 3—5% coefficient of variation at the 20-μg level. Florkowski et al. [3] reported a few experiments, using extraction with 8-quinolinol into chloroform or with trioctylamine into xylene for radioisotope-excited x.r.s. measurements on polluted waters at the 1—5 mg l^{-1} level.

An ingenious way of target preparation was proposed by Magyar and Lobanov [132] who extracted into molten 8-quinolinol, and subsequently dried, remelted, cooled, ground and pelletized the organic phase. Such a method partially avoids the problems inherent in separating a small volume of organic phase from the aqueous sample and in adhesion of the organic solvent to the wall of the vessel. The procedure is claimed to be useful for trace metal determinations in fresh water, but the enrichment factors are typically 10—50 only. Similarly, Kawase et al. [133] extracted the APDC chelates of Ni, Cu, Zn, Cd, Pb and Bi from hot solutions into disks, and measured by e.d.x.r.s.

In general, again, very little attention has been paid to specific problems that might be encountered in extraction preconcentration for natural waters. In a recent intercomparison study of preconcentration methods, disappointing results were often found for APDC extractions from natural waters [17].

CHELATION AND SUBSEQUENT SORPTION IMMOBILIZATION

While liquid—liquid extraction involves handling large volumes of extract and time-consuming evaporations or another target preparation step, reversed-phase techniques with organic solvents adsorbed on the surface of a small particle support seem more interesting. Such processes correspond to repeated extraction, and quantitative yields can therefore be expected even with relatively low distribution constants. In their original approach, Knapp et al. [134] formed the transition metals chelates with NaDDTC and subsequently adsorbed the chelates onto Chromosorb W-DMCS columns. They observed complete sorption of Fe, Co, Ni, Cu, Zn, Cd, Hg and Pb at pH 4 or 5. The carbamates were eluted with 2 ml of chloroform onto a filter paper in a special teflon container for w.d.x.r.s. measurement. For 100-ml samples, the detection limits were 0.1—1.1 μg.

Such reversed-phase techniques with subsequent elution can be combined advantageously with e.d.x.r.s. by using a totally reflecting sample holder. In this technique, because of the small angle of incidence of a few minutes of arc, the primary incident rays almost cannot penetrate the sample support. Thus the usual scattered irradiation caused by the sample support is almost completely eliminated and determinations of 10^{-10} g become possible. In water analysis, Knöchel and Prange [104, 135] formed the transition metal chelates with DDTC, adsorbed the chelates on a Chromosorb column and eluted with chloroform as a thin film onto a totally reflecting quartz glass support. The yield for many elements was nearly quantitative, reproducibilities of 3—6% were achieved in spite of the deposit not being homogeneous, and the detection limits calculated from peak-to-background ratios were typically 0.01 $\mu g\ l^{-1}$; but even with special precautions, the blank contributions increased the detection limits to 0.02—0.3 $\mu g\ l^{-1}$. Yet, Fe, Ni, Cu, Zn, Hg and Pb could be determined conveniently in seawater in this way. Knoth and Schwenke [136] similarly formed the transition metals—APDC chelates after pipetting a 100-μl sample volume onto a siliconized quartz glass support, rinsing off the unreacted material and measuring by total reflection e.d.x.r.s.; they obtained quantitative collections of numerous elements, even from 3% NaCl solutions, and detection limits at the 20 pg level (i.e., 0.2 $\mu g\ l^{-1}$).

Another promising procedure consists in chelation followed by immobilization on activated carbon, the most traditional of all adsorbents. Activated charcoal is known to be a good adsorber for organic and colloidal material, and so probably also for the species of trace metals that are bound to naturally occurring organic and colloidal matter. Free ions are not quantitatively adsorbed onto activated carbon, but addition of a chelating agent will convert them to an adsorbable form. The addition of a chelating agent and the subsequent adsorption of activated carbon should thus constitute a powerful technique for collecting both originally free and colloidal and organic trace metal species. Jackwerth et al. [137] were probably the first to exploit this idea for preconcentrations in atomic absorption spectroscopy. It has been concluded [138] that 8-quinolinol is a particularly suitable multielement chelating agent, because the chelates exhibit high stability constants at nearly natural pH levels for many transition metal ions, but not for alkali and alkaline earth ions; further, the 8-quinolinolates can be adsorbed onto activated carbon very efficiently and straightforwardly. The optimal preconcentration procedure depends somewhat on the type of water under test but consists roughly of adding 10 mg of 8-quinolinol per liter of water sample at pH 8 (either adding solid 8-quinolinol and heating the sample to 60° C, or adding a 10% 8-quinolinol solution in acetone), adding 100 mg of activated carbon after an equilibration for 30 min, and filtering off the suspension. Quantitative recoveries with enrichment factors near 10 000 were demonstrated for about 20 ions from various media independent of the alkali and alkaline earth content. When the filters loaded with 8-quinolinol/

activated carbon were examined by e.d.x.r.s. [139], the responses were linear up to 1 mg l^{-1} metal concentrations, and the reproducibility was 5%. In synthetic or natural waters containing up to 10 mg l^{-1} of humic substances, quantitative recoveries can be maintained [124], even for the trivalent ions that are strongly bound to humic matter, if sufficient activated carbon is used, i.e., if some x.r.s. sensitivity is sacrificed. The results obtained on natural waters via the 8-quinolinol chelation/activated carbon adsorption procedure are somewhat higher than those obtained by other preconcentration procedures, because collection of the naturally occurring organic and colloidal trace metal species is more complete. Although this procedure is not as simple as some other preconcentration techniques, and requires some previous knowledge of the major ion composition of the water sample (at least if optimal sensitivities are to be reached), it is considered very valuable in every case where organic or colloidal material effects could interfere with the recovery of the total transition metal concentration, and its merits were established quite well in intercomparison studies [17—19]. Recently, Johansson and Akselsson [140] used oxine or APDC chelation and activated carbon adsorption in combination with p.i.x.e. analysis to obtain typical detection limits in the range 0.02—2 μg l^{-1} for brackish and distilled water, while Fou [141] qualitatively detected trace elements in household tap water by p.i.x.e. after a, probably incomplete, direct collection in an activated charcoal filter.

ELECTRODEPOSITION

Preconcentrations by electrodeposition imply a very different approach and somewhat more sophisticated equipment. Cathodic deposition has been applied in combination with x.r.s. for preconcentrations from simple solutions. Vassos et al. [142] determined 2—40 μg of Cr, Co, Cu, Hg, Ni or Zn by constant-current electrodeposition on 1-cm diameter graphite-rod electrodes, in 15 ml of solution containing low concentrations of supporting electrolyte to simulate natural waters. Marshall and Page [143] determined Cd, Ni and Zn by e.d.x.r.s. of deposits prepared by flow electrolysis on graphite cloth electrodes, but warned that the mechanisms of the electrodeposition of alloys and metal mixtures must be studied before this approach can be generally applied in the analysis of water samples.

Wündt et al. [144] proposed a procedure for transition elements based on electrodeposition of the anionic organo-complexes from mixed organic aqueous media in a high potential electric field, and tested it on complex synthetic samples simulating river water. They first collected all cations at pH 2 on Dowex 50-W cation-exchange resin, and then eluted the anionic cyano- and oxo-complexes of transition metals with a potassium cyanide solution at pH 11 (while Ca^{2+} and Mg^{2+} remained on the resin). On addition of about a 0.8 mole fraction of 2-propanol (to increase the solute solvating power while the dielectric constant was kept low), the complexes of Co, Ni, Cu, Zn and Cd were deposited in a high potential field (300—1500 V) onto an aluminium anode. Good collection yields and detection limits around

TABLE 2

Single element preconcentration methods for x.r.s. of environmental water

Preconcentration type	Procedure	Type of water studied	Determination characteristics[a]	Ref.
Uranium				
Chelex-100 resin	Stir 60 mg resin in 1 l of water at pH 4 for 3 h, filter off, pelletize with binder and boric acid; w.d.x.r.s.	Ground water with alkaline earths and HCO_3^- (ca. 15 μg U l^{-1})	Ca-interference minimal at pH 4 s = 4% at 30 μg l^{-1} DL = 2 μg l^{-1} (100 s counting)	145
Cellulose phosphate paper	Pass 100 ml solution of pH 2.5 five times at 15 ml min^{-1} through Whatman P.81 ion-exchange paper in NH_4-form, wash; w.d.x.r.s.	Natural waters, drinking water	Linear response to 1 mg U s = 14% at 5 μg U, 6% at 10 μg U DL = 0.3 μg U if 0.5-l sample (100 s counting)	146
Silica gel powder treated with *N*-2-aminoethyl-3-amino-propyltriethoxy-silane (Fig. 1)	Heat 20 ml with HCl to destroy carbonates, add NH_4OH to pH 7, add $(NH_4)_2CO_3$ to 0.1 M, stir with 100 mg silylated silica gel for 20 min, filter off, pelletize with binder; w.d.x.r.s. and e.d.x.r.s.	Carbonate solutions (solution mining)	Linear response to 2 mg U Interference of Mo and V s = 3% at 0.08 mg U, 0.4% at 0.8 mg U, 0.22% at 1.5 mg U DL = 2.5 μg U or 0.12 ppm in 20 ml (100 s counting)	147
Silica-cellulose filter treated with *N*-2-ethyl-3-amino-propyltri-methoxysilane	Acidify the sample to pH 2, boil, neutralize, add $(NH_4)_2CO_3$, cycle 25 ml during 60 min through the 25 mm diameter silylated silica-cellulose filter, wash; direct w.d.x.r.s.	Carbonate solutions (solution mining)	Recoveries from 95 to 70% for 0.5—10 ppm U at pH 6—8 s = 3.5% DL = 5.4 μg U or 0.2 ppm in 25 ml (100 s counting)	148
Precipitation as Ba diuranate	Acidify to pH 1, boil, neutralize, add $(NH_4)_2CO_3$ to 0.002 M, bring pH to 12.3, add Ba^{2+}, filter through Ag-membrane; w.d.x.r.s.	Carbonate solutions (solution mining)	Ag-membrane enhances the U-fluorescence. Strong influence of CO_3^{2-} SO_4^{2-}, Mo and V conc. Linear reponse to 50 ppm U s = 5% at 1 ppm U, 1.4% at 50 ppm U. DL = 60 ppb U	149

Cellulose ion-exchanger Hyphan (Fig. 1)	Pass 2 l at pH 6 through Hyphan column, elute U with 25 ml 1 M HCl, neutralize, stir 30 min with 0.1 g Hyphan powder, filter off; e.d.x.r.s.	Natural and drinking water	High distribution coefficients for U Capacity: 0.5 mmol U per g Hyphan DL = 0.3 ppb U in 5 l Waters with 0.4—12 ppb U	150
Anion-exchange resin	Stir 25 ml with 1 g Amberlite IRA-400 resin for 2 h, filter off, spread the resin on a Mylar film; e.d.x.r.s.	Carbonate solutions	Quantitative recovery to 50 g l^{-1} Na_2CO_3 and 20 g l^{-1} $NaHCO_3$ DL = 5 μg U or 20 ppb in 200 ml (300 s counting)	151
Halides				
No preconcentration (for Br)	Standard additions; w.d.x.r.s.	Saline natural waters and synthetic brines	200—600 ppm Br	152
Evaporation (for Br)	Evaporate 2 l to dryness, and dry 10 mg residue with Na_2SeO_4 internal standard on filter paper; w.d.x.r.s.	River waters	10—600 μg l^{-1}	153
Direct measurement of Ag remaining in solution after precipitation (for Cl, Br, I)	Add Ag^+ (and Cd^{2+} internal standard) to 50 ml sample, stir, centrifuge off the AgCl (+ AgBr + AgI); direct w.d.x.r.s. of Ag remaining in solution	Natural and waste waters	1—5 ppm Cl^- s = 10% for a few ppm Cl, 2% for high levels	154
No preconcentration (for Br)	Direct w.d.x.r.s. in liquid specimen cell; use ratio of Br-K_α to background as measure for Br	Sea water, lake water, synthetic solutions	No interference of 5% NaCl and 2% $MgCl_2$. Accuracy 2% or better, down to 10 ppm Br	155
Coprecipitation with AgSCN (for Cl)	Add NH_4SCN and $AgNO_3$ to 50-ml sample at pH 5, stir for 10 min, filter off; w.d.x.r.s. measurement of Cl-K_α/S-K_α ratio	Drinking water	10^{-5}—10^{-4} M. s = 3% at 4 ppm	156
Precipitation with $AgNO_3$ (for Cl, Br, I)	Add $AgNO_3$, filter off; w.d.x.r.s.	Water samples	Linear response for 0—100 μg DL $\leqslant$ 0.2 ppm (40 s counting)	157

TABLE 2 (continued)

Preconcentration type	Procedure	Type of water studied	Determination characteristics[a]	Ref.
No preconcentration (for Br and Cl)	Direct w.d.x.r.s. under He flux after Se internal standard addition (for Br) or after Ba addition to precipitate interfering anions (for Cl)	Natural waters and brines	(Precipitation with Ag^+ or evaporation are unsatisfactory.) Considerable interference on Br and Cl by NaCl, Ca^{2+}, Mg^{2+}, Sr^{2+}, K^+, if no internal standard is used; linear response for 0.6—100 ppm Br with Se internal standard. Considerable interference on Cl from SO_4^{2-}, HCO_3^- and CO_3^{2-} Linear response for 0.05—150 $\mu g\ l^{-1}$ Cl after Ba^{2+} addition to precipitate interferences; s = 1%	158
Anion filter paper (for Br)	Pass 40-ml sample 7 times through three SB-2 anion-exchange papers at high pH; w.d.x.r.s.	Natural waters and brines	Linear response for 0.06—1 ppm Br	158
Precipitation with La^{3+} and Pd^{2+} (for F and I, respectively)	Add to 200—500 ml sample 60 mg $La(NO_3)_3$ and 40 mg $Pd(NO_3)_2$, adjust to pH 2.8, heat for 35 min, filter LaF_3 and PdI_2 mixture. E.d.x.r.s. of La-L_α (for F) and I-K_α (for I)	Geothermal waters	Of all investigated components only PO_4^{3-} interferes with F^- and excesses of S^{2-} and $S_2O_3^{2-}$ with I^- s = 4% DL = 0.2 ppm I^- and 4 ppm F^-	159
Precipitation with Ag^+ and adsorption on activated carbon (for I)	Add 150 mg activated carbon and 200 μg Ag^+ to 60 ml (pH 1), stir for 1 min, filter; w.d.x.r.s.	Ground water	Dilution necessary for concs. >10 ppm. No interferences of $S_2O_3^{2-}$, SCN^- and NH_4^+ in realistic ground water samples s = 8% at 1 ppm level DL = 0.12 ppm for 60 ml	161

Sulphur				
Direct measurement of Ba^{2+} in solution after precipitation (for SO_4^{2-})	Add Ba^{2+} (and Cs^+ internal standard) to 50-ml sample, stir, centrifuge; direct w.d.x.r.s. of Ba remaining in solution	Natural and waste waters	2-120 ppm SO_4^{2-} s = 10% for a few ppm SO_4^{2+}, 2% for high levels	154
Exchange reaction on thin silver halide layers (for S^{2-})	Add 400 mg EDTA per l of sample (stabilized with Zn^{2+}) at pH 4, stir 1 h, filter through AgI or AgCl layer (containing 300 μg Ag); wash filter with water; w.d.x.r.s.	Environmental and drinking water	Sulfide is stabilized with Zn^{2+} for if immediate analysis is not possible. Procedure optimized with respect to pH, temperature, filtration rate, deposit thickness. Interferences of Hg^{2+}, Sn^{2+}, CrO_4^{2-}, $S_2O_3^{2-}$, SO_3^{2-} and AsO_3^{3-}; other interferences eliminated by EDTA-masking or buffering. Applicable in the ppb and ppm range; 1—18 μg S^{2-} l^{-1} found in river waters. DL = 0.1 μg S (ca. 200 s counting) s = 2.3% at 10 μg	162
No preconcentration (for SO_4^{2-} and SO_3^{2-})	Direct w.d.x.r.s. in liquid sample cell under atmospheric pressure; S—K_α to scatter background ratio is used as a measure for S-content	Seawater	No interference of NaCl. Results compare well with gravimetry s = 1% at 900 ppm S	163
Coprecipitation with $BaCrO_4$ (for SO_4^{2-})	Add K_2CrO_4 and $BaCl_2$ to unacidified 50—100 ml sample, stir for 10 min, filter off; w.d.x.r.s. of S—K_α/Cr—K_α ratio	Drinking water	Applicable at 10^{-5}—10^{-4} M level s = 4% at 15 ppm SO_4^{2-} level	156
No preconcentration	Direct radioisotope-excited vacuum e.d.x.r.s. of 4 ml in liquid sample cell	Mineral water	No interference of NaCl. DL = 30 ppm (1 h counting) s = 1.5% at 3500 ppm	164

TABLE 2 (continued)

Preconcentration type	Procedure	Type of water studied	Determination characteristics[a]	Ref.
Selenium Coprecipitation with APDC	Add to 500 ml water of pH 4 100 mg APDC (and 200 μg Fe^{3+} carrier if Fe conc. <400 ppb), stir for 30 min, filter; radioisotope-excited e.d.x.r.s.	Environmental water	Linear range 4—100 ppb DL = 0.6 ppb (2000 s counting) s = 4.1% at 10 ppb	165
Reduction with ascorbic acid, adsorption of Se on activated carbon (selective for SeO_3^{2-})	Add to 1 h sample of pH 2 some 3 g ascorbic acid and 100 mg activated carbon, stir for 15 min, filter; e.d.x.r.s.	River, lake, ground and drinking water, sea water, rain	Procedure optimized with respect to pH, reagent concs. and type, and reaction time. No influence of various salts, humic material and SeO_4^{2-}. Linear range 0.05—50 ppb s = 6% at 0.5 ppb. DL = 0.05 ppb SeO_3^{2-} (3000 s counting) Procedure applied in environmental screening [168], in the range 0.05—2 ppb Se(IV)	166
Reduction by thourea/H_2SO_4 refluxing, adsorption of Se on activated carbon (for total dissolved Se)	Add to 1 l water: 50 ml H_2SO_4, 1 g thiourea and 100 mg activated carbon, reflux for 15 min, filter; e.d.x.r.s.	River, lake, ground and drinking water, sea water, rain	Procedure optimized with respect to all reduction reaction parameters. No influence of sample salinity, Fe^{3+} and humic material. Linear range 0.06—10 ppb for SeO_4^{2-} and SeO_3^{2-}. s = 25% at 0.1 ppb, 11% for 0.1—1 ppb, 5% for 1—25 ppb, 3% for 100 ppb Se DL = 0.06 ppb Se (3000 s counting) Procedure applied in environmental screening [168], in the range 0.06—2 ppb Se	167

Chromium				
Chelex-100 resin (for Cr^{3+} and after reduction for total dissolved Cr)	Add triethanolamine buffer and 200 mg Chelex-100 resin to the sample, stir for 30 min, filter, pelletize; w.d.x.r.s. (for Cr^{3+}). Reduce CrO_4^{2-} to Cr^{3+} by boiling for 5 min with 50 mg $NaHSO_3$, then as above (for total dissolved Cr)	Aqueous samples	Procedure optimized for pH, reagent conc. and reaction conditions. s = 1% for 50 μg Cr^{3+}, 3% for 50 μg total Cr	169
Coprecipitation with Fe^{3+} (for Cr^{3+})	Add 100 μg Fe^{3+} to 100 ml water, bring pH to 8.5, filter after 1 h; w.d.x.r.s.	Estuarine water	No influence of CrO_4^{2-}, NaCl or other components at realistic levels. Linear response to 100 ppb. s = 6% at 1 ppb, 2% at 10 ppb 1% at 100 ppb DL = 0.1 ppb (100 s counting)	170
Coprecipitation with APDC + Co^{2+} (for CrO_4^{2-}, after Cr^{3+} separation)	To the eluate of above procedure brought to pH 4, add 100 μg Co^{2+} and 20 mg ADPC, filter after 1 h; w.d.x.r.s.	Estuarine water	No significant interferences. Linear reponse up to 100 ppb s = 7% at 1 ppb, 3% at 10 ppb, 1% at 100 ppb DL = 0.1 ppb (100 s counting)	170
Phosphorus				
Extraction of molybdophosphoric acid and absorption on silylated silica gel (for PO_4^{3-})	Bring 50-ml sample to pH 1, add 250 mg $Na_2MoO_4 \cdot 2H_2O$, stir, extract with 10 ml ethyl acetate. Add 10 ml water to the extract, stir, add 10 mg silica gel silylated with N-β-amino-ethyl-γ-aminopropyl-triethoxysilane, filter and pelletize with cellulose; w.d.x.r.s. for Mo—K_α	Natural waters	Positive interference of AsO_4^{2-} but not silicate s = 3% at 15 ppb Linear response to 3 ppm	171
Potassium				
Precipitation with tetraphenylborate	To a 2—5 ml water sample, add NH_4^+ as carrier, adjust to pH 2—4, add Na-tetraphenylborate, stir, filter; vacuum e.d.x.r.s.	Aqueous samples	If an excess of NH_4^+ is present, decompose by heating. Applicable for 0.1—1000 μg K s = 0.1% for 1000 μg to 5% for 0.1 μg K	172

TABLE 2 (continued)

Preconcentration type	Procedure	Type of water studied	Determination characteristics[a]	Ref.
Iron				
Evaporation on chromatographic paper	Spot 0.5 ml of two-fold diluted sample spiked with Cr as internal standard on Whatman 3 MM chromatographic paper disc; dry; w.d.x.r.s.	Polluted stream water	Linear response to 400 ppm s = 8% at 100 ppm DL = 5 ppm (100 s counting)	173
Nickel				
Sorption on naphthalene powder with 1-(2-thiazolylazo)-2-naphthol	To a sample buffered at pH 6.9, add 2 g of naphthalene homogeneously doped with 4 mg 1-(2-thiazolylazo)-2-naphthol, stir, filter, pelletize; x.r.s.	Water samples	Quantitative collection of 10 μg Ni from 200 ml water Linear response for 0—18 μg Ni	174
Arsenic				
Gutzeit method	Add 5 ml H_2SO_4 and 10 g Zn powder to 100 ml sample, capture evolving hydride on $AgNO_3$ test paper, w.d.x.r.s.	Water samples	Reaction parameters optimized Linear responses to 50 μg s = 4% at 10 μg	175
Molybdenum				
Chelation by tetramethylenedithiocarbamate and adsorption on activated carbon	Add acetate buffer and 300 mg NH_4-tetramethylenedithiocarbamate to 2 l sample; pass in 20 min through layer of 20 mg activated carbon on filter carrier, dry; w.d.x.r.s.	Sea water	Quantitative recovery for 25 ppb Risk of losses on container walls Results of 3.6 ppb in sea water	176

Barium				
Cation-exchange paper, after chemical separations	Add $Pb(NO_3)_2$ and hexamine to 1 l sample, adjust pH to 5.5, add $K_2Cr_2O_7$, filter after 12 h. Dissolve precipitate of $BaCrO_4$ and $PbCrO_4$, add 1,2-diaminocyclohexanetetra-acetic acid to mask Pb^{2+}, cycle 5 times through an SA-2 cation-exchange paper; w.d.x.r.s.	Mineral water and sea water	No interference of Ca^{2+} Linear response to 10 ppm Ba s = 2% at 1 ppm DL = 10 ppb (100 s counting)	177
Mercury				
Anion-exchange paper	To 50 ml sample, add HCl to 0.2 M to form $HgCl_4^{2-}$; cycle 10 times through SB-2 anion-exchange paper; w.d.x.r.s.	Water samples	No significant interferences noted. About 65% recovery of organic Hg following u.v. irradiation or Cl_2 oxidation s = 3.8% at 1 ppm Hg DL = 20 ppb (100 s counting)	178

[a] s is standard deviation per measurement; DL is the limit of detection.

1 $\mu g\ l^{-1}$ were claimed. It is clear that the various reagent additions imply serious contamination risks, and that the environmental applicability of this approach requires further demonstration.

PRECONCENTRATIONS OF SINGLE ELEMENTS

In view of its inherent selectivity, x.r.s. is naturally most appropriate for multi-element determinations. Yet it can, of course, be used as a detection method after a highly selective preconcentration for determinations of single elements. Many such examples are available in the literature for various fields of application.

The literature pertaining to applications of x.r.s. in water analysis for a single element or only two elements simultaneously is summarized in Table 2. The detail in the summary reflects to some extent the degree of detail in the original publication. Of course, many x.r.s. procedures for various matrices often also pass through a dissolution step and an aqueous phase. In Table 2, however, only those methods are included that deal directly with natural waters, or were developed for the purpose of water analyses, or pertain to concentration levels that are realistic in some waters.

It appears, not unexpectedly, that most of these single-element procedures have been proposed for uranium assays. Also, several references are available for the halides, for sulphur, selenium and chromium species, and for a few other ions. The characteristics of these procedures, as included in Table 2, allow a relative evaluation in each particular case.

CONCLUSION

It must be emphasized that this literature review did not reveal any panacea for preconcentration prior to x.r.s. in water analysis. Indeed, no method is simultaneously extremely sensitive, applicable over an infinite concentration range, free of interference and matrix effects, capable of determining all elements in their different oxidation states and chemical speciations, and very simple, fast and economic. Moreover, a method of choice cannot be selected in a straightforward way, because too much depends on the type and variability of samples, on the number and concentration of elements to be assayed, and on the relative importance that one attributes to speed, quality and cost of the analysis.

Mainly because of the confusion, size and complexity of the literature, many research laboratories are now seen to embark on developing a preconcentration procedure of their own rather than applying or adapting a published method. It is hoped that the present wide review will be of some help to the analytical chemist who has to make an intelligent selection of a preconcentration method when faced with application of x-ray spectrometry to water samples.

REFERENCES

1 E. Jackwerth, A. Mizuike, Y. A. Zolotov, H. Berndt, R. Höhn and N. M. Kuzmin, Pure Appl. Chem., 51 (1979) 1105.
2 R. van Grieken, K. Bresseleers, J. Smits, B. Vanderborght and M. Vanderstappen, Adv. X-ray Anal., 19 (1976) 435.

3 T. Florkowski, B. Holynska and J. Niewodniczanski in Nuclear Techniques in Environmental Pollution, International Atomic Energy Agency, Vienna, 1971, p. 335.
4 M. A. Kalam, A. Hussam, M. Kahliquzzaman, A. H. Kahn, M. M. Islam, M. B. Zaman and M. Husain, J. Radioanal. Chem., 46 (1978) 285.
5 J. G. Dick, C. C. Wan and R. Difruscia, X-Ray Spectrom., 6 (1977) 212.
6 P. Clechet, G. Eschalier, J. Jose and C. Michou-Sauchet, Analusis, 5 (1977) 49.
7 J. R. Cann and C. K. Winter, Mar. Geol., 11 (1971) M33.
8 V. Subramanian, and B. F. d'Anglejan, Mar. Geol., 22 (1976) M1.
9 E. R. Sholkovitz, R. Van Grieken and D. Eisma, Neth. J. Sea Res., 12 (1978) 407.
10 T. Florkowski and B. Holynska, Radiochem. Radioanal. Lett., 11 (1972) 229.
11 M. Vanderstappen and R. Van Grieken, Fresenius Z. Anal. Chem., 282 (1976) 25.
12 J. M. Martin, A. J. Thomas and R. Van Grieken, Neth. J. Sea Res., 12 (1978) 414.
13 K. M. Varier, G. K. Mehta and S. Sen, Nucl. Instrum. Methods, 181 (1981) 217.
14 Y. Hashimoto, Y. Osada, S. Tanaka, R. Chiba and H. Yokota, Nucl. Instrum. Methods, 181 (1981) 227.
15 W. C. Burnett and G. T. Mitchum, Nucl. Instrum. Methods, 181 (1981) 231.
16 S. Monaro, R. Lecomte, P. Paradis, S. Landsberger and G. Desaulniers, Nucl. Instrum. Methods, 181 (1981) 239.
17 J. Smits, J. Nelissen and R. Van Grieken, Anal. Chim. Acta, 111 (1979) 215.
18 D. E. Leyden, W. Wegscheider, W. B. Bodnar, E. D. Sexton and W. K. Nonidez, in J. Albaiges (Ed.), Proc. Int. Congress on Analytical Techniques in Environmental Chemistry, Pergamon Press, Oxford, 1980, p. 469.
19 D. E. Leyden, W. Wegscheider and W. B. Bodnar, Int. J. Environ. Anal. Chem., 7 (1979) 85.
20 D. E. Leyden, W. B. Bodnar, W. Wegscheider, B. B. Jablonski and A. T. Ellis, Abstracts of the 12th Annual Symposium on the Analytical Chemistry of Pollutants, Amsterdam, April, 1982, p. 36; Anal. Chim. Acta, in press.
21 K. Haberer, Jahrbuch Vom Wasser, 32 (1965) 128.
22 H. Meier, E. Unger, W. Albrecht, D. Bösche, W. Hecker, P. Menge, G. Zeitler and E. Zimmerhackl, Mikrochim. Acta, (I) (1975) 505.
23 J. Cornil and G. Ledent, Analusis, 3 (1975) 11.
24 K. Fenkart, E. Eng and U. Frey, Fresenius Z. Anal. Chem., 293 (1978) 364.
25 P. Van Dyck, Ph.D. Thesis, University of Antwerp (UIA), Wilrijk, Belgium, 1982.
26 F. A. Rickey, K. Mueller, P. C. Simms and B. D. Michael in, T. G. Dzubay (Ed.), X-ray Fluorescence Analysis of Environmental Samples, Ann Arbor Science Publishers, Ann Arbor, MI, 1977, p. 135.
27 P. C. Simms and F. A. Rickey, The Multielemental Analysis of Drinking Water using Proton-induced X-ray Emission, EPA Report 600/1-78-058, NTIS, Springfield, VA, 1978, p. 49.
28 M. E. Alexander, E. K. Biegert, J. K. Jones, R. S. Thurston, V. Valkovic, R. M. Wheeler, C. A. Wingate and T. Zabel, Int. J. Appl. Radiat. Isot., 25 (1974) 229.
29 K. C. Chan, B. L. Cohen, J. O. Frohliger and L. Shabason, Tellus, 28 (1976) 24.
30 R. Hight and C. C. Foster, Adv. X-Ray Anal., 18 (1975) 333.
31 Y.-C. L. Lien, R. R. Zombola and R. C. Bearse, Nucl. Instrum. Methods, 146 (1977) 609.
32 S. Tanaka, M. Darzi and J. W. Winchester, Environ. Sci. Technol., 15 (1981) 354.
33 A. Pape, J. C. Sens, P. Fintz, A. Gallmann, H. E. Gove, G. Guillaume and D. M. Stupin, Nucl. Instrum. Methods, 105 (1972) 161.
34 P. Sioshansi, A. S. Lodhi and H. Payrovan, Nucl. Instrum. Methods, 142 (1977) 285.
35 G. Robaye, G. Weber, J. M. Delbrouck-Habaru, M. C. Depauw and I. Roelandts, Nucl. Instrum. Methods, 172 (1980) 535.
36 H. G. Pfeiffer and P. D. Zemany, Nature, 174 (1954) 397.
37 E. J. Felten, I. Fankuchen and J. Steigman, Anal. Chem., 31 (1959) 1771.
38 G. Ackermann, R.-K. Koch, H. Ehrhardt and G. Janner, Talanta, 19 (1972) 293.
39 J. C. Johnson and B. E. Nagel, Mikrochim. Acta, (1963) 525.
40 J. Smits and R. Van Grieken, Anal. Chim. Acta, 88 (1977) 97.

41 R. D. Giauque, R. B. Garrett and L. Y. Goda, in T. G. Dzubay (Ed.), X-ray Fluorescence Analysis of Environmental Samples, Ann Arbor Science Publishers, Ann Arbor, MI, 1977, p. 153.
42 D. C. Camp, J. A. Cooper and J. R. Rhodes, X-ray Spectrom., 3 (1974) 47.
43 H. P. M. Kivits, F. A. J. De Rooij and G. P. J. Wijnhoven, Nucl. Instrum. Methods, 164 (1979) 225.
44 A. L. Allen and V. C. Rose, Adv. X-ray Anal., 15 (1972) 534.
45 R. Cesareo, S. Sciuti and G. E. Gigante, Int. J. Appl. Radiat. Isot., 27 (1976) 58.
46 M. Murata and M. Noguchi, Anal. Chim. Acta, 71 (1974) 295.
47 T. Florkowski, B. Holynska and S. Piorek, in Measurement, Detection and Control of Environmental Pollutants, International Atomic Energy Agency, Vienna, 1976, p. 213.
48 F. Clanet and R. Deloncle, Anal. Chim. Acta, 117 (1980) 343.
49 F. Clanet, R. Deloncle and G. Popoff, Analusis, 9 (1981) 276.
50 F. Clanet, R. Deloncle and G. Popoff, Water Res., 15 (1981) 591.
51 D. E. Leyden, T. A. Patterson and J. J. Alberts, Anal. Chem., 47 (1975) 733.
52 P. Burba and K. H. Lieser, Fresenius Z. Anal. Chem., 286 (1977) 191.
53 K. H. Lieser, E. Breitwieser, P. Burba, M. Röber and R. Spatz, Mikrochim. Acta, (I) (1978) 363.
54 P. Burba, K. H. Lieser, V. Neitzert and H. M. Röber, Fresenius Z. Anal. Chem., 291 (1978) 273.
55 K. H. Lieser, P. Burba, W. Calmano, W. Dyck, E. Heuss and S. Sondermeyer, Mikrochim. Acta, (II) (1980) 445.
56 P. Burba, Fresenius Z. Anal. Chem., 306 (1981) 233.
57 D. E. Leyden, in T. G. Dzubay (Ed.), X-ray Fluorescence Analysis of Environment Samples, Ann Arbor Science Publishers, Ann Arbor, MI, 1977, p. 145.
58 D. E. Leyden and G. H. Luttrell, Anal. Chem., 47 (1975) 1612.
59 D. E. Leyden, G. H. Luttrell, W. K. Nonidez and D. B. Werho, Anal. Chem., 48 (1976) 67.
60 D. E. Leyden, G. H. Luttrell, A. E. Sloan and N. J. De Angelis, Anal. Chim. Acta, 84 (1976) 97.
61 K. Hirayama and N. Unohara, Bunseki Kagaku, 29 (1980) 452.
62 T. M. Florence and G. E. Batley, Talanta, 23 (1976) 179.
63 M. I. Abdullah, O. A. El-Rayis and J. P. Riley, Anal. Chim. Acta, 84 (1976) 363.
64 D. T. Carlton and J. C. Russ, X-ray Spectrom., 5 (1976) 172.
65 W. T. Grubb and P. D. Zemany, Nature, 176 (1955) 221.
66 W. J. Campbell, E. F. Spano and T. E. Green, Anal. Chem., 38 (1966) 987.
67 W. J. Campbell, T. E. Green and S. L. Law, Am. Lab., June (1970) 28.
68 S. L. Law and W. J. Campbell, Adv. X-ray Anal., 17 (1973) 279.
69 S. N. Ndam and V. C. Rose, Engineerings, XLIV (1968) 2.
70 C. J. Toussaint, G. Aina and J. Broothaerts, in Report EUR-5060, Joint Research Centre, Ispra, Italy, Annual Report 1972, p. 376.
71 M. B. Blasius, S. J. Kerkhoff, R. S. Wright and C. R. Cothern, Water Resour. Bull., 8 (1972) 704.
72 P. G. Burkhalter, Report NRL 7637, Naval Research Laboratory, Washington, D.C., 1973, 18 pp.
73 A. Robert and R. Valles, Radiochem. Radioanal. Lett., 15 (1973) 279.
74 B. Holynska, M. Leszko and E. Nahlik, J. Radioanal. Chem., 13 (1973) 401.
75 D. B. Lister, Anal. Instrum., 13 (1975) 143.
76 F. C. Smith Jr. and O. H. Masi, Adv. X-ray Anal., 19 (1976) 449.
77 C. J. Toussaint, G. Aina and F. Bo, Anal. Chim. Acta, 88 (1977) 193.
78 P. Clechet and G. Eschalier, Proc. 4th Int. Colloquium on Anal. Methods using X-rays, Strasbourg, France, May 1977, p. 205.
79 M. M. Ulrich and P. K. Hopke, Res./Dev., 28 (1977) 34.
80 R. Cesareo and G. E. Gigante, Water, Air Soil Pollut., 9 (1978) 99.
81 H. Kingston and P. A. Pella, Anal. Chem., 53 (1981) 223.
82 C. H. Lochmüller, J. W. Galbraith and R. L. Walter, Anal. Chem., 46 (1974) 440.

83 R. E. Van Grieken, C. M. Bresseleers and B. M. Vanderborght, Anal. Chem., 49 (1977) 1326.
84 K. H. Lieser, H.-M. Röber and P. Burba, Fresenius Z. Anal. Chem., 284 (1979) 361.
85 P. Burba and K. H. Lieser, Fresenius Z. Anal. Chem., 297 (1979) 374.
86 G. Gendre, W. Haerdi, H. R. Linder, B. Schreiber and R. W. Frei, Int. J. Environ. Anal. Chem., 5 (1977) 63.
87 A. Disam, P. Tschöpel and G. Tölg, Fresenius Z. Anal. Chem., 295 (1979) 97.
88 J. Smits and R. Van Grieken, Angew. Makromol. Chem., 72 (1978) 105.
89 J. A. Smits and R. E. Van Grieken, Anal. Chem., 52 (1980) 1479.
90 J. Smits and R. Van Grieken, Anal. Chim. Acta, 123 (1981) 9.
91 J. Smits and R. Van Grieken, Int. J. Environ. Anal. Chem., 9 (1981) 81.
92 G. Smiricz, Siemens Review XXXIX, 6th Special Issue, X-ray and Electron Microscopy News, 1972, p. 7.
93 A. J. Ellgren, Union Carbide Technical Memorandum, TTC-41, 1974.
94 C. L. Luke, Anal. Chim. Acta, 41 (1968) 237.
95 H. Watanabe, J. Berman and D. S. Russell, Talanta, 19 (1972) 1363.
96 B. Holynska and K. Bisiniek, J. Radioanal. Chem., 31 (1976) 159.
97 N. Moriyama, K. Kimata and S. Andou, Adv. X-ray Anal. Jpn., 5 (1973) 93.
98 H. Sasuga, A. Abe, T. Nakamura, E. Asada and T. Aota, Adv. X-ray Anal. Jpn., 8 (1976) 79.
99 T. Tanoue, H. Nara and S. Yamaguchi, Adv. X-ray Anal. Jpn., 11 (1979) 81.
100 K. Hirokawa, Adv. X-ray Anal. Jpn., 12 (1980) 51.
101 J. E. Kessler and S. M. Vincent, Pittsburgh Conf. on Anal. Chem. and Appl. Spectrosc., March 1972, paper 70.
102 C. J. Toussaint and R. Boniforti, Int. J. Environ. Anal. Chem., 6 (1979) 217.
103 H. Hellmann and A. Griffatong, Fresenius Z. Anal. Chem., 257 (1971) 343.
104 A. Knöchel and A. Prange, Fresenius Z. Anal. Chem., 306 (1981) 252.
105 J. F. Elder, S. K. Perry and F. P. Brady, Environ. Sci. Technol., 9 (1975) 1039.
106 H. Meier and E. Unger, J. Radioanal. Chem., 32 (1976) 413.
107 A. H. Pradzynski, R. E. Henry and J. S. Stewart, J. Radioanal. Chem., 32 (1976) 219.
108 A. H. Pradzynsky, R. E. Henry and E. L. Draper, Jr., Proc. ERDA. Symp. X- and Gamma-ray Sources and Applications, Ann Arbor, MI, May, 1976, p. 175.
109 T. Tanoue, H. Nara and S. Yamaguchi, Adv. X-ray Anal. Jpn., 11 (1979) 69.
110 S. Brüggerhoff, E. Jackwerth, B. Raith, A. Stratmann and B. Gonsior, Fresenius Z. Anal. Chem., 311 (1982) 252.
111 S. Takemoto, H. Kitamura, Y. Kuge, S. Nakagawa, K. Murata and S. Ikeda, Bunseki Kagaku, 25 (1976) 40.
112 E. Scheubeck, Ch. Jörrens and H. Hoffmann, Fresenius Z. Anal. Chem., 303 (1980) 257.
113 E. Scheubeck, Mikrochim. Acta, (II) (1980) 283.
114 H. R. Lindner, H. D. Seltner and B. Schreiber, Anal. Chem., 50 (1978) 896.
115 I. Watanabe and Y. Kose, Adv. X-ray Anal. Jpn., 12 (1980) 55.
116 R. Panayappan, D. L. Venezky, J. V. Gilfrich and L. S. Birks, Anal. Chem., 50 (1978) 1125.
117 C. Bergerioux and W. Haerdi, Analusis, 8 (1980) 169.
118 R. Püschel, Talanta, 16 (1969) 351.
119 M. Vanderstappen and R. E. Van Grieken, Talanta, 25 (1978) 653.
120 L. Van't dack, unpublished results.
121 E. Bruninx and E. van Meyl, Anal. Chim. Acta, 80 (1975) 85.
122 E. Bruninx, A. van Eenbergen and A. Schouten, Anal. Chim. Acta, 109 (1979) 419.
123 R. Chakravorty and R. Van Grieken, Int. J. Environ. Anal. Chem., 11 (1982) 67.
124 B. M. Vanderborght and R. E. Van Grieken, Int. J. Environ. Anal. Chem., 5 (1978) 221.
125 K. Hirokawa, Fresenius Z. Anal. Chem., 260 (1972) 4.
126 H. Watanabe and T. Ueda, Bull. Chem. Soc. Jpn., 53 (1980) 411.
127 F. A. J. Armstrong, P. M. Williams and J. D. H. Strickland, Nature, 30 (1966) 481.
128 K. Bächmann, CRC Crit. Rev. Analyt. Chem., 12 (1981) 1.
129 F. J. Marcie, Environ. Sci. Technol., 1 (1967) 164.
130 K. Iwasaki, K. Tanaka and N. Takagi, Bunseki Kagaku, 23 (1974) 1179.

131 T. Kuroha and S. Shibuya, Bunseki Kagaku, 17 (1968) 801.
132 B. Magyar and F. I. Lobanov, Talanta, 20 (1973) 55.
133 A. Kawase, S. Nakamura and N. Fudagawa, Bunseki Kagaku, 30 (1981) 229.
134 G. Knapp, B. Schreiber and R. W. Frei, Anal. Chim. Acta, 77 (1975) 293.
135 A. Knöchel and A. Prange, Mikrochim. Acta, (II) (1980) 395.
136 J. Knoth and H. Schwenke, Fresenius Z. Anal. Chem., 294 (1979) 273.
137 E. Jackwerth, J. Lohmer and G. Wittler, Fresenius Z. Anal. Chem., 266 (1973) 1.
138 B. M. Vanderborght and R. E. Van Grieken, Anal. Chem., 49 (1977) 311.
139 B. Vanderborght, J. Verbeeck and R. Van Grieken, Bull. Soc. Chim. Belg., 86 (1977) 23.
140 E. M. Johansson and K. R. Akselsson, Nucl. Instrum. Methods, 181 (1981) 221.
141 C.-M. Fou, Nucl. Instrum. Methods, 186 (1981) 599.
142 B. S. Vassos, R. F. Hirsch and H. Letterman, Anal. Chem., 45 (1973) 792.
143 H. Marshall and J. A. Page, Spectrochim. Acta, Part B, 33 (1978) 795.
144 K. Wündt, H. Duschner and K. Starke, Anal. Chem., 51 (1979) 1487.
145 L. R. Hathaway and G. W. James, Anal. Chem., 47 (1975) 2035.
146 P. Minkkinen, Finn. Chem. Lett., (1977) 134.
147 B. B. Jablonski and D. E. Leyden, Adv. X-ray Anal., 21 (1978) 59.
148 J. T. Cronin and D. E. Leyden, Int. J. Environ. Anal. Chem., 6 (1979) 255.
149 B. B. Jablonski and D. E. Leyden, Anal. Chem., 51 (1979) 681.
150 P. Burba, B. Gleitsmann and K. H. Lieser, Fresenius Z. Anal. Chem., 289 (1978) 28.
151 H. Feldstein and I. Gilath, J. Radioanal. Chem., 57 (1980) 47.
152 H. J. Rose, Jr. and F. Cuttitta, Adv. X-ray Anal., 11 (1968) 23.
153 O. Erämetsä and M. Särkkä, Suom. Kemistil., B43 (1970) 4.
154 A. Heres, O. Girard-Devasson, J. Gaudet and J.-C. Spuig, Analusis, 1 (1976) 408.
155 Y. Deutsch, Anal. Chem., 46 (1974) 437.
156 B. Magyar and G. Kaufmann, Talanta, 22 (1975) 267.
157 M. Yasuno, Adv. X-ray Anal. Jpn., 10 (1978) 87.
158 M.-C. Sichere, F. Cesbron and G.-M. Zuppi, Anal. Chim. Acta, 98 (1978) 299.
159 Y. Buelens, M.Sc. Thesis, Department of Chemistry, University of Antwerp (U.I.A.), 1977.
160 R. Van Grieken, R. Gijbels, W. Blommaert, R. Vandelannoote and L. Van't dack in Nuclear Methods in Environmental Research, CONF-771072, NTIS, U.S. Dept. of Commerce, Springfield, VA, 1977, p. 368.
161 P. T. Howe, Report AECL-6444, Atomic Energy of Canada Ltd., 1980, p. 11.
162 P. Tschöpel, A. Disam, V. Kriváň and G. Tölg, Fresenius Z. Anal. Chem., 271 (1974) 106.
163 S. A. Gallo, D. L. Taylor and H. Zeitlin, Int. J. Environ. Anal. Chem., 3 (1974) 317.
164 S. M. Al-Jobori, S. Szegedi and A. Pazsit, Radiochem. Radioanal. Lett., 30 (1977) 45.
165 A. H. Pradzynski, R. E. Henry and J. L. S. Stewart, Radiochem. Radioanal. Lett., 21 (1975) 277.
166 H. Robberecht, R. Van Grieken and H. A. Van der Sloot, in J. Albaiges (Ed.), Analytical Techniques in Environmental Chemistry, Pergamon Press, Oxford, 1980, p. 463.
167 H. J. Robberecht and R. E. Van Grieken, Anal. Chem., 52 (1980) 449.
168 H. Robberecht, R. Van Grieken, D. Vanden Berghe, M. Van Sprundel and H. Deelstra, Sci. Total Environ., in press.
169 D. E. Leyden, R. E. Channell and C. W. Blount, Anal. Chem., 44 (1972) 607.
170 A. J. Pik, J. M. Eckert and K. J. Williams, Anal. Chim. Acta, 124 (1981) 351.
171 D. E. Leyden, W. K. Nonidez and P. W. Carr, Anal. Chem., 47 (1975) 1449.
172 H. Menke, Fresenius Z. Anal. Chem., 296 (1979) 32.
173 S. L. Tackett and M. A. Brocious, Anal. Lett., 2 (1969) 649.
174 T. Fujinaga, M. Satake and J. Miura, Talanta, 26 (1979) 964.
175 K. Kato and M. Murano, Bunseki Kagaku, 22 (1973) 1312.
176 H. Monien, R. Bovenkerk, K. P. Kringe and D. Rath, Fresenius Z. Anal. Chem., 300 (1980) 363.
177 P. Clechet and G. Eschalier, Analusis, 9 (1981) 125.
178 P. Clechet, G. Eschalier, C. Rampon and C. Vallouy, Analusis, 5 (1977) 366.

Analytica Chimica Acta, 143 (1982) 35—44
Elsevier Scientific Publishing Company, Amsterdam — Printed in The Netherlands

COMPUTER-ASSISTED STRUCTURE—CARCINOGENICITY STUDIES ON POLYNUCLEAR AROMATIC HYDROCARBONS BY PATTERN RECOGNITION METHODS
The Role of the Bay and L-Regions

YOSHIKATSU MIYASHITA, YOSHIMASA TAKAHASHI, SHIN-ICHI DAIBA, HIDETSUGU ABE and SHIN-ICHI SASAKI*

School of Materials Science, Toyohashi University of Technology, Tempaku, Toyohashi, Aichi 440 (Japan)

(Received 29th March 1982)

SUMMARY

Computer-assisted studies of structure—carcinogenicity relations for unsubstituted polynuclear aromatic hydrocarbons (PAHs) are described. On the basis of the bay and the K- and L-region theories, the carcinogenic process for each PAH is expressed by multi-dimensional descriptors. Factor analysis is used to group these descriptors. Descriptors grouped by the method were found to be useful in understanding the physicochemical properties related to the carcinogenic process, and both the L-region and the bay region were shown to play important roles in the explanation of the carcinogenicity of PAHs.

Several theoretical studies of the carcinogenic properties of polynuclear aromatic hydrocarbons (PAHs) have been reported. The K- and L-region theory, by Pullman and Pullman [1], is an early representative. However, Scribner [2] pointed out that not only the reactivity of the parent PAH but also its transport and metabolic processes to yield an ultimate carcinogen must be considered in explaining the carcinogenesis. On the basis of studies of the metabolism of PAHs [3, 4], Jerina et al. [5, 6] proposed the bay region theory. This theory postulates that for a given PAH a carbocation which forms part of a bay region that is typified by the hindered region between the 1- and 12-positions in benz[a]anthracene should be the most mutagenic and carcinogenic. In PAHs, the bay region is the terminal ring consisting of an A-region which is the presumptive initial epoxidation site and a B-region which is the final epoxidation site. The metabolic pathway is shown in Fig. 1. On the basis of this theory, the relations between the reactivities of these metabolites and their carcinogenicities have been studied by Smith et al. [7]; the reactivity indices of the metabolites were calculated by the Hückel molecular orbital method. Loew et al. [8, 9] calculated the electronic properties of the bay region relevant to epoxidations and hydroxylations, to examine the metabolism of PAHs. Pullman [10] has discussed critically the mechanism of chemical carcinogenesis. Present knowledge of

0003-2670/82/0000-0000/$02.75

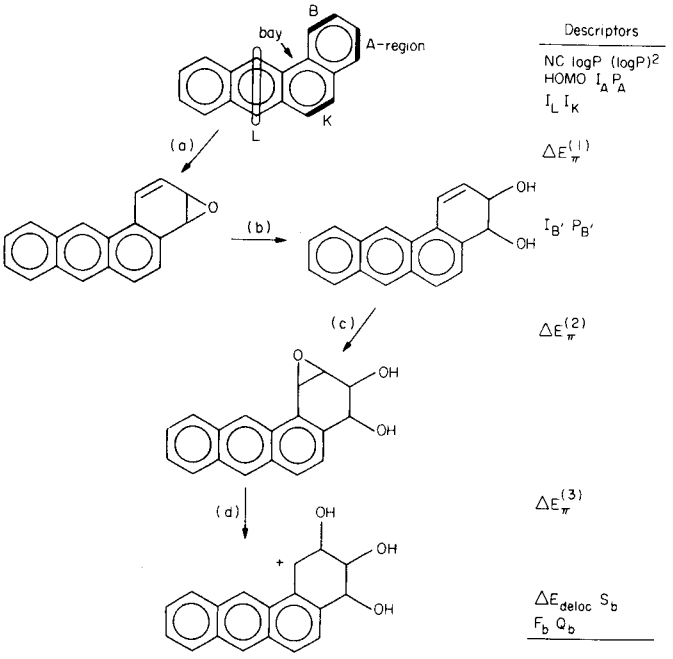

Fig. 1. Pathway for the metabolic conversion of benz[a]anthracene and the relevant descriptors.

the fundamental mechanisms involved in chemical carcinogenesis has been reviewed [11].

Pattern recognition techniques have been used for the investigation of structure—activity relationships for a variety of compounds [12—19]. These techniques also have been applied to structure—carcinogenicity relationships [15, 20—26]. However, most of these studies have focussed on only the description of parent compounds, except for the carcinogenesis studies of nitrosamine by Dunn and Wold [21] and Petit et al. [24]. Also, Dunn and Wold [21] doubted the validity of the binary classification study.

A study of structure—carcinogenicity relationships has been reported in which theoretical indices relating to a series of metabolic transformations obtained by Smith et al. [7] were used [15]. Here, in order to extend the previous studies, the data set involving additional K- and L-region indices is examined by pattern recognition methods including factor analysis. Factor analysis has been applied in studies of chemical problems [27] including drug design [28—30] and spectral analysis [31]; it is useful in establishing the minimum number of factors. These factors can be interpreted in relation to the original chemical properties. Factor analysis can thus help in interpreting the relation between chemical profiles and biological activity.

DATA SET

The carcinogen data for 24 unsubstituted PAHs were taken from Jerina et al. [5, 6]. In order to represent the reactivities and properties of PAHs, the chemical profile for each PAH possibly related to a carcinogenic process can be represented by 17 descriptors

$$x_i = (\mathrm{NC}, \log P, (\log P)^2, \mathrm{HOMO}, I_A, P_A, \Delta E_\pi^{(1)}, I_{B'}, P_{B'}, \Delta E_\pi^{(2)}, \Delta E_\pi^{(3)}, \Delta E_{\mathrm{deloc}}, S_b, F_b, Q_b, I_L, I_K) \quad (1)$$

where x_i is a pattern vector for the i-th PAH; the chemical meanings of these descriptors are shown in Table 1. The carcinogenicities of PAHs and some of the descriptor values are shown in Table 2. The I_K and I_L values for PAHs without K- and L-regions are assigned to zero in this study. This assignment is according to the study of structure—activity relationships by Cammarata and Menon [32]. The carcinogenicities are expressed by an arbitrary scale J with values of 0, 1, 2, 3 and 4 for inactive(−), slight(+), moderate(2+), more active(3+) and very active compounds(4+), respectively [33]. The reason why K- and L-region descriptors are used here together with the descriptors used in the previously reported study is that examination of the roles of these chemically reactive sites is obviously necessary. The importance

TABLE 1

The meanings of the seventeen descriptors

Symbol	Descriptor
NC	Number of carbon atoms
$\log P$	Log of partition coefficient P for the parent compound
$(\log P)^2$	Square of $\log P$
HOMO	Highest occupied molecular orbital energy for parent compound (β unit)
I_A	Bond superdelocalizability on A-region for parent compound
P_A	Bond order for A-region parent compound
$\Delta E_\pi^{(1)}$	Energy change in forming A-region dihydrodiol from parent compound (β unit)
$I_{B'}$	Bond superdelocalizability for B-region of A-region dihydrodiol form
$P_{B'}$	Bond order for B-region of A-region dihydrodiol form
$\Delta E_\pi^{(2)}$	Energy change in forming the dihydrodiol-epoxide from the A-region dihydrodiol (β unit)
$\Delta E_\pi^{(3)}$	Energy change in forming the trihydrotriol carbocation from the dihydrodiol-epoxide (β unit)
$\Delta E_{\mathrm{deloc}}$	Change in delocalization energy (β unit)
S_b	Carbocation atomic superdelocalizability
F_b	Carbocation free valence
Q_b	Carbocation charge density at the benzylic carbon position
I_L	Sum of two atomic superdelocalizabilities involved in L-region for parent compound
I_K	Bond superdelocalizability on K-region for parent compound

TABLE 2

Carcinogenicity[a] and descriptor values[b] for 24 PAHs

No.	Name	Carcinogenicity	$\Delta E_{\pi}^{(1)}$	ΔE_{deloc}	I_L
1	Naphthalene	—	−3.2588	0.488	0.000
2	Anthracene	—	−3.2023	0.544	2.606
3	Tetracene	—	−3.1859	0.628	3.010
4	Pentacene	—	−3.1806	0.710	3.590
5	Benz[a]anthracene	+	−3.3368	0.766	2.438
6	Benzo[a]tetracene	—	−3.3427	0.846	2.863
7	Phenanthrene	—	−3.3185	0.658	0.000
8	Benzo[c]phenanthrene	+	−3.2990	0.600	0.000
9	Chrysene	+	−3.2992	0.640	0.000
10	Benzo[b]chrysene	—	−3.2928	0.647	2.512
11	Picene	—	−3.3052	0.662	0.000
12	Triphenylene	—	−3.3799	0.664	0.000
13	Benzo[g]chrysene	2+	−3.3671	0.728	0.000
14	Dibenz[a,c]anthracene	+	−3.3919	0.722	2.306
15	Dibenz[a,j]anthracene	+	−3.3292	0.722	2.294
16	Dibenz[a,h]anthracene	2+	−3.3292	0.738	2.292
17	Naphtho[2,3-a]pyrene	2+	−3.2072	0.690	2.724
18	Benzo[a]pyrene	4+	−3.2611	0.794	0.000
19	Benzo[e]pyrene	+	−3.3836	0.714	0.000
20	Dibenzo[a,l]pyrene	2+	−3.3681	0.808	0.000
21	Dibenzo[a,i]pyrene	4+	−3.2740	0.870	0.000
22	Dibenzo[a,e]pyrene	3+	−3.3934	0.778	0.000
23	Dibenzo[a,h]pyrene	4+	−3.2486	0.845	0.000
24	Tribenzo[a,e,i]pyrene	2+	−3.4000	0.818	0.000

[a]From Refs. [5, 6]. [b]From Ref. [7].

of these regions has been pointed out by Pullman [10]. Smith et al. [7] have suggested the importance of the deactivating L-region for some PAHs having such regions.

FACTOR ANALYSIS

Factor analysis is a well-developed computerized multivariate statistical technique; it involves the simultaneous analysis of multiple measurements on many compounds. In the present study, measurements are the descriptors concerning the carcinogenic process of PAHs.

It is likely that there are redundant and highly correlated descriptors in a descriptor space. In such cases, R factor analysis is useful for examining relations among descriptors. In R factor analysis [27, 34], an $n \times d$ data matrix $\mathbf{X}$ can be decomposed into an $n \times r$ factor score matrix $\mathbf{F}$ and $d \times r$ factor loading matrix $\mathbf{A}$

$$\mathbf{X} = \begin{pmatrix} x_1 \\ x_2 \\ \vdots \\ x_n \end{pmatrix} = \mathbf{F}\,\mathbf{A}^t$$

where n is the number of compounds, d is that of descriptors, and r is the intrinsic dimensionality of the data matrix. $\mathbf{A}^t$ is a transposed matrix of A.

The procedure of R factor analysis is as follows. In the first step, from a data matrix, a $d \times d$ correlation or covariance matrix is calculated. Eigenanalysis of this symmetric matrix produces d eigenvectors and eigenvalues. The eigenvalues arranged in decreasing order can be used to determine the dimensionality r of the original data. This procedure is equivalent to construction of an orthogonal set of reference axes in a subspace. In the next step, these reference axes are rotated so that the rotated axes can be related more closely to chemically significant properties. Usually, in order to maximize the number of high and low loading descriptors, the varimax rotation (i.e., the orthogonal transformation) is employed.

Here R factor analysis is used to cluster 17 descriptors for 24 PAHs into several groups of mutually correlated descriptors. Because the descriptor data set was multisource, the 17×17 correlation matrix was diagonalized. Table 3 shows the eigenvalues and cumulative percent variances obtained by eigenvalues. There are several methods of determining the intrinsic dimensionality of data by eigenanalysis from a correlation matrix [27]. In this study, the criterion adopted is that the intrinsic dimensionality is the number of eigenvalues necessary to explain 95% of the variance in the data [29]. Table 3 suggests that the number of factors which explain 95% of the total variance is five, and only 1.1% augmentation in the total variance is given by the sixth factor. Therefore the intrinsic dimensionality of the data matrix is considered to be 5.

According to the R analysis studies described by Martin [28], the carcinogenicities for PAHs are also included in the data matrix. The 18×18 correlation matrix was diagonalized. Next, the varimax rotation was employed. The loading resulting from a correlation matrix is the cosine of the angle between each descriptor and each factor. The larger the loading, then the closer to the corresponding factor is the descriptor. The factor loadings for each descriptor on each factor are shown in Table 4. The final row in Table 4 contains the

TABLE 3

Eigenvalues (λ) and cumulative percent variances (%Var) obtained by eigenanalysis for 24 PAHs

Factor no.	1	2	3	4	5	6	7
λ	10.14	4.30	0.98	0.69	0.54	0.20	0.07
%Var	59.7	85.0	90.8	94.8	98.0	99.1	99.5

TABLE 4

The factor loadings for each descriptor on each factor for 24 PAHs

Descriptors	Factor				
	1	2	3	4	5
NC	−0.86	0.12	0.45	−0.05	0.17
log P	−0.89	−0.13	0.42	0.06	0.08
$(\log P)^2$	−0.89	−0.16	0.39	0.04	0.05
HOMO	0.57	0.68	−0.31	−0.24	0.00
I_A	−0.41	−0.85	−0.07	0.04	−0.24
P_A	0.10	−0.92	−0.33	0.09	−0.01
$\Delta E_\pi^{(1)}$	0.07	−0.94	−0.29	0.10	−0.01
$I_{B'}$	−0.34	0.08	0.92	−0.10	0.10
$P_{B'}$	0.20	−0.31	−0.88	0.17	−0.21
$\Delta E_\pi^{(2)}$	0.16	−0.37	−0.85	0.19	−0.24
$\Delta E_\pi^{(3)}$	−0.28	0.20	0.91	−0.11	0.17
ΔE_{deloc}	−0.43	0.06	0.89	−0.03	0.08
S_b	−0.57	−0.09	0.77	0.10	−0.03
F_b	0.26	−0.26	−0.90	0.11	−0.19
Q_b	0.44	−0.07	−0.89	0.01	−0.09
I_L	−0.19	−0.35	−0.12	0.87	−0.11
I_K	−0.17	0.15	0.44	−0.18	0.84
Carcinogenicity	−0.23	−0.20	0.64	−0.59	0.16

loadings of carcinogenicity for each factor. On the basis of the factor loadings for each factor, these descriptors are divided into 5 groups, the absolute value of the threshold factor loading being set as 0.68. Each factor can then be considered as follows: (1) transport property of a parent PAH, (2) formation of A-region metabolites from a parent PAH, (3) formation of B-region metabolites and an ultimate carcinogen from the A-region dihydrodiol, (4) chemical reactivity of the L-region, and (5) chemical reactivity of the K-region. Further, when the relations between carcinogenicity and each factor are considered, the third and fourth factors especially affect the carcinogenicity. In our previous work [15], the dimensionality was 3; that result is consistent with the present work because two descriptors, I_L and I_K, were not included in the previous analysis.

The factor analysis technique was then employed, using the same descriptors, for only 15 carcinogenic PAHs. The eigenvalues and cumulative percent variances are shown in Table 5. In this eigenanalysis, 98.2% of the total variance can be explained by 5 factors and only 1.2% augmentation in the total variance is given by 6 factors. Therefore in this case the intrinsic dimensionality is also considered to be 5.

The 18 × 18 correlation matrix of the 17 descriptors and carcinogenicity data for PAHs was diagonalized. The factor loadings rotated are shown in Table 6. These descriptors were divided into five groups. This grouping of descriptors for carcinogenic PAHs is almost identical to the one that was

TABLE 5

Eigenvalues (λ) and cumulative percent variances (%Var) obtained by eigenanalysis for 15 PAHs

Factor no.	1	2	3	4	5	6	7
λ	9.57	3.51	1.97	1.13	0.52	0.21	0.07
%Var	56.3	76.9	88.5	94.9	98.2	99.4	99.8

TABLE 6

The factor loadings for each descriptor on each factor for 15 PAHs

Descriptors	Factor				
	1	2	3	4	5
NC	0.94	0.12	0.27	−0.06	−0.02
log P	0.95	−0.10	0.29	0.00	−0.01
$(\log P)^2$	0.95	−0.10	0.27	−0.01	−0.02
HOMO	−0.64	0.58	−0.42	−0.08	0.12
I_A	0.62	−0.69	0.13	−0.12	−0.23
P_A	−0.04	−0.97	−0.13	0.06	−0.11
$\Delta E_\pi^{(1)}$	−0.01	−0.98	−0.10	0.07	−0.12
$I_{B'}$	0.35	−0.09	0.92	−0.05	−0.05
$P_{B'}$	−0.11	−0.08	−0.97	0.15	−0.01
$\Delta E_\pi^{(2)}$	−0.05	−0.13	−0.96	0.20	0.00
$\Delta E_\pi^{(3)}$	0.22	−0.02	0.97	−0.08	−0.02
ΔE_{deloc}	0.44	−0.05	0.89	−0.01	−0.08
S_b	0.65	−0.07	0.72	0.08	−0.13
F_b	−0.18	−0.04	−0.98	0.07	0.01
Q_b	−0.45	0.05	−0.89	−0.02	0.08
I_L	0.01	−0.07	−0.22	0.95	0.17
I_K	0.06	−0.31	0.07	−0.19	−0.92
Carcinogenicity	0.32	−0.53	0.64	−0.36	−0.03

obtained by using descriptors for noncarcinogenic and carcinogenic PAHs, except that HOMO is assigned to the first factor. As HOMO is a property of the parent compound, this grouping is natural. Among the various relationships between carcinogenicity and each factor, the second and third factors have the greatest influence on the carcinogenic potency.

This descriptor grouping is useful for the development of regression equations for carcinogenicity, because this information allows the selection of a set of descriptors which span the descriptor space in a relatively uncorrelated manner. This procedure is one of the most useful feature selection methods.

MULTIPLE REGRESSION ANALYSIS

The five factors obtained by R factor analysis were reasonably interpreted in terms of physicochemical properties. Then, an attempt was made to relate

carcinogenicity to the descriptors by selecting one descriptor for each group. First, linear regression equations were generated for 15 carcinogens. The following equation is the most significant of all the equations obtained, from the chemical and statistical points of view. The level of significance of each of the terms was judged by the F and Student's t test

$$J = 9.47\Delta E_{\pi}^{(1)} + 10.78\Delta E_{\text{deloc}} - 0.32I_{\text{L}} + 25.73 \qquad (2)$$

(5.28) (4.34) (0.27) (17.86)

$n = 15$ $s = 0.53$ $r = 0.92$ $F = 18.80$

In this equation and Eqn. (3), n, s, r, and F are, respectively, the number of compounds, the standard deviation, the multiple correlation coefficient, and the F-value of the correlation. The numbers in parentheses are the 95% confidence intervals. The $\Delta E_{\pi}^{(1)}$ and ΔE_{deloc} terms are justified above the 99.5% level by the t test. The I_{L} term is justified at a level between 97.5 and 99%. The descriptor values in Eqn. (2) and the following equation are listed in Table 2.

Equation (2) shows that the smaller the energy change in forming the A-region dihydrodiol from a parent compound, the greater the change in delocalization energy during carbocation formation; and that the smaller the sum of atom superdelocalizability of the L-region, the greater is the carcinogenicity. The carcinogenicity of noncarcinogens can be calculated by Eqn. (2). As shown in Table 7, the calculated values are in reasonable agreement with the observed ones for all noncarcinogens except for 3 PAHs (pentacene, benzo[a]tetracene, and picene) for which the deviations are rather large.

Thus, the three exceptional PAHs were removed in further analysis as outliers. The remaining six noncarcinogens were added to the group of carcinogens and regression equations were generated as described above

$$J = 8.64\Delta E_{\pi}^{(1)} + 12.43\Delta E_{\text{deloc}} - 0.34I_{\text{L}} + 21.61 \qquad (3)$$

(5.04) (3.25) (0.25) (16.21)

$n = 21$ $s = 0.62$ $r = 0.91$ $F = 26.45$

Equation (3), which has the same descriptors as Eqn. (2), is the most significant. Furthermore, comparison of Eqns. (2) and (3), taking into account the 95% confidence interval, indicates that the slopes of each term are very close. The carcinogenicity of all 24 PAHs was calculated by Eqn. (3) (Table 7). The removed three PAHs as outliers, however, cannot be explained by this model equation.

Conclusion

The 17 descriptors related to the carcinogenic processes of PAHs can be divided into five groups with physicochemically significant properties by factor analysis. This facilitates the development of regression equations for

TABLE 7

Carcinogenicity observed and calculated by Eqn. (2) and Eqn. (3)

Compound number[a]	Observed	Eqn. (2)		Eqn. (3)	
		Calcd.	Error[b]	Calcd.	Error[b]
1	0[c]	0.14[e]	−0.14	−0.48	0.48
2	0[c]	0.45[e]	−0.45	−0.19	0.19
3	0[c]	1.39[e]	−1.39	0.86	−0.86
4	0[c,d]	2.13[e]	−2.13	1.72[e]	−1.72
5	1	1.63	−0.63	1.47	−0.47
6	0[c,d]	2.30[e]	−2.30	2.26[e]	−2.26
7	0[c]	1.42[e]	−1.42	1.13	−1.13
8	1	0.97	0.03	0.57	0.43
9	1	1.40	−0.40	1.07	−0.07
10	0[c]	0.74[e]	−0.74	0.34	−0.34
11	0[c,d]	1.58[e]	−1.58	1.29[e]	−1.29
12	0[c]	0.89[e]	−0.89	0.67	−0.67
13	2	1.71	0.29	1.57	0.43
14	1	0.67	0.33	0.49	0.51
15	1	1.27	−0.27	1.04	−0.04
16	2	1.45	0.55	1.24	0.76
17	2	1.95	0.05	1.55	0.45
18	4	3.42	0.58	3.31	0.69
19	1	1.40	−0.40	1.25	−0.25
20	2	2.56	−0.56	2.56	−0.56
21	4	4.12	−0.12	4.14	−0.14
22	3	2.00	1.00	1.97	1.03
23	4	4.09	−0.09	4.05	−0.05
24	2	2.37	−0.37	2.41	−0.41

[a]See Table 2. [b]Error = observed minus calculated value. [c]These data were not included in generating Eqn. (2). [d]These data were not included in generating Eqn. (3). [e]Calculated from regression equation.

carcinogenicity. The problem of collinearity among descriptors can be removed by this grouping. Thus, factor analysis is shown to be a useful feature selection method.

The previous report [15] showed the importance of the metabolic pathway based on the bay region theory for carcinogenicity. This work proves the significance of the L-region reactivity in addition to the bay region reactivity. This model for carcinogenic activity could not, however, explain the noncarcinogenicity of the three exceptional PAHs. This deviation may be due to other metabolic pathways and/or presently unknown factors in carcinogenesis.

The authors thank the Computer Center, Institute of Molecular Science, for the use of the HITAC M-200H computer, and Dr. C. Takayama for invaluable discussions, and Dr. C. Jochum for many useful suggestions concerning factor analysis.

REFERENCES

1 A. Pullman and B. Pullman, Adv. Cancer Res., 3 (1955) 117.
2 J. D. Scribner, J. Natl. Cancer Inst., 55 (1975) 1035.
3 A. Borgen, H. Darvey, N. Castagnoli, T. T. Crocker, R. E. Rasmussen and I. Y. Wang, J. Med. Chem., 16 (1973) 502.
4 P. Sims, P. L. Grover, A. Swaisland, K. Pal and A. Hewer, Nature, 252 (1974) 326.
5 D. M. Jerina and R. E. Lehr, in V. Ullrich, I. Roots, A. G. Hildebrant, R. W. Estabrook and A. H. Conney (Eds.), Microsomes and Oxidations, Pergamon, Oxford, 1977, p. 709.
6 D. M. Jerina, R. Lehr, M. Schaefer-Ridder, H. Yagi, J. M. Karle, D. R. Thakker, A. H. Wood, A. Y. H. Lu, D. Rayn, S. West, W. Levin and A. H. Conney, in H. Hiatt, J. D. Watson and I. Winstin (Eds.), Origins of Human Cancer, Cold Spring Harbor Laboratory, Cold Spring Harbor, NY, 1977, p. 639.
7 I. A. Smith, G. D. Berger, P. G. Seybold and M. P. Servé, Cancer Res., 38 (1978) 2968.
8 G. H. Loew, J. Phillips, J. Wong, L. Hjelmeland and G. Pack, Cancer Biochem. Biophys., 2 (1978) 113.
9 G. H. Loew, J. Wong, J. Phillips, L. Hjelmeland and G. Pack, Cancer Biochem. Biophys., 2 (1978) 123.
10 B. Pullman, Int. J. Quantum Chem., 16 (1979) 669.
11 B. Pullman, P. O. P. Ts'o and H. Gelboin (Eds.), Carcinogenesis: Fundamental Mechanisms and Environmental Effects, D. Reidel Publishing Co., Dordrecht, The Netherlands, 1980.
12 G. L. Kirschner and B. R. Kowalski, in E. J. Ariëns (Ed.), Drug Design, Vol. 8, Academic Press, New York, 1979, p. 73.
13 P. J. Lewi, in E. J. Ariëns (Ed.), Drug Design, Vol. 7, Academic Press, New York, 1976, p. 209.
14 P. J. Lewi, in E. J. Ariëns (Ed.), Drug Design, Vol. 10, Academic Press, New York, 1981, p. 307.
15 Y. Miyashita, T. Seki, Y. Takahashi, S. Daiba, Y. Tanaka, Y. Yotsui, H. Abe and S. Sasaki, Anal. Chim. Acta, 133 (1981) 603.
16 Y. Miyashita, Y. Takahashi, Y. Yotsui, H. Abe and S. Sasaki, CODATA Bull., 41 (1981) 37; Anal. Chim. Acta, 133 (1981) 615.
17 A. J. Stuper, W. E. Brügger and P. C. Jurs, Computer-Assisted Studies of Chemical Structure and Biological Function, Wiley—Interscience, New York, 1979.
18 Y. Takahashi, Y. Miyashita, H. Abe, S. Sasaki, Y. Yotsui and M. Sano, Anal. Chim. Acta, 122 (1980) 241.
19 K. Varmuza, Pattern Recognition in Chemistry, Springer-Verlag, Berlin, 1980.
20 J. T. Chou and P. C. Jurs, J. Med. Chem., 22 (1979) 792.
21 W. J. Dunn, III and S. Wold, J. Chem. Inf. Comput. Sci., 21 (1981) 8; J. Med. Chem., 21 (1979) 1001.
22 P. C. Jurs, J. T. Chou and M. Yuan, J. Med. Chem., 22 (1979) 476.
23 B. Nordén, U. Edlund and S. Wold, Acta Chem. Scand., B32 (1978) 602.
24 B. Petit, R. Potenzone, Jr., A. J. Hopfinger, G. Klopman and M. Shapiro, in E. C. Olson and R. E. Christoffersen (Eds.), Computer-Assisted Drug Design (ACS Symp. Ser. 112), Am. Chem. Soc., Washington, DC, 1979, p. 553.
25 M. Yuan and P. C. Jurs, Toxicol. Appl. Pharmacol., 52 (1980) 294.
26 K. Yuta and P. C. Jurs, J. Med. Chem., 24 (1981) 241.
27 E. R. Malinowski and D. G. Howery, Factor Analysis in Chemistry, Wiley—Interscience, New York, 1980.
28 Y. C. Martin, Quantitative Drug Design, Dekker, New York, 1978.
29 Y. C. Martin and H. N. Panas, J. Med. Chem., 22 (1979) 784.
30 M. L. Wiener and P. Wiener, J. Med. Chem., 16 (1973) 655.
31 R. W. Rozett and E. M. Petersen, Anal. Chem., 47 (1975) 1301, 2377; 48 (1976) 817.
32 A. Cammarata and G. K. Menon, J. Med. Chem., 19 (1976) 739.
33 R. Franke, Chem.—Biol. Interact., 6 (1973) 1.
34 R. J. Rummel, Applied Factor Analysis, Northwestern University Press, Evanston, IL, 1970.

Analytica Chimica Acta, 143 (1982) 45—77
Elsevier Scientific Publishing Company, Amsterdam — Printed in The Netherlands

COMPUTER-CONTROLLED TITRATIONS
Part 1. Considerations Based on Systems Theory

J. C. SMIT[a] and H. C. SMIT*

Laboratory for Analytical Chemistry, University of Amsterdam, Nieuwe Achtergracht 166, 1018 WV Amsterdam (The Netherlands)

(Received 8th February 1982)

SUMMARY

Automated titrimetric procedures are considered on the basis of systems theory, with emphasis on the dynamic behaviour of the system. In the case of continuous addition of titrant, conditions are derived for the maximum addition speed and a correction procedure is given. Control algorithms for discontinuous addition of titrant are given, including an algorithm for on-line estimation of the dynamic (overall) effects of the titration system; this is useful for determining the waiting time between two successive additions of titrant. Shannon's theorem is utilized in order to decide on the sampling of the titration curve, both for continuous and discontinuous additions of titrant. Finally, confidence intervals for the end-point determination are derived, based on zero crossing statistics, and applied on the second derivative of a sigmoidal titration curve.

Titrimetric methods are widely used in chemical analysis because of their precision, accuracy and simplicity. The analytical result, which is based on the end-point volume corresponding to a rapid change in the concentration of some species involved in the reaction, can be obtained only by measuring relative concentrations. These well established chemical techniques are time- and manpower-consuming, but their combination with chemometrics and computer facilities will probably increase their present popularity. In particular, broader applications in process control can be expected. At this moment, titration techniques are not very widely used for direct control purposes because their time requirement is the limiting factor. The control of a process requires both accuracy and speed from the analytical method used. Therefore, it is appropriate to study the parameters which determine the results of an automated titration and to develop optimal automation of titrimetric analysis. To achieve this final aim, the dynamics of the titration procedure have also to be investigated. The use of systems and signal theory is indispensable for these studies. A short introduction is given below.

---

[a]Present address: Laboratory for Neurology, St. Radboud Hospital, Catholic University Nijmegen, Reinier Postlaan 4, 6500 HB Nijmegen, The Netherlands.

BASICS OF SYSTEMS THEORY

The behaviour of many physical and chemical systems can be described in more or less simplified form by means of a mathematical model. Deterministic models are based on conservation law (e.g., for mass, momentum or energy) and stochastic models are based on statistical information about the system. The solution of the mathematical model, in general involving a differential equation, describes the output $y(t)$ of the system on a defined input stimulus $x(t)$. If linearity is assumed, two approaches are possible in systems theory. The first is to calculate the functional dependence between an input signal $x(t)$ and an output signal $y(t)$ by using an integral transformation. The operator, obtained by applying the Laplace transformation, for example, is defined as the system transfer function $H(s)$, which is the transformed impulse response of the system considered. The Laplace transform $Y(s)$ of the output $y(t)$ is now simply given by $X(s)H(s)$, where $X(s)$ is the transform of the input $x(t)$. In a similar way, the complex frequency response function $H(j\omega)$ is obtained. In the following paragraphs, some general properties used in systems theory are mentioned without going into detail. More information is easily available [1—3]. A second, more general approach than that indicated above is given by the so-called state space theory [2] which will not be described here.

First, it is necessary to investigate the mathematical properties of a descriptive model, restricted to linear, time-invariant causal systems with a single input signal $x(t)$ and a single output signal $y(t)$. The relation between the input signal $x(t)$ and the resulting output response $y(t)$ is given, for example, by the following differential equation:

$$a_0 y(t) + a_1 \mathrm{d}y(t)/\mathrm{d}t + \ldots a_n \mathrm{d}^n y(t)/\mathrm{d}t^n = x(t) \tag{1}$$

for $t > 0$, where $y(t)$ is subjected to the following initial conditions

$$\lim_{t \downarrow 0} y^{(j)}(t) = 0 \qquad (j = 0, \ldots, n-1) \tag{2}$$

Equations (1) and (2) represent a so-called causal system, with the property that a non-zero response occurs only after the input has been altered. The system transfer function $H(s)$ is the Laplace transform of the response $h(t)$ of the system on the "unit pulse function", represented by the delta function of Dirac $\delta(t)$. Because the Laplace transform of $\delta(t)$ is 1, we obtain for the system transfer function of the system

$$\sum_{j=0}^{n} a_j y^{(j)}(t) = \delta(t)$$

$$\text{with } y^{(j)}(0) = 0 \qquad (j = 0, \ldots, n-1) \tag{3}$$

$$H(s) = 1 \Big/ \sum_{j=0}^{n} a_j s^j$$

For the Laplace transform $Y(s)$ of the response $y(t)$ on the input signal $x(t)$ as represented by Eqn. (1)

$$Y(s) = L\{y\}(s) = H(s)L\{x\}(s) = H(s)X(s) = X(s) \Big/ \sum_{j=0}^{n} a_j s^j \tag{4}$$

and hence

$$y(t) = L^{-1}\left[X(s) \Big/ \sum_{j=0}^{n} a_j s^j \right] = \int_0^t x(\tau) h(t - \tau) \mathrm{d}\tau \tag{5}$$

where $h(t)$ is the response on the unit pulse in the time domain.

The systems theoretical calculations on combinations of systems (series, parallel, closed loop or open loop) are considerably simplified by the use of the properties of the Laplace transformation. Let $H_1(s)$, $H_2(s)$ and $H_3(s)$ be the system transfer functions of linear, time-invariant causal systems. If a system consists of two non-interacting parallel systems with transfer function $H_1(s)$ and $H_2(s)$, then the system transfer function of the composite system is

$$H(s) = H_1(s) + H_2(s) \qquad \text{(sum)} \tag{6}$$

If a system consists of two non-interacting systems in series, with transfer functions $H_1(s)$ and $H_2(s)$, the transfer function of the composite system is

$$H(s) = H_1(s)H_2(s) \qquad \text{(product)} \tag{7}$$

A composite system consisting of non-interacting systems, parallel and/or in series, has a transfer function which can be formed from the transfer functions of the individual systems by applying the well known rules of commutativity, associativity and distributivity of algebra, e.g.

$$H_1(s)\{H_2(s) + H_3(s)\} = H_1(s)H_2(s) + H_1(s)H_3(s) \tag{8}$$

Equations (6), (7) and (8) permit subdividing of complicated systems in separate parts or inversely the combination of subsystems.

A descriptive "systems theoretical model" of a system or subsystem can be obtained from the output response on any well defined input signal. The input signal can consist of, e.g., sine functions, Heaviside's unit function, a noise signal or a unit pulse function; the latter gives directly the system transfer function. Any input is sufficient to give a rough description of the overall effect of a system or subsystem without consideration of its physical or chemical properties. However, it must be realized that this descriptive model has no physical meaning (except in some very simple first- or second-order systems), although it is of great practical value for interpreting the behaviour of systems in open or closed loops.

THE TITRATION SYSTEM

If it is assumed that systems theory may be applied to titration assemblies, the total titration system can be divided into four subsystems as presented in Fig. 1. The input of the mixing system is a defined addition of titrant with a constant concentration $C_{titrant}$. The output reflects a concentration change of the added and mixed reagent. The response of the chemical reaction system giving this output depends on the formation of the reaction product. The detection system, e.g., a pH electrode, an ion-selective electrode or a photometer, converts the concentration changes of the reaction product or the reagent to an electric signal. In most cases, the final subsystem will be an amplifier in combination with a data-handling system or at least a recorder. In the following sections, the influence of the dominant subsystems on systematic and random errors in an automated end-point determination will be discussed.

Mixing system

The mixing process of a perfectly mixed solution in a vessel can be described by a first-order differential equation; on the assumption that the change of volume caused by the addition of titrant may be neglected, the differential equation is

$$q(t) = [V/C_{titrant}]\,[dC_m(t)/dt] \tag{9}$$

where the input variable of the system $q(t)$ denotes the addition of titrant in $m^3\ s^{-1}$, $C_{titrant}$ is the concentration of the titrant in mol m^{-3} and $C_m(t)$ is the output of the mixing system, being the titrant concentration after mixing in a volume V in m^3. For the initial condition $C_m(0) = 0$, the system transfer function is obtained by taking $q(t) = \delta(t)$

$$H_{m1}(s) = 1/\tau_{m1}s \tag{10}$$

where $\tau_{m1} = V/C_{titrant}$ is the system time constant. This quantity determines the dynamic behaviour of the system. Usually, in systems where input and output have the same dimensions, the time constants have the dimension of time. In this particular case, with different dimensions of input and output signal, τ_{m1} does not have the dimension of time.

If the increase in volume after an addition of titrant cannot be neglected, e.g., in spectrophotometric titrations in 10-ml cells, the time constant τ_{m1} will increase. This effect can be illustrated very simply by the differential equation

$$q(t) = [1/C_{titrant}]\,[d(V(t)C_m(t))/dt] \qquad (\text{for } t > 0) \tag{11}$$

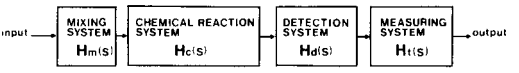

Fig. 1. Block diagram of a titration process.

For a constant addition of titrant $q(t) \equiv m$ m^3 s^{-1}, $V(t)$ will be $V(0) + mt$, and Eqn. (11) can be written as

$$m = [(V(0) + mt)/C_{\text{titrant}}]\,[\mathrm{d}C_m(t)/\mathrm{d}t] + [m/C_{\text{titrant}}]\,C_m(t) \tag{12}$$

where $V(0)$ denotes the volume at $t = 0$. The coefficient of the dynamic part of Eqn. (12), being the time constant of the system, is time-dependent and a non-constant parameter system is obtained.

In automatic titrators, other than coulometric titrators, the titrant is usually added from a burette equipped with a stepping motor. With such burettes, it is possible either to inject a single pulse of titrant or to inject almost continuously at a speed depending on the frequency of the stepping motor. With the aid of Eqns. (4) and (10), the following expressions are obtained for a continuous addition $q(t) \equiv m$ m^3 s^{-1}

$$C_m(t) = L^{-1}[Q(s)H_{m1}(s)] = mt/\tau_{m1} \tag{13}$$

for $t > 0$, with $Q(s) = L[q(t)] = m/s$

A discontinuous small addition of titrant can be described by a Dirac delta function $m\delta(t)$. Application of Eqn. (4) gives

$$C_m(t) = L^{-1}[mH_{m1}(s)] = [m/\tau_{m1}]\,\breve{u}(t) \tag{14}$$

where $\breve{u}(t)$ denotes Heaviside's unit function or unit step function. Both functions $\delta(t)$ and $\breve{u}(t)$ (generalized functions in the sense of distributions), are often used as input functions in macroscopic system descriptions [1].

The perfect mixer model $H_{m1}(s)$ will differ from a practical mixing system. Two effects may be distinguished. The first is the distortion of the ideal mixer responses as calculated in Eqns. (13) and (14), caused by the hydrodynamic properties of the titration vessel. The second effect of non-ideal mixing is random fluctuation in the output signal. The characteristics of these fluctuations are determined by the geometry of the titration vessel including the burette tip and electrodes and the stirring mechanism. Experimental and theoretical studies are needed to relate these mixing effects to an adequate system description. For the purpose of automation, a phenomenological description of the two non-ideal mixing effects suffices. Therefore, the effects are approximated by an additional first-order system with a system transfer function $H_{m2}(s)$ and a first-order, band-limited, white noise signal $\underline{n}(t)$ (the underline refers to the stochastic properties of the signal in the time domain). The output response to an input signal $q(t) = m\delta(t)$ becomes finally the signal $\underline{c}(t) = z(t) + \underline{e}(t)$, as indicated in Fig. 2.

The response on both the deterministic input signal $q(t)$ and the stochastic signal $\underline{n}(t)$ is described by

$$\underline{c}(t) = L^{-1}\{Q(s)H_{m1}(s)H_{m2}(s)\} + [L^{-1}\{Q(s)H_{m1}(s)(1 - H_{m2}(s))\}]\,\underline{n}(t) \tag{15}$$

The first part of the right-hand side of Eqn. (15) is the deterministic system response $z(t)$, while the second part describes the mixing noise effects $\underline{e}(t)$. The deterministic system response $z(t)$ is simply obtained by substituting

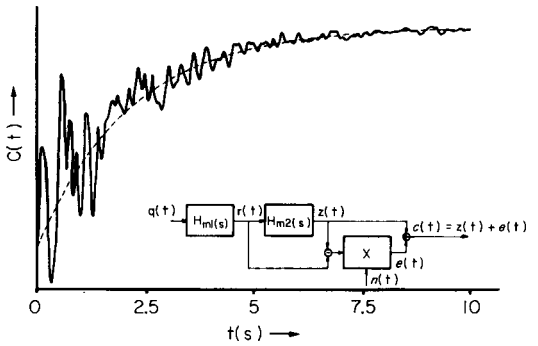

Fig. 2. Analog computer simulation of a non-perfect mixer with an impulse-shaped input signal, achieved with a Telefunken RA742 analog computer and a Hewlett-Packard HOI-3722 noise generator with Gaussian bandwidth of 5 Hz; time constant of $H_{m2}(s)$ is 2 s.

into Eqn. (15) the system transfer function $H_{m1}(s) = 1/(\tau_{m1}s)$ and the additional first-order transfer function $H_{m2}(s)$. The function $H_{m2}(s)$ is chosen as $1/(1 + \tau_{m2}s)$. So we get for the performance of a continuous addition $q(t) \equiv m$ with a concentration C_{titrant}

$$z(t) = (m/\tau_{m1})\{t - \tau_{m2} + \tau_{m2} \exp(-t/\tau_{m2})\} \qquad (\text{for } t > 0) \tag{16}$$

When this result is compared with Eqn. (13), which is the response of a perfect mixer, two effects of the non-ideal mixing behaviour can be distinguished. The first effect is the contribution of the so-called transient state term, which describes the slowness of the system. When this effect is eliminated ($t > 5\tau_{m2}$), a second effect will remain in the form of a time shift τ_{m2} of the signal.

A similar calculation is possible for discontinuous addition of titrant, viz. $q(t) \equiv \delta(t)m$. This yields

$$z(t) = (m/\tau_{m1})\{1 - \exp(-t/\tau_{m2})\} \qquad (\text{for } t > 0) \tag{17}$$

Compared with the result of Eqn. (14), the unit step function is replaced by a typical first-order response.

For the computation of the stochastic signal $\underline{e}(t)$, an approach based on signal theory has to be followed. In this case, the most elegant way is to describe signals in the frequency domain. An arbitrary real-valued signal $\underline{n}(t)$ is then represented by a power spectral density function (psdf) $G_{nn}(\omega)$. The physical meaning of the psdf can be clarified by a short description. Let the Fourier transform of a real-valued stochastic signal be (assuming $N(\omega)$ exists)

$$N(\omega) = F\{\underline{n}(t)\} = \int_{-\infty}^{+\infty} e^{-j\omega t}\, \underline{n}(t)\mathrm{d}t \tag{18}$$

After $N(\omega)$ has been multiplied by

$$\phi(\omega, \omega_0, \Delta\omega) = \begin{cases} 1 & \omega_0 - \Delta\omega/2 < \omega < \omega_0 + \Delta\omega/2 \\ 0 & \text{else} \end{cases}$$

inverse transformation yields

$$\underline{n}(t, \omega_0, \Delta\omega) = \frac{1}{2\pi} \int_{-\infty}^{+\infty} e^{j\omega t} \phi(\omega, \omega_0, \Delta\omega) N(\omega) d\omega \tag{19}$$

where $\underline{n}(t, \omega_0, \Delta\omega)$ is the time signal, containing only frequencies with a bandwidth $\Delta\omega$ centered at ω_0. The total average power of the signal $\underline{n}(t, \omega_0, \Delta\omega)$ is estimated by

$$\hat{P}(\omega_0, \Delta\omega, T) = \frac{1}{T} \int_{-T/2}^{T/2} \underline{n}^2(t, \omega_0, \Delta\omega) dt$$

and as T approaches infinity, this estimate will approach the true mean value:

$$P(\omega_0, \Delta\omega) = \lim_{T \to \infty} \frac{1}{T} \int_{-T/2}^{T/2} \underline{n}^2(t, \omega_0, \Delta\omega) dt \tag{20}$$

It can be proved that the estimate is unbiased and consistent. This quantity still depends on the bandwidth $\Delta\omega$. Finally the psdf is defined by

$$G_{nn}(\omega_0) = \lim_{\Delta\omega \to 0} [P(\omega_0, \Delta\omega)/\Delta\omega] \tag{21}$$

The total power of the signal $\underline{n}(t)$ is defined by

$$\lim_{T \to \infty} \frac{1}{T} \int_{-T/2}^{+T/2} \underline{n}^2(t) dt \tag{22}$$

and so is equal to the value of the autocovariance function

$$R_{nn}(\tau) = \lim_{T \to \infty} \frac{1}{T} \int_{-T/2}^{+T/2} \underline{n}(t)\underline{n}(t + \tau) dt \tag{23}$$

in the point $\tau = 0$. According to the Wiener—Khinchin relation

$$R_{nn}(\tau) = F^{-1}\{G_{nn}(\omega)\} \tag{24}$$

the total power of the signal $\underline{n}(t)$ is given by

$$R_{nn}(0) = \frac{1}{2\pi} \int_{-\infty}^{+\infty} G_{nn}(\omega) d\omega \tag{25}$$

Moreover, it is clear that this total power is equal to the variance σ_n^2 of the stochastic signal.

If the signal $\underline{n}(t)$, generated in the mixing vessel, is a stationary first-order, band-limited, white noise, $\underline{n}(t)$ can be described as the output of a first-order system with input signal $\underline{x}(t)$, being a stationary white noise (Fig. 3). Thus we have $G_{xx}(\omega) = k$ and a complex frequency response function, defined as the Fourier transform of the unit pulse response, given by $H(j\omega) = 1/(1 + j\omega\tau_{m2})$. The psdf of the output signal $\underline{n}(t)$ is obtained by using the Wiener—Khinchin relation and the convolution property of the Fourier transform. This results in

$$G_{nn}(\omega) = |H(j\omega)|^2 G_{xx}(\omega) = k/(1 + \omega^2\tau_{m2}^2) \tag{26}$$

Application of Eqn. (25) finally yields

$$\sigma_n^2 = R_{nn}(0) = \frac{1}{2\pi} \int_{-\infty}^{+\infty} [k/(1 + \omega^2\tau_{m2}^2)]\,\mathrm{d}\omega = k/2\tau_{m2} \tag{27}$$

and substitution of Eqn. (27) into (26) gives

$$G_{nn}(\omega) = 2\tau_{m2}\sigma_n^2/(1 + \omega^2\tau_{m2}^2) \tag{28}$$

The fluctuations in concentration will disappear after some time when the added titrant has been mixed homogeneously. Therefore the signal $\underline{n}(t)$ has been multiplied by $[r(t) - z(t)]$, resulting in the stochast $\underline{e}(t)$ (see Fig. 2). To investigate the stochastic behaviour of $\underline{e}(t)$ on an input stimulus $q(t)$, it is first assumed that $q(t) \equiv m$ (continuous addition of titrant). Then when Eqns. (13) and (16) are used for $r(t)$ and $z(t)$, respectively, the expression for $\underline{e}(t)$ at $t > 0$ becomes

$$\underline{e}(t) = \{m\tau_{m2}/\tau_{m1}(1 - \exp(-t/\tau_{m2}))\}\underline{n}(t) \tag{29}$$

which yields a non-stationary noise signal. However, for $t > 5\tau_{m2}$ the noise signal may be considered as stationary with a total power

$$\sigma_e^2 = (m\tau_{m2}/\tau_{m1})^2\sigma_n^2 \tag{30}$$

In the case of discontinuous addition of titrant, the "disturbance signal" $\underline{e}(t) = \underline{n}(t)[r(t) - z(t)]$ is obtained by substitution of the results from Eqns. (14) and (17) into $r(t)$ and $z(t)$, respectively, which results in the non-stationary noise signal

$$\underline{e}(t) \begin{cases} 0 & t = 0 \\ \dfrac{m}{\tau_{m1}} \exp(-t/\tau_{m2})\underline{n}(t) & 0 < t < 5\tau_{m2} \\ \text{approximately zero for} & t \geqslant 5\tau_{m2} \end{cases} \tag{31}$$

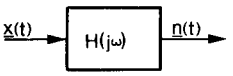

Fig. 3. Representation of a first-order, band-limited noise $\underline{n}(t)$ as an output of a first-order system $H(j\omega)$.

Finally, the total system response of the non-ideal mixer for continuous or discontinuous addition of titrant may be described by the superposition of the results of Eqns. (16) and (29), or Eqns. (17) and (31).

Chemical reaction system

In titrimetric analysis, many types of reaction can be utilized. Cover and Meites [4] pointed out various types of reaction that are suitable for the purpose of automated titrations with continuous addition of titrant. Most reaction types are mono- or bi-molecular equilibrium reactions with or without side-reactions. For a mono-molecular reaction system, represented by the scheme

$$A_0 \underset{k_{b_1}}{\overset{k_{f_1}}{\rightleftharpoons}} A_1 \underset{k_{b_2}}{\overset{k_{f_2}}{\rightleftharpoons}} A_2 \ldots A_{n-1} \underset{k_{b_n}}{\overset{k_{f_n}}{\rightleftharpoons}} A_n$$

the total system may be described by a set of first-order differential equations

$$\begin{aligned}
d[A_0]/dt &= -k_{f_1}[A_0] + k_{b_1}[A_1] \\
&\vdots \\
d[A_p]/dt &= +k_{f_p}[A_{p-1}] - k_{b_p}[A_p] + k_{b_{p+1}}[A_{p+1}] - k_{f_{p+1}}[A_p] \qquad (32) \\
&\vdots \\
d[A_n]/dt &= +k_{f_n}[A_{n-1}] - k_{b_n}[A_n]
\end{aligned}$$

with the initial condition $[A_0](0) = \alpha$ and $[A_p](0) = 0$, $p = 1, \ldots n$. Let us consider the chemical reaction as a system with a concentration change of A_0 (the added and mixed titrant) as input, and the concentration of A_n as output. With the assumptions that the volume change is negligible during titration, and that the forward reactions (k_f) are faster than the reverse reactions (k_b), the total system can be solved by solving consecutively each single equation. When distribution theory is used, the first initial value problem $d[A_0]/dt + k_{f_1}[A_0] = 0$ with the initial condition $[A_0] = 0$ for $t < 0$ and $[A_0] = \alpha$ for $t = 0$, may be transformed as follows:

$$(d[A_0]/dt) + (k_{f_1}[A_0]) = [A_0](0)\delta(t) \quad \text{for } t \geqslant 0 \quad \text{and} \quad [A_0] \equiv 0 \text{ for } t < 0 \qquad (33)$$

The system (33) is now again a causal system with input $[A_0](0)\delta(t) = \alpha\delta(t)$ and output $[A_n](t)$. Laplace transformation yields

$$\begin{aligned}
L\{[A_0]\} &= \tau_{c_1}(1 + \tau_{c_1}s)^{-1}[A_0](0) \\
&\vdots \\
L\{[A_p]\} &= (\tau_{c_{p+1}}/\tau_{c_p})(1 + \tau_{c_{p+1}}s)^{-1}L(A_{p-1}) \qquad (\text{for } p = 1, \ldots n-1) \qquad (34) \\
&\vdots \\
L\{[A_n]\} &= (\tau_{c_n}s)^{-1}L\{[A_{n-1}]\}
\end{aligned}$$

with $\tau_{c_p} = 1/k_{f_p}$

Hence, the system transfer function for $[A_0](0) = 1$ is

$$L\{[A_n]\} \equiv H_c(s) = (1/s)\left[\prod_{p=1}^{n} (1 + \tau_{cp}s)^{-1}\right] \tag{35}$$

Finally, it is possible to make the crude assumption that q coefficients, say τ_{cp_i}, $i = 1, \ldots q$, are small compared with the other coefficients τ_{cp_i}, $i = q + 1, \ldots n$. Then $H_c(s)$ can be written as

$$H_c(s) = \frac{1}{s}\prod_{i=1}^{q} (1 + \tau_{cp_i}s)^{-1} \prod_{i=q+1}^{n} (1 + \tau_{cp_i}s)^{-1} \tag{36}$$

and the first factor can be approximated by

$$\prod_{i=1}^{q} (1 + \tau_{cp_i}s)^{-1} \approx 1 - \left(\sum_{i=1}^{q} \tau_{cp_i}\right)s \approx \exp\left[-\left(\sum_{i=1}^{q} \tau_{cp_i}\right)s\right] \tag{37}$$

For simple acid—base reactions, $\tau_{c_2} \ldots \tau_{c_{n-q}}$ become zero and τ_{c_1} is of the order of 0.1 s, while for some complexiметric reactions, $\tau_{c1} \ldots \tau_{cn-q}$ can be some minutes. In this latter case, the effects of the dominant time constants must be taken into account when an automated titrator is to be developed.

Bimolecular reactions without side-reaction are represented by the reaction scheme

$$A + B \underset{k_{f_1}}{\overset{k_{b_1}}{\rightleftharpoons}} AB + B \underset{k_{f_2}}{\overset{k_{b_2}}{\rightleftharpoons}} AB_2 + \ldots AB_{n-1} + B \underset{k_{f_n}}{\overset{k_{b_n}}{\rightleftharpoons}} AB_n \tag{38}$$

The reaction is considered as a system with a concentration change of A as input and a concentration change of AB_n as output. If it is again assumed that the forward reactions are relatively fast, then for $t > 0$ the set of differential equations (39) is obtained. In the case that the first reaction step is the dominant reaction with the initial ($t = 0$) conditions: $[A](0) = a$, $[B](0) = b_1$, and $[AB](0) = 0$, then with $[A](t) = x$, $[B](t) = y$, and $[AB](t) = z$, the initial value problem Eqn. (40) is obtained

$$\begin{aligned}
d[A]/dt &= -k_{f_1}[A][B] \\
d[AB]/dt &= k_{f_1}[A][B] - k_{f_2}[AB][B] \\
&\vdots \\
d[AB_n]/dt &= k_{f_n}[AB_{n-1}][B] \\
d[B]/dt &= -k_{f_1}[A][B] - k_{f_2}[AB][B] - \ldots - k_{f_n}[AB_{n-1}][B]
\end{aligned} \tag{39}$$

$$\begin{aligned}
dx/dt &= -k_{f_1}xy \\
dy/dt &= -k_{f_1}xy \\
dz/dt &= +k_{f_1}xy
\end{aligned} \tag{40}$$

with $x(0) = a$, $y(0) = b_1$, and $z(0) = 0$

From these relations it follows immediately that for $t \geqslant 0$

$$a - x = b_1 - y = z \tag{41}$$

Integration of Eqn. (40) yields for $a < b_1$ the result

$$\begin{aligned}
[\mathrm{A}] &= x = [a(a - b_1) \exp(-t/\tau_c)] / [a \exp(-t/\tau_c) - b_1] \\
[\mathrm{B}] &= y = b_1(a - b_1) / [a \exp(-t/\tau_c) - b_1] \\
[\mathrm{AB}] &= z = ab_1[1 - \exp(-t/\tau_c)] / [b_1 - a \exp(-t/\tau_c)] \\
\text{with } \tau_c &= 1/k_{f_1}(b_1 - a)
\end{aligned} \tag{42}$$

while for $t > \tau_c$, set (42) tends to $[\mathrm{A}] = x \approx 0$; $[\mathrm{B}] = y \approx b_1 - a = b_2$; and $[\mathrm{AB}] = z \approx a$.

After every new addition of titrant the time constant τ_c will increase to a maximum until the end-point is reached. At the beginning of the titration, where $b_1 \gg a$ and the value b_1 does not change very much, Eqn. (42) may be described as

$$\begin{aligned}
[\mathrm{A}] &= x \approx a \exp(-k_{f_1} b_1 t) \\
[\mathrm{B}] &= y \approx b_1 \\
[\mathrm{AB}] &= z \approx a[1 - \exp(-k_{f_1} b_1 t)]
\end{aligned} \tag{43}$$

Hence, for $b_1 \gg a$, the chemical reaction system is approximated by a pseudo-first-order chemical reaction [5].

Mathematical as well as modelling problems will arise when one has to consider chemical reaction systems where the dominant time constant is no longer a constant. These non-constant parameter systems have to be treated in a different way, because they cannot be described by a simple system transfer function. In general, a monomolecular reaction system or a bimolecular reaction system, acting as a pseudo-first-order reaction, can be described by the general form of Eqn. (36).

Finally, some attention must be paid to the proportionality factor μ_c^*, which gives the ratio of input (concentration of mixed titrant) and output (concentration of the reaction product) in the equilibrium state. After the end-point, the concentration of the reaction product will stay constant, while before the end-point the concentration of the reaction product changes proportionally to the added volume of titrant (neglecting volume changes). An extensive example is presented in the following section on "systematic errors in titrations with continuous addition of titrant".

The transfer function of the combination of the mixing system and that of the chemical reactions is not simply the product of the transfer functions $H_m(s)$ and $H_c(s)$. These transfer functions both contain a factor $1/s$, representing an integration with respect to t, which means, in physical terms, a storage of each output. Because there is no storage between the two phases of the mixing and the chemical reaction processes, the following expression

is obtained for the transfer function of the combination of the mixing system and the chemical reaction system:

$$H_{mc}(s) = H_m(s)H_c(s)s$$

$$\text{with } H_m(s) = [\tau_{m1}s(1 + \tau_{m2}s)]^{-1} \tag{44}$$

$$\text{and } H_c(s) = [s(1 + \tau_{c1}s)(1 + \tau_{c2})]^{-1} \exp(-\tau_{\text{delay}}s)\mu_c^*$$

where $H_c(s)$ is supposed to have two dominant time constants and a delay time (see Eqn. (36) for $n - q = 2$).

In the case where the reaction is very fast and consequently the time constants τ may be neglected, the relation between the input and output concentrations of the chemical reaction system, $C_i(t)$ and $C_0(t)$, respectively, is given by $C_0(t) = \mu_c^* \bar{u}(t_{eq} - t)C_i(t)$, where t_{eq} is the time needed to reach equivalence. The function $\mu_c^* \bar{u}(t_{eq} - t)$ is not linear and therefore the chemical reaction cannot be described by a system transfer function. Otherwise the important algebraic relations (6), (7) and (8) would be violated. This is the reason why formula (44) is only applicable as long as the equivalence point has not been reached.

Detection system

Most detectors used in potentiometric titrations are ion-selective electrodes. The most widely used ion-selective electrodes are the glass membrane electrodes for pH measurements. Adequate descriptions of the dynamic properties of such glass electrodes have been given by many workers in the field of electroanalytical sciences [6—15]. The mathematical description is based on Fick's law, on the assumption that the diffusion process through the boundary layer is the slowest electrode process. For a stepwise change of the sample concentration, this results in an exponential change of the activity in the boundary layer. An exception must be made for electrodes of the neutral-carrier type. According to Morf et al. [13], a stepwise change of the sample concentration or activity can be described by

$$a_{i_{\text{bulk}}}(t) = \begin{cases} 0 & t < 0 \\ a_{\text{bulk}} & t > 0 \end{cases} \tag{45}$$

and the corresponding change of the activity in the boundary layer is represented by

$$a_i(t) = a_{\text{bulk}}[1 - \exp(-t/\tau_d)] \tag{46}$$

with $\tau_d = 4\delta^2/\pi^2 D$, where $a_i(t)$ is the activity in the boundary layer, a_{bulk} is the activity in the bulk sample solution at $t > 0$, δ is the thickness of the diffusion layer, and D is the diffusion coefficient of the aqueous boundary layer. If Eqn. (46) is considered as the output response of a system and Eqn. (45) as an input stimulus, the system transfer function can be obtained with the use of Eqn. (4)

$$H_d(s) = \frac{L\{a_{bulk}[1 - \exp(-t/\tau_d)]\}}{L\{a_{bulk}\bar{u}(t)\}} = \frac{s^{-1} - (s + 1/\tau_d)^{-1}}{s^{-1}} = 1/(1 + \tau_d s) \qquad (47)$$

The transducing step from the activity in the layer boundary to an electric voltage is given by a simplified Nernst equation, if contributions of liquid junction potentials are neglected:

$$E(t) = E_i^0 + S \log a_i(t) \qquad (48)$$

where $E(t)$ is the electrode (cell) potential, E_i^0 the standard potential of the electrode assembly, and S the Nernstian slope. As the logarithm operation is not a linear operation, the relation between $E(t)$ and $a_i(t)$ cannot simply be defined in terms of a system transfer function with the validity of the properties given in Eqns. (6), (7) and (8). This step in the system chain can only be described with the aid of Eqn. (48) in the time domain. In block diagrams, the non-linear operation is usually represented by double lines, as shown in Fig. 4. In this particular case the transfer in the time domain is denoted by the functional μ_d: $\mu_d[a_i(t)] = E_i^0 + S \log a_i(t) = E(t)$. The same phenomenon has been met already in the case of fast chemical reactions.

It is worthwhile to comment on the detector model. First, the time constant τ_d depends on the rate of mixing, because the average thickness of the diffusion layer δ is influenced by the mixing speed (Eqn. 46). It has been shown in the experimental work of Lindner et al. [11, 13] that these effects should not be neglected. A second effect is an extra noise contribution in the electrode signal $E(t)$ caused by stirring. The authors have not investigated the properties of this noise contribution and the relation of these properties with the diffusion layer thickness. Probably, it will be a first-order band-limited noise with a disturbance time constant equal to τ_d. Therefore, the model must be extended by an extra white noise contribution $\underline{n}(t)$, as shown in Fig. 4.

For spectrophotometric detection, a similar detector model may be obtained. However, in this case, τ_d will be very small in practice and μ_d is described by the Lambert—Beer law.

Transducer and measuring system

In the final part of the analytical chain, electronic instruments are applied in order to adapt the signals from the detector for registration, data handling and data reduction. These instruments may be electrometric amplifiers in potentiometric titrations or photomultipliers in spectrophotometric titrations,

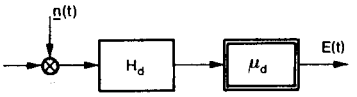

Fig. 4. Block diagram of a detection system with a non-linear subsystem μ_d and an additional noise contribution in the diffusion layer.

combined with a recorder, an analog-to-digital converter (ADC) and a computer for calculating and displaying the results. Time effects in such instruments are usually very small and negligible in comparison with the other time constants in the analytical chain. Therefore, the system transfer function of the transducer and measuring system may be approximated by

$$H_t(s) = \mu_t \tag{49}$$

where μ_t is only a scaling factor.

SYSTEMATIC ERRORS IN TITRATIONS WITH CONTINUOUS ADDITION OF TITRANT

To automate a titration system, aimed at the determination of either a titration curve or one or more end-points, there are two approaches. The first is continuous addition of titrant. This approach is only of practical value if the system parameters of the several subsystems are constant during titration. If the system parameters of one or more of the subsystems change during titration, discontinuous addition of titrant is more practical. In the investigation of systematic errors, caused by dominant and constant system parameters, a simplified model of a complexiметric titration will be considered, with dominant mixer time constants and a dominant detector time constant. The chemical reaction is assumed to be very fast, while the contributions of stochastic signals, from mixing, are neglected for the moment (see Fig. 5).

Let $q(t) = m$ m^3 s^{-1} be the input of the system, which is a continuous addition of titrant (ligand, L) of concentration C_{titrant}. The output of the mixing system, with a system transfer function $H_m = (\tau_{m1}s)^{-1}(1 + \tau_{m2}s)^{-1}$, will be the concentration of the added and mixed ligand $C_L(t)$. The chemical reaction of the complexiметric reaction can be described by a bimolecular equilibrium reaction

$$M + L \underset{k_b}{\overset{k_f}{\rightleftharpoons}} ML \tag{50}$$

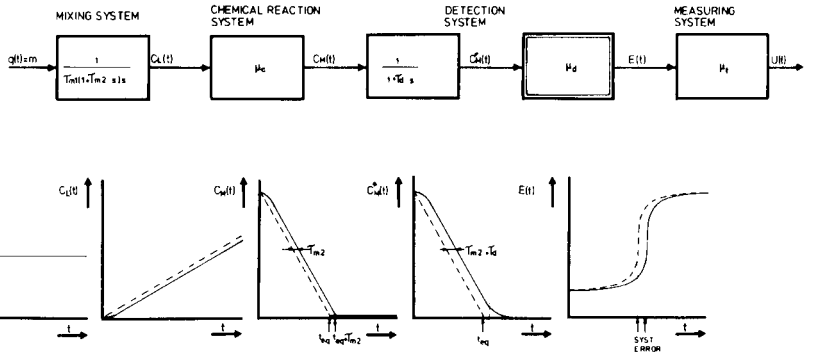

Fig. 5. Representation of a simplified complexiметric titration indicated with an ion-selective electrode.

with $k_b \ll k_f$. Considering the chemical reaction as a system with the concentration of the ligand $C_L(t) \equiv [L](t)$ as input, and the concentration $C_M(t) \equiv [M](t)$ of the metal M as output, the system can be described by a non-linear differential equation of the Bernoulli—Ricatti type [14, 15]. When the reaction is relatively fast, the chemical reaction time constants can be neglected and the system transfer function $H_c(s) = \mu_c^*/s$. The combination of the mixer and the chemical reaction system (Eqn. 44) yields

$$H_{mc}(s) = (1/\tau_{m1}s)[1/(1 + \tau_{m2}s)]\mu_c^* \tag{51}$$

The functional μ_c^* is only determined in the time domain by the equilibrium relation

$$K \equiv k_f/k_b = [ML]/[M][L] \tag{52}$$

and the stoichiometric relations

$$[M] + [ML] = C_M(0) \text{ and } [L] + [ML] = C_L(t) \tag{53}$$

Substituting $[M] = C_M(0) - [M]$ and $[L] = C_L(t) + [M] - C_M(0)$ into Eqn. (52) and solving the resulting quadratic equation for [M] yields

$$[M] = C_M(t) = 0.5\{-(C_L(t) - C_M(0) + 1/K) + [(C_L(t) - C_M(0) + 1/K)^2 + 4C_M(0)/K]^{1/2}\} \tag{54}$$

The total time necessary for delivery of the amount of titrant, equivalent to $C_M(0)$, will be denoted by t_{eq}. For sufficiently large values of K (about 10^{19} for Cu/EDTA), Eqn. (54) can be written as

$$C_M(t) = \mu_c^*[C_L(t)] = [C_M(0) - C_L(t)]\,u(t_{eq} - t) \tag{55}$$

where the functional μ_c^*, which is defined by the right-hand side of Eqn. (55), denotes the system transfer function in the time domain.

The conversion of the metal ion concentration $C_M(t)$ to an electric signal is achieved by an ion-selective electrode, with a dominant time constant τ_d, and may be described by a system transfer function $H_d(s) = 1/(1 + \tau_d s)$ and a non-linear operation μ_d (see Eqns. 47 and 48). The transducer and measuring system is a combination of an amplifier, an ADC and a computer with an algorithm which produces the inverse of the operator μ_d. In principle, the signal now obtained is a direct measure of the concentration $C_M^*(t)$.

The same result is obtained in the case of a spectrophotometric detector, with one difference, viz. that the time constant τ_d is relatively small. With the aid of Eqn. (51), in this particular case

$$C_M(t) = \mu_c^*\{L^{-1}[m(\tau_{m1}s)^{-1}(1 + \tau_{m2}s)^{-1}]\} = \mu_c^*[C_L(t)] \tag{56}$$

After the inverse Laplace transform, $C_L(t)$ is given by

$$C_L(t) = (m/\tau_{m1})[t - \tau_{m2} + \tau_{m2} \exp(-t/\tau_{m2})] \tag{57}$$

For $t \gg 5\tau_{m2}$, the concentration change of $C_L(t)$ is proportional to $(t - \tau_{m2})$. The measured end-point will be shifted over a time interval τ_{m2}. Taking this into account, Eqn. (56) can be described as

$$C_M(t) = \begin{cases} C_M(0) - (m/\tau_{m1})[t - \tau_{m2} + \tau_{m2} \exp(-t/\tau_{m2})] & 0 < t < t_{eq} + \tau_{m2} \\ 0 & t > t_{eq} + \tau_{m2} \end{cases} \tag{58}$$

To obtain the concentration $C_M^*(t)$ in the boundary layer of the electrode, we assume that Eqn. (58) describes the input of the electrode system with a system transfer function $H_d(s) = 1/(1 + \tau_d s)$. Let $h_d(t)$ be the impulse response on the unit impulse stimulated at $t = 0$, then the response at time t on an arbitrary signal $x(t)$ is given by Eqn. (5). Applying this equation for an input stimulus $C_M(t)$, which is zero for $t > t_{eq} + \tau_{m2}$, we find

$$C_M^*(t) = \int_0^t C_M(\tau) h_d(t - \tau) d\tau \qquad \text{for } 0 < t < t_{eq} + \tau_{m2}$$

$$\text{and } C_M^*(t) = \int_0^{t_{eq} + \tau_{m2}} C_M(\tau) h_d(t - \tau) d\tau \qquad \text{for } t > t_{eq} + \tau_{m2} \tag{59}$$

Substitution of $h_d(t - \tau) = 1/\tau_d \exp(-(t - \tau)/\tau_d)$ and Eqn. (58) into Eqn. (59) yields for $0 < t < t_{eq} + \tau_{m2}$

$$C_M^*(t) = C_M(0) - \frac{m}{\tau_{m1}} \{t - \tau_d - \tau_{m2}\} + \frac{m}{\tau_{m1}} \left\{ \frac{\tau_d^2}{(\tau_{m2} - \tau_d)} \exp(-t/\tau_d) - \frac{\tau_{m2}^2}{(\tau_{m2} - \tau_d)} \exp(-t/\tau_{m2}) \right\} \tag{60}$$

and for $t \geqslant t_{eq} + \tau_{m2}$

$$C_M^*(t) = C_M(0) - \frac{m}{\tau_{m1}} \{t_{eq} - \tau_d\} \exp\{-(t - \tau_{eq} - \tau_{m2})/\tau_d\} + \frac{m}{\tau_{m1}} \left[\frac{\tau_d^2}{(\tau_{m2} - \tau_d)} \exp\{-t/\tau_d\} - \frac{\tau_{m2}^2}{(\tau_{m2} - \tau_d)} \exp\{-t/\tau_{m2}\} \times \exp\{-(t - t_{eq} - \tau_{m2})/\tau_d\} \right] \tag{61}$$

Considering Eqn. (60) in a time interval 5 MAX $\{\tau_{m2}, \tau_d\} < t < t_{eq} + \tau_{m2}$, where MAX$\{\tau_{m2}, \tau_d\}$ denotes the larger of the two time constants, the transient parts may be neglected, and so

$$C_M^*(t) = C_M(0) - (m/\tau_{m1})(t - \tau_d - \tau_{m2}) \text{ for } 5 \text{ MAX}\{\tau_{m2}, \tau_d\} < t < t_{eq} + \tau_{m2} \tag{62}$$

On the same assumption, Eqn. (61) can be simplified to

$$C_M^*(t) = C_M(0) - \frac{m}{\tau_{m1}} \{t_{eq} - \tau_d\} \exp\{-(t - t_{eq} - \tau_{m2})/\tau_d\} \text{ for } t > t_{eq} + \tau_{m2} \quad (63)$$

To obtain some practical rules for continuous titrations with constant and known system parameters, the former theoretical considerations may be used with the aid of Eqns. (62) and (63). It is now clear that under the condition

$$5\,\text{MAX}\{\tau_d, \tau_{m2}\} \ll t_{eq} \quad (64)$$

the systematic error in the obtained end-point volume will be $m(\tau_{m2} + \tau_d)$, hence the measured end-point volume $v_{\text{end-point}} = v_{eq} + m(\tau_{m2} + \tau_d)$.

In considering continuous titration processes where the mixer and the detector time constants are no longer dominant, it becomes necessary to introduce the chemical reaction time constants τ_c, as explained before. Because they all appear as indicated in Eqn. (44), it is found that the condition

$$5\,\text{MAX}\{\text{all time constants}\} \ll t_{eq} \quad (65)$$

yields approximately a systematic error of

$$\text{Error} = m\Sigma\{\text{all time constants}\} \quad (66)$$

When the electrode potential $E(t)$ is used directly for end-point determination without converting the signal (maximum slope determination), the same rules as derived before are valid, but with the extra condition that τ_d should be small. In that case the sigmoidal titration curve is shifted over a time interval equal to Σ(all time constants), without distortion in the end-point area. The theory can also be used in procedures to obtain the overall time constant (= Σ all time constants).

When several titrations are done at different addition speeds, the relation of addition speed versus uncorrected end-points is a straight line. The intersection of the line with the end-point axis is the correct end-point, while the slope is the overall time constant (see Fig. 6).

DISCONTINUOUS ADDITION OF TITRANT: SAMPLING FREQUENCY

If the dominant time constants are unknown and dependent on actual concentrations during the titration, a better approach is discontinuous addition, i.e., a new volume of titrant is added after equilibrium has been attained. This approach is generally used in manual titrations. When these titrations are automated, it is necessary to decide how many additions are required either to construct a complete titration curve or to determine the end-point, and how long one has to wait between two additions of titrant. A combination of both will influence the total time of analysis. Two applications of titrimetry must be distinguished. One is in solution equilibrium studies, to obtain very precise and accurate equilibrium constants [16, 17]. The other is

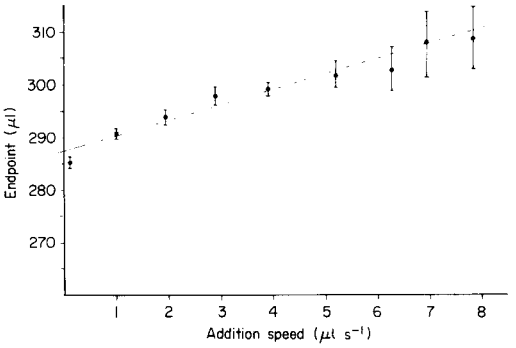

Fig. 6. Uncorrected end-point as a function of the addition speed. Titration of 0.001 M Cu(II) with 0.1 M EDTA indicated by an Orion Cu^{2+}-selective 94-92 A electrode. The t_{ep} values are measured and end-point volumes including their standard deviation are calculated from $v_{ep} = mt_{ep}$ and $\sigma^2_{v(ep)} = m^2\sigma^2_{t(ep)}$. A weighted fit is used to determine the coefficients of the model function $y = A + Bx$. The value of A is the end-point volume without a systematic error and the slope B is the overall time constant to the titration process. A = 288 μl, S_A = 0.75 μl, B = 3 s, S_B = 0.22 s.

in routine analysis to locate end-points which then may be used for open or closed loop control. In the latter application of titrimetry, the duration of the measurements may be as important as the precision and accuracy for the required control (see, e.g., [18]).

The number of required equilibrium points will depend strongly on the selected titration procedure (sigmoidal or segmented titration curves) and on the method selected for calculating the end-point. Frequently, the result from a sigmoidal curve is based on visual estimation of the volume corresponding to the maximum slope of the titration curve, $E = E(v)$; this volume has also been evaluated from the maximum of the first derivative or the zero crossing of the second derivative. Reliable values for the end-point volume require that a large number of equilibrium points be measured in the neighbourhood of the potential jump, whereas in principle no measurements are needed in the flat parts of the sigmoidal curve.

Here, the number of points necessary to describe the potential jump adequately with a minimum loss of information and without introducing aliasing effects, is based on the sampling theorem of Shannon [19]. This theorem will be explained when it is applied later.

The steepest part of a symmetrical sigmoidal titration curve can be described by a model function (see Fig. 7A)

$$y(v) = (A/\pi)\ \text{arctg}\ (v/B) \tag{67}$$

where $y(v)$ is the detector output, v the volume of added titrant, and A and B are model parameters. Equation (67) can be rewritten in the form

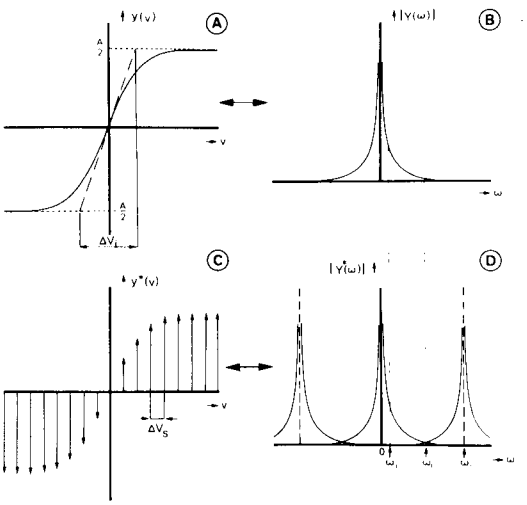

Fig. 7. A, Representation of a sigmoidal titration curve. B, Representation of the Fourier transform of function A. C, Representation of an equidistant-sampled sigmoidal titration curve. D, Representation of the Fourier transform of function C.

$$y(v) = y_1(v) + y_2(v)$$

$$\text{with } y_1(v) = \begin{cases} A - (A/\pi)\ \text{arccotg}\ (v/B) & t < 0 \\ -(A/\pi)\ \text{arccotg}\ (v/B) & t > 0 \end{cases} \tag{68}$$

$$\text{and } y_2(v) = A/2\ \text{sgn}\ (v) = \begin{cases} -A/2 & t < 0 \\ A/2 & t > 0 \end{cases}$$

The Fourier transform of $y(v)$ is given by $F\{y(v)\}(\omega) = F\{y_1(v)\}(\omega) + F\{y_2(v)\}(\omega)$ with $F\{y_1(v)\}(\omega) = -(A/j\omega) + (A/j\omega)\exp\{-\omega B\}$ and $F\{y_2(v)\}(\omega) = A/j\omega$, where $F\{y_2(v)\}(\omega)$ is obtained after applying the Fourier transform in a distributional sense [20]. Finally, the amplitude spectrum is given by

$$|\dot{Y}(\omega)| = |F\{y(v)\}(\omega)| = |(A/\omega)\exp\{-\omega B\}| \tag{69}$$

Information on distribution theory is readily available [20, 21]. In the steepest part of the titration curve, waveforms with higher frequencies, say $|\omega| > \omega_i$, are necessary to describe the jump. The potential jump is estimated by the first derivative of $y(v)$ with respect to v

$$(dy(v)/dv)_{v=0} = A/B\pi \tag{70}$$

The intersections of the tangent in the inflection point and the lines $y = A/2$ and $y = -A/2$ can be calculated by using Eqn. (70), resulting in the points

$(\pm B\pi/2,\ \pm A/2)$ and an interval $\Delta V_i = B\pi$. In the next section, Shannon's theorem is applied in order to relate ΔV_i to the sampling volume ΔV_s by using $\omega_i = 2\pi/\Delta V_i$ and $\omega_s = 2\pi/\Delta V_s$. If the function $y(v)$ is sampled with a sampling interval ΔV_s, which interval is so far unknown, the function obtained (Fig. 7C) can be described by

$$y^*(v) = y(v) \sum_{n=-\infty}^{+\infty} \delta(v - n\Delta V_s) = y(v)\delta_{\Delta V_s}(v) \tag{71}$$

where $\delta_{\Delta V_s}(v)$ denotes the sampling function. Fourier transform of Eqn. (71) yields

$$Y^*(\omega) = F\{y(v)\delta_{\Delta V_s}(v)\}(\omega) = (1/2\pi)F\{y(v)\}(\omega) * F\{\delta_{\Delta V_s}(v)\}(\omega) \tag{72}$$

When the distribution theory is applied again, the Fourier transform of the sampling function is obtained, resulting in

$$F\{\delta_{\Delta V_s}(v)\}(\omega) = \sum_{n=-\infty}^{+\infty} e^{jn\Delta V_s\omega} = \omega_s \sum_{n=-\infty}^{+\infty} \delta(\omega - n\omega_s) \tag{73}$$

From Eqns. (72) and (73)

$$Y^*(\omega) = \frac{\omega_s}{2\pi} Y(\omega) * \sum_{n=-\infty}^{+\infty} \delta(\omega - n\omega_s) = \frac{\omega_s}{2\pi} \sum_{n=-\infty}^{+\infty} Y(\omega - n\omega_s) \tag{74}$$

Equation (74) is only valid for band-limited signals, i.e., $Y(\omega) = 0$ for $|\omega| > \omega_c$, where ω_c is the cut-off frequency. It follows from Eqn. (74) that the spectrum $Y^*(\omega)$ of a sampled function $y(v)$ is a composite of a repeated function $Y(\omega)$, only if $\omega_s > 2\omega_c$ (see Fig. 7D). Hence, in order to obtain a sampling interval ΔV_s which does not introduce aliasing effects, we need

$$\Delta V_S < \pi/\omega_c \tag{75}$$

which is simply Shannon's theorem. From this theorem, it follows that all information about a signal $y(v)$ is present in $Y^*(\omega)$ if the spectra have no overlap. Hence, it must be remarked that the signal $Y(\omega) = F\{A/\pi \text{ arctg } v/B\}(\omega)$ is not band-limited. By using Eqn. (69), it is observed that truncation of the signal in the frequency domain at a point $|Y(\omega_c)| = 0.01\ |Y(\omega_i)|$ will not yield large errors. Hence

$$(1/\omega_c) \exp(-B/\omega_c) = 0.01\ (1/\omega_i) \exp(-B/\omega_i) \tag{76}$$

and substitution of $\omega_c = 2\pi/\Delta V_c$, $\omega_i = 2\pi/\Delta V_i$, and $\Delta V_i = B\pi$ into Eqn. (76) gives

$$(\Delta V_c/\Delta V_i) \exp[(-2\Delta V_i)/\Delta V_c + 2] - 0.01 = 0 \tag{77}$$

which yields in numerical approximation, by applying the Newton—Raphson iteration procedure

$$\Delta V_c/\Delta V_i \approx 0.36 \tag{78}$$

For the required sample volume ΔV_s, the relations (75) and (78) give the upper boundary

$$\Delta V_s < \pi/\omega_c = \Delta V_c/2 \approx 0.18\,\Delta V_i \tag{79}$$

Another method of obtaining end-points is to linearize the sigmoidal curves. This method, the Gran method [22] is based on dv/dE values. A symmetrical sigmoidal titration curve is represented by the inverse hyperbolic function

$$E(v) = B + A\,\ln[x + (x^2 + 1)^{1/2}] \tag{80}$$

with $x = f(v) = av + b$, where v is the volume of added titrant and A, B, a and b are parameters; the equivalence point lies at $x = 0$. For a simple acid—base titration, a and b are determined respectively by $a = -c/(2v_{eq}K_w^{1/2})$ and $b = +c/(2K_w^{1/2})$, while $b/a = -v_{eq}$ (c is the start concentration and K_w the equilibrium constant 10^{-14}). If a small area $[v_{eq} - \zeta, v_{eq} + \zeta]$, centered at v_{eq}, is taken, Eqn. (80) may be described approximately for $0 \leqslant v \leqslant v_{eq} - \zeta$ by

$$E(v) = B + A\,\ln(2x) \approx C + A\,\ln(x) = C + A\,\ln(f(v)) \tag{81}$$

with $C = B + A\,\ln 2$, and for $v_{eq} + \zeta \leqslant v \leqslant 2v_{eq}$ by

$$E(v) = B + A\,\ln x[1 - (1 + 1/x^2)^{1/2}] \approx D - A\,\ln(-x) = D - A\,\ln[-f(v)] \tag{82}$$

with $D = B - A\,\ln 2$, because for $0 \leqslant v \leqslant v_{eq} - \zeta$ and for $v_{eq} + \zeta \leqslant v \leqslant 2v_{eq}$, the values of x are respectively $+10^6$ and -10^6. Now the functions

$$dv/dE = +A^{-1}v - v_{eq}/A \qquad \text{for } 0 \leqslant v \leqslant v_{eq} - \zeta$$

$$\text{and } dv/dE = -A^{-1}v + v_{eq}/A \qquad \text{for } v_{eq} + \zeta \leqslant v \leqslant 2v_{eq}$$

are linear functions with respect to the volume, with a point of intersection at $v = v_{eq}$.

In the original work [22] Gran pointed out that for a large variety of acid—base, precipitation, complexiметric and oxidation-reduction titrations, the intersection of the two lines obtained corresponds to the end-point volume. The introduction of linear regression and asymmetry coefficients [23] and corrections for side-reactions [24] are useful extensions of the Gran method in the sense of accuracy and precision in end-point determinations carried out by computer programs.

The minimum number of points needed to describe such linearized sigmoidal titration curves depends on the mathematical approximation of the linear segments. However, the number of samplings needed for the $\Delta V/\Delta E$ procedure in order to obtain the linear segments with minimal loss of information, is determined by condition (79).

When multiparametric fitting procedures are used, where titration curves are expressed by means of a mathematical approximation based on equilibrium, mass conservation or other physical laws, the number of samplings

needed depends on the number of unknown parameters in the approximation and on the requirements of accuracy and precision in the end-point determination. Many workers in this field have developed models, procedures and computer programs for a large variety of titration techniques [25—30].

DISCONTINUOUS ADDITION OF TITRANT: EQUIDISTANT ΔE VALUES

For linearly indicated titrations and for many other titrations where the titration curve consists of two or more nearly linear segments, the titrant can be added with equidistant additions, ΔV. For sigmoidal curves, however, the minimum addition necessary to describe the neighbourhood of the potential jump, implies a large number of equidistant minimum additions. For this kind of titration, where the end-point calculations are based on dE/dv or d^2E/dv^2 methods, it is preferable to use non-equidistant additions in such a way that the ΔE values are constant. This can be established by means of an algorithm which controls the motor burette. The algorithm will be derived first. A large class of symmetrical sigmoidal titration curves can be represented by an inverse hyperbolic function as shown in Eqn. (80). To derive the algorithm, only a single part of the titration curve, described by Eqn. (81), need be considered. The task is as follows: given three values of E, say E_{n-2}, E_{n-1} and E_n with $E_{n-1} - E_{n-2} = E_n - E_{n-1} = \Delta E$, and given the corresponding values v_{n-2}, v_{n-1} with $\Delta V_{\text{old}} = v_{n-1} - v_{n-2}$, the corresponding value v_n and consecutively $\Delta V_{\text{new}} = v_n - v_{n-1}$ must be determined (see Fig. 8). With the aid of the derivatives of $E(v)$ (Eqn. 81) in the points v_{n-2} and v_{n-1}, viz.

$$\begin{aligned}(dv/dE)_{v=v_{n-2}} &= A^{-1}v_{n-2} + b/Aa =: y_{n-2}\\ \text{and } (dv/dE)_{v=v_{n-1}} &= A^{-1}v_{n-1} + b/Aa =: y_{n-1}\end{aligned} \tag{83}$$

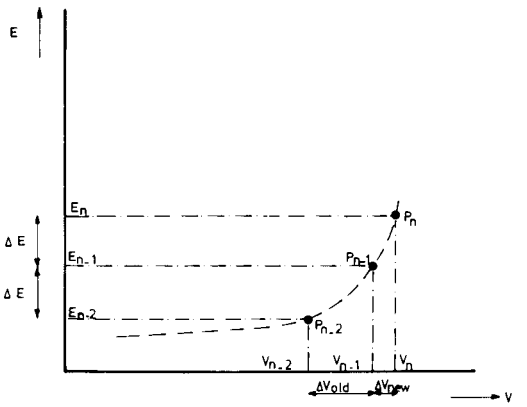

Fig. 8. Outline of a control algorithm, controlling constant ΔE values in potentiometric titrations.

the values of the quantities A^{-1} and b/Aa can be converted to y_{n-2} and y_{n-1}. Substituting this into the expression for the derivative in the point v_n yields

$$\left(\frac{dv}{dE}\right)_{v=v_n} = \left(\frac{y_{n-2}-y_{n-1}}{v_{n-2}-v_{n-1}}\right) vn + \frac{v_{n-2}y_{n-1}-v_{n-1}y_{n-2}}{v_{n-2}-v_{n-1}} =: y_n \tag{84}$$

When Eqn. (84) is used for v_n and v_{n-1} it follows that

$$y_n - y_{n-1} = [(y_{n-1}-y_{n-2})/(v_{n-1}-v_{n-2})](v_n - v_{n-1}) \tag{85}$$

$$\text{or } \Delta V_{new} = \Delta V_{old}/[(y_{n-1}-y_{n-2})/(y_n - y_{n-1})] \tag{86}$$

where $\Delta V_{new} = v_n - v_{n-1}$ denotes the new addition of titrant and $\Delta V_{old} = v_{n-1} - v_{n-2}$ is the last added quantity. If $(E_n - E_{n-1}) = (E_{n-1} - E_{n-2}) = \Delta E = \Delta E_{old}$, then according to Eqn. (81):

$$(av_n + b)/(av_{n-1} + b) = (av_{n-1} + b)/(av_{n-2} + b) \tag{87}$$

As $Aay = av + b$, Eqn. (87) can be rewritten as

$$y_n y_{n-2}/(y_{n-1})^2 = 1 \quad \text{or} \quad y_n = (y_{n-1})^2/y_{n-2} \tag{88}$$

With the aid of Eqn. (88), the denominator of Eqn. (86) becomes

$$(y_{n-1}-y_{n-2})/(y_n - y_{n-1}) = y_{n-2}/y_{n-1} \tag{89}$$

and hence by Eqns. (83) and (81)

$$(y_{n-1}-y_{n-2})/(y_n - y_{n-1}) = y_{n-2}/y_{n-1} = \exp(\Delta E/A) = k_1 \tag{90}$$

and so

$$\Delta V_{new} = \Delta V_{old}/k_1 \tag{91}$$

From Eqn. (91) it follows that any new addition is obtained by dividing the former addition by a factor k_1, which results in equidistant ΔE values. When Eqn. (91) is applied to control the motor burette, there will be no feedback of the measured ΔE_{old} values. The introduction of a deviation factor $\epsilon = \Delta E/\Delta E_{old}$, where ΔE denotes the set value and ΔE_{old} the measured value, makes the control algorithm complete

$$\Delta V_{new} = \epsilon(\Delta V_{old}/k_1) \tag{92}$$

with $\epsilon > 1$ for $\Delta E > \Delta E_{old}$, and $0 < \epsilon < 1$ for $\Delta E < \Delta E_{old}$. The feedback is shown schematically in Fig. 9. Rewriting Eqn. (92) provides an algorithm for the first part of the titration curve

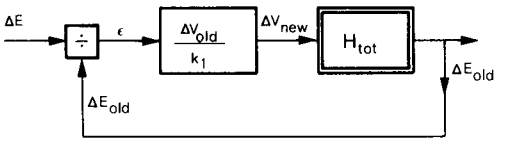

Fig. 9. Representation of an algorithm for closed loop control for equidistant ΔE values in sigmoidal titration curves. H_{tot} denotes the complete titration equipment.

$$\Delta V_{new} = \Delta V_{old}\, \Delta E/\Delta E_{old}\, k_1 \tag{93}$$

with $k_1 = \exp(\Delta E/A)$ for $0 \leqslant v \leqslant v_{eq} - \zeta$.

In a similar way an algorithm for the second part of the titration curve can be derived from Eqn. (82), which results in

$$\Delta V_{new} = (\Delta V_{old}/\Delta E_{old}) - (\Delta E/k_2) \tag{94}$$

with $k_2 = \exp[-\Delta E/A]$ for $v_{eq} + \zeta \leqslant v \leqslant 2v_{eq}$.

If ΔE is small compared to A, Eqns. (93) and (94) may be replaced by a single control algorithm for the complete titration curve

$$\Delta V_{new} = (\Delta V_{old}/\Delta E_{old}) - (\Delta E/k') \tag{95}$$

with $k' = (k_1 + k_2)/2$. In order to apply the control algorithm, the slope A is the only parameter which should be determined.

The algorithm expressed in Eqn. (95) has the disadvantage that it is not very stable in the flat parts of the titration curve. The reason is that the value of the difference quotient $\Delta E_{old}/\Delta V_{old}$ in the flat parts of the titration curve is extremely sensitive to instrumental noise. The new addition ΔV_{new} will then be determined by the stochastic character of the noise in the detector signal. If accidentally the value ΔE_{old} becomes very small, the new addition ΔV_{new} becomes unrealistically high. A second disadvantage is that the algorithm is not self-starting, because at least one addition has to be made before the algorithm can work. To solve both problems, an extra parameter ΔV_{max} is introduced, denoting the maximum possible addition during titration, and further the absolute value of the difference quotient $\Delta E_{old}/\Delta V_{old}$ is used. The titration starts with a first addition, equal to ΔV_{max}, and equidistant ΔE values will then be controlled

$$\Delta V_{new} = \Delta V_{max}/\{1 + k|\Delta E_{old}/\Delta V_{old}|\} \tag{96}$$

with $k = \Delta V_{max}\{[\exp(-\Delta E/A) + \exp(\Delta E/A)]/2\}$

The algorithm of Eqn. (96) is quite simple and stable, and is easy to implement in a microcomputer-based apparatus. Furthermore, it can be used in titrimetric analysis with one or more end-points [31].

The above-mentioned method for the calculation of new additions may be improved by an algorithm, not based on linear extrapolation but on hyperbolic extrapolation. It is assumed that small parts of the titration curve may be described by the hyperbolic function

$$E(v) = [A/(B + v)] + C \tag{97}$$

with three parameters A, B and C. Given four values, E, say E_{n-3}, E_{n-2}, E_{n-1} and E_n, with only $E_n - E_{n-1} = \Delta E$ being the set value, and given the corresponding values v_{n-3}, v_{n-2} and v_{n-1}, the task is now to determine the value v_n and consecutively $\Delta V_{new} = v_n - v_{n-1}$. To simplify the calculations, a scaling and shifting factor is introduced for the E coordinate as well as for the v coordinate in such a way that $(v'_{n-3}, E'_{n-3}) = (0, 0)$ and $(v'_{n-2}, E'_{n-2}) = (1,1)$. Equation (97) may then be described as

$$E'(v') = A'/(B' + v') + C'$$

$$\text{with } v' = (v - v_{n-3})/(v_{n-2} - v_{n-3}) \text{ and } E' = (E - E_{n-3})/(E_{n-2} - E_{n-3}) \tag{98}$$

The new parameters A', B' and C' can be expressed as E'_{n-1} and v'_{n-1} by substituting (0,0), (1,1) into Eqn. (98), which gives

$$A' = -B'(B' + 1); C' = B' + 1; B' = v'_{n-1}(1 - E'_{n-1})/(E'_{n-1} - v'_{n-1}) \tag{99}$$

By using Eqns. (98) and (99), the value v_n and also ΔV_{new} can be calculated, assuming $E_n - E_{n-1} = \Delta E$. The solution is expressed in eight steps, each step can be written as a statement in a computer program written in Fortran-IV:

$$(1)\ v'_{n-1} = (v_{n-1} - v_{n-3})/(v_{n-2} - v_{n-3})$$

$$(2)\ E'_{n-1} = (E_{n-1} - E_{n-3})/(E_{n-2} - E_{n-3})$$

$$(3)\ B' = v'_{n-1}(1 - E'_{n-1})/(E'_{n-1} - v'_{n-1})$$

$$(4)\ A' = -B'(B' + 1) \tag{100}$$

$$(5)\ T_1 = A'(E_{n-2} - E_{n-3})$$

$$(6)\ T_2 = \Delta E(B' + v'_{n-1})$$

$$(7)\ v'_n = (T_1 v'_{n-1} - T_2 B')/(T_1 + T_2)$$

$$(8)\ \Delta V_{new} = v'_n(v_{n-2} - v_{n-3}) + v_{n-3} - v_{n-1}$$

This rather stable algorithm cannot be implemented easily in a microcomputer-based apparatus, but it can be applied successfully in a computer network, where, for example, the control and measuring functions are done by a microcomputer in the laboratory and functions like Eqn. (100) are calculated by a coupled host computer. This approach to laboratory automation is under study [33].

EQUILIBRIUM DETECTION

In automatic titrations with discontinuous addition of titrant, it is necessary to know how long to wait before equilibrium is established in the system. A fixed waiting time, based on the largest observed process time constant, may be very inefficient, especially when the dominant time constant changes significantly during titration. It is obvious that zero detection of the first derivative of the signal $E(t)$ would be a proper criterion for determining the equilibrium state of the system. However, such methods based on zero slope will fail when noise $\underline{n}(t)$ is superimposed on the signal $E(t)$. To explain why, noise that is first-order band-limited with a cut-off frequency $\omega_c = 1/\tau_n$, and a psdf similar to Eqn. (28) are considered

$$G_{nn}(\omega) = 2\tau_n\sigma_n^2/(1 + \omega^2\tau_n^2) \tag{101}$$

The total power of the noise is σ_n^2. Differentiation of the signal $\underline{n}(t)$ gives $\underline{n}'(t)$ with a psdf

$$G_{n'n'}(\omega) = G_{nn}(\omega)|j\omega|^2 = 2\omega^2\tau_n\sigma_n^2/(1 + \omega^2\tau_n^2) \tag{102}$$

Considering the spectrum $G_{n'n'}(t)$ for $\omega\tau_n \gg 1$,

$$G_{n'n'}(\omega) \approx 2\sigma_n^2/\tau_n \tag{103}$$

which is an unlimited white noise with infinite high-frequency contributions and with infinite power. This effect, inherent in differentiation signals, was recognized by Goode [30], who used the first and second derivatives on his spectrophotometric data. The use of filters or "tamed differentiators" can suppress the noise contributions in the higher frequencies, but will probably distort the original signal $E(t)$, implying longer waiting times and also a longer time of titration.

The equilibrium detection method, described in this section, is based on integrating the signal $E(t)$, where $E(t)$ is assumed to be a step response of a system with a dominant time constant τ_{max}.

First, however, some attention must be given to the sampling of signal $E(t)$ with additional noise $\underline{n}(t)$, where the psdf of the noise depends on the place where the noise signal is introduced in the system. From Fig. 10, two approaches are possible. The first is to select a sampling frequency ω_s in such a way that aliasing effects are practically avoided, i.e.

$$G_{nn}(\omega_s) < 0.01\ G_{nn}(0) \tag{104}$$

With the aid of expressions (104) and (101) and $\omega_{min} = 1/\tau_{min}$ and $\omega_s = 2\pi/T_s$ the condition for the sampling time T_s is obtained as $T_s < 0.63\,\tau_{min}$. If, for technical reasons, this sampling frequency cannot be reached, a second approach is to introduce a first-order anti-aliasing filter with a time constant τ_f and a complex frequency response function $H_f(j\omega) = 1/(1 + j\omega\tau_f)$. The filter time constant must be based on τ_{max} to avoid distortion of the signal $E(t)$, whereas the sampling time T_s must be based on τ_f. For the filter cut-off frequency $\omega_f = 1/\tau_f$ a value is chosen where $G_{EE}(\omega_f) < 0.01\ G_{EE}(0)$, i.e., the signal spectrum is clipped for signals with frequencies larger than $10\ \omega_{max}$. The sampling frequency $\omega_s = 2\pi/T_s$ is chosen in such a way that

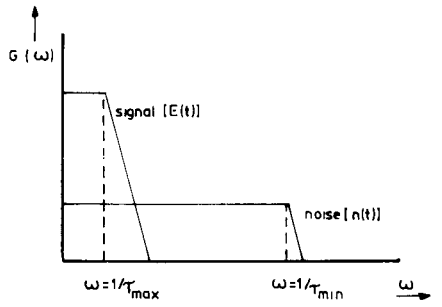

Fig. 10. Schematic representation of a signal and noise power spectral density function.

$$|H_f(j\omega_s)|^2 = 1/(1 + \omega_s^2\tau_f^2) < 0.01 \qquad (105)$$

i.e., the contributions of possibly filtered noise $\underline{n}(t)$ are reduced to 0.1 of the original value. From Eqn. (105) and the above discussion, it follows that $\tau_f < 0.1\ \tau_{max}$ and $T_s < 0.63\ \tau_f$. This provides a practical condition for determining the filter time constant τ_f and the sampling time T_s, to avoid signal distortion and aliasing effects for sampling a composite signal $\underline{E}(t) = E(t) + \underline{n}(t)$. This sampled signal will be used to estimate the dominant time constant of the system, and also the changes in time constant in the neighbourhood of the end-point. The estimated value $\hat{\tau}_{max}$ is used to monitor the waiting time necessary to reach the equilibrium state after a single addition of titrant.

Starting with a first-order step response $E(t) = A[1 - \exp(-t/\tau)]$, the normalized area Q may be expressed by

$$Q(T) = \int_0^T E(t)\mathrm{d}t/[T\,E(t)] - 0.5 = [1 - \exp(-T/\tau)]^{-1} - (\tau/T) - 0.5 \qquad (106)$$

A similar equation is obtained for responses $E(t) = A \exp(-t/\tau)$. From Eqn. (106), the numerical value of τ can be approximated by a given $Q(T)$ and T, applying a Newton—Raphson iteration procedure given by

$$x_n = x_{n-1} - [f(x_{n-1})/f'(x_{n-1})] \qquad (107)$$

with $f(x) = (1 - e^x)^{-1} + x^{-1} - 0.5 - Q(T) = 0$ and $x = -T/\tau$.

In an on-line approach, however, where during data acquisition (sampling) Eqn. (107) has to be evaluated, the number of iterations and so the calculation time can affect the timing of the data acquisition. Therefore, it is necessary to investigate the behaviour of Eqn. (106) to find an approximate formula with a constant calculating time. For large values of the time T, Eqn. (106) can be simplified by

$$\tau \approx T(\tfrac{1}{2} - Q(T)) \qquad (\text{for } T > 5\tau) \qquad (108)$$

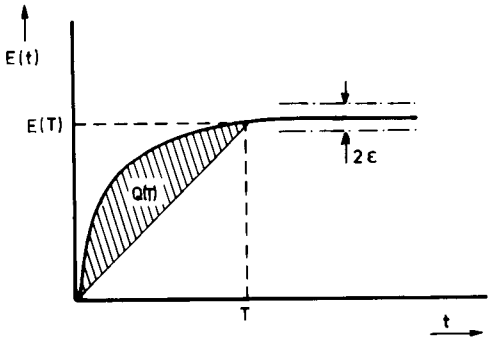

Fig. 11. Representation of a step response of a dominant first-order system.

For small values of T, and $y = Q(T)$ and $x = -T/\tau$, Eqn. (106) can be rewritten as

$$y = [1 - \exp(x)]^{-1} + x^{-1} - 0.5 \tag{109}$$

After substitution of a Taylor series expansion for $1 - \exp(x)$ into Eqn. (109), the final expression, for $x \to 0$, is $\lim_{x \to 0} y/x = -1/12$. Alternatively, with $y = Q(T)$ and $x = -T/\tau$, one gets

$$\tau \approx T/12Q(T) \qquad (\text{for } 0 < T < \tau) \tag{110}$$

As shown in Fig. 12, expression (110) causes inadmissible errors for the larger values of T/τ. To keep the errors within certain limits, $Q(T)$ in expression (110) is replaced by $\text{tg}(\pi Q(T))/\pi$, yielding

$$\tau \approx T\pi/12\text{tg}[\pi Q(T)] \qquad (\text{for } 0 < T < \tau) \tag{111}$$

The estimated value τ, obtained by the approximation (108) or (111), depending on the value of Q, is applied to predict the waiting time. The easiest procedure is to set a waiting time equal to 5τ. Another approach, used in our computer programs, is to calculate the asymptotic value A of the step response $E(t) = A(1 - \exp(-t/\tau))$ and error boundaries $[A - \epsilon, A + \epsilon]$, where ϵ is an arbitrarily chosen value. Shortly after the addition of titrant, an interval for the equilibrium state can be calculated

$$A - \epsilon < E(t_{\text{equilibrium}}) < A + \epsilon \tag{112}$$

with $A = [E(0) - E(T)]/[\exp(-T/\tau) - 1]$.

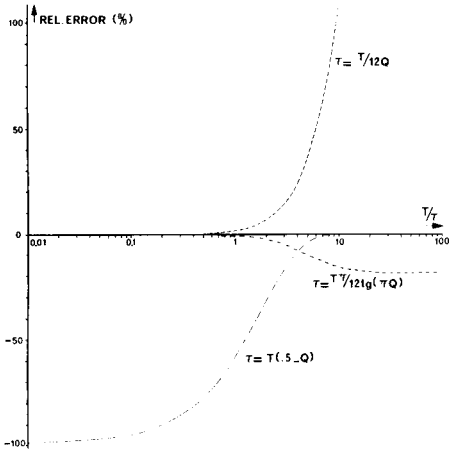

Fig. 12. Relative errors in time constant determination algorithms. See also Eqns. (108), (110) and (111).

END-POINT DETERMINATION BY SECOND DERIVATIVE METHODS

When the zero crossing of the second derivative of the sigmoidal titration curve is used for end-point determination, random errors in the crossing will again be present. The origin of these random errors is the second derivative of the instrumental noise, superimposed on the sigmoidal titration curve. Here, it is assumed that the sigmoidal curve can be represented by m points, obtained after discontinuous additions of titrant by means of an equilibrium detection method. The time between two successive measurements is assumed to be large (at least five times the dominant time constant), and the covariance (i.e., the expected value of the product $\underline{n}_i\underline{n}_{i+1}$) is negligible and $\underline{n}_i$ and $\underline{n}_{i+1}$ for $i = 1 \ldots m$ are mutually independent. The second derivative curve may be approximated in the neighbourhood of the equivalence point by a model function of the form

$$\underline{E}_i'' = a + B(v_i - \bar{v}) + \underline{n}_i'' \tag{113}$$

with $\bar{v} = \Sigma_i v_i/N$, where E_i'' denotes the twice-differentiated electrode potential, corresponding to the added volume v_i; $\underline{n}_i''$, for all i, is a normally distributed stochastic variable with an expected value equal to zero and a variance $\mathrm{VAR}\{\mathrm{n}_i''\} = (\sigma'')^2$. For a sufficient number of data pairs (E_i'', v_i), a linear regression line can be estimated, for N points given by

$$\hat{E}_i'' = \hat{a} + \hat{B}(v_i - \bar{v})$$

$$\text{with } \hat{a} = \left(\sum_i \underline{E}_i''\right)\Big/N,\ \hat{B} = \left[N\sum_i v_i\underline{E}_i'' - \sum_i v_i \sum_i \underline{E}_i''\right]\Big/\left[N\sum_i v_i^2 - \left(\sum_i v_i\right)^2\right]$$

$$s_{\hat{a}}^2 = s_{Ev}^2/N,\ s_{\hat{B}}^2 = s_{Ev}^2/(N-1)s_v^2,\ s_v^2 = (N-1)^{-1}\left[\sum_i v_i^2 - \left(\sum_i v_i\right)^2\Big/N\right],$$

$$s_{Ev}^2 = (N-2)^{-1}\sum_i \left\{\underline{E}_i'' - \left[\hat{a} + \hat{B}\left(v_i - \sum_i v_i/N\right)\right]\right\}^2 \tag{114}$$

The intersection of the regression line with the v-axis will give the estimated end-point, described by

$$\hat{v}_{ep} = \bar{v} - \hat{a}/\hat{B} \qquad (\text{for } \hat{B} \neq 0) \tag{115}$$

Dependent on the stochastic variable, there are more possible crossings, each crossing having its own probability. To obtain a confidence interval, the distribution of $\hat{v}_{ep}$ should be known. As $\hat{a}$ and $\hat{B}$ are normally distributed, the quotient of the estimated $\hat{a}$ and $\hat{B}$ will have a Cauchy-like distribution without the existence of an expected value and variance. To approximate a confidence interval, usable in practice, it is necessary to make a joint confidence region for a and B. The contour of the confidence ellipse in the parameter

space (i.e., in coordinates (a, B) for a given $100(1-\alpha)\%$ confidence region) is for mutually independent values of $\hat{a}$ and $\hat{B}$ given [32] by

$$(a-\hat{a})^2/s_{\hat{a}}^2 + (B-\hat{B})^2/s_{\hat{B}}^2 = H^2 \tag{116}$$

where H^2 is F-distributed with 2 and $(N-2)$ degrees of freedom, respectively, at a level of significance equal to $(1-\alpha)$, i.e., $H^2 = 2F_{2,N-2,1-\alpha}$. In the $a/s_{\hat{a}}$, $B/s_{\hat{B}}$ space, the contour of the confidence circle is obtained with radius H and a centre at $P(\hat{B}/s_{\hat{B}}, \hat{a}/s_{\hat{a}})$ (see Fig. 13). As the end-point is estimated with a model function for the equivalence point by

$$v_{eq} = \bar{v} - a/B = \bar{v} + M \tag{117}$$

the confidence interval for M and also for v_{eq} can be approximated by a set of straight lines from the origin (0,0) with a slope of $-Ms_{\hat{a}}/s_{\hat{B}}$, crossing the critical confidence contour. This means that the set of values M, resulting in different straight lines intersecting the confidence circle, will determine the confidence interval of v_{eq}. The set of distances d between the point $P(\hat{B}/s_{\hat{B}}, \hat{a}/s_{\hat{a}})$ and the set of straight lines

$$B/s_{\hat{B}} - a/s_{\hat{a}}(Ms_{\hat{a}}/s_{\hat{B}}) = 0 \tag{118}$$

must be smaller than, or equal to, the radius H of the confidence circle, resulting in the inequality

$$d^2 = |[(\hat{a}/s_{\hat{a}})M + (\hat{B}/s_{\hat{B}})]/(M^2+1)^{1/2}| \leqslant H^2 \tag{119}$$

This inequality will give the total of all acceptable M values with a chosen percentage confidence. Rewriting inequality (119) gives a quadratic equation in M

$$M^2[(\hat{B}/s_{\hat{B}})^2 - H^2] + 2M(\hat{a}/s_{\hat{a}})(\hat{B}/s_{\hat{B}}) + (\hat{a}/s_{\hat{a}})^2 - M^2 \leqslant 0 \tag{120}$$

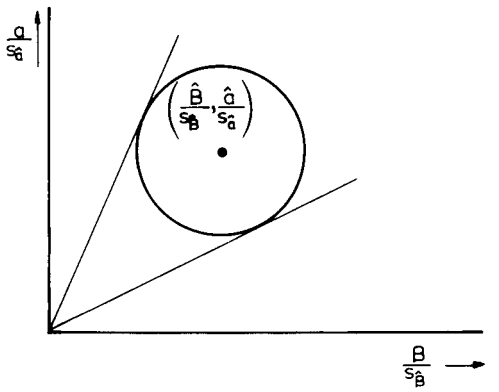

Fig. 13. Representation of a confidence circle for the estimated values $\hat{B}/s_{\hat{B}}$ and $\hat{a}/s_{\hat{a}}$.

Solving this expression, with the assumption that $M_1 < M_2$, gives

$$M_{1,2} = (\hat{B}^2 - H^2 s_{\hat{B}}^2)^{-1} \{-\hat{a}\hat{B} \pm s_{\hat{a}} s_{\hat{B}} [H^2((\hat{a}/s_{\hat{a}})^2 + (\hat{B}/s_{\hat{B}})^2 - H^2)]^{1/2}\} \quad (121)$$

The confidence intervals for v_{eq} are represented by $[\bar{v} + M_1, \bar{v} - M_2]$ for a given percentage confidence, and are listed in Fig. 14.

One remark is necessary concerning the change in statistical properties of the twice-differentiated noise $\underline{n}_i$ for non-equidistant sampled data. When a differentiation algorithm is applied to equidistantly distributed data, expressed by

$$\underline{n}_i'' = (\underline{n}_{i+1} - 2\underline{n}_i + \underline{n}_{i-1})/\Delta V^2 \quad (122)$$

the variance of $\underline{n}_i''$ is obtained by using the well known error propagation rule:

$$\mathrm{VAR}\{\underline{n}_i''\} = 6\sigma^2/(\Delta V)^4 = (\sigma'')^2 \quad (123)$$

where σ^2 is the variance of $\underline{n}_i$ for all i. As can be observed from Eqn. (123), the variance of the twice differentiated noise $\underline{n}_i$ is inversely proportional to the fourth power of a chosen value ΔV. For non-equidistant ΔV values, the variance $\mathrm{VAR}\{\underline{n}_i''\}$ is a function of $v_{i+1} - v_i$ and $v_i - v_{i-1}$. In that case, the variance of $\underline{n}_i''$ is no longer constant for all i, and the linear regression procedure described in Eqn. (114) is no longer valid.

CONCLUSIONS

The results described above show that a rather fast continuous addition of titrant will provide acceptable final results in well defined titration systems

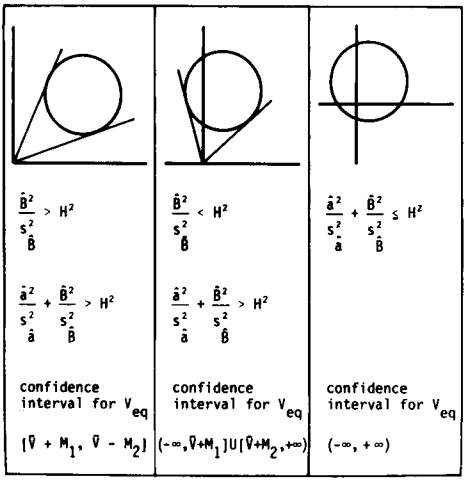

Fig. 14. Confidence intervals for end-point determination, detected by the zero crossing of the second derivative of a sigmoidal titration curve.

with constant parameters. When the derived conditions (Eqn. 64 or 65) are used, systematic errors can be corrected. For systems where the system parameters are dependent on the concentration, or in general for variable parameter systems, no rules for correcting systematic errors are derived. In these cases, the approach of discontinuous titrant addition is necessary with waiting times for equilibrium to be achieved between successive additions of titrant. The investigation of this approach has resulted in a simple rule (Eqn. 79) to determine the minimum additions in the neighbourhood of the end-point, that allow the titration curve to be described with minimum loss of information. This rule can be used for equidistant additions of titrant. For non-equidistant volume steps, corresponding to equidistant ΔpH or ΔE values, two control algorithms are derived which can be used in titration equipment with computer-controlled motor burettes. The first (Eqn. 96) can easily be implemented in a microcomputer and is optimal for symmetrical or nearly symmetrical sigmoidal titration curves; it can also be successfully applied in titrations with more than one end-point. More sophisticated is the algorithm expressed in Eqn. (100), where a hyperbolic extrapolation is used. For detecting the equilibrium state after a small addition of titrant, the algorithm used (Eqn. 111) is based on the assumption that the system acts like a dominant first-order system in that particular area. In contrast to a zero slope detection method, where the observed signal is differentiated, this algorithm is based on integrating the signal, with the advantage that the signal-to-noise ratio will not increase. Possibilities for extending the equilibrium detection algorithm by a numerical filter procedure with a signal-dependent time constant are being investigated. The properties of that filter can best be described as a filter with a maximum time constant (maximum filter effect) in the equilibrium state of the system, without distortion of the original signal.

The accuracy achieved in the end-point determination by detecting the zero crossing of the second derivative of a sigmoidal titration curve is also considered. For discontinuous addition of titrant, with the assumption that the stochastic variables in each sampled point are mutually independent, a confidence interval for the end-point is derived (Fig. 14). Further research is needed on continuous addition of titrant, where the noise has to be considered as a stochastic process $\underline{n}(t)$ and the covariance is no longer zero. Experiments based on the algorithms derived above are described in Part 2 of this series [31].

The authors express their gratitude to Drs. E. Edens for valuable discussions on the statistical part in the final section, and to Prof. Dr. E. M. de Jager for his advice during the preparation of the manuscript.

REFERENCES

1 S. W. Director and R. A. Rohrer, Introduction to Systems Theory, McGraw-Hill, New York, 1972.
2 D. M. Wiberg, State Space and Linear Systems, McGraw-Hill, New York, 1971.

3 J. S. Bendat, Principles and Applications of Random Noise Theory, Wiley, New York, 1958.
4 R. E. Cover and L. Meites, J. Phys. Chem., 67 (1963) 1528.
5 C. H. Bamford and C. F. H. Tipper (Eds.), Comprehensive Chemical Kinetics, Vol. 2 (Theory of kinetics), Elsevier, Amsterdam, 1969.
6 G. A. Rechnitz and H. F. Hameka, Fresenius Z. Anal. Chem., 214 (1965) 252.
7 G. Johansson and K. Norberg, J. Electroanal. Chem., 18 (1968) 239.
8 R. P. Buck, J. Electroanal. Chem., 18 (1968) 363, 381, 387.
9 G. A. Rechnitz and G. C. Kugler, Anal. Chem., 39 (1967) 1682.
10 B. Karlberg, Anal. Chim. Acta, 66 (1973) 93.
11 E. Lindner, K. Toth and E. Pungor, Anal. Chem., 48 (1976) 1071.
12 R. Rangarajan and G. A. Rechnitz, Anal. Chem., 47 (1975) 324.
13 W. E. Morf, E. Lindner and W. Simon, Anal. Chem., 47 (1975) 1596.
14 P. W. Carr and J. Jordan, Anal. Chem., 45 (1973) 643.
15 W. E. van der Linden, Anal. Chim. Acta, 77 (1975) 327.
16 H. S. Rossotti, Talanta, 21 (1974) 809.
17 G. J. M. Heijne and W. E. van der Linden, Talanta, 22 (1975) 925.
18 P. M. E. M. van der Grinten and J. M. N. Lenoir, Statistische Procesbeheersing, Het Spectrum, Utrecht, 1973, p. 292.
19 C. E. Shannon, Bell System Tech. J., 27 (1948) 379, 623.
20 I. M. Gelfand and D. V. Shilov, Veralgemeinerte Funktionen, VEB Verlag, Bd. I. Berlin, 1960.
21 E. M. de Jager (Ed.), Mathematics Applied to Physics, Springer Verlag, Berlin, 1970, Chapter 2.
22 G. Gran, Acta Chem. Scand., 4 (1950) 559; The Analyst, 77 (1952) 661.
23 C. Liteanu and D. Cörmös, Talanta, 7 (1960) 18.
24 F. Ingman and E. Still, Talanta, 13 (1960) 18.
25 J. G. McCullough and L. Meites, Anal. Chem., 47 (1975) 1081.
26 A. F. Isbell, Jr., R. L. Pecsok, R. H. Davies and J. H. Purnell, Anal. Chem., 45 (1973) 2326.
27 J. W. Frazer, W. Selig and L. P. Rigdon, Anal. Chem., 49 (1977) 1250.
28 D. M. Barry and L. Meites, Anal. Chim. Acta, 68 (1974) 435.
29 D. M. Barry, L. Meites and B. H. Campbell, Anal. Chim. Acta, 69 (1974) 143.
30 S. R. Goode, Anal. Chem., 49 (1977) 1408.
31 J. C. Smit, H. C. Smit, H. Steigstra and U. Hannema, Anal. Chim. Acta, 143 (1982) 79.
32 D. M. Himmelblau, Process Analysis by Statistical Methods, Wiley, New York, 1970, p. 119.
33 R. P. J. Duursma, H. Steigstra, R. G. Logchies and H. C. Smit, Anal. Chim. Acta, to be submitted.

Analytica Chimica Acta, 143 (1982) 79—94
Elsevier Scientific Publishing Company, Amsterdam — Printed in The Netherlands

COMPUTER-CONTROLLED TITRATIONS
Part 2. Equipment and Performance

J. C. SMIT[a], H. C. SMIT*, H. STEIGSTRA and U. HANNEMA

Laboratory for Analytical Chemistry, University of Amsterdam, Nieuwe Achtergracht 166, 1018 WV Amsterdam (The Netherlands)

(Received 8th February 1982)

SUMMARY

Experimental verification of the theoretical considerations in Part 1 is reported for automated titrations. The most advanced approach is based on the use of a general computer network with a host computer and satellite microcomputers. The combination of the calculation facilities of the host computer and the control functions of the microprocessor makes it possible to control titrations in a sophisticated manner. Several algorithms for both continuous and discontinuous titrations are tested. For comparison, the description of the network concept is preceded by consideration of a simple dedicated microcomputer system, which is more usual in automated titrations because of the cheap hardware. A powerful control algorithm, which is quite easy to understand, is tested in several potentiometric titrations with one or more end-points.

Manual titrations, whether done to a simple end-point or based on a titration curve, are time- and manpower-consuming. Yet, titrimetric analysis is one of the most important techniques for routine work. Thus, it is not surprising that many attempts have been made to automate the procedures. The first automatic titrators used mechanical coupling between the burette and the recorder (e.g., Radiometer, Jouan). More advanced automation became practicable with the introduction of computers, and particularly microprocessors. Apart from instrument manufacturers, many workers have directed their attention to the application of microcomputers in automation of titrimetric analysis [1—14], in order to reduce time and manpower requirements in routine work.

Automated titrators have to meet a number of requirements, which depend on the purpose of the titrator and which may be contradictory. The ideal is a cheap instrument that will provide automatically 100% accurate, precise and directly available results. The real titrator is a compromise and it will be very difficult to design an automated titrator that can replace fully a good analyst.

The aim of this paper is to report on the performance of the algorithms derived in Part 1 [15] when they are implemented in a universal computer

[a]Present address: Laboratory for Neurology, St. Radboud Hospital, Catholic University Nijmegen, Reinier Postlaan 4, 6500 HB Nijmegen, The Netherlands.

0003-2670/82/0000-0000/$02.75

network and in a dedicated microprocessor-based instrument, the latter being more usual in automated titrations. In addition, more insight into computer applications will be given for potential daily users who are unskilled in computer techniques and automation.

DESIGN CONSIDERATIONS

The simple dedicated microcomputer concept

In recent years, experience has been gained with a simple microprocessor-based automated titrator, suitable for routine potentiometric titrations; the simplest time-consuming human actions in the titration procedure are mechanized, but no more. In this titrator the algorithm derived in Part 1 [15] was implemented and tested. The algorithm is a compromise between simplicity, accuracy and speed; it was developed with the intention of obtaining automatically a complete titration curve with an accuracy and a time duration of the same order as in manual titrations.

In such titrations, the additions of titrant have first to decrease to a minimum in the vicinity of the end-point in the case of non-linear titrations. The change of pH or mV value after a certain titrant addition is frequently used; such changes are indicated by the slope of the titration curve. The increments of titrant to be added can be chosen in an approximately inversely proportional relation to the first derivative of the titration curve. An increment is added only when the effects of the previous increment have reached an equilibrium state. This means that the automated titrator must find the slope of the time-dependent pH (or mV) signal for determining equilibrium. These and other considerations result in the following titrator design: first, the analog signal from a pH or mV meter is amplified. An anti-aliasing filter prior to analog-to-digital conversion is necessary to prevent folding (conversion) of high-frequency noise to lower frequencies in the frequency range of the signal. The low-frequency noise cannot be removed by filter procedures later. The cut-off frequency of the simple first-order low-pass filter used is 10 Hz. In the next stage, the signal is converted to a 10-bit digital number of means of an analog-to-digital converter (ADC). To determine the equilibrium state, the computer takes samples at regular front-adjustable times Δt. The minimum slope is obtained by comparing two successive readings with an accuracy determined by the resolution (quantization) error of the ADC

$$\begin{aligned} &|\{U[(n+1)\Delta t] - U[n\Delta t]\}/\Delta t| \leqslant \epsilon \qquad && U_{\text{new}} = U[(n+1)\Delta t] \\ &n > 10 && U_{\text{new}} = U(11\Delta t) \end{aligned} \tag{1}$$

where ϵ denotes the absolute value of the resolution error. If no successive readings are equal, the tenth reading is used for U_{new}. The computer then calculates the value of ΔU from the new and old value, i.e., after and before addition of titrant. A measure of the slope of the titration curve in

equilibrium is thus obtained. Further titrant increments are calculated by means of the algorithm [15]

$$\Delta V_{NC} = \Delta V_{MAX}[1 + k\Delta U/\Delta V_{OA}]^{-1} \quad (2)$$

where ΔV_{MAX} denotes the maximum addition of titrant, ΔV_{NC} the calculated volume of titrant to be added, ΔV_{OA} the titrant volume of the previous increment, k the feedback factor, and ΔU the difference in voltage at the input of the titrator as a result of the last increment of titrant. The volume ΔV_{NA}, the volume which is in fact added, is limited by the chosen limits

$$\begin{aligned} \Delta V_{NA} &= \Delta V_{NC} \quad \text{for} \quad 2\Delta V_{OC} \geqslant \Delta V_{NC} \geqslant \tfrac{1}{2}\Delta V_{OC} \\ \Delta V_{NA} &= 2\Delta V_{OC} \quad \text{for} \quad \Delta V_{NC} > 2\Delta V_{OC} \\ \Delta V_{NA} &= 2\Delta V_{OC} \quad \text{for} \quad \Delta V_{NC} < \tfrac{1}{2}\Delta V_{OC} \end{aligned} \quad (3)$$

where ΔV_{OC} denotes the calculated volume of the previous addition. Moreover, the addition is limited by ΔV_{MIN} and ΔV_{MAX} when ΔV_{NC} crosses these ultimate boundaries. The values ΔV_{MAX} and ΔV_{MIN} and also the total volume of titrant, V_{TOT}, are chosen by the operator by setting thumbwheel switches on the front of the titrator.

After the start of the titration, the x—y recorder prints a point at $x = 0$, (i.e., a volume zero) and at $y = U$ (e.g., the first pH value). Then the pen is lifted and the first volume of titrant is added from the stepping motor-driven burette. The computer waits for equilibrium, indicated by the minimum slope of the input signal calculated by Eqn. (1). After this condition has been fulfilled, a second point (x, y) is printed.

In the case of pH versus V titrations, the value of $\Delta U/\Delta V$ increases upto the end-point and the new increments of titrant diminish according to Eqns. (2) and (3). After the end-point the opposite happens. In linear titrations, such as photometric titrations, where the measure of absorbance A is a function of the titrant volume V, $\Delta A/\Delta V$ does not change and consequently ΔV remains unchanged, except at the end-point where the slope alters.

For completeness, the original hardware is described below, without great detail. The heart of the titrator (Fig. 1) is an 8-bit microprocessor chip (type 8008). The available random access memory (RAM) for storing data during execution of the titration program is 2 kbyte (1 byte is 8 bits). A 2-kbyte reprogrammable read only memory (pROM) is also available; the titrator program is stored in the pROM.

In developing the specific titrator software, a microcomputer system (GNC-8; Great Northern Computers) was used; this system is also based on an 8008 microprocessor chip, with 48 basic instructions and a teletype as input/output station. To communicate with the microcomputer, the system is equipped with a software package which makes it possible to load, dump, and edit instructions. Such a software package (in this case called Monitor 8, which is part of the GNC-8 system) is absolutely necessary for developing special purpose software. The automatic titrator programs were stored in pROMs. The pROMs for the titrator programs were built into the hardware configuration of the titrator; this configuration is identical to that of the

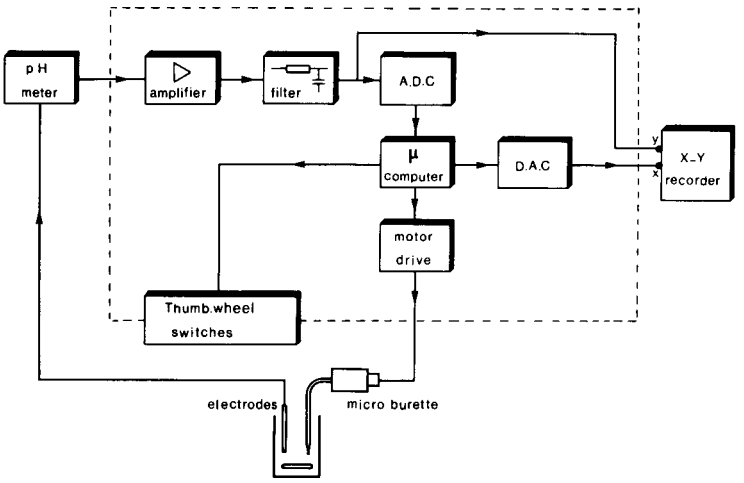

Fig. 1. Block diagram of the automatic titrator.

developing system without the extras of the latter. A simple pushbutton is used to start the program. Other important parts are the microprocessor-controlled ADC, converting the amplified and filtered input signal to a digital number, and the digital-to-analog converter (DAC) for conversion of the total added volume of titrant, expressed by a digital number, to an analog signal (see Fig. 1). A 0.5-ml Metrohm microburette type E457 is used. The burette is equipped with a Berger stepping motor type D080 also controlled by the microprocessor. The combination of the burette and the stepping motor allows a minimum addition of 1/32 μl of titrant and can reach a maximum addition speed of 2 μl s^{-1}.

The computer network concept

Not only the great variety of titrations, but also the other analytical techniques used in research or routine laboratories, can justify the choice of a general-purpose computer network instead of dedicated computers. The computer network concept with a central minicomputer system coupled with satellite microcomputers is suitable for general automation purposes [16, 17]. An advantage of such networks is the combination of fast calculation facilities on the central (host) computer with the data acquisition capabilities of the microcomputer. Such combinations have led to more sophisticated automation.

The operation of the computer network used here (see Fig. 2) may be explained as follows. On the local terminal two keyboard modes are possible: a terminal mode and an interpreter mode. In the terminal mode, it is possible to communicate with the host computer with all facilities served by the operating system. The master program can be written in a higher computer language (FORTRAN IV here) with the advantage that an extensive FORTRAN library is available, containing subroutines and subprograms

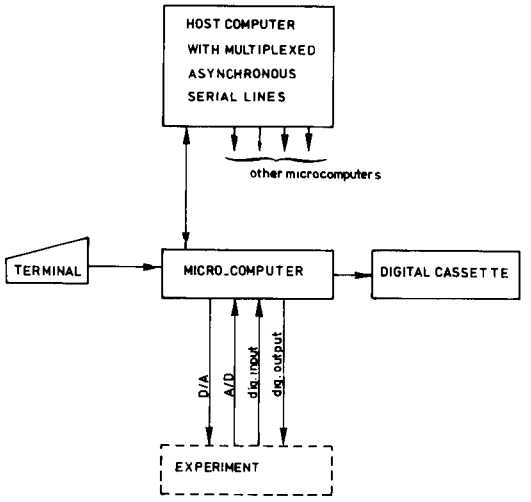

Fig. 2. Block diagram of the computer network used.

for curve fitting, interpolation, plotting, Fourier transform, etc. In the interpreter mode, the keyboard is connected with the microcomputer. In the microcomputer, an interpreter language program developed in this laboratory makes it possible to build programs structured like BASIC, but with instructions absent in commercially available programming languages. With these interpreter instructions, input and output ports can be simply controlled, e.g., ADC or DAC, relays, stepping motors, etc. Delay times can be introduced between the several instructions. The transfer of variable names and their values between microcomputer and host computer is achieved by a protocol [17]. The user can synchronize the master program running in the host computer, with the interpreter program running in the microcomputer, with special WRITE/READ subroutines as extensions of the FORTRAN library and the GET FROM/SEND TO HOST statements in the interpreter. For titrations, the pH or mV values are sampled by the microcomputer and transferred to the host computer. Values calculated by the host computer (e.g., addition of titrant) are sent back to the interpreter program (see Fig. 3). With simple keyboard escape commands, the user can switch from the

```
 1 ACQUIRE V FROM INPUT PORT 1                                    :
 2 SEND TO HOST: V →→→→→→→→→→→→→→→→→→→→→→→→→→→→CALL UCRD(V,.....)
 3 PAUSE 10                                                       :
 :                                                                :
 :                                                                :
10 GET FROM HOST: NSTEP ←←←←←←←←←←←←←←←←←←←←←←CALL UCWR(NSTEP,..)
11 STEP NSTEP TO OUTPUT PORT 3                                    :
 :                                                                :
 :                                                                :
    INTERPRETER PROGRAM                          FORTRAN PROGRAM
```

Fig. 3. Dialogue between interpreter program and FORTRAN program.

terminal to interpreter mode and vice versa. Detailed information about the interpreter language will be published [17]. In general, the combination between the powerful programming and calculating facilities of the host computer and the control and timing facilities of the interpreter program is very valuable.

DEDICATED MICROCOMPUTER APPLICATIONS

Experimental

The results given below were obtained by means of the automated titrator described above, with a Philips PW 9408 pH meter and combined glass—calomel electrode (Electrofact 7GR111). For the complexiметric titrations, a mercury indicating electrode was used [18]; a gold rod sealed in a glass tube was cleaned with concentrated nitric acid, rinsed with water, dipped in mercury, and then rinsed successively with water, diluted EDTA solution and water. The x—y recorder used was a Hewlett—Packard type 7045A. The volume of solution titrated was 50 ml in a 100-ml beaker. Solutions were stirred magnetically.

Performance of the algorithm

The performance of the algorithm was tested for various titrations with different parameter settings.

Figure 4 shows that only Curve 4 with the largest possible $\Delta V_{MAX} = 99$ µl leads to an uncertainty in the determination of the end-point. In the other titrations, the end-point could be determined to 0.5 mm, corresponding to 0.5 µl. Titration 3 was repeated 12 times, the result being $\bar{x} = 334.63$ µl with a standard deviation in the mean of 0.24 µl. The duration of these 12 titrations varied considerably, the average being 618.5 s with extreme values of 870.0 s and 520.0 s. This large variation can probably be ascribed to differences in mixing of acid and base caused by differences in relative

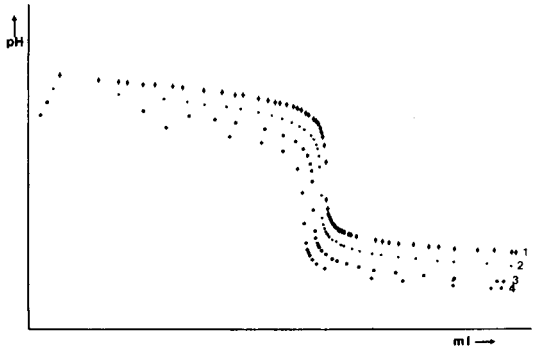

Fig. 4. Effect of maximum addition V_{MAX} in the titration of borax with 3.5 M HCl. Curves: (1) $V_{MAX} = 30$ µl, $k = 9$, time = 29 min; (2) $V_{MAX} = 50$ µl, $k = 9$, time = 15 min; (3) $V_{MAX} = 75$ µl, $k = 9$, time = 11 min; (4) $V_{MAX} = 99$ µl, $k = 9$, time = 10 min.

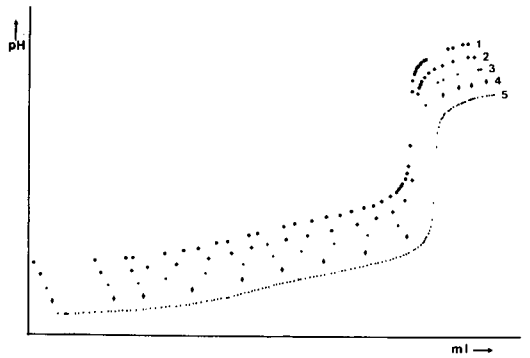

Fig. 5. Effect of choice of feedback factor k in the titration of oxalic acid with 3.3 M NaOH. Curves: (1) V_{MAX} = 50 µl, k = 8, time = 16 min; (2) V_{MAX} = 50 µl, k = 4, time = 11 min; (3) V_{MAX} = 50 µl, k = 2, time = 9 min; (4) V_{MAX} = 50 µl, k = 1, time = 7 min; (5) V_{MAX} = 5 µl, k = 1, time = 31 min.

position of the combined electrode, the tip of the burette and the stirring rod in the beaker.

Figure 5 shows that only Curve 1, with k = 8, gives the feasibility of precise end-point determination. Curve 5 is given for comparison; only in this curve is any inflection point to be seen half-way towards the end-point. With another setting of the titrator (ΔV_{MAX} = 75 µl and k = 9), seven titrations were done to test the system. The end-point was found to lie at 299.57 µl with a standard deviation of 0.13 µl in the mean. The average duration of the titration was 789.0 s with extremes of 945.0 and 646.0 s.

Figure 6 shows that titrations with more than one end-point can be handled by the automatic titrator. With a proper choice of the value of the feedback factor (k = 6—9) both end-points can be found.

The titration of copper ions with EDTA, with potentiometric indication by means of Hg/Hg(II) [19], was examined because of the asymmetric

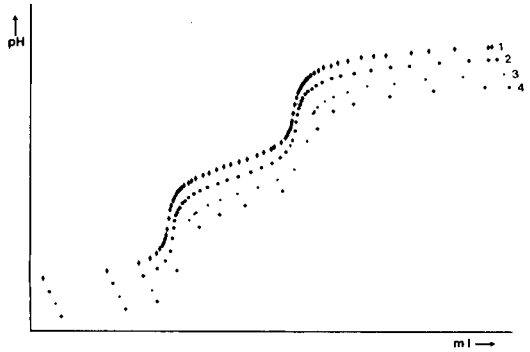

Fig. 6. Effect of feedback factor k in the titration of phosphoric acid with 3.5 M NaOH. Curves: (1) V_{MAX} = 50 µl, k = 9; (2) V_{MAX} = 50 µl, k = 6; (3) V_{MAX} = 50 µl, k = 3; (4) V_{MAX} = 50 µl, k = 1.

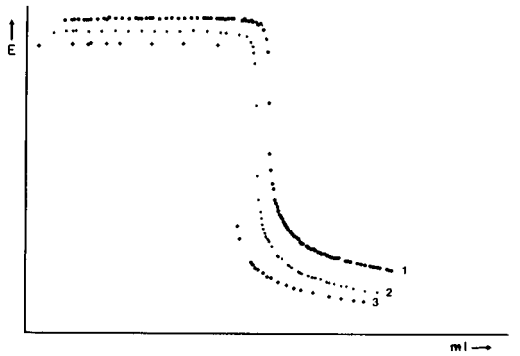

Fig. 7. Effect of the choice of maximum addition V_{MAX} on the titration of Cu(II) (+ 1% Hg(II)) with 0.26 EDTA. Curves: (1) V_{MAX} = 5 μl, k = 8; (2) V_{MAX} = 10 μl, k = 8; (3) V_{MAX} = 25 μl, k = 8.

shape of the titration curve (Fig. 7). In the sense of visual measurement of the end-point, it appears that, as might be expected, only small values of ΔV_{MAX} yield a good representation of the titration curve. Photometric titrations of copper(II) with triethylenetetramine were also tested with the apparatus combined with a Zeiss PMQ II spectrophotometer; when absorbance versus volume of titrant was recorded, two straight lines were found.

COMPUTER NETWORK APPLICATIONS

Experimental

The computer network consisted of a host computer (VARIAN type V76 minicomputer) and a microcomputer system based on a ZILOG Z-80 microprocessor [17]. The Metrohm microburette and the stepping motor (see above) were controlled by the interpreter program running in the microcomputer. For end-point indication, a combined glass electrode (see above) and a Cu^{2+}-selective electrode (Orion type 94-92A) were used with the PW9408 pH/mV meter; the analog output was connected to one of the eight available 12-bit A/D converters in the microcomputer system. In these experiments, 25.00 ml of sample solution was diluted with about 50 ml of water in a 100-ml vessel. Solutions were stirred magnetically.

For spectrophotometric titrations, a Zeiss PMQ II spectrophotometer with an analog output signal proportional to the transmittance was used. The titrations were done in 10-ml cells (2-cm path length) and solutions were stirred magnetically.

Rapid potentiometric titrations of copper(II) with EDTA

Conditions as derived in Part 1 [15] have to be fulfilled (Eqns (65) and (66)) for rapid automated titrations. For the titration of 0.001 M Cu(II) with 0.07 M EDTA, a total titration time of 100 s is chosen. The relatively fast titration is indicated by the ion-selective electrode, which has a dominant time constant of about 3 s. The stepping motor of the burette is controlled

by the interpreter program which generates a pulse-train of 16 000 pulses with a speed of 160 pulses s^{-1}, equivalent to a speed of addition $m = 5\ \mu l\ s^{-1}$. After a time $t > 5\tau$ (where τ denotes the overall time constant of the system), the transient effects are quenched and the Cu(II) concentration changes linearly with the time until the end-point t_{eq} is reached. The concentration of the copper(II), $C(t)$, can be approximated as a function of time

$$C(t) = b - a(t - \tau) \quad (\text{for } 5\tau < t < t_{eq}) \tag{4}$$

It can be assumed that the electrode response is Nernstian, and so the electrode potential will be

$$E(t) = A \ln[b - a(t - \tau)] + C' \tag{5}$$

The expected concentration changes of the sample ion versus time are illustrated in Fig. 8, assuming a dominant and constant detector time constant on the interval $(5\tau, t_{eq})$.

Rewriting of Eqn. (5) gives

$$E(t) = A \ln(B - t) + C \quad (\text{for } 5\tau < t < t_{eq}) \tag{6}$$

with $C = C' + A \ln a$ and $B = (b + a\tau)/a$. Here B denotes the intersection of the straight part of the concentration versus time curve with the time axis. The data, sampled with a frequency of 4 Hz, are transferred to the master program for end-point calculation. The sampled data are fitted with the function of Eqn. (6). The gradient expansion algorithm of Marguardt, used in the master program, has been described completely, including FORTRAN subroutines, by Bevington [20]. The fitting procedure stops if a preselected decrease in the chi-square value is reached. The calculated value for B is identical to t_{end}, and the obtained end-point volume Bm in ml of titrant (EDTA) has only to be corrected for a constant factor. The correct end-point

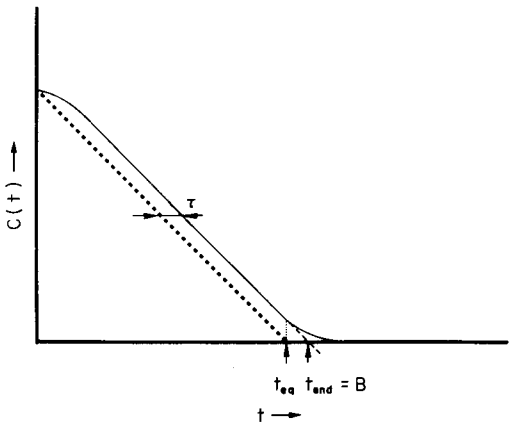

Fig. 8. Schematic representation of the concentration change of the sample ion versus time with continuous addition of titrant.

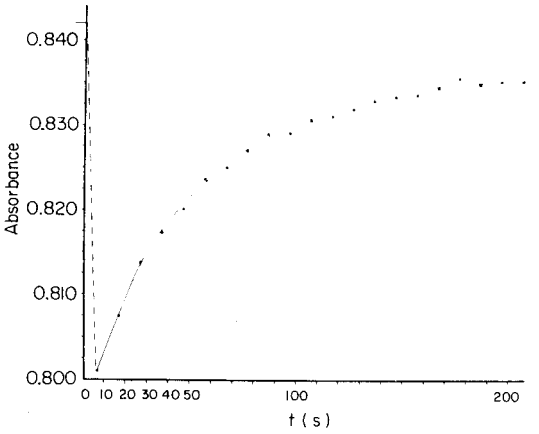

Fig. 9. Concentration change (absorbance) after a pulse-shaped addition of titrant in the spectrophotometric Cu(II)/Fe(III)—EDTA titration. Addition of 40 μl from 160 μl to 200 μl (before the first end-point). (·—·—·) Addition time of 6.4 s; (—) response after addition upto 200 s.

volume will then be $(Bm - \tau m)$ ml EDTA. To find an estimated value for the overall time constant τ, a simple exponential function with τ as parameter is fitted through the first data points, assuming that the overall system response is dominant first order. The average values of three experiments are listed in Table 1. The large variance in the obtained value C, which is the scaling factor of the titration curve in the E-direction, is caused by the addition of only approximately 50 ml of water to the 25.00 ml of Cu(II) solution in the titration vessel. But this effect will not influence the precision of the end-point determination obtained by the fitted value of B.

The same data were fitted with an arctg function

$$E(t) = A + B \text{ arctg } [C(t - D)] \tag{7}$$

also using the gradient expansion algorithm of Marguardt. The estimated values for D and A are the coordinates of the end-point corresponding to the t_{end} value and mV value of $E(t_{end})$, respectively. Corrections, made by using the estimated value of τ, result in an average value for the end-point and are also listed in Table 1.

TABLE 1

Calculated end-points obtained by applying Eqns. (6) and (7) with corrections for systematic errors in the potentiometric Cu(II)—EDTA titration. Constant addition speed, 5 μl s^{-1}; Orion 94-92A Cu^{2+}-selective electrode

A	$= -332 \pm 8.6$
mB	$= 363.4 \pm 0.6$ μl
C	$= 440 \pm 53$
Correction τm	$= 10 \pm 2.0$
End-point	$= 353.7 \pm 1.4$ μl (fitted with Eqn. (6) and corrected)
End-point	$= 353.6 \pm 1.7$ μl (fitted with Eqn. (7) arctg and corrected)

Discontinuous potentiometric titrations

As an illustration of the use of the hyperbolic extrapolation algorithm, a Cu(II)—EDTA titration was done with discontinuous addition of titrant, using the equilibrium detection algorithm (Eqns 100 and 111 of part 1) [15]. The electrode signal is amplified and shifted by an additional offset voltage in such a way that the voltage over the A/D converter changes from −10 V to +10 V during titration. In an interactive way, the parameters for the extrapolation algorithm can be inserted as maximum step size and equidistant ΔE value. In this experiment, the step size was limited to a maximum of 25 μl (800 steps of the stepping motor) and a ΔE value of 0.5 V was chosen. The results are listed in Table 2. The values are the calculated values of the computer program and will suggest unjustly some significance in the third decimal. As can be seen in the table, in the flat part of the sigmoidal curve (Points 1—9) the computer added the maximum addition of 25 μl of titrant. From Points 9 to 25, the motor burette comes under the control of the algorithm and consequently the additions are decreased. In the end-point

TABLE 2

Data obtained by applying a hyperbolic extrapolation routine in a potentiometric Cu(II)—EDTA titration

Point number	Input ADC E (V)	Titrant added (μl)	Totally added (μl)	Point number	Input ADC E (V)	Titrant added (μl)	Totally added (μl)
1	−9.254	00.000	00.000	25	0.745	0.188	282.687
2	−9.191	25.000	25.000	26	1.798	0.188	282.875
3	−9.091	25.000	50.000	27	1.940	0.031	282.906
4	−8.975	25.000	75.000	28	2.301	0.063	282.969
5	−8.815	25.000	100.000	29	2.593	0.063	283.031
6	−8.622	25.000	125.000	30	5.181	0.094	283.125
7	−8.370	25.000	150.000	31	5.225	0.031	283.156
8	−8.044	25.000	175.000	32	5.300	0.031	283.187
9	−7.623	25.000	200.000	33	6.112	0.063	283.250
10	−7.111	22.469	222.469	34	6.144	0.031	283.281
11	−6.579	16.531	239.000	35	6.205	0.031	283.312
12	−6.054	11.594	250.594	36	7.328	0.063	283.375
13	−5.534	8.312	258.906	37	7.383	0.031	283.406
14	−5.036	6.062	264.969	38	7.431	0.031	283.437
15	−4.503	4.812	269.781	39	7.521	0.063	283.500
16	−4.012	3.469	273.250	40	7.649	0.125	283.625
17	−3.452	2.875	276.125	41	8.013	0.250	283.875
18	−2.934	1.937	278.062	42	8.254	0.219	284.094
19	−2.428	1.437	279.500	43	8.345	0.344	284.437
20	−1.895	1.125	280.625	44	8.406	0.438	284.875
21	−1.218	0.813	281.437	45	8.506	0.875	285.750
22	−0.873	0.375	281.812	46	8.622	1.750	287.500
23	−0.100	0.500	282.312	47	8.748	3.500	291.000
24	0.305	0.188	282.500	48	8.803	7.000	298.000

area (Points 26—37), the additions vary from 0.031 to 0.094 μl, corresponding to 1—3 steps of the stepping motor. In the steepest part of the sigmoidal curve, from Points 29 to 30, a potential jump is measured of about 250 mV. In this area the algorithm can hardly control the process, because fractions of a single step would be needed to achieve equidistant ΔE values. A secondary effect is the relatively large influence of the subsequent delivery of titrant from the burette tip in this area. The totally added volumes of titrant corresponding to the Points 29 and 30 are respectively 283.0(31) and 283.1(25) μl (the brackets denote the inaccuracy of the last two digits). After the end-point area (Points 37—48), the additions are doubled. The algorithm is protected against overshooting in such a way that a new addition of titrant is never more than twice the previous addition. For this restriction, a price must be paid: the potential values directly after the end-point are not distributed quite so equidistantly. The end-point is calculated by fitting an arctg function (Eqn. 7) through five points in the steepest part of the titration curve, resulting in an end-point of 283.0(86) μl. The titration procedure took 23 min 21 s. (This experiment served as an illustration for the hyperbolic extrapolation algorithm; with another parameter setting the procedure could take much less than 23 min.)

Discontinuous spectrophotometric titrations

Titration of copper(II) with EDTA. Titrations were tested on 10.00-ml aliquots of a solution containing 5.00 ml of 0.05 M Cu(II) and 50 ml of 0.5 M monochloroacetic acid/monochloroacetate buffer (pH 2), diluted to 100 ml with 0.01 M perchloric acid. The titrant was 0.1 M EDTA. The end-point is indicated by the formation of the Cu(II)—EDTA complex, with maximum absorbance at 745 nm. The data sampled by the microcomputer are transmittance values. The master program transforms these values to absorbance and then corrects them for dilution during the titration by means of the equation:

$$A_{\text{corr.}} = \{-\log(T)[V_{\text{added}} + V_{\text{start}}]\}/V_{\text{start}} \quad (8)$$

where T denotes transmittance, $A_{\text{corr.}}$ is the absorbance after volume correction, V_{start} is the starting volume of the sample solution in the titration cell and V_{added} is the total volume of titrant added up to the point considered. In the master program, the equilibrium algorithm is used for determining the waiting time, while the end-points are calculated from the intersection of the two straight lines fitted through the two segments. The titrations are done under the condition of equidistant absorbance steps, controlled by the hyperbolic extrapolation routine. The average values of three titrations are listed in Table 3.

In this kind of titration, the application of the hyperbolic extrapolation routine is not necessary, as the segments (absorbance versus volume of titrant) are also nearly linear. The motive for applying this routine was to check the results on slightly curved segments, which results were satisfactory.

TABLE 3

Spectrophotometric Cu(II)—EDTA titrations, with a hyperbolic extrapolation routine. Calculated end-points are given with volume correction for dilution during titration

End-point volume (μl)	Approximate titration time (min)	Number of points
246.0 ± 0.9	4	11
247.4 ± 1.0	10	32

Titration of copper(II) and iron(III) with EDTA. This type of spectrophotometric titration was used to test the equilibrium algorithm in a system where the dynamic system parameters change significantly. The titrations were done in 10.00-ml aliquots of a solution containing 4.00 ml of 0.05 M Fe(III), 4.00 ml of 0.05 M Cu(II), 50 ml of 0.5 M monochloroacetic acid/monochloroacetate buffer (pH 2) and diluted to 100.00 ml with 0.01 M perchloric acid. The total Cu(II)/Fe(III) was titrated with 0.1 M EDTA and the end-point was indicated by the Cu(II)—EDTA complex at 745 nm. Upto the first end-point, the EDTA added reacts immediately with Cu(II) to form the Cu(II)—EDTA complex. Because the conditional stability constant of Fe(III)—EDTA is several orders of magnitude higher than the conditional stability constant of Cu(II)—EDTA, quantitative conversion to the Fe(III)—EDTA complex will occur. As the formation of the Fe(III)—EDTA complex is slow compared to that of the Cu(II)—EDTA complex, the response of the spectrophotometer will be as illustrated in Fig. 9. The estimated overall time constants, obtained by applying the equilibrium algorithm, vary from 13 s at the start of the titration to 188 s in the neighbourhood of the first end-point. Here also, it is assumed that the overall system response is predominantly first order in the interval between two additions. During the titration, when the first end-point is passed, the overall time constant will change to fractions of a second. The average results of three experiments are shown in Fig. 10. The end-points are calculated from the intersections of the straight lines fitted through the segments, and neglecting the points sampled near both end-points. As in the former experiment, the hyperbolic extrapolation algorithm is used to control equidistant absorbance values.

Discontinuous spectrophotometric titrations with indicator added

This type of spectrophotometric titration was examined to test the end-point calculation for a case in which one of the segments of the absorbance versus volume curve is slightly curved. A solution containing 3.00 ml of 10^{-5} M ytterbium, 5.00 ml of 1 M hexamethylenetetraamine buffer (pH $\approx$ 5.5) and 1.00 ml of 10^{-4} M xylenol orange indicator in a 10-ml titration cell was titrated with 10^{-4} M EDTA. The end-point is indicated by means of the xylenol orange—ytterbium complex at 575 nm. The titrations are done in triplicate. Ytterbium was also titrated similarly after (1 + 1) dilution of the 10^{-5} M solution with 0.01 M HNO_3. Average results of the two sets of three titrations each are listed in Table 4.

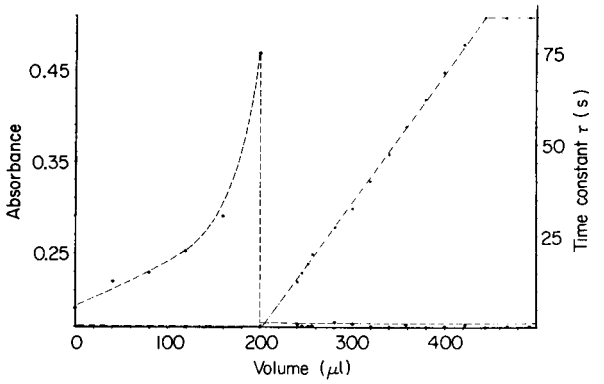

Fig. 10. Spectrophotometric titration of Cu(II)/Fe(III) with EDTA: (- - - -) time constant versus titration volume; (-·-·-) absorbance versus titration volume. First end-point at 201.5 ± 10 μl; second end-point 445.3 ± 0.4 μl; titration time about 50 min.

CONCLUSIONS

The dedicated titrator described here meets the requirements outlined initially. Of course, the microprocessed system offers more possibilities than used in this design. Obvious extensions would be the calculation of the second derivative of the titration curve for end-point determination, linearization of the titration curve, volume corrections, etc. In an earlier approach [21], hardware solutions were used for linearization and volume corrections, which could be applied in combination with the automated titrator or with manual titration systems [22]. The progress in microcomputer technology facilitates cheap software solutions for such functions.

The simple titrator described needs some parameter settings before the titration. Depending on the applications, an automated titrator can be designed to operate either fully automatically or to utilize the prior knowledge of the operator. In principle, optimum results will be achieved by using skilled analytical knowledge in addition to the calculating capabilities of the instrument.

The development of a fully automatic titrator still requires much investigation of titration systems. System parameters, such as time constants,

TABLE 4

Calculated end-points of spectrophotometric titrations of ytterbium with EDTA (xylenol orange indicator)

Dilution	End-point (automated titration)	End-point (manual titration)	Titration time (automated titration)	Number of points
Without dilution	307.0 ± 1.0	294.3 ± 1.5	± 4½ min	15
(1 + 1) dilution	159.0 ± 1.7	157.0 ± 2.0	± 7 min	15

their dependence on the signal, and their influence on the systematic error have to be determined as well as the statistical properties and the origin of fluctuations (noise) of the signal. Such studies [15] are used in the computer network concept. Depending on the type of the titration curve (segmented or sigmoidal) and on the dynamic behaviour of the titration system (parameters of mixing, chemical and detection processes), the master program running in the host computer can be changed and adapted very easily to the requirements of the analysis. Modular FORTRAN software, combined with the control facilities served by the interpreter program, will be a powerful and flexible tool in the automation of titrimetric analysis. The system is also suitable for other techniques used in the analytical laboratory.

The algorithm for rapid potentiometric titrations can be applied only to cases in which the system parameters are constant or nearly constant during titration. These limitations may be overcome by developing algorithms for handling variable parameters as well. For spectrophotometric titrations, especially time-consuming ones, automation is very useful. The experiments showed good reproducibility of results in such titrations. Moreover, titrations of low concentrations of metal ions with an indicator added can be successfully automated. A weak point in the present method of end-point calculation, based on the volume corresponding to the intersection of two fitted straight lines through two segmented parts, is the accuracy of the coordinates of the obtained intersection point. When the titration time has to be decreased for control reasons, the number of sample points must also be decreased. This increases the uncertainty in the estimated parameters of the straight lines and also in the coordinates of the point of intersection of the two straight lines. So far, it has not been possible to find a satisfactory answer or a theoretical basis to the problem of how decreased titration time influences the accuracy and confidence limits of the end-points found. This is also true for the assessment of end-points on sigmoidal curves by means of the arctg fit.

The authors thank Mr. P. M. Boon and Mr. R. G. Logchies for their assistance in the microprocessor hardware and software development and to Drs. L. G. Decnop-Weever for her assistance during the experiments.

REFERENCES

1 D. J. Leggett, Anal. Chem., 50 (1978) 718.
2 N. Busch, P. Freyer and H. Szamelt, Anal. Chem., 50 (1978) 2166.
3 A. H. B. Wu and H. V. Malmstadt, Anal. Chem., 50 (1978) 2090.
4 P. U. Früh, L. Meier and H. Rutishauer, Anal. Chim. Acta, 95 (1977) 97.
5 D. Betteridge, E. L. Dagless, P. David, D. R. Deans, G. E. Penketh and P. Shawcross, Analyst, 101 (1976) 409.
6 W. E. Earle and K. S. Fletcher, Chem. Instrum., 7 (1976) 101.
7 L. M. Doane, J. T. Stock and J. D. Stuart, J. Chem. Educ., 56 (1979) 415.
8 A. H. B. Wu, T. Rotunno and H. V. Malmstadt, J. Assoc. Off. Anal. Chem., 62 (1979) 969.

9 L. Andersson, A. Granéli and M. Strandberg, Anal. Chim. Acta, 103 (1978) 489.
10 R. W. Hendler, D. Songco and T. R. Clem, Anal. Chem., 49 (1977) 1908.
11 R. W. Hendler, Anal. Chem., 49 (1977) 1914.
12 C. R. Martin and H. Freiser, Anal. Chem., 51 (1979) 803.
13 S. Firstenberg and H. Malmvig, Am. Lab., 10 (1978) 119; Chimia, 32 (1978) 514.
14 T. F. Christiansen, J. E. Busch and S. C. Krogh, Anal. Chem., 48 (1976) 1051.
15 J. C. Smit and H. C. Smit, Anal. Chim. Acta, 143 (1982).
16 H. C. Smit, Anal. Chim. Acta, 122 (1980) 201.
17 R. P. J. Duursma, H. Steigstra, R. G. Logchies and H. C. Smit, Anal. Chim. Acta, to be submitted.
18 C. N. Reilley and R. W. Schmidt, Anal. Chem., 29 (1957) 264.
19 U. Hannema, G. J. van Rossum and G. den Boef, Fresenius Z. Anal. Chem., 250 (1970) 302.
20 P. R. Bevington, Data Reduction and Error Analysis for the Physical Sciences. McGraw-Hill, New York, 1969.
21 J. M. van der Meer and J. C. Smit, Anal. Chim. Acta, 83 (1976) 367.
22 G. J. M. Heijne, Ph.D. Thesis, University of Amsterdam, The Netherlands, 1977.

Analytica Chimica Acta, 143 (1982) 95—110
Elsevier Scientific Publishing Company, Amsterdam — Printed in The Netherlands

A GENERAL-PURPOSE MINICOMPUTER SYSTEM FOR ELECTROCHEMICAL STUDIES

D. BRITZ

Kemisk Institut, Aarhus Universitet, 8000 Aarhus C (Denmark)

(Received 13th April 1982)

SUMMARY

A software system (SYS) is described for a 16-bit minicomputer interfaced to a potentiostat and electrochemical cells, as well as various display and signal devices. The software controls the functions common to all electrochemical experiments, such as applying cell voltage, timing, sampling signals, displaying these on graphic devices, and smoothing data; it also loads specific user programs into core, for experiments requiring these functions. In this way, a new experiment can quickly be programmed and running; the software also contains some debugging aids. While the system described is specific to the minicomputer used, its general structure should be capable of implementation on any mini- or microcomputer.

The minicomputer (or microcomputer) is no longer a rarity in electrochemical research, principally because the cost of a minicomputer and its peripherals is now at a level which does not dominate the total equipment cost. What is still rare, however, is a generally useful software system that can be adapted quickly to a new experiment; as a rule, considerable programming effort dedicated to a single experiment is needed [1]. Clearly, there is a need for a set of standards for a computerized set-up, so that a relatively inexperienced research worker can buy what is required and then construct a flexible system in a structured manner. The system used in this institute is an attempt in this direction, and is described in this paper.

The system

To run electroanalytical experiments, the computer should function as a controller of a given potentiostat. It should thus be a programmable signal source (D/A converters), be capable of measuring signals from the potentiostat (A/D converters), and produce a few pulses and short circuits on demand to control various other devices. The computer software system should have built into it the usual basic tasks (handling of peripheral devices and simple processes), as well as some commonly used experimental techniques such as polarography with controlled drop time, comparative impedance measurements, and perhaps cyclic voltammetry. The system should produce output to display devices (usually a video unit and an X-Y plotter) and hand over

stored data to another computer (or perhaps store it for access by a higher-level system running on the same computer).

The computer need not take over functions that are done well by the analog equipment; for example, a computer can be a digital potentiostat [2] but a simple analog device is more effective. The same applies to signal conditioning (rectifying, filtering, amplifying), although occasionally digital treatment is advantageous, e.g., in on-line FFT work [3]. On the software side, the system should allow quick programming for new experiments. No complex data handling is generally needed, as this can be done off-line. As far as possible, user/system interaction should be "friendly", i.e., not too rigid. The program structure should allow a reasonable possibility of transport to another computer without drastic changes at levels higher than the machine-code level.

Most of the above requirements appear to have been achieved in the present system; transportation has not been tried. Programming for new experiments and tests is quick after some practice. Students take a week or so to learn the assembly code and then write their own experiment programs, generally in a few hours. A peek/poke facility, allowing direct access to core, helps with debugging. A large collection of three-character commands provides a reasonable number of standard processes (displays, data moving/handling, smoothing, sampling, setting of D/A outputs, etc.).

HARDWARE

Figure 1 shows the hardware schematically. The computer, a Computer Automation Alpha LSI 16-bit machine with 8K of volatile memory and a

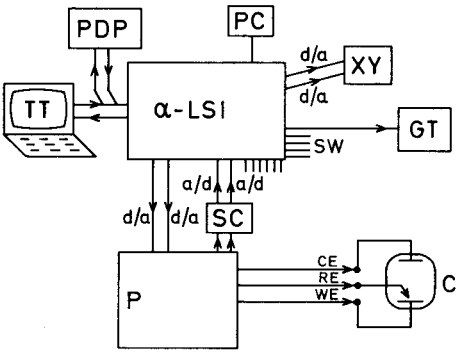

Fig. 1. Hardware system. The Alpha LSI minicomputer is connected to a remote PDP 11/44 and some local devices. TT is a keyboard terminal, and PC is a programmable clock with 12-bit A/D converters (eight channels); there are four D/A converter channels, two of which address the X-Y recorder; GT is a video dot-matrix screen (192 × 256 points); P is the potentiostat, fed from the Alpha by a D/A output and presenting (normally) the current-readout and cell voltage to two A/D inputs for reading, through the signal-conditioning units SC. C is the electrochemical cell with its counter, reference and working electrodes, CE, RE and WE, respectively. The SW (switches) device is used variously to control external events.

64-word ROM containing the bootstrap loader, communicates with the operator terminal TT and/or a remote PDP11 computer. The Alpha has four D/A outputs, eight channels of A/D input, eight on/off switch "outputs" which also deliver TTL pulses from other pins, and four variable-length pulses. Two of the D/A outputs are attached to an X-Y recorder; the other two can feed the potentiostat P with control signals. Typically, the A/D inputs sample the electrode current and potential, timed by a programmable clock device PC. The on/off switches and TTL pulses can be used for such jobs as activating a drop-knocker, an automatic burette [4] or a floating switch within the potentiostat, which isolates the cell from the control amplifier, thus interrupting the current, for potentiometric stripping work [5]. Besides the X-Y recorder, there is a graphic terminal (GT), which is a video unit with a dot matrix (256 × 192 points).

The potentiostat is a standard laboratory-built unit based on the design of Brown et al. [6]; it incorporates damped positive feedback iR compensation [7], current-follower current read-out and the above-mentioned floating switch. The signal conditioning module (SC) consists of a precision d.c. amplifier, one a.c. amplifier, one full-wave rectifier for a.c. work, one variable high-pass filter, and three variable low-pass filters (all with FET inputs). Filtering, often neglected, can reduce noise levels and is dictated by the sampling theorem [8]. The electrochemical parts vary with the experiment; a Metrohm E554 polarographic stand (with drop-timer input) and a PAR 303 static mercury drop electrode stand have been used.

A remote PDP 11/44 can be connected to the TT or the Alpha. In the configuration used here, the PDP is used for higher-level tasks; it contains, for example, a cross-assembler for the Alpha assembler code, and it generates the Alpha machine code as an ASCII file that can be read into the Alpha by its loader. The PDP can also receive data from the Alpha. Of course, floppy disk storage, and even an independent (disk) operating system, can be attached to the minicomputer; this would then take over the tasks of the PDP. Such systems will generally be less powerful than the PDP system (RSX), which further communicates with a larger VAX 11 system in this department. In any case, the electrochemical software system would remain substantially the same if disk storage and operating system were available.

For users contemplating the purchase of such equipment, the cross-assembler could present a problem, if a system is not provided with the minicomputer. Fortunately, some general-purpose assemblers that can be adapted for the commoner commercial microprocessors are now becoming available.

THE SYS SOFTWARE

The system program (SYS) is described below in sufficient detail to make its design and operation understood; the machine code details are not given because these are specific to the machine.

Alpha architecture and conventions

The Alpha LSI has 16 bits per word. Hexadecimal notation is indicated by a colon before the number, e.g., :1000 = 4096. For hardware (coding) reasons, only the first 128 locations (the scratch pad area) can be addressed from anywhere in memory; this area is a valuable part of memory. Logically, in this area are sited such quantities as hardware flags, constants, pointers to (i.e., addresses of) system subroutines which must reside in higher memory, and, for convenience and if there is space, a globally accessible data area for use by any user segment (see later). It so happens that most (but not all) hardware interrupt vectors are also sited in this area (see below). To save memory, this area contains no subroutines but only pointers to them. The interrupt vector codes are mostly one-word items. At the time of writing, there are vectors, flags, constants and a "load" address, from 0 to :18, a block of forty words for a globally accessible data area and finally about sixty subroutine pointers, leaving some spare words.

The Alpha has two registers, A and X; these are fast-access 16-bit words and are needed for many machine operations.

The following hardware devices are peripheral to the machine (cf. Fig. 1). The keyboard terminal (TT) is an ADM 3A terminal. The programmable clock (PC), coupled to an eight-channel multiplexed A/D converter, has an automatic-in feature, somewhat like a direct memory access. The on/off switch device (SW, eight switches) is a row of reed switches acting within some 50 μs; this device also incorporates the D/A converters, i.e., they share the same I/O channel. The real-time clock (RC) is controlled by mains frequency (50 Hz) with pulses at 10 ms intervals. The console interrupt (CO) is a pushbutton with a corresponding interrupt vector, and is used as an emergency exit from any condition.

In addition to the graphic terminal (GT), there is an X-Y plotter (Philips PM-8041) which is controlled by one SW channel, which lifts or drops the pen, and two D/A channels, which control the two axes. Thus, there is no machine code that activates the plotter as such, but at the next higher coding level it is convenient to think of the plotter as a device.

All real devices have special machine codes to control them. Each is given a hardware channel number, and a small number of code patterns performs such operations as enabling/disabling the interrupt capability of the device, sending control information to it or reading information from it. These codes are specific to the computer used, as well as the device structure, and will not be described further.

The SYS structure

Table 1 shows a rough memory map of SYS, which is a self-contained program complex with all hardware handlers (interrupt service routines, etc.), subroutines and a large number of command procedures. The load command LOA will effect the reading into memory of a given additional USER segment. The general outline of SYS is as follows.

TABLE 1

Memory map of SYS

:0000	Scratchpad	Hardware interrupt vectors, flags, global constants, subroutine pointers, globally accessible data area
:007F	Trap vectors CO, RC vectors	
	TT monitor (ISR) and TT input buffer	
	TT command interpreter	
	SYS routines	Hardware handlers (TT, GT, XY, PC, SW) and routines Software subroutines
	Experiment routines	POLAR, IMP, *POT
	PRELIM, SETUP, MAIN	
:0B80	USER	USER TT command interpreter; USER program(s)
:1000 :1FFF	Data area	

Immediately following the trap, CO and RC vectors, is the TT monitor section, containing the relatively short TT interrupt service routine and the command interpreter through which all actions originate. Then there are the device handlers and routines, and a series of general subroutines including the above-mentioned peek/poke facility, a TT memory dump display, a loader for the user-specific segment, some arithmetic routines (multiply, divide, 2**N, etc.), several data-handling routines (smoothing, moving, inverting, differentiating, etc.), some routines to convert ASCII strings to binary numbers and some standard electrochemical experimental routines, e.g., for polarographic and timed impedance measurements. Lastly, there is a preliminary routine, to be executed once, upon loading of SYS into memory, and a set-up routine, which restores conditions to normal upon pushing the console button. The last few words of SYS are formally the "main" program, where SYS waits for commands (it is a prompt plus a two-word wait loop) and a dummy USER segment. This, when SYS has been freshly read in, contains only a return code; it is the place from which an actual USER segment will be written when it is loaded.

At present, SYS, up to the (main) wait loop, is about 3K words in length. Most user programs are not more than a few hundred words in length. Thus, the top 4K of memory is always available for data and a data stack commonly starts at address :1000 or 4096.

The handling of SYS

The start-up sequence is as follows. First, the computer, the terminal and all other devices are turned on. There is a switch on the front panel, connecting either the TT with the remote PDP11, the TT with the Alpha, or the PDP11 with the Alpha and TT in parallel. Secondly, TT is connected with the PDP, and the operator logs on. Then TT is switched to PDP/Alpha + TT, and the Alpha is set to LOAD; it contains a small bootstrap loader which is read into a high memory location. This loader will read into memory binary code, which it translates from ASCII hexadecimal code. Thirdly, the PDP (RSX) utility program PIP is prompted to display the SYS code file, which is read in by the Alpha bootstrap loader. Upon completion, the Alpha goes through some initializing procedures and ends up in the MAIN wait loop.

Normally, in the fourth step, a USER segment is also wanted (SYS is usually kept in memory). The operator again logs onto the PDP, switches over to the Alpha and enters the command LOA. This actuates the SYS loader, which, like the ROM loader, reads in ASCII hexadecimal code coming from the PDP (a USER program, sent by PIP) but now writes this into memory starting from the USER location. Any older USER is thus overwritten. At the baud rate used here (2400 baud) this takes only a few seconds, while SYS requires 2—3 min.

It is thus possible to write relatively short USER (experiment-specific) programs on the PDP, cross-assemble these as separate units into an ASCII code file and read these in quickly as wanted, and debug them with the PEE (peek/poke) command.

In the fifth step, the experiment is run. Mostly, the experiment produces GT displays, and X-Y plots can be obtained by the manual PLT command. Finally, if the acquired data are to be sent to the PDP for higher-level processing, they are displayed on the TT by the Alpha, and simultaneously read by the PDP, in the edit mode.

Details of the SYS routines

In the following paragraphs, subroutines are usually named by their scratchpad pointer names; this is indicated by a leading asterisk, e.g., *CHARO points to the actual routine ZCHO.

Interrupt service routines. With the Alpha, a successful interrupt transfers control to the respective interrupt vector location, which may contain a machine instruction. For all devices except the TT, the interrupt vector normally contains the IMS (increment memory) instruction, i.e., the flag word for the device is incremented on interrupt, and this can be detected by the calling process.

TT interrupts are more complex; it is necessary to handle typed text, stack it into a sixty-word line buffer and, eventually, on a line-terminator (carriage-return, CR or line-feed, LF), act on the contents of that line. The TT interrupt vector is therefore a call to the TT interrupt service routine, or keyboard monitor. For most typed characters, this routine, TTISR,

(see Fig. 2) reads the typed character, echoes it, and adds it to the line already accumulated in the line buffer. Some special cases are as follows: (a) a control-S followed by a control-Q provides halt and restart of a display on the TT; (b) a control-U invalidates the line being typed and starts a new one, echoing U and a CR/LF; (c) a RUB backtracks one space; (d) a CR or LF indicates that the accumulated line is now ready for interpreting (i.e., it is a complete command line); a CR/LF is echoed, the line buffer pointer is reset to the start and the command interpreter subroutine is called, which itself will call one or more processes.

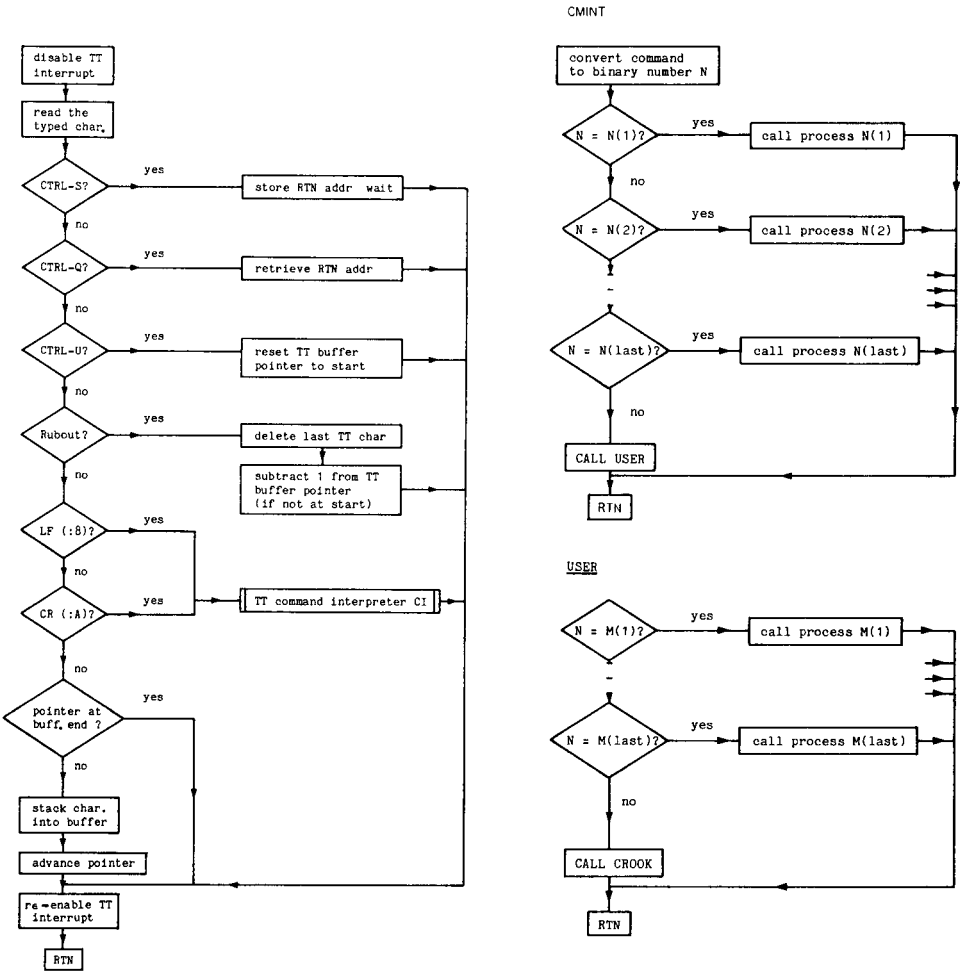

Fig. 2. Flow diagram of the TT interrupt action (TTISR). "RTN" means "return to interrupted process".

Fig. 3. Flow diagram of command interpreter CI (sectioning, discussed in text, not shown). $N(1), N(2), \ldots N(\text{last})$ are command numbers, from radix-40 conversions of command texts.

The command interpreter CMINT. Figure 3 shows a flow diagram of CMINT. CMINT is entered from the TTISR, and the first 1, 2 or 3 ASCII characters in the line buffer are converted to a number, by using radix-40, which allows condensation of any three-letter string into a unique binary number. This command "value" is now compared with a string of known, expected values. A successful hit calls the required part of SYS, and a RTN is effected on completion. If no hit is found anywhere, it is assumed that the command must lie in the USER segment, and this is called. There, the search is continued until a hit is obtained or until the segment has been searched. If no hit is found at all, the command was a bad one and the routine *CROOK (which gives suitable warning) is called before the return.

An overview of some of the actual commands *N*1, . . . and their function is shown in Table 2. A few more minor ones are not shown. Most commands are followed by (normally) numerical parameters and these must be read in and converted from the ASCII strings in the buffer, to the intended binary value. The routine *ASBIN does this conversion (see below), delivering a number. Many of the commands have "memory", i.e., the subroutine called stores the previous parameter set and if the command is given later without parameters (*ASBIN then returns a string of zeroes), the zero values lead to repeated use of these "remembered" values. This is very convenient with multiparameter commands such as PLT, SAM, SMU, POL, which are, in practice, called many times during an experimental run, with the same parameters.

The command POL sets the Alpha to producing a polarogram; at given intervals, the current is sampled (average of twenty readings at 1000 Hz, to eliminate 50-Hz line hum) and stacked, and the mercury drop is knocked off. The new potential is then also set. With a minicomputer, the easiest form of potential scan to generate is a staircase scan that holds the potential constant over the life of each drop, the dE/dt component of classical polarography is then absent. It is also quite easy to program alternate-drop polarography [9], which eliminates depletion effects of one drop on the next.

This type of polarography (which can be d.c. or simple a.c., depending on what is fed to the A/D converter) is useful for a close look at a new system with unknown behaviour. Single-drop sweep techniques, which are sometimes advantageous [4, 10], are less well suited to preliminary observations.

The command IMP initiates an infinite loop, in which at drop-life intervals TD the current is read at a fixed potential E (again, average of twenty readings) and displayed on the TT, and the drop is dislodged. This is useful in impedance measurements [11]. The infinite loop is ended by pressing the console-interrupt button, which forces a return to MAIN.

Hardware and pseudo-hardware routines

The SYS subroutines handling hardware functions are outlined here to convey the principles involved. The idea is that simple functions will be required repeatedly and it should not be necessary in writing an experiment program (USER) to be concerned with basic tasks such as writing a number

TABLE 2

An overview of the commands and their functions

Group	Mnemonic	Parameters	Function
General	PEE	addr 1	Examine/modify a location
	DMP	addr 1, addr 2	Display core contents
	JMP	addr	Jump there
	LOA		Load USER segment
	RAD	1, 2 or 3 char.	Give radix-40 value of string
	PDP	*n*, addr	Transfer *n* numbers, starting at addr, to PDP 11/44
Switch	SWI	N 1/0	Switch switch N on/off
	DAC	N, mV	Set D/A N to mV
GT	GTC		Clear GT monitor screen
	GTO	*n*, scale-down, addr, *x*-gain	Display *n* locations, centered, from addr, on GT, with scale-down and *x*-expansion
X-Y plotter	PLM	X, Y	Move pen (up) there
	PLB		Put dots in 4 outer corners
	PEN	1/0	Drop/lift pen
	PLT	*n*, dy, *y*-gain, *x*-gain, addr	Plot the *n* points on XY, offsetting by +dy, with *y*-gain, and *x*-gain, from location addr
PC	ADC	*n*	Single-shot A/D conversion on ch. *n*, display as mV on TT
	SAM	*n*, ch., *f*, addr	Sample *n* points on A/D ch. at *f* Hz; stack these from addr
Data handling	CLR	*n*, addr	Clear *n* words of core from addr
	MOV	*n*, addr 1, addr 2	Copy *n* words from addr 1 . . . to addr 2 . . .
	SMU	*n*, w, addr, n	Smooth an *n*-word sequence from addr, with smoothing window w, *n* times
	INV	*n*, addr	Change sign of *n* words from addr
	DER	*n*, addr	Differentiate *n* words from addr
Electrochemical	POL	(see text)	Take a polarogram
	IMP	(see text)	Repeatedly display current measurement

on the TT or getting the PC ready to sample data. There is a hierarchy of such routines; e.g., the TT has a dedicated routine for printing one character (*CHARO) and this is utilized by the higher-level routine *STRO (string out).

The terminal device, TT. The two most basic routines here are *CHARO and *TTENA. The *CHARO routine writes a single ASCII character, passed via the A-register, on the screen. It must first test whether the TT device is ready for such an entry (and wait if it is not). Then the proper code is sent to the TT device. The wait/test loop plus device addressing are thus conveniently combined into on subroutine call, CALL *CHARO, with prior loading of the character into the A-register.

The *TTENA routine enables interrupts by the TT (i.e., the input from the keyboard part), after completing a data read from the TT to clear a possibly unread character (some TT's demand this) and making sure that the proper code is in the TT interrupt vector, by placing it there; it should be the "call TTISR" code, but may accidentally have been overwritten.

Certain characters are "printed" frequently, e.g., CR/LF, space, colon, the "bell" tone, and the prompt character, normally the asterisk. These have their own routines *CRLF, *SPACE, *COLON, *BELL and *PROMPT, and all make use of *CHARO. This saves loading the A-register with the appropriate ASCII code.

The subroutine *STRO (string out) displays a text string, specified via the X-register by its starting address in memory, on the TT. The routine writes the string, using *CHARO, until it finds a null (binary zero); such a string must therefore be terminated with a null. This is useful for system (error) messages, or for printing numbers, first processed into character strings (e.g., by *DECO or *HEXO; see below).

A useful routine is *TTIN: this enables TT interrupt, and simply locally waits for any character to be typed by the operator, returning the code value after again disabling the interrupt. In this way, one can program an operator-controlled wait. This has been used, for example, for computer-controlled titrations [11] where *TTIN allowed a wait for the next titration increment, and simultaneously read in the number of volume increments to be added.

The graphic terminal device, GT. Here there are only two bottom-level, hardware-addressing routines: *GTO and *GTCLR. The former places a dot on the GT at coordinates passed via the A- and X-registers, while *GTCLR clears the screen, interrupts and waits for 100 ms, which is demanded by the terminal used here.

There is also a higher-level subroutine, *GTOUT, which uses *GTO to reproduce a given data buffer as a graphic display. There are too many parameters to pass via the registers, so they are passed via a data block containing the parameter addresses, following the call:

```
CALL    *GTOUT
DATA    N
DATA    YSCL
DATA    BUFAD
DATA    XINC
```

with N the number of points, YSCL the y-axis (down) scaling, BUFAD the starting address of the buffer (i.e., the number series) and XINC the x-scaling. The buffer is displayed as a contiguous time-series, centered along the x-axis. A sampled set of data points (up to 256 points) can thus be displayed quickly. Conveniently, this routine has "memory" for the parameters, and the GTO command can thus be given without them after the first time.

The programmable clock device, PC. This is both a programmable clock and an A/D converter. Several bottom- and higher-level routines are concerned with this device. Thus *PCOFF stops clocking, converting and interrupting. The routine *PCRDY, with the parameters frequency and channel number passed via the A- and X-registers, prepares PC to clock at the required rate and to cause an interrupt at each A/D conversion. The *PCWTC routine waits for the next PC interrupt (detected by the raised PC flag) and clears the flag again; a reading of the A/D conversion may then be taken. The *PCIMS routine places the "increment PC flag" code into the PC interrupt vector, in case it has been replaced by different code; it also clears the PC flag. The *PCSFR routine sets the PC's clocking frequency but does not start the PC; this hardware routine is used by *PCRDY. The *SAMPLE routine, with a data block, initiates a data-sampling sequence, using the automatic-in feature. Parameters are *N* (number of samples), channel number, frequency, and the buffer address from which the acquired data is to be written. The *ADCON routine provides a single-shot immediate A/D conversion and returns the value to the A-register, by using the single-shot mode of PC.

The switch device, SW. The *SWITCH routine turns a certain switch number (A-register) on or off, depending on the X-register contents; also included is the basic routine *PULSE, which outputs a TTL pulse on the given channel (A-register) to the front-panel sockets. This is used, among other things, by the higher-level routine *KNOCK, which applies a pulse on the channel dedicated to the Metrohm drop-knocker input. To knock off a mercury drop, only CALL *KNOCK need be written into the program.

The SW I/O channel is shared by the D/A converters, and so *DACON is also placed here. The latter routine sets one of the D/A output terminals to the required voltage (passed as mV, and converted to counts by the routine).

The X-Y plotter pseudo-device, PL. This is a "soft" device; channels 3 and 4 of the D/A converter are attached only to the X-Y recorder, as is one of the on/off switches, to actuate the pen. Thus the lowest-level hardware routines are in reality addressing the SW device, via subroutines *DACON and *SWITCH.

Here, there are several low-level routines. Thus, for example, *PLPEN lifts or lowers the pen, depending on the A-register value passed, and then waits 150 ms to give the movement time for completion; *PLGO moves the pen (whether up or down) to new coordinates, which are output via the D/A channels, and a return from *PLGO is effected after a 500-ms wait. The *PLMOV routine first lifts the pen and moves it to the new coordinates (using *PLPEN and *PLGO); and the *PLDOT routine lifts the pen, moves it to new coordinates, drops it there briefly, and lifts it again, thus printing a dot. All pen movements for these routines are effected via *PLGO, which also records in memory the new coordinates.

Next there is a subroutine *PLDRW. This draws a straight line from present coordinates (held in memory) to the new given ones. The problem here (i.e., why *PLGO cannot just be used with the pen down) is that the pen must travel fairly slowly, and must draw a good straight line joining the coordinates. Clearly, as the D/A converters driving the pen have a minimum resolution, a series of steps in X and Y will be produced and the series that lies closest to the ideal straight line must be found. The recorder pen movement is the sum of many very small movements with intervening wait periods; in practice, the length of the wait period is adjusted until the drawing speed is acceptable, producing good lines.

The highest-level X-Y plotter routine is *PLOT, which draws a stored time-series, using *PLDRW to draw straight lines from point to point. The data is taken to be a sequential function and is drawn with scaling parameters as passed by the call. This routine can be called directly (and usually is called only) by the command PLT. The parameters are N (number of values in sequence), y-offset (in mV), gain or attenuation, X-scaling factor (time/axis increment, or multiple of one D/A unit) and data buffer start address. This routine, which usually is called repeatedly during an experiment, has the memory feature.

Miscellaneous SYS subroutines

Roughly the second half of SYS comprises subroutines that are not directly concerned with hardware activity; some of these are number conversion and arithmetic routines, and some write information on the terminal. These are described briefly. Generally, there are no problems in programming these and with more recent microprocessors, multiply and divide are available as hard-wired functions as well as double-word addition.

Memory display/correction. The routine PEEK, only ever called by the command PEE plus address, allows display (in decimal and hexadecimal) of specified memory locations. The TT cursor halts after the display and if the operator types in a new number (in either hex or decimal form), this will replace the original contents and the next location will be displayed. Typing a slash (/) causes the next location to be displayed and with a back slash (\) the previous location is displayed; typing a point (.) ends the PEEK run. With this, it is possible to check the memory contents and correct them, or place data manually into memory, e.g., for test purposes.

DUMP (command DMP) prints a table of memory contents on the TT, both in decimal and hex, alongside the addresses, between two specified addresses.

All display routines, writing numbers on the TT, make use of the conversion routines *HEXO and *DECO, which receive a binary number and write it out in formatted ASCII code (see below).

The subroutine *CROOK, the complaint routine, prints two question marks on the TT and sounds the bell tone, to indicate some bad conditions, e.g., trying to write into the SYS area, or inputting a non-existent command, etc.

Data-handling routines. Several operations on data arrays are available. The *MOVX routine (command MOV) copies a specified array to another memory area. This is useful for saving experimental data until the end of an experiment, for final plotting. The *INVRT routine (command INV) changes the sign of an array of numbers. DERIV (DER) performs a simple central-difference differentiation. CONDI (CON), a signal-conditioning routine, can offset and scale (up or down). *SMUTH (SMU) will smooth an array, using an equal-weights, moving-average technique, with a specified window size.

Arithmetic routines. These operate on single numbers or pairs of numbers at a time. The *MPY routine multiplies two numbers, placing the result with double-word precision into the X- and A-registers. *DIV divides a double-word number, as *MPY places it in the registers, by another integer. *IABS returns the absolute value of a number and *EXP2 returns the base-2 exponential (required for some hardware codes). *SQRT computes the square root, using Newton's method, of a double-word integer.

A double-word adding routine, *DADD, adds an integer to a double-word number in memory, specified by the address of the high word. This is needed when several numbers are averaged and their sum exceeds the maximum size for a 16-bit word, 32767.

Number (code) conversions. First, *HEXO and *DECO convert a binary integer to an ASCII code string that can then be displayed on the TT screen as a four-digit hexadecimal number or a signed six-field decimal, respectively. The routine *RAD40 receives a string with up to three characters (a command string) and converts it to a single number by the radix-40 method.

There are also the two conversion routines *ADMV and *MVDA. The first takes an A/D count (i.e., the result of an A/D conversion) and converts it to a (milli)voltage by scaling. *MVDA computes the counts that must be presented to the D/A converter to cause it to produce the given (milli)-voltage.

Lastly, there is the most important routine *ASBIN. Most commands are followed by number parameters, in either hex or decimal ASCII code (or a mixture). These must be decoded. The usual convention is adopted that hex numbers are preceded by a colon and decimals are typed as (signed or unsigned) numbers. These codes lie embedded in the TT input buffer on typing a CR/LF. The X-register is used as buffer pointer. First the command itself is converted to the radix-40 form and the appropriate subroutine (or program section) is entered, moving the pointer to the character just past the command. *ASBIN now advances the pointer, for every parameter to be found, until it finds a non-blank character, which may be a colon, a sign (+ or −) or a digit. It then interprets the code following this, ended by either a blank or a null (line end), as either a hex or decimal number and computes that number, returning it via the A-register. The X-register pointer is moved on past the code string, ready for the next, if any. The decoding and computing is a relatively simple task, computationally. If anything is wrong with

the string (illegal, uninterpretable characters) or there is no string where expected, the routine returns zero as the result(s). This is useful for those commands calling routines with memory; the first call might be the command with a number of parameters, and subsequent calls simply the command itself; *ASBIN will then "read" all parameters as zero, which causes the called subroutine to use the previous values.

Other routines. The wait routine *DELAY can provide timed waits, counted either in 10 or 0.1 ms units. In the first case, the 100-Hz real-time clock RC is used to count down the given (passed) number of ticks. If the passed argument, the number of ticks, is negative, it is interpreted as a (positive) 0.1 ms unit, and a software timing routine is used, which is simply a loop of dummy statements, carefully adjusted to exactly 0.1 ms. Such delays are needed in many experiments; examples are drop timing, or waiting (e.g., 1 ms) after applying a new electrode potential before taking a measurement, or holding the electrode at a deposition potential for 1 min in anodic stripping, etc.

The subroutine LOAD, called only by the LOA command, reads in a USER segment from the PDP (set to write this on the TT), converts each four-digit hex ASCII code string to a binary number, and stacks it in the USER memory section. To change from one experiment to another, or to use a new version of the USER program, the new program text file on the PDP is assembled into an Alpha machine code file and loaded via LOAD. These segments are usually short and require only a few seconds to load. The body of SYS is then preserved and may remain resident in the machine for weeks on end.

The USER segment invariably begins with its own command interpreter chain, ending with a call to *CROOK, if no commands are found, and contains some specific experimental subroutines; all of these subroutines have, of course, access to all global SYS routines that have their pointers in the scratchpad. These global SYS addresses are defined in a symbol table appended to each USER assembler-code file.

Standard electrochemical routines. There are three electrochemical routines: *POT, POLAR and IMPED, which happen to be very commonly used in this laboratory. *POT applies a given (milli)voltage to D/A output no. 1 (dedicated to the external control input of the potentiostat), using the *DACON routine after a *MVDA conversion. *POLAR runs a polarogram with the Metrohm stand, via the POL command, and IMPED by the command IMP (see above).

(Re)Starting routines PRLIM, SETUP. When a new program (SYS or just USER) is loaded into memory, the last code word is a transfer address, i.e., the address from which the computer will start executing after loading. Because the status of the various devices is highly uncertain at that point, it is best to start by resetting them all. PRLIM disables all interrupts, and devices are turned off. A message on the TT then prompts the operator to press the console interrupt button, CI (CO interrupt is, of course, enabled).

Whenever CI is pressed (also at any other time), the routine SETUP is called. SETUP resets certain memory locations to their normal state: e.g., the TT interrupt vector may have had a "no operation" in it, and receives the normal "call TTISR" code; the command interpreter pointer is set to point at the command interpreter (it may have been the local PEEK interpreter), the TT input buffer pointer is reset to the buffer start, all D/A channels are set to zero, switches are turned off and, lastly, the TT is enabled to interrupt. An asterisk prompt is printed on the TT. Control is then handed to what must be regarded as SYS's "main" program, which is simply a two-word wait loop. The processor cycles here until the operator starts typing a command, each typed character causing a TT interrupt, transfer to the service routine, which stacks the character, until a CR or LF is typed, whereupon it hands over to the command interpreter, etc. The chain ends with a prompt asterisk on the TT and a return, from the TT service routine, to the MAIN wait loop.

OTHER SYSTEMS

This paper has dealt specifically with the system used in this laboratory, based on a minicomputer that is now somewhat out-of-date. At the present time, a similar system could be constructed in much the same form with a cheaper microprocessor which has extra hard-wired mathematical capabilities. Such basic systems, however, require considerable cooperation with an electronics workshop. It may therefore be preferable to buy a more sophisticated minicomputer system, more or less ready-made, such as the Digital Equipment MINC 11, based on a PDP 11. Such systems will be more costly, but can also be used at higher levels, and are usually disk-based, incorporating an operating system, text editor, assembler for assembly code and sometimes a FORTRAN compiler. The big difference then will be that hardware handling is part of the operating system, and that the most demanding programming, that for the first part of SYS (see Table 1), is not needed. Instead of SYS, separate programs would be written, starting at the level of Experiment routines (Table 1). Some processes such as setting electrode potentials (by a D/A converter) would still appear as subroutines to be linked with experiment programs. The data area used by SYS would be replaced by arrays within any such program and these arrays would be written into a disk file for further processing. Some hardware routines would still be required, e.g., for a video display or switches and TTL pulse outputs; these would also be separately compiled/assembled subroutines, and could be stored in a suitable library facility.

The author thanks Mr. Peter Hougaard for writing the square-root subroutine and for helpful comment, Mr. John Mortensen for useful discussion, and Ms. Lisbeth Heilesen for patient typing of the paper.

REFERENCES

1 M. Bos, Anal. Chim. Acta, 81 (1976) 21.
2 W. W. Goldsworthy and R. G. Clem, Anal. Chem., 44 (1972) 1360.
3 S. C. Creason and D. E. Smith, Anal. Chem., 45 (1973) 2401.
4 D. Britz and J. Mortensen, J. Electroanal. Chem., 127 (1981) 231.
5 D. Jagner and A. Graneli, Anal. Chim. Acta, 83 (1976) 19.
6 E. R. Brown, T. G. McCord, D. E. Smith and D. D. DeFord, Anal. Chem., 38 (1966) 1119.
7 D. Britz, Electrochim. Acta, 25 (1980) 1449.
8 J. S. Bendat and A. G. Piersol, Random Data: Analysis and Measurement Procedures, Wiley-Interscience, New York, 1971.
9 J. H. Christie, L. L. Jackson and R. A. Osteryoung, Anal. Chem., 48 (1976) 242.
10 D. Britz, Anal. Chim. Acta, 115 (1980) 327.
11 D. Britz, Anal. Chem., 52 (1980) 1166.

Analytica Chimica Acta, 143 (1982) 111—120
Elsevier Scientific Publishing Company, Amsterdam — Printed in The Netherlands

DETERMINATION OF TRACES OF METALS BY ANODIC STRIPPING VOLTAMMETRY AT A ROTATING GLASSY CARBON RING—DISC ELECTRODE

Part 1. Method and Instrumentation with Evaluation of some Parameters

C. BRIHAYE and G. DUYCKAERTS*

Laboratoire de Chimie Analytique, Université de Liège au Sart Tilman, B6, B-4000 Liège (Belgium)

(Received 28th May 1982)

SUMMARY

The equipment and procedure are described for the determination without preconcentration of several heavy metals based on d.c. anodic stripping voltammetry at a rotating ring—disc glassy carbon electrode with in situ mercury plating. During stripping of the metals deposited on the disc, the current from the reduction of the ions collected at the ring is measured. Some parameters (scan rate, thickness of the mercury film, electrode rotation and deposition time) influencing the ring collection peak current are examined experimentally. The results are compared with the theoretical considerations given by de Vries and van Dalen for anodic stripping voltammetry on a stationary mercury film electrode and by Bakanov et al. for a rotating mercury film electrode.

For several years, special techniques of anodic stripping voltammetry (a.s.v.) different from the conventional d.c. and differential pulse methods have been developed, to improve the sensitivity and lower the detection limits. With small volumes of solution, Stulik and Stulikova [1] showed that it was possible to increase the sensitivity. Eisner et al. [2] examined a mercury film glassy carbon electrode for a.s.v. with a staircase wave as the applied signal. To minimize the background current, Steeman et al. [3] used a subtractive technique with two identical cells provided with twin mercury film electrodes; one cell contained a blank solution, and the other the test solution. Magjer and Branica [4] introduced into the cell a perforated disc vibrating at 50 Hz to assist transport of the electroactive species towards a stationary mercury-plated glassy carbon electrode. Schieffer and Blaedel [5] built a cell provided with two tubular glassy carbon electrodes in series; these electrodes were separated by a thin teflon spacer. The solution flowed through the electrodes. Trace metal cations deposited on the first electrode during pre-electrolysis were stripped by means of a potential scan and collected by the second electrode held at a constant cathodic potential. Sipos et al. [6] examined subtractive a.s.v. with a rotating mercury-coated

0003-2670/82/0000-0000/$02.75

glassy carbon split-disc electrode. The metal cations were deposited on both electrodes; at the end of the plating time, one electrode was cleaned by holding at an anodic potential, and then an anodic potential scan was applied to both electrodes. The difference between the currents was recorded. Goto et al. [7] developed an anodic stripping semidifferential method with a mercury film electrode formed in situ; in this technique, an analog circuit was used to measure the semidifferential of the current with respect to time as a function of electrode potential. Johnson and Allen [8, 9] described a new technique, called anodic stripping voltammetry with collection, using a rotating ring—disc electrode (RRDE). Later, Laser and Ariel [10] applied this method with a glassy carbon RRDE, mercury-plated in situ, to the determination of zinc, lead and copper in an acetate buffer.

In the work described here, a detailed study was made of a.s.v. with collection at a rotating glassy carbon ring—disc electrode, mercury-plated in situ, in order to define the possibilities and limitations of the system. In later papers, a comparison of various a.s.v. techniques, and their application to the determination of heavy metals in different matrices, will be reported.

THEORETICAL ASPECTS

The rotating ring—disc electrode was developed by Frumkin and Nekrasov [11] to detect the intermediates of electrode reactions. In a.s.v. with collection [8, 9], while the electrode rotates constantly, the disc is first set for a certain period of time at a potential E_D located in the limiting current plateau of the reaction $M^{n+} + ne \rightarrow M^0$ (electrolysis step). Afterwards, an anodic potential scan applied to the disc induces the oxidation of the deposited metal (stripping step). During this step, the ring is held at a constant cathodic potential of the reduction reaction $M^{n+} + ne \rightarrow M^0$. A fraction N_0 of the ions produced by the potential scan is collected by the ring. As the ring potential remains constant, the measured ring current (i_R) has no capacitive component and therefore the ring base line must be flat.

The limiting convection/diffusion current at the disc ($i^0_{D,l}$) during the electrolysis step is given by the following relation derived by Levich

$$i^0_{D,l} = 0.62\, nF\pi r_1^2 D^{2/3} \nu^{-1/6} \omega^{1/2} C \qquad (1)$$

where r_1 is the radius of the disc electrode (cm), ν is the kinematic viscosity ($cm^2\ s^{-1}$), ω is the rotation speed of the electrode (rad s^{-1}), and C is the bulk concentration of the electroactive species (mol ml^{-1}).

In the same way, the limiting current at the ring electrode ($i^0_{R,l}$) is given by the relation

$$i^0_{R,l} = 0.62\, nF\pi (r_3^3 - r_2^3)^{2/3} D^{2/3} \nu^{-1/6} \omega^{1/2} C \qquad (2)$$

where r_2 and r_3 are the inner and outer radii of the ring electrode, respectively.

A ring—disc electrode is characterized by three parameters [12]. First, the collection efficiency N_0 is the fraction of material produced at the disc

reaching the ring. Hence, for the above-mentioned reaction, $N_0 = -i_{R,1}/i_{D,1}$. A relation established by Albery and Bruckenstein [13, 14] allows N_0 to be calculated from r_1, r_2 and r_3. Second, the term $\beta^{2/3}$ is the ratio of the limiting currents at the ring and at the disc $\beta^{2/3} = i^0_{R,1}/i^0_{D,1}$. The third parameter is the shielding factor S: if no potential is applied to the disc, the measured current at the ring held at potential E_R in the convection/diffusion current plateau of the electrochemical reaction is $i^0_{R,1}$. However, if the disc is brought to potential E_D in the same plateau, the flux of matter reaching the ring will decrease because the reaction also takes place at the disc. In consequence, the measured current at the ring ($i_{R,1}$) will be lower. The proportionality factor between $i_{R,1}$ and $i^0_{R,1}$ is called the shielding factor S.

In actual practice, the above-outlined process of a.s.v. with collection is more complicated. If the charging current on the disc is not taken into account, voltammograms similar to those shown in Fig. 1 are obtained. In order to analyse these schemes, the disc potential (E_D) range is best considered as divided into three zones I, II and III.

Zone I. The reduction $M^{n+} + ne \rightarrow M^0$ occurs on the disc ($i^0_{D,1}$), which involves shielding of the ring. Therefore, $i_{R,I} = S\, i^0_{R,1}$.

Zone II. At the disc, there is production of M^{n+}, of which fraction N_0 reaches the ring. In consequence, the reduction current on the ring increases: $i_{R,II} = -N^0\, i_{D,II}$.

Zone III. There is no reduction of M^{n+} at the disc, and the ring is not shielded by the disc: $i_{R,III} = i^0_{R,1}$.

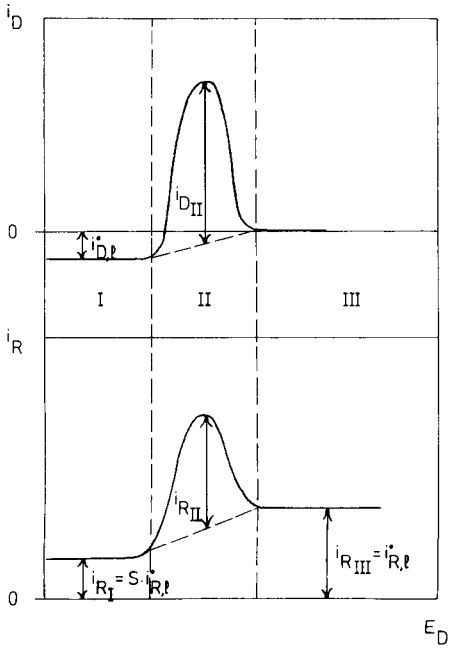

Fig. 1. Description of the stripping and collection peaks in a.s.v. with collection.

It follows that a rotating ring–disc electrode used in a.s.v. with collection should have the following characteristics: N_0 has to be as high as possible in order to increase the ring signal, and S has to be near unity so that the base line of the ring current is flat (i.e., $i_{R,I} = i_{R,III}$). In fact, $i_{R,II} \gg i^0_{R,1}$ and the term $(i_{R,III} - i_{R,I})$ can be neglected with respect to $i_{R,II}$. That means that the slope of the base line on the ring is very slight in relation to the collection peak height. The ring base line can therefore be considered as practically flat in a.s.v. with collection.

Provided that the number of exchanged electrons is the same in the reduction and oxidation, the number of coulombs resulting from the stripping of the plated metal on the disc during the period of time t_{dep} is given by the relation $Q_D = i^0_{D,1}\, t_{dep}$, and the number of coulombs relative to the collection of the metal cations is given [8, 9] by

$$Q_R = -N_0\, Q_D = -N_0\, 0.62\, nF\pi r_1^2\, \omega^{1/2} \nu^{-1/6} D^{2/3} C t_{dep} \qquad (3)$$

EXPERIMENTAL

Equipment

A glassy carbon electrode constructed in the laboratory workshop was used; a schematic diagram is shown in Fig. 2. The electrical contacts were made with mercury. To minimize lateral eccentricity, the electrode rotation was contained within two sets of ball-bearings separated by 10 cm. The active surface of the electrode was brought to a final mirror finish by successive polishing with 5-μm, 0.3-μm and 0.05-μm alumina. The electrode was driven by a stepping motor allowing rotation speeds of up to 3000 rpm. The electrode radii were $r_1 = 0.261$ cm, $r_2 = 0.290$ cm and $r_3 = 0.394$ cm. Table 1 shows the correspondence between the calculated values of the characteristic parameters and those measured from the reduction waves of potassium hexacyanoferrate(III) in 0.1 M NaOH—0.56 M Na_2SO_4 solution. The bipotentiostat was similar to that described by Napp et al. [15].

For the heavy metal determinations, mercury was plated in situ following the procedure described by Florence [16].

Procedures

Heavy metals in seawater were determined as follows. The pH of the seawater was adjusted to pH 2.5 with diluted hydrochloric acid (Suprapur, Merck). Then 40 ml of the solution was introduced into the cell, followed by a volume of a Hg^{2+} solution such that the final mercury concentration lay between 10^{-5} and 2.5×10^{-5} M. Oxygen was removed by bubbling pure nitrogen for 20 min. During this time, the electrode was polished with 0.05-μm alumina on filter paper. After rinsing with high-purity water, the electrode was introduced into the cell and rotation at 1500 rpm was started.

The mercury film was plated by setting the disc and the ring at —0.9 V for 30 min. Afterwards, the films were cleaned by stripping the heavy metals

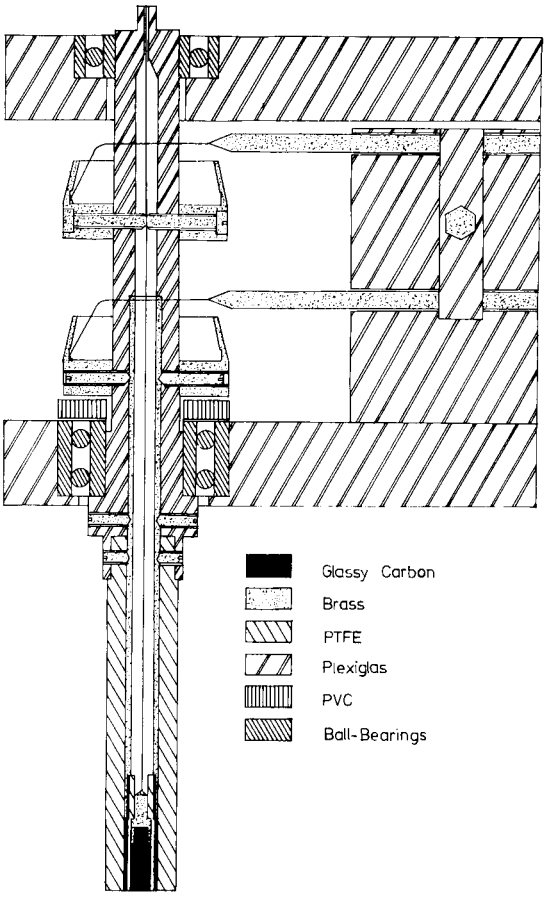

Fig. 2. Schematic diagram of the rotating glassy carbon ring—disc electrode.

TABLE 1

Characteristic parameters of the rotating ring—disc electrode used

	N_0	$\beta^{2/3}$	S
Calculated	0.425	1.62	0.74
Measured	0.414	1.49	0.69

deposited together with the mercury by means of a potential scan from —0.9 to —0.1 V at a rate of 3 V min^{-1}; the potentials of both electrodes were held at —0.1 V for 5 s. All potentials given are vs. Ag/AgCl, 0.1 M KCl.

For the actual measurements, the disc and the ring were set at —0.9 V during a suitable period of time (electrolysis step). An anodic potential scan from —0.9 to —0.1 V at a rate of 3 V min^{-1} was applied to the disc; the ring

potential was kept constant at —0.9 V. The ring current was recorded (stripping and collection step). The disc and the ring were cleaned by a potential scan followed by a stop at —0.1 V for 5 s.

Figure 3 shows a voltammogram obtained by determining cadmium, lead and copper in a sample of seawater from the North Sea. The water was found to contain 0.56 μg Cd l^{-1}, 2.4 μg Pb l^{-1} and 0.81 μg Cu l^{-1}.

RESULTS AND DISCUSSION

Different parameters of the a.s.v. with collection were examined experimentally to define the potentialities and the limitations of the method.

Verification of the applicability of the a.s.v. theory for a planar mercury film electrode to a.s.v. with collection

De Vries and van Dalen [17] derived theoretical relationships between various parameters in a.s.v. with a planar stationary electrode covered with a mercury film: (a) i_p (peak current) against v (potential scan rate) with d (film thickness) as a parameter; (b) i_p against d with v as a parameter; (c) $w_{1/2}$ (width at half-height) against v with d as a parameter; (d) $w_{1/2}$ against d with v as a parameter; (e) $E_p - E_{1/2}$ (peak potential referred to $E_{1/2}$) against d with v as a parameter; (f) $E_p - E_{1/2}$ against v with d as a parameter. Later, Bakanov et

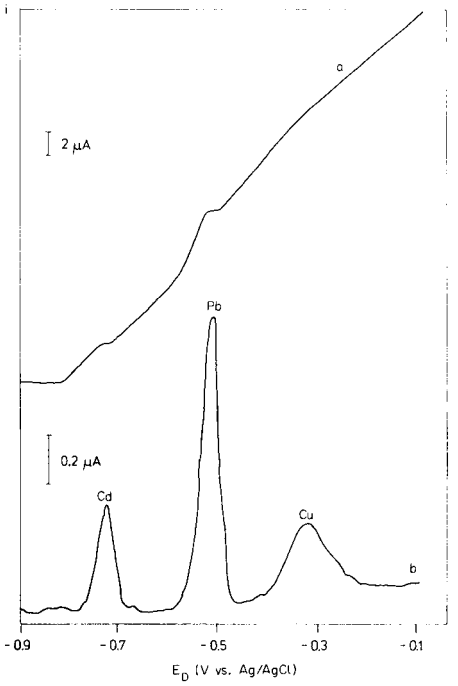

Fig. 3. Voltammogram for Cd, Pb and Cu in seawater by a.s.v. with collection. (a) Disc; (b) ring. $[Hg^{2+}] = 1.63 \times 10^{-5}$ M, $\omega = 1500$ rpm, $t_{dep} = 5$ min, $v = 3$ V min^{-1}.

al. [18] showed that these relationships can also be applied to a rotating mercury film electrode. Further, they derived relationships between the above-mentioned parameters and the rotation speed of the electrode ω (rpm).

The applicability of these relationships was verified here for the collection peak of lead in 0.5 M NaCl solution at pH 2.5.

(a) $i_{p,R}$ *as a function of the potential scan rate* v. Figure 4 shows the experimental relation between $i_{p,R}$ and v, for a film thickness, d, of 0.04 μm. The relationship between the collection peak height and the potential scan rate is linear up to 3 V min^{-1}.

(b) $i_{p,R}$ *as a function of the mercury film thickness* d. Table 2 shows the values of the peak current against mercury plating time for v = 1 V min^{-1}. The value of $i_{p,R}$ appears to be independent of the plating time and, consequently, of the mercury film thickness.

(c) $w_{1/2}$ *as a function of* v, ω *and* d. Table 3 shows the variation of the width at half-height of the collection peak as a function of v, ω and d.

All these results show that, for analytical needs, a.s.v. with collection follows sufficiently closely the relations derived by de Vries and van Dalen [17], as well as those derived by Bakanov et al. [18].

Calibration graphs and detection limits

Figure 5 shows the lines passing through the origin obtained by plotting the collection peak heights of cadmium, lead and copper as a function of the bulk concentrations added to a seawater sample.

For a rotation speed of 1500 rpm and a mercury concentration of 1.63 $\times$ 10^{-5} M, the background deviation (i.e., the maximal peak-to-peak variation) of the ring current is 10 nA. If the detection limit is regarded as the concentration giving a signal equal to 3 times the background deviation, the detection limit calculated from the calibration graphs is about 6 ng l^{-1} under the following experimental conditions: v = 3 V min^{-1}, t_{dep} = 1 h, ω = 1500 rpm and $[Hg^{2+}]$ = 1.63 $\times$ 10^{-5} M.

Figure 6 shows the voltammograms obtained by determining Cd, Pb and Cu in a seawater sample which had been purified by electrolysis on a mercury pool for 48 h. The concentrations of Cd, Pb and Cu found were 8, 10 and 7 ng l^{-1}, respectively. If it is assumed that half the lead peak and two-thirds of the cadmium and copper peaks can be measured acceptably, the experimental detection limit is about 5 ng l^{-1}. This value agrees well with that determined from the background deviation.

Precision and accuracy

The precision was evaluated by calculating the relative standard deviations of the collection peak heights for Cd, Pb and Cu from five successive voltammograms in water from the North Sea. The sample of seawater was previously electrolysed on a mercury pool (E = —0.9 V) for 48 h. The concentrations of Cd, Pb and Cu were adjusted by addition to 0.01 μg l^{-1} in the first series of measurements and to 0.9, 1.1 and 1.6 μg l^{-1}, respectively, in the second

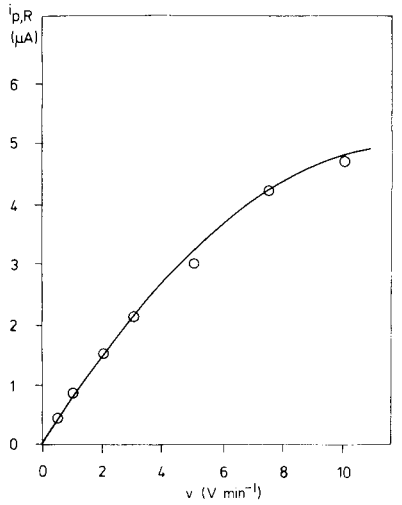

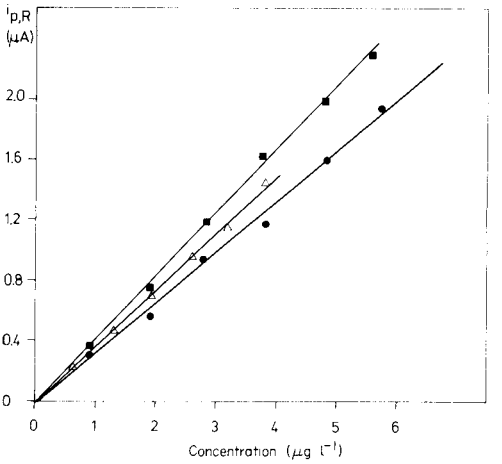

Fig. 4. Variation of the collection peak current of lead as a function of the potential scan rate v in 0.5 M NaCl solution at pH 2.5. $[Hg^{2+}] = 1.63 \times 10^{-5}$ M, $[Pb^{2+}] = 4$ μg l^{-1}, $t_{dep,Pb} = 5$ min, $\omega = 1500$ rpm, $d = 0.04$ μm.

Fig. 5. Collection peak currents as a function of concentration added to seawater previously purified by electrolysis: (■) Pb; (△) Cd; (●) Cu. $[Hg^{2+}] = 1.63 \times 10^{-5}$ M, $d = 0.04$ μm, $\omega = 1500$ rpm, $v = 3$ V min^{-1}, $t_{dep,Cd,Pb,Cu} = 5$ min.

TABLE 2

Collection peak current of lead as a function of mercury plating time (0.5 M NaCl solution, pH 2.5, $[Hg^{2+}] = 1.63 \times 10^{-5}$ M, $\omega = 1500$ rpm, $[Pb^{2+}] = 10$ μg l^{-1}, $t_{dep,Pb} = 5$ min, $v = 1$ V min^{-1})

$i_{p,R}$ (μA)	2.8	3.1	2.9	2.9
$t_{dep,Hg}$ (h)	0.5	1.0	3.0	5.0

series. The relative standard deviations of the means at the 95% confidence level are shown in Table 4.

The accuracy of the method was assessed by determining lead and copper in the NBS standard reference material, Orchard Leaves (SRM 1571). The procedure was as follows: the dried and weighed samples (ca. 100 mg) were ashed in a low-temperature asher with activated oxygen (LTA 600, Tracerlab) for 48 h. The residues were digested with 0.5 ml of 70% perchloric acid (Suprapur, Merck) for 2 h. The solutions were evaporated on hot plates under pyrex bell-jars swept by filtered nitrogen. The residues were dissolved in 1 ml of concentrated hydrochloric acid (Suprapur, Merck) and the solutions were diluted to 250 ml with high-purity water.

Table 5 shows a comparison between the measured contents and the NBS certified values. These results indicate that the method studied provides values that are accurate and adequately precise.

TABLE 3

Width at half-height of the collection peak of lead as a function of the potential scan rate v, the rotation speed ω, and the mercury plating time. (0.5 M NaCl solution, pH 2.5, $[Hg^{2+}] = 1.63 \times 10^{-5}$ M, $[Pb^{2+}] = 2.5\ \mu g\ l^{-1}$, $t_{dep,Pb} = 5$ min)

Scan rate as variable[a]					
$w_{1/2}$ (mV)	33	33	33	35	
v (V min^{-1})	0.5	1.0	2.0	3.0	
Rotation speed as variable[b]					
$w_{1/2}$ (mV)	37	33	33	33	35
ω (rpm)	250	500	1000	1500	2000
Mercury plating time as variable[c]					
$w_{1/2}$ (mV)	35	33	33	35	
$t_{dep,Hg}$ (h)	0.5	1.0	3.0	5.0	

[a] $\omega = 1500$ rpm, $d = 0.04\ \mu$m.
[b] $v = 1$ V min^{-1}, $d = 0.04\ \mu$m.
[c] $v = 1$ V min^{-1}, $\omega = 1500$ rpm.

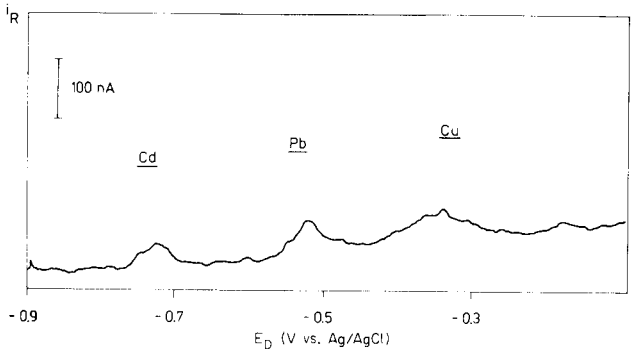

Fig. 6. Voltammogram by a.s.v. with collection from seawater previously purified by electrolysis. $[Hg^{2+}] = 1.63 \times 10^{-5}$ M, $d = 0.04\ \mu$m, $\omega = 1500$ rpm, $v = 3$ V min^{-1}, $t_{dep,Cd,Pb,Cu} = 1$ h, $[Cd^{2+}] = 8$ ng l^{-1}, $[Pb^{2+}] = 10$ ng l^{-1}, $[Cu^{2+}] = 7$ ng l^{-1}.

CONCLUSION

Anodic stripping voltammetry with collection at a rotating ring—disc glassy carbon electrode covered in situ with a mercury film follows the relations derived by de Vries and van Dalen as well as those proposed by Bakanov et al.

The detection limit is ca. 5 ng l^{-1} for the determination of Cd, Pb and Cu in seawater from the North Sea. The precision is ca. 25% at a concentration level of 0.01 μg l^{-1} and 6% at a concentration of 1 μg l^{-1}. The concentrations measured by this method can be regarded as accurate. Thus, a.s.v. with collection appears to be one of the most promising electrochemical techniques for ultratrace determinations.

TABLE 4

Relative standard deviations of the mean peak heights for Cd, Pb and Cu (5 replicates, $[Hg^{2+}] = 1.63 \times 10^{-5}$ M, $d = 0.04$ μm, $\omega = 1500$ rpm, $v = 3$ V min^{-1}, $t_{dep} = 1$ h and 5 min)

	Cd	Pb	Cu
Concentration (μg l^{-1})	0.01	0.01	0.01
$s_m t\ 100/\bar{x}$ (%)	19	29	26
Concentration (μg l^{-1})	0.9	1.1	1.6
$s_m t\ 100/\bar{x}$ (%)	6.4	5.6	7.0

TABLE 5

Lead and copper content in Orchard Leaves (SRM 1571)

	Metal content (μg g^{-1})	
	Measured[a]	Certified
Pb	46.7 ± 2.5	45 ± 3
Cu	11.9 ± 1.6	12 ± 1

[a]Mean and standard deviation from 3 separate samples.

The authors are very grateful to Mr P. Lemaire for the construction of the rotating electrode and to Mr L. Swennen who built the electronic set-up.

REFERENCES

1 K. Stulik and M. Stulikova, Anal. Lett., 6 (1973) 441.
2 U. Eisner, J. A. Turner and R. A. Osteryoung, Anal. Chem., 48 (1976) 1608.
3 E. Steeman, E. Temmerman and R. Verbinnen, Anal. Chim. Acta, 96 (1968) 177.
4 T. Magjer and M. Branica, Croat. Chem. Acta, 49 (1977) L1.
5 G. W. Schieffer and W. J. Blaedel, Anal. Chem., 49 (1977) 49.
6 L. Sipos, S. Kozar, I. Kontusic and M. Branica, J. Electroanal. Chem., 87 (1978) 347.
7 M. Goto, K. Ikenoja and D. Ishii, Anal. Chem., 51 (1979) 110.
8 D. C. Johnson and R. E. Allen, Talanta, 20 (1973) 305.
9 R. E. Allen and D. C. Johnson, Talanta, 20 (1973) 799.
10 D. Laser and M. Ariel, J. Electroanal. Chem., 49 (1974) 123.
11 A. N. Frumkin and L. I. Nekrasov, Dokl. Akad. Nauk SSSR, 126 (1959) 115.
12 W. J. Albery and M. L. Hitchman, Ring—Disc Electrodes, Oxford Science Research Papers, Clarendon Press, Oxford, 1971.
13 W. J. Albery, Trans. Faraday Soc., 62 (1966) 1915.
14 W. J. Albery and S. Bruckenstein, Trans. Faraday Soc., 62 (1966) 1920.
15 D. T. Napp, D. C. Johnson and S. Bruckenstein, Anal. Chem., 39 (1967) 481.
16 T. M. Florence, J. Electroanal. Chem., 27 (1970) 273.
17 W. T. de Vries and E. van Dalen, J. Electroanal. Chem., 9 (1965) 448.
18 V. I. Bakanov, P. S. Zakharov, V. A. Antip'eva and A. P. Grigorchenko, Zh. Anal. Khim., 28 (1973) 2292.

Analytica Chimica Acta, 143 (1982) 121—130
Elsevier Scientific Publishing Company, Amsterdam — Printed in The Netherlands

DETERMINATION OF TRACES OF SELENIUM(IV) BY CATHODIC STRIPPING VOLTAMMETRY AT THE HANGING MERCURY DROP ELECTRODE

GRAŻYNA JARZĄBEK and ZENON KUBLIK*
Department of Chemistry, University of Warsaw, Pasteura 1, Warsaw 02093 (Poland)
(Received 26th April 1982)

SUMMARY

Conditions convenient for the determination of traces of selenium(IV) by cathodic stripping technique are described. Several electrolytes were tested. Three procedures are given in which the troublesome splitting of the stripping peak is eliminated. Suitable conditions include perchloric acid solution at elevated temperature, hydrochloric acid solution after preconcentration at zero current, and perchloric acid solution containing a small amount of iodide. The detection limits are 5×10^{-9}, 2×10^{-9} and 5×10^{-10} mol dm^{-3}, respectively. The time required for the entire procedure is about 30 min starting with a soluble selenium(IV) sample.

The problem of the determination of selenium at trace levels has received much attention recently as a consequence of the recognition of the biological importance of this element. Selenium is an essential nutrient at trace level but toxic in excess [1, 2]. When selenium is present in animal feeds at concentrations less than 0.1 ppm, deficiency symptoms develop, but when it is present at concentrations exceeding 5 ppm, chronic selenosis occurs. The determination of traces of selenium is also of interest because selenium tends to weaken the toxic action of some heavy metals in animal and human organisms [3, 4].

Electroreduction of selenium(IV) at mercury electrodes proceeds in acidic solutions with intermediate formation of a deposit which usually accumulates on the electrode surface. There are some discrepancies in the literature on the nature of this deposit. According to several authors [5—15], the deposit corresponds to mercury selenide, whereas other authors claim that it corresponds to elemental selenium [16—19]. Some recent results [20] firmly support the formation of mercury selenide. Irrespective of the real nature of the deposit, its accumulation on the electrode surface has often been exploited for the determination of selenium(IV) traces by cathodic stripping voltammetry [6—15], [18, 19]. However, under some conditions, multiple stripping peaks were observed during the electroreduction of the deposit, which led to serious difficulties in quantitative work.

The main purpose of the present investigation was therefore to establish conditions for the electroreduction of mercury selenide without formation of multiple stripping peaks or at least without any important effect of peak splitting on the measurements. A secondary purpose was to verify the utility of preconcentration of the mercury selenide deposit on the electrode surface at zero current. According to Speranskaya [16] and Toropova et al. [21], such deposition proceeds at mercury electrodes only in rather concentrated hydrochloric acid solutions.

EXPERIMENTAL

The voltammetric curves were recorded with a Radelkis OH-105 polarograph using a conventional three-electrode arrangement. The reference electrode was a slightly modified, saturated calomel electrode, in which potassium chloride was replaced by sodium chloride to avoid precipitation of potassium perchlorate in the salt bridge. All the potentials reported here are versus this reference electrode. The auxiliary electrode was a platinum foil with a surface area of 2 cm^2. The indicating electrode was a hanging mercury drop electrode (HMDE) of the type described by Kemula and Kublik [22] with a surface area of 0.024 cm^2. Several experiments were done with a conventional dropping mercury electrode. The deposition step was done either under zero-current conditions (i.e., open circuit) or under the usual conditions at an appropriate applied potential. During deposition, the solution was stirred magnetically. All the solutions were prepared as described earlier [23]. Prior to measurement, all solutions were deaerated with pure argon. Most experiments were done at 22° C; elevated temperatures were sometimes used, as noted below.

RESULTS

The influence of the supporting electrolyte

There are few comparative studies of the voltammetric behaviour of selenium(IV) in acidic solutions. According to Vajda [8], voltammetric curves obtained from hydrochloric acid differ markedly from the curves obtained from perchloric acid solution. Yet Alam et al. [17] did not observe any essential differences between voltammograms obtained from these two acids.

Figure 1 shows a comparison of two cyclic curves obtained for a moderate concentration of selenium(IV) in solutions of perchloric and hydrochloric acids. Curve 1 obtained from perchloric acid solution shows two cathodic peaks. The first, elongated peak, c_1, corresponds to the electroreduction of selenous acid to mercury selenide. The second peak, c_2, corresponding to the electroreduction of mercury selenide is poorly developed. The height of this peak, and the positions and magnitudes of the humps on the descending portion of the peak, are not very reproducible. The presence of humps suggests that the deposit is inhomogeneous. The cathodic portion of the

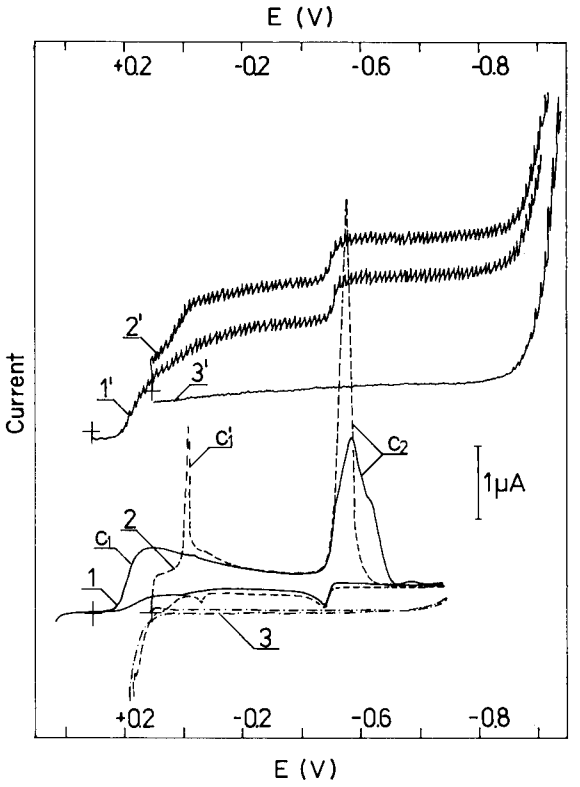

Fig. 1. Voltammetric and polarographic curves obtained for 1×10^{-4} mol dm^{-3} Se(IV) in a 0.1 mol dm^{-3} solution of: (1, 1′) perchloric acid; (2, 2′) hydrochloric acid. (3) Blank test for curve 2; (3′) blank test for curve 2′. Voltage scan rate for curves 1 and 2 is 1 V min^{-1}.

cyclic curve 2, obtained from hydrochloric acid solution differs in several points from curve 1. First, the start of peak c_1 is overlapped by the mercury dissolution current, so that it cannot be recorded fully. Second, an additional sharp peak, c_1', is superimposed on the plateau of the first peak. Third, peak c_2 obtained under these conditions is significantly higher than peak c_2 obtained from perchloric acid solution and does not show humps on its descending portion.

The differences in the selenium(IV) electroreduction process are not confined to the voltammetric conditions. The starting portion of the polarographic curve obtained from hydrochloric acid solution (curve 2′) shows a split whereas no split is observed on curve 1′. Thus, the electroreduction of selenium(IV) at mercury electrodes in hydrochloric and perchloric acid solutions proceeds by different mechanisms in the potential range 0.0 to —0.1 V.

The shapes of peak c_2 obtained for selenium(IV) in solutions of other acids can be divided into two groups. The curves obtained from sulphuric, nitric, phosphoric and citric acid solutions are similar to those obtained from perchloric acid solution. The curves obtained from perchloric acid solutions containing a halide, however, are similar to those from hydrochloric acid solution. The concentrations of halide ions necessary to cause the changed shape of the peak c_2 are $\geqslant 5 \times 10^{-6}$ mol dm^{-3} for iodide, $\geqslant 1 \times 10^{-3}$ mol dm^{-3} for bromide, $\geqslant 1 \times 10^{-2}$ mol dm^{-3} for chloride, and $\geqslant 0.1$ mol dm^{-3} for thiocyanate.

Electroreduction of selenium(IV) in perchloric acid solutions

Decrease in the Se(IV) concentration has little influence on the shape of the first peak on curve 1 of Fig. 1, but the second peak splits into three overlapped peaks. At 1.5×10^{-7} mol dm^{-3} selenium(IV), two of these peaks become well separated (Fig. 2, curve 1).

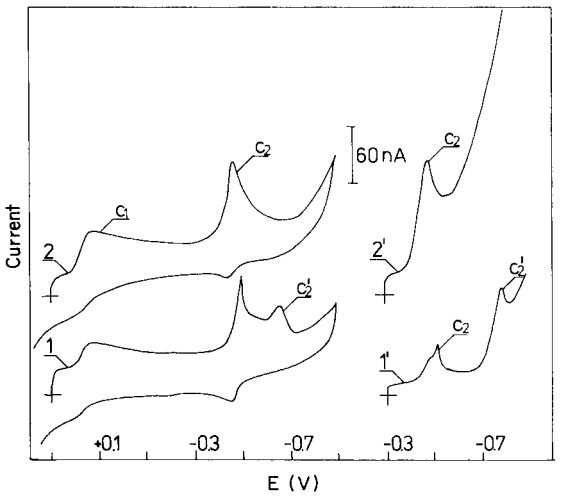

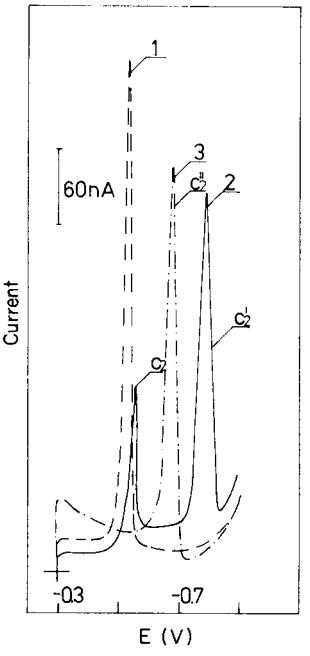

Fig. 2. Cyclic and stripping voltammetric curves obtained for Se(IV) in 0.1 mol dm^{-3} perchloric acid. Concentration of Se(IV): (1, 2) 3×10^{-6}; (1', 2') 1.5×10^{-7} mol dm^{-3}. Deposition time: (1', 2') 3 min at —0.3 V. Temperature: (1, 1') 20°C; (2, 2') 70°C. Voltage scan rate 1 V min^{-1}.

Fig. 3. Cathodic stripping voltammetric curves obtained for 5×10^{-7} mol dm^{-3} Se(IV) in 0.1 mol dm^{-3} hydrochloric acid after deposition for 3 min: (1) at zero current; (2) at —0.3 V; (3) as (2) but in the presence of 2×10^{-5} mol dm^{-3} Cu(II). Voltage scan rate 1 V min^{-1}.

Under stripping conditions, the occurrence of a single or double peak depends on the Se(IV) concentration. At concentrations higher than 1×10^{-7} mol dm^{-3}, curves were of type 1′ (Fig. 2) whereas there was only a single peak at concentrations lower than 1×10^{-7} mol dm^{-3}. However, the concentration range where this single peak appeared was narrow, and the peak vanished at concentrations lower than 2×10^{-8} mol dm^{-3} even after very long preconcentration times. The calibration plot obtained for perchloric acid solutions was linear only in the range 2×10^{-8}—1×10^{-7} mol dm^{-3}. There were marked deviations from linearity when the second stripping peak occurred on the voltammograms.

Attempts to eliminate the additional stripping peak by variation in the deposition potential or by application of deposition at zero current were unsuccessful. Variations in the deposition potential led only to the small changes in the height of the stripping peak. Deposition at zero current gave a peak at the same potential as peak c_2, but the peak height was only about a sixth of the peak height after deposition at —0.3 V. The additional stripping peak could easily be eliminated by increasing the temperature. Curves 2 and 2′ (Fig. 2) obtained at 70° C did not show any splitting of the second peak. The calibration plot obtained at 70° C after deposition for 5 min at —0.3 V in stirred solution was linear in the concentration range 5×10^{-9}—5×10^{-6} mol dm^{-3}. An increase in temperature improves, therefore, not only the linear range of the calibration plot but also the detection limit which was 2×10^{-8} mol dm^{-3} at room temperature.

The electroreduction of selenium(IV) in hydrochloric acid solutions

Under cyclic conditions in 0.1 mol dm^{-3} hydrochloric acid supporting electrolyte, variations in selenium(IV) concentration in the range 1×10^{-4}—1.5×10^{-6} mol dm^{-3} did not lead to occurrence of the additional peak c_2'. Also under stripping conditions, the additional stripping peak was not observed for $< 1 \times 10^{-7}$ mol dm^{-3} Se(IV) concentrations. At higher Se(IV) concentrations, the shape of the stripping curves depended markedly on the deposition potential. Maintenance of the deposition potential in the range +0.05—0.0 V led to formation of a single peak, whereas deposition at negative potentials led to two well separated stripping peaks (Fig. 3, curve 2). From an analytical point of view, the additional peak creates problems because the calibration plot then deviates from linearity.

Attempts to eliminate the additional stripping peak showed that this peak did not appear when the deposit was formed at zero current (Fig. 3, curve 1), when the deposition proceeded in the rather narrow range of potential from +0.05 to 0.00 V, or when the solution contained copper(II) ions (curve 3). The addition of only traces of copper(II) led to slight decreases in peaks c_2 and c_2' and to the appearance of a new small peak c_2''. An increase in the Cu(II) concentration led to a further decrease of peaks c_2 and c_2' accompanied by a systematic increase in peak c_2''. At sufficiently high copper(II) concentration, only the peak c_2'' remained on the voltammo-

gram (curve 3). The stripping peak obtained after deposition at zero current had the same position and height as the single peak obtained after deposition at +0.05 V. Under zero-current conditions, peak c_1' also increased but this effect was not studied in detail because it offered no analytical advantages compared to peak c_2.

Figure 4 presents the stripping peaks obtained for very small concentrations of selenium(IV) after deposition at zero current. It is evident that the stripping peak obtained for Se(IV) concentration as low as 3×10^{-9} mol dm^{-3} is quite well developed. The logarithmic calibration plot of current (nA) vs. concentration is linear over the range 3×10^{-9}—3×10^{-7} mol dm^{-3} Se(IV).

Figure 5 illustrates the influence of various factors on the height of the stripping peak obtained after deposition at zero current for 5×10^{-8} mol dm^{-3} Se(IV) solution. The peak height was strictly proportional to the deposition time up to 12 min. An increase in the chloride ion concentration at constant acidity led to a marked increase in the peak height. An increase in the acidity at constant chloride concentration decreased the peak height. For solutions containing 0.1 mol dm^{-3} hydrochloric acid and 0.9 mol dm^{-3} sodium chloride, the detection limit for selenium(IV) was 2×10^{-9} mol dm^{-3}.

Interferences from other ions were investigated for 5×10^{-8} mol dm^{-3} Se(IV) solution with zero-current deposition lasting 5 or 10 min. The presence of a 100-fold amount of zinc(II), which is a common contaminant of

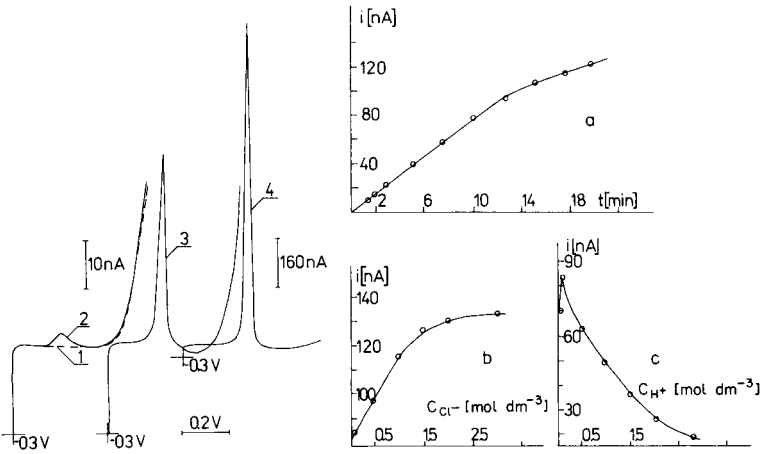

Fig. 4. Cathodic stripping curves obtained for increasing selenium(IV) concentration in 0.1 mol dm^{-3} hydrochloric acid. Se(IV) concentration: (1) 0; (2) 3×10^{-9}; (3) 3×10^{-8}; (4) 3×10^{-7} mol dm^{-3}. Deposition for 10 min at zero current in stirred solutions. Sensitivity: (1—3) 10 nA; (4) 160 nA. Voltage scan rate 1 V min^{-1}.

Fig. 5. The dependence of the height of the cathodic stripping peak obtained for 5×10^{-8} mol dm^{-3} Se(IV) after preconcentration at zero current on: (a) deposition time in 0.1 mol dm^{-3} HCl; (b) chloride ion concentration at 0.1 mol dm^{-3} hydrogen ion for 10-min deposition; (c) hydrogen ion concentration at 0.1 mol dm^{-3} chloride for 10-min deposition.

many solutions, had no significant effect on the selenium stripping peak. No interferences were observed from a 10-fold amount of lead(II) ions or a 5-fold amount of iron(III) ions. An equivalent concentration of copper(II) led to a small decrease in the selenium stripping peak height. At higher copper(II) concentrations, the deposition became less effective. As shown above (Fig. 3, curve 3), increasing the concentration of copper(II) caused the eventual disappearance of peaks c_2 and c_2' and the appearance of a new stripping peak corresponding to electroreduction of copper selenide.

Electroreduction of selenium(IV) in the presence of iodide

Arlt and Neuman [12], studying the influence of various substances on the cathodic stripping peak of selenium(IV), found that the addition of a little iodide did not significantly affect the peak shape or height. Under polarographic conditions, Christian et al. [24] found that 1×10^{-3} mol dm^{-3} iodide caused some "cutting" of the starting portion of the first selenium-(IV) reduction wave but did not affect the second wave.

In the present work, significant concentrations of iodides caused problems. In solutions containing 0.1 mol dm^{-3} perchloric acid, 0.1 mol dm^{-3} iodide and 1×10^{-4} mol dm^{-3} Se(IV), a brown suspension appeared and the voltammetric curve showed no peaks corresponding to reduction of Se(IV). Obviously, under these conditions selenous acid is reduced to the element with formation of iodine, as in the reaction often used for titration of selenous acid [25]. Yet the addition of a small amount of iodide appears to be very useful.

The cyclic voltammetric curves obtained for selenium(IV) in the absence and presence of 5×10^{-6} mol dm^{-3} iodide are compared in Fig. 6. Curve 2' shows that the presence of 5×10^{-6} mol dm^{-3} iodide produces only a small cathodic peak on the blank. According to Kemula et al. [26] this peak corresponds to the reduction of Hg_2I_2 deposited on the electrode surface. When this amount of iodide is present along with selenium(IV), the first reduction peak is hardly affected whereas the second peak becomes sharper and higher. The quantity of electricity consumed during the formation of peak c_2 remains unchanged whether or not iodide is present, which indicates that the same amount of deposit is formed on the mercury surface in both cases. The cyclic curves recorded again in the same solution after one hour had the same shape, which means that the above-mentioned reduction of selenous acid to selenium does not proceed in very dilute iodide solutions. Even when 5×10^{-4} mol dm^{-3} iodide was added, the features of the second peak were maintained.

The presence of small amounts of iodide also exerted a useful effect on the shape of the reduction peak of mercury selenide on stripping. Deposition at potentials at which HgSe and Hg_2I_2 were plated simultaneously led to a large reduction peak of Hg_2I_2 but after the decay of this current, a very well defined peak corresponding to the electroreduction of HgSe appeared. The stripping curves obtained under such conditions for very small concen-

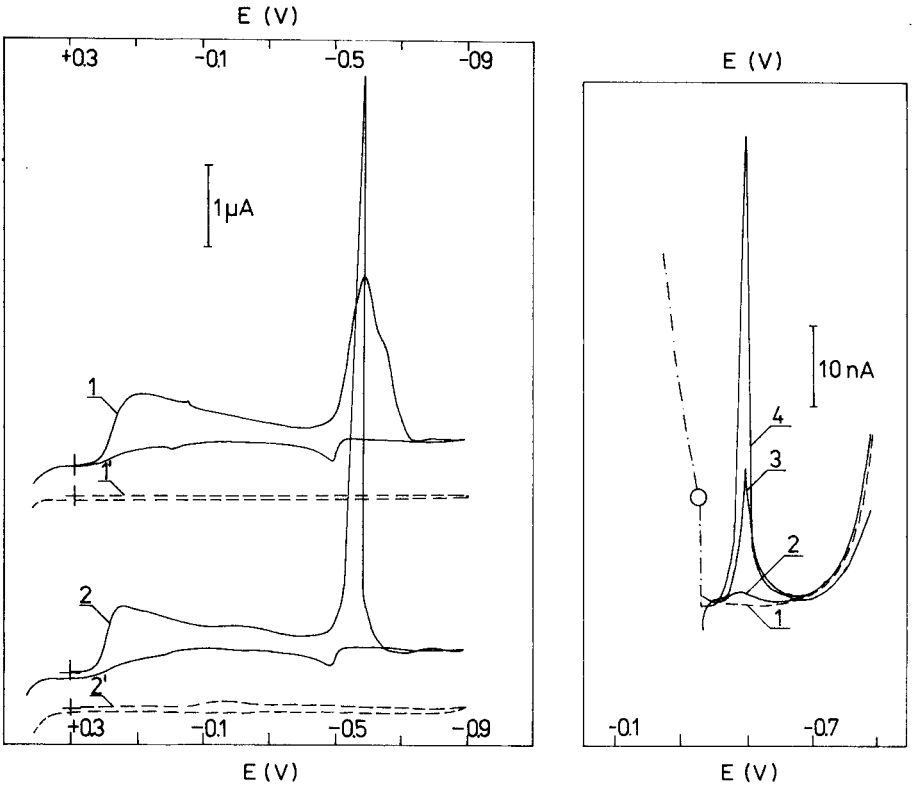

Fig. 6. The influence of iodide on the cyclic curves obtained for 1×10^{-4} mol dm^{-3} Se(IV) in 0.1 mol dm^{-3} perchloric acid. Concentration of iodide: (1) 0; (2) 5×10^{-6} mol dm^{-3}. (1') Blank test for curve 1; (2') blank test for curve 2. Voltage scan rate 1 V min^{-1}.

Fig. 7. Cathodic stripping curves obtained for Se(IV) in 0.1 mol dm^{-3} $HClO_4$ with 2×10^{-5} mol dm^{-3} iodide. Se(IV) concentration: (1) 0; (2) 4.8×10^{-10}; (3) 5.6×10^{-9}; (4) 4.5×10^{-8} mol dm^{-3}. Deposition time: (1, 2, 3) 21 min; (4) 5 min at —0.1 V. Voltage scan rate 1 V min^{-1}. At the potential designated by the circle, the recording was stopped for 60 s.

trations of Se(IV) are shown in Fig. 7. The detection limit attained in solutions containing a little iodide after deposition for 21 min at —0.1 V was 5×10^{-10} mol dm^{-3}. For a deposition time of 21 min, the calibration plot was linear in the range 5×10^{-10}—8×10^{-9} mol dm^{-3} selenium(IV). For higher Se(IV) concentrations, linear plots were obtained for deposition times of 5 min.

The curves obtained after preconcentration on open circuit were similar to the curves shown in Fig. 7. The selenium stripping peaks obtained after deposition at more negative potentials, i.e., under conditions where iodides did not react with mercury, were less well defined.

DISCUSSION

The results presented above suggest several new variants of the cathodic stripping technique for determining traces of selenium(IV). The use of supporting electrolytes containing halide ions is more convenient, from an analytical point of view, than the use of other electrolytes. Particular sensitivity is provided by perchloric acid solutions containing a little iodide. The detection limit attained in this medium, 5×10^{-10} mol dm^{-3}, is the lowest so far reported for selenium(IV) at mercury electrodes.

Many facts connected with the use of halide-containing electrolytes remain unclear. To explain the effects observed in hydrochloric acid solution, Vajda [8] suggested that selenous acid is converted to $SeCl_6^{2-}$. However, this seems unlikely because $SeCl_6^{2-}$ ions exist only in concentrated hydrochloric acid solutions [27].

The appearance of the additional peak c_1' on the voltammograms obtained from hydrochloric acid solutions indicates that in this medium the electroreduction of Se(IV) to mercury selenide proceeds, at least partly, via some intermediate product (cf. polarogram 2', Fig. 1). These results confirm an opinion given many years ago by Schwaer and Suchy [28] that Se(IV) is reduced polarographically in three reduction steps. The intermediate product formed in the first reduction step accumulates on the electrode surface and is then reduced in peak c_1'. It is difficult to elucidate the nature of the product responsible for the formation of this peak.

The results presented show clearly that the reduction of Se(IV) at open circuit proceeds not only in the concentrated hydrochloric acid, as claimed by Speranskaya [16] and Toropova et al. [21], but also in more dilute hydrochloric acid as suggested by Vajda [8]. From thermodynamic data, Se(IV) can be reduced by mercury in acidic solutions containing halide ions according to the equations

$$H_2SeO_3 + 4\ Hg + 4\ Cl^- \rightarrow Se + 2\ Hg_2Cl_2 + 2\ H_2O \quad (1)$$

$$H_2SeO_3 + 5\ Hg + 4\ Cl^- \rightarrow HgSe + 2\ Hg_2Cl_2 + 2\ H_2O \quad (2)$$

Speranskaya [16] and Toropova et al. [21] suggested that reaction (1) was appropriate. However, the present results show that the main product of the reaction is reduced in peak c_2, i.e., reaction (2) is more likely. However, the preconcentration at open circuit also leads to an increase in the height of peak c_1'; this indicates that the reaction between Se(IV) and mercury in hydrochloric acid solutions is more complicated than those described by reactions (1) or (2).

The present experiments show that electroreduction of the deposited mercury selenide is sometimes accompanied by the formation of multiple peaks. The additional peaks are inconvenient from the analytical point of view because the calibration plot usually becomes distorted. Multiple peaks appear often during the formation or reduction of multilayers of deposits. However, this cause seems unlikely here because the formation of multiple

peaks was observed even when the amount of deposited material was distinctly smaller than the amount needed for a monolayer of deposit. Additional peaks may also occur when the solution contains contaminants that react with the substance to be determined. Selenide forms slightly soluble precipitates with copper(II) ions, but deposition of copper selenide is not responsible for the peak discussed, as is clear from Fig. 3. Clearly, the true nature of the multiple peaks found requires more extensive investigations.

REFERENCES

1 V. V. Yermakov and N. V. Kovalski, Biologicheskiye Znachenie Selena, Moskva, Nauka, 1974.
2 R. W. Andrews and D. C. Johnson, Anal. Chem., 47 (1975) 294.
3 E. M. Bem, Chem. Anal. (Warsaw), 24 (1979) 155.
4 R. A. Zingaro and W. C. Cooper, Selenium, Van Nostrand Reinhold, New York, 1974, p. 594.
5 J. J. Lingane and L. W. Niedrach, J. Am. Chem. Soc., 71 (1949) 196.
6 J. Lewinson, Thesis, University of Wisconsin, 1964; cited in R. Neeb, Inverse Polarographie, Akad. Verlag, Berlin, 1969, p. 177.
7 R. G. Pac and T. V. Semochkina, Zavod. Lab., 33 (1967) 1491.
8 F. Vajda, Acta Chim. Acad. Sci. Hung., 63 (1970) 257.
9 B. Ya. Kaplan and O. A. Shiryaeva, Zh. Anal. Chim., 25 (1970) 185.
10 B. Ya. Kaplan and O. A. Shiryaeva, Zavod. Lab., 36 (1970) 1178.
11 A. Russu, L. S. Kopanskaya and V. A. Voznesenski, Zh. Anal. Khim., 30 (1975) 1153.
12 C. Arlt and R. Neuman, Fresenius Z. Anal. Chem., 282 (1976) 463.
13 W. Holak, J. Assoc. Off. Anal. Chem., 59 (1976) 650.
14 M. W. Blades, J. A. Dalziel and C. M. Elson, J. Assoc. Off. Anal. Chem., 59 (1976) 1234.
15 S. Forbes, G. P. Bonds and T. S. West, Talanta, 26 (1978) 473.
16 E. F. Speranskaya, Zh. Anal. Khim., 17 (1962) 347.
17 A. M. Shafiqul Alam, O. Vittori and M. Porthault, J. Electroanal. Chem., 61 (1975) 191.
18 A. M. Shafiqul Alam, O. Vittori and M. Porthault, Anal. Chim. Acta, 87 (1976) 437.
19 G. Henze, P. Monks, G. Tölg, F. Umland and E. Wessling, Fresenius Z. Anal. Chem., 295 (1979) 1.
20 G. Jarząbek and Z. Kublik, J. Electroanal. Chem., 137 (1982) 247.
21 V. F. Toropova, Yu. N. Polyakova, E. A. Naumova and O. W. Kopylova, Zh. Anal. Khim., 35 (1980) 296.
22 W. Kemula and Z. Kublik, Anal. Chim. Acta, 18 (1958) 104.
23 G. Jarząbek and Z. Kublik, J. Electroanal. Chem., 114 (1980) 165.
24 G. D. Christian, E. C. Knoblock and W. C. Purdy, Anal. Chem., 35 (1963) 1128.
25 I. M. Kolthoff, R. Belcher, V. A. Stenger and G. Metsuyama, Volumetric Analysis, Vol. III, Interscience, New York, 1957.
26 W. Kemula, Z. Kublik and J. Taraszewska, Chem. Anal. (Warsaw), 8 (1963) 171.
27 W. Petzold, Z. Anorg. Allg. Chem., 209 (1932) 267.
28 K. Schwaer and K. Suchy, Collect. Czech. Chem. Commun., 7 (1935) 25.

Analytica Chimica Acta, 143 (1982) 131—142
Elsevier Scientific Publishing Company, Amsterdam — Printed in The Netherlands

A STUDY OF THE EFFECT OF SOME POLLUTANT GASES ON CATHODES USED IN MEMBRANE-COVERED AMPEROMETRIC OXYGEN DETECTORS

MICHAEL L. HITCHMAN* and SALMA KAUSER

Department of Chemistry and Applied Chemistry, University of Salford, Salford, M5 4WT (Gt. Britain)

(Received 4th June 1982)

SUMMARY

The effects of various gaseous pollutants on the electrochemical activity of materials used as cathodes for membrane-covered amperometric oxygen detectors are described. It is shown that gold and platinum cathodes are not unduly affected by concentrations of sulphur dioxide and chlorine many times greater than those likely to be encountered in test solutions, and that a gold cathode is also unaffected by hydrogen sulphide. A platinum cathode is rapidly and significantly poisoned on contact with hydrogen sulphide; an analysis of the fall in the rate of oxygen reduction as a function of time indicates that the poisoning occurs by the blocking of surface sites by sulphide. The effect of hydrogen sulphide on silver, nickel and nickel sulphide electrodes is also reported. Of these materials, only nickel sulphide is an effective electrocatalyst for oxygen reduction in the presence of sulphide.

Membrane-covered amperometric detectors are extensively used for the measurement of gaseous and dissolved oxygen in a wide variety of environments [1—6]. The major advantages of such detectors over other electrochemical systems are, first, that the membrane protects the electrodes from contamination or poisoning by electroactive and surface-active impurities in the sample, and, second, that for dissolved oxygen measurements in situ the electrochemical cell is not affected by changes in the composition of electrolyte in the sample solutions. However, membranes commonly used with such detectors, although showing different permeabilities to different gases, do not usually exhibit any high degree of preferential permeability to oxygen over other gases [6]. Therefore, gaseous impurities in the environment are not prevented from entering the electrochemical cell and contaminating the cathode, the anode and the electrolyte. The overall effect of contamination by gaseous pollutants on these detectors has long been recognised [7], but there has been no systematic, detailed study of it. This paper is concerned with the effects on platinum and gold, which are widely used as cathodes in these oxygen detectors, of SO_2, Cl_2 and H_2S which are found in aqueous environments and which are potential poisons for electrocatalytic processes. Results for the effect of H_2S on silver, nickel and nickel sulphide electrodes are also given.

0003-2670/82/0000-0000/$02.75

EXPERIMENTAL

Equipment

The effect of the pollutant gases on the activity of oxygen cathodes was not investigated by using a membrane-covered oxygen detector directly because of interfering effects on the anode and electrolyte composition occurring at the same time. Instead, studies were made with the cathode materials in the form of rotating wire electrodes (RWE) [8] in a conventional electrochemical cell. These electrodes consisted of the wire (diameter 0.5—2 mm) sealed coaxially into one end of a stainless steel shaft with a conducting cement (Eccobond solder 56C; Emerson and Cumming). An insulating lacquer (Lacomit) painted onto the shaft and the cement and overlapping onto the electrode ensured that electrochemical reaction only occurred on the wire. Electrical contact was made to the electrode by means of a wire dipping into a well in the top of the shaft containing mercury. The reference electrode was an Ag/AgCl electrode in direct contact with the electrolyte in the cell and used in conjunction with a Luggin capillary; the tip of the capillary was kept close to the rotating wire. The auxiliary electrode was a platinum foil.

The electrolyte used was KCl (2 M)/KOH (0.01 M). Oxygen detectors usually contain KCl, so that chloride ions are present to complete the Ag/AgCl reference electrode but because of the reduction of oxygen to hydroxide at the cathode, the thin layer of solution between the cathode and membrane rapidly becomes alkaline [9]. The electrolyte used in this study simulated conditions found near the cathode of the usual detector. The electrolyte solution was either deaerated with nitrogen for the recording of residual currents or aerated for the recording of a current—voltage curve for oxygen reduction. The cell was thermostatted at 25 ± 0.1°C.

The shafts of the wire electrodes were supported in a bearing block, surmounted by a pulley and rotated by coupling to a servodrive unit (Chemical Electronics Type RD1). The rotation speed was monitored by using a stroboscopic disc. Rotation speeds in the range 5—20 Hz were used, with most experiments being done at 10 Hz. The potential of the RWE was controlled by means of a single operational amplifier potentiostat [10]. This potential was changed manually and was measured with a digital voltmeter. The current through the cell at each potential was monitored with a galvanometer.

Procedures

The effect of a gas on cathodic activity was studied by recording a current—voltage curve for oxygen reduction before the RWE came into contact with the pollutant gas and then again after contact. The contact with the various gases was effected by removing the RWE from the electrochemical cell and then dipping it into another sample of electrolyte solution contaminated with a known concentration of the pollutant. The contaminated solutions were made either by bubbling controlled amounts of the appropriate gas into the solution, or, more simply and reliably, by adding the sodium salt

of the anion that would result from the gas reacting with a high pH electrolyte. Thus, a solution of sodium sulphide (0.01—0.1 M) was taken as being equivalent to H_2S in the electrolyte, sodium sulphite solution (0.01—2 M) as equivalent to SO_2, and sodium hypochlorite solution (0.4—1.7 M) as equivalent to Cl_2. Contact times varied from a few minutes to 15 h.

To record the cathodic activity of a fresh electrode surface again after contamination, it was necessary to clean the RWE. Various methods are suggested in the literature for cleaning poisoned electrodes, but it was found that reproducible current—voltage curves could only be obtained by using the following methods. For platinum, hot chromic acid was used. For gold, a hot mixture of concentrated hydrochloric acid with a few drops of hydrogen peroxide added was successful. For silver, a solution of 6 M nitric acid was used, and for nickel concentrated hydrochloric acid The duration of the cleaning depended on the degree of poisoning of the electrode, but cleaning was taken as being successful when a current—voltage curve with a well defined oxygen reduction plateau was obtained.

The nickel sulphide RWE were made by leaving a nickel wire in contact with a sulphide solution overnight and no cleaning was necessary because, as discussed below, there was no effect of H_2S on the electrode activity.

RESULTS AND DISCUSSION

General behaviour of rotating wire electrodes

Prior to studying the effect of the gases on the cathodic activity for oxygen reduction, the RWE were tested to ensure that they were showing the expected hydrodynamic behaviour. Provided that the electrodes were cleaned by the methods described above, reproducible current—voltage curves for oxygen reduction were obtained with wide transport-controlled plateau regions in all cases. Limiting currents (i_l) were found to depend on (rotation speed)$^{0.4}$. A value for the exponent of 0.4 lies in the range 0.25—0.64 commonly found for RWE [8], and so the rotating wires were functioning satisfactorily as hydrodynamic electrodes.

Results for contamination by sulphur dioxide

Treatment of the gold RWE showed that with either 0.5 M sulphite solution and contact times from 10 min to 15 h, or 0.01—2 M solution and a contact time of 1 h, there was no dramatic change in the shape of the current—voltage curve or in the height of the transport-limited plateau for oxygen. The limiting current (i_l) measured at the centre of the plateau (—0.9 V) remained constant to within ±8% of the average value obtained with an uncontaminated surface. It was found that the reproducibility of i_l even in the absence of contamination was of this order; errors of up to ±10% readily arise from accidental bending of the wire. The half-wave potential ($E_{1/2}$), the value of which reflects the catalytic activity of the electrode, did show a tendency to shift to slightly more negative potentials after

treatment with sulphite solutions; i.e., there was a reduction in electrode activity. In the worst case, though, that of overnight treatment with 0.5 M sulphite, $E_{1/2}$ was only 50 mV more negative than that of an untreated electrode.

Very similar results were obtained under the same conditions of treatment for a platinum RWE. In particular, i_l (at −0.5 V) remained constant to within ±9% of its original value, and there was practically no variation in $E_{1/2}$.

Typical concentrations of SO_2 found, for example, in effluent from industrial waste treatment lie in the range 100—400 mg l^{-1} (i.e., 1.5—6.3 mM) [11] while in wine a maximum acceptable value is about 100 mg l^{-1} [12]. If the SO_2 permeates the membrane of the oxygen detector then, as discussed above, alkaline sulphite solution is produced. If rapid conversion is assumed, then a typical sulphite concentration coming into contact with the electrode will also be about 1.5—6.3 mM. The results reported above for $[SO_3^{2-}]$ in the range 10 mM—2 M show that both gold and platinum should be suitable for use as cathodes in membrane-covered oxygen detectors for prolonged periods in SO_2-containing environments without any deleterious effects.

Results for contamination by chlorine

Treatment of the gold RWE with 1.7 M hypochlorite for up to 4 h did not significantly shift $E_{1/2}$ for oxygen nor did i_l vary by more than ±10%. With the platinum RWE similar results were obtained with the variation in i_l being ±11%.

Adequate disinfection of secondary effluent is achieved with a Cl_2 dosage of 8—15 mg l^{-1} (0.1—0.2 mM) while the recommended maximum residual chlorine in undiluted effluents is 0.1—0.5 mg l^{-1} (1.5—7 μM) [13]. Treatment of an electrode with an alkaline hypochlorite solution will simulate the conditions actually present in a membrane-covered detector if Cl_2 permeates the membrane, and so at the chlorine levels likely to be encountered by such a detector there should be no adverse effects resulting from contamination of gold or platinum cathodes.

Results for contamination by hydrogen sulphide

Figure 1 A and B show respectively current—voltage (i—E) curves obtained with a gold RWE when treated with a 0.05 M sulphide solution for up to 4 h and with sulphide solutions in the range 0.01—0.1 M for 1 h. In neither case is there any dramatic effect on the shape of the curves or on the transport-limited current. The average value of $E_{1/2}$ in Fig. 1A is (−0.34 ± 0.06) V and in Fig. 1B it is (−0.53 ± 0.03) V; i.e., there is no apparent loss of catalytic activity for either electrode on treatment with sulphide. At −0.9 V in Fig. 1A, the average value of i_l is (57 ± 5) μA and in Fig. 1B it is (170 ± 10) μA. As already indicated, variations of this order are comparable to the precision of the experiment.

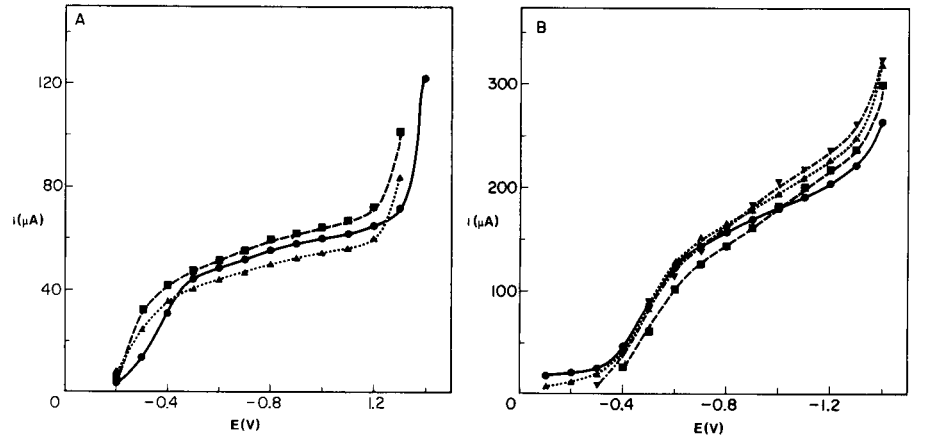

Fig. 1. Oxygen reduction at a gold electrode treated with sulphide solutions. (Reference electrode, Ag/AgCl/Cl$^-$ (2 M)). A, Treated with 0.05 M sulphide for various times: (•) untreated and 1 h; (▲) 2 h; (■) 4 h. B, Treated for 1 h with various sulphide concentrations: (•) untreated; (▲) 0.01 M; (■) 0.05 M; (▼) 0.1 M.

These results with gold are to be contrasted with those obtained with platinum under comparable conditions. Figure 2A shows the i—E curves for platinum treated with 0.05 M sulphide solution for up to 4 h, and Fig. 2B shows the curves after treatment for 1 h with sulphide solutions with concentrations in the range 0.01—0.05 M. The results shown in Fig. 2B are characteristic of electrode poisoning: the reduction in catalytic activity is shown by a shift of $E_{1/2}$ to more negative potentials and a higher interfacial resistance to charge transfer is shown by a decrease in di/dE before the transport-controlled region. Both these effects result in a plateau which does not begin

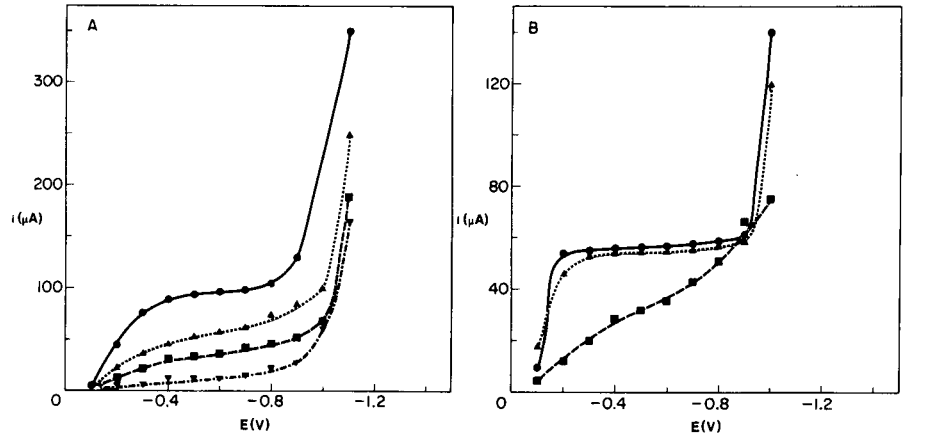

Fig. 2. Oxygen reduction at a platinum electrode treated with sulphide solutions. (Reference electrode, Ag/AgCl/Cl$^-$ (2 M)). A, Treated with 0.05 M sulphide for various times: (•) untreated; (▲) 1 h; (■) 2 h; (▼) 4 h. B, Treated for 1 h with various sulphide concentrations: (•) untreated; (▲) 0.01 M; (■) 0.05 M.

to develop fully until quite negative voltages and which is therefore poorly defined because of interference from solvent decomposition. In Fig. 2A the destruction of the current—voltage curve is even more dramatic with no characteristic sigmoid form remaining after treatment of just a few hours in 50 mM sulphide solution.

Hydrogen sulphide in an effluent stream, for example, will permeate the membrane of the oxygen detector and will be involved in the following equilibria:

$$H_2S \rightleftharpoons H^+ + HS^-; HS^- \rightleftharpoons H^+ + S^{2-}$$

the pK_a values being 7.04 and 11.96, respectively. With the electrolyte in the cathode region having pH 13—14, the predominant species will be S^{2-}. Concentrations of H_2S in effluents can be as high as 100—200 mg l^{-1} [11, 14]. Therefore, the concentration of S^{2-} in contact with the cathode could be 3—6 mM. The present results show quite clearly that a gold cathode in an oxygen detector would not be unduly affected by such concentrations whereas an oxygen detector with a platinum cathode used in H_2S-contaminated effluents would be affected even after relatively short contact times.

An idea of the way in which poisoning of a platinum cathode by S^{2-} occurs can be obtained by considering the kinetics of the poisoning process. The rate of electrochemical reduction of oxygen on a clean surface site ($\vec{j}_0$) at any potential can be written [15] as

$$\vec{j}_0 = AC_O^\infty/[(k_H')^{-1} + (k_D')^{-1}] \text{ mol s}^{-1} \quad (1)$$

where A is the electrode area, C_O^∞ is the concentration (mol cm^{-3}) of dissolved oxygen in the bulk solution, k_H' is the rate constant (cm s^{-1}) for the reduction by heterogeneous kinetics, and k_D' is the rate constant (cm s^{-1}) for the electroactive species (O_2) crossing any diffusion boundary layer from the bulk solution to the electrode surface. Equation (1) can be rewritten in the form $\vec{j}_0 = k' AC_O^\infty$, where k' is an empirical rate constant (cm s^{-1}) having contributions from both kinetics and transport. This equation can also be written as $\vec{j}_0 = k AC_O^a$, where C_O^a is the amount of oxygen adsorbed per unit area of the electrode surface (mol cm^{-2}) and k is a rate constant (s^{-1}) relating k' and the equilibrium constant for the adsorption of oxygen on the surface prior to reduction, i.e., O_2 (solution) $\rightleftharpoons$ O_2 (adsorbed).

In the presence of sulphide ions, C_O^a will be reduced by a factor of $(1 - \theta)$ if a fraction θ of the surface sites are poisoned by S^{2-}. Hence the rate of reduction on a poisoned surface ($\vec{j}_S$) will be given by $\vec{j}_S = k\ A\ C_O^a\ (1 - \theta)$. Provided that there is no change in the relative contributions of k_H' and k_D' to k' and hence to k, then at a given potential the rate of electrochemical reduction in the presence of poisoning compared with that in the absence of poisoning will be $\vec{j}_S/\vec{j}_0 = (1 - \theta)$, which, since rates are equivalent to currents, can be written as

$$i_S/i_o = (1 - \theta) \quad (2)$$

If the poisoning of surface sites is written as

$$S^{2-}(aq) + Pt(s) \underset{k_d}{\overset{k_a}{\rightleftharpoons}} PtS(s) + 2e^-$$

then the net rate at which the fraction of surface sites are formed will be given by

$$n\, d\theta/dt = k_a (1 - \theta) n_S - k_d n\theta \tag{3}$$

where n is the total number of sites available per cm^2, k_a is the rate constant for adsorption (cm s^{-1}), k_d is the rate constant for desorption (s^{-1}), and n_S is the concentration of S^{2-} in solution (molecules cm^{-3}).

The minimum concentration of S^{2-} used in the experiments (0.01 M) corresponds to a value of $n_S \approx 6 \times 10^{18}$ molecules cm^{-3} which is much greater than the total number of surface sites available for poisoning, $n \approx 10^{15}$ sites cm^{-2}. Thus, it is reasonable to integrate Eqn. (3) to give

$$\theta = \theta_e [1 - \exp(-k_a n_S t/n\theta_e)] \tag{4}$$

where θ_e is the fraction of the surface covered once equilibrium has been achieved. The results of Fig. 2A suggest that since as $t \to \infty$, $i_S \to 0$ then $\theta_e \to 1$; i.e., all the surface sites are blocked for oxygen reduction by the presence of sulphide ions. In this case, Eqn. (4) has a simple form when expressed as $(1 - \theta)$ and Eqn. (2) becomes

$$i_S/i_0 = \exp(-k_a n_S t/n) \tag{5}$$

A simple test of this equation is to consider the case where $i_S/i_0 = 0.5$. The half-life ($t_{1/2}$) for the current decay will be

$$t_{1/2} = \ln 2/(k_a/n)\, n_S \tag{6}$$

Figure 3 shows the variation with time of i_S/i_o at a fixed potential of −0.6 V and for different sulphide ion concentrations. A plot of the values of $t_{1/2}$ from Fig. 3 against the reciprocal of the sulphide concentration (M) according to Eqn. (6) gave a straight line passing through the origin, which suggests that the model for poisoning is reasonable. From the slope of the plot, a value for the second-order rate constant (k_aL/n where L is Avogadro's number) was calculated: 0.31 cm^3 mol^{-1} s^{-1}.

A more rigorous test of the model is to plot the results for the full decay curves of Fig. 3 according to Eqn. (5) in the form

$$\ln(i_S/i_0) = -(k_a/n)\, n_S\, t \tag{7}$$

This is done in Fig. 4. For 0.05 M and 0.1 M sulphide solutions at times less than about 30 s, Eqn. (7) clearly holds. From the slopes of the plots, a value of k_aL/n of 0.44 cm^3 mol^{-1} s^{-1} was calculated for 0.05 M sulphide and a value of 0.36 cm^3 mol^{-1} s^{-1} for 0.1 M sulphide. Both these values are in reasonable agreement with that obtained from the above-mentioned $t_{1/2}$ vs. C_s^{-1} plot. At longer times than 30 s there are clear deviations from

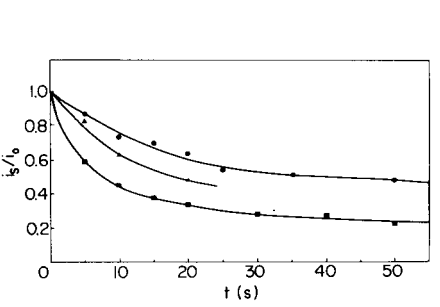

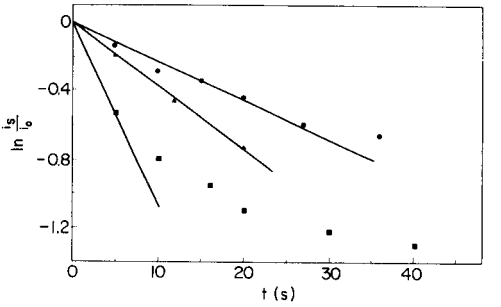

Fig. 3. Plots of variation of current with time for platinum electrode treated with various concentrations of sulphide solution: (•) 0.05 M; (▲) 0.1 M; (■) 0.5 M.

Fig. 4. Test of Eqn. (7) for data from Fig. 3. Sulphide ion concentrations: (•) 0.05 M; (▲) 0.1 M; (■) 0.5 M.

linearity. This could arise as a result of two reactions occurring in parallel [16].

The original electrode surface would be expected to have not only Pt sites but also sites covered by some form of oxide, especially as hot chromic acid was used to clean the electrodes before treatment with sulphide. Oxygen reduction can occur on both clean Pt sites and on oxide-covered sites [17]. The rate of poisoning of these two types of sites by sulphide ions would be expected to be rather different from each other. Possible reactions are

$$S^{2-} + Pt \rightleftharpoons PtS + 2e^-; \quad S^{2-} + PtOH \rightleftharpoons PtS + OH^- + e^-$$

Two parallel pseudo-first order reactions producing a common product lead to curvature of a simple first-order plot of the type shown in Fig. 4 [16]. At short times the kinetics are dominated by reaction of sulphide with the more active sites, but at longer times when all these sites have been poisoned, the kinetics are those of the reaction with the less active sites. Taking the results from Fig. 2A for i_S/i_0 at −0.6 V and plotting them according to Eqn. (7) shows that at long times there is again a linear relationship (Fig. 5) and from the slope of the plot a rate constant for poisoning of the less active sites is obtained: 2.8×10^{-3} cm^3 mol^{-1} s^{-1}. This rate constant is about 100 times less than that for the poisoning of the more active sites.

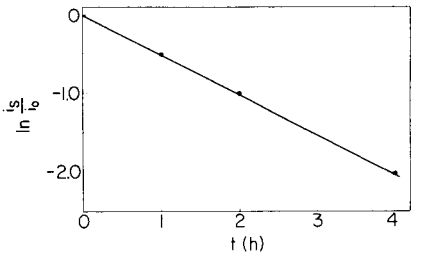

Fig. 5. Test of Eqn. (7) for data from Fig. 2A.

Thus, one has a model for the poisoning of platinum by sulphide which suggests that there is initially a rapid poisoning of some of the surface sites followed by a slower poisoning of the remainder of the sites. From a practical viewpoint, however, it can be seen that the initial poisoning of the more active sites is both rapid enough (<1 min) and extensive enough (≈50% fall in O_2 reduction current in 1 min) to make a platinum cathode unsuitable for use in H_2S-polluted environments.

Other cathode materials

The results presented in the previous sections have been exclusively concerned with platinum and gold because these are the most widely used materials for oxygen detectors. Silver is also often used as a cathode in these oxygen detectors [6], but as the results of Schmid and Mancy [7] indicate it is sensitive to H_2S. Figure 6 shows this clearly. Treatment with a 0.1 M sulphide solution for 30 min leads to a considerable loss of activity of the electrode with i_l at −0.9 V being reduced from about 40 μA to 20 μA. Similar loss of activity results from treatment with 0.05 M sulphide for varying lengths of time. For example, a 10% reduction in i_l was obtained after treatment for only 1 min. Thus silver, like platinum, is unsuitable for use as an oxygen cathode in H_2S-contaminated environments.

Replacement of a metal by a metal sulphide has been suggested [18] as a means of overcoming the problem of cathode contamination by H_2S. This has been investigated further. Figure 7 shows current—voltage curves obtained for a nickel electrode after treatment with 0.1 M sulphide for different times. There is initially a loss of catalytic activity as shown by the decrease

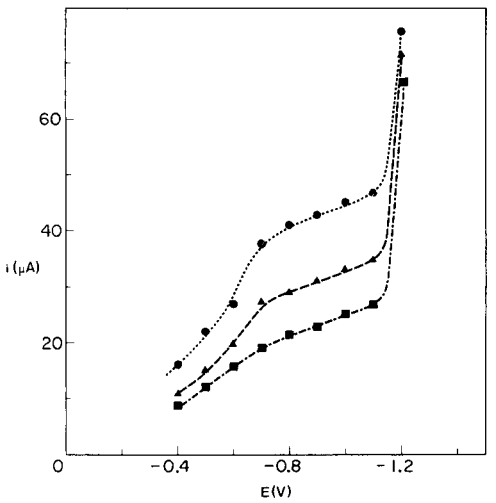

Fig. 6. Oxygen reduction at a silver electrode treated for 30 min with various concentrations of sulphide: (•) untreated; (▲) 0.05 M; (■) 0.1 M. (Reference electrode, Ag/AgCl/Cl^- (2 M)).

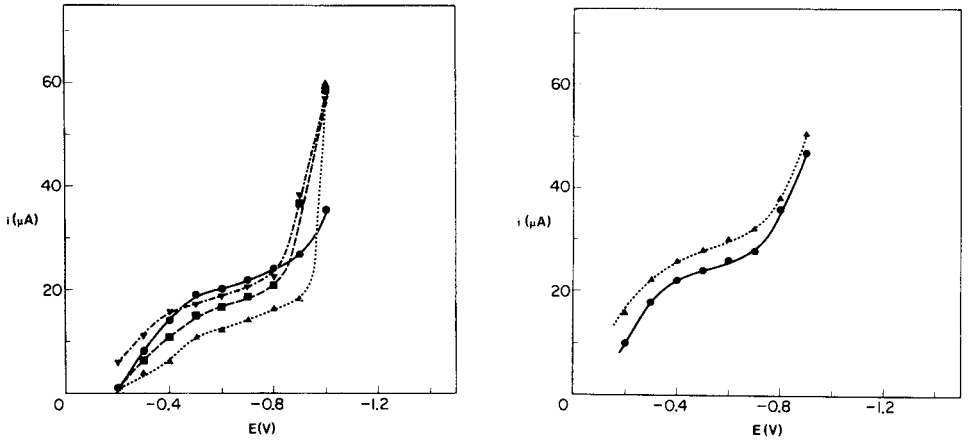

Fig. 7. Oxygen reduction at nickel electrode treated with 0.1 M sulphide solution for various times: (•) untreated; (▲) 15 min; (■) 1 h; (▼) 2 h. (Reference electrode, Ag/AgCl/Cl^- (2 M)).

Fig. 8. Oxygen reduction at nickel and nickel sulphide electrodes: (•) Ni; (▲) NiS. (Reference electrode, Ag/AgCl/Cl^- (2 M)).

in the slope of the $i - E$ curves and the significant fall in i_l. On more prolonged treatment of the electrode with sulphide, however, there is a restoration of the activity of the electrode for oxygen reduction and after 2 h i_l is comparable to that for the untreated electrode.

A possible explanation for this behaviour is that during initial contact of the nickel with sulphide, the sulphide ions are physically adsorbed onto the nickel and block the surface sites for oxygen reduction. With more prolonged contact, the adsorbed sulphide has time to react with the nickel to form nickel sulphide and this is an effective catalyst for oxygen reduction [19]. This type of explanation is supported by the results shown in Fig. 8 where $i - E$ curves are given for a pure nickel wire and for the same wire after conversion of the surface to nickel sulphide; the higher currents for the nickel sulphide probably arise simply from the increase in surface area on formation of the nickel sulphide.

Treatment of a nickel sulphide electrode with sulphide solution was found to have no further effect on either the shape of the $i - E$ curve or on i_l. Thus nickel sulphide is not only an effective catalyst for oxygen reduction, but is also resistant to poisoning by H_2S. It is therefore a potentially interesting candidate for a cathode in an oxygen detector for use in H_2S-contaminated environments.

Effect of contamination on overall operation of a membrane-covered oxygen detector

All the results given have been for the effects of contaminants on the cathode of the oxygen detectors. In practice, of course, a gas permeating through

the membrane can also contaminate the anode of the detector. However, because the anode does not have to be immediately behind the inner surface of the membrane, measures can be taken to minimise contact between the contaminant gas and the anode; e.g., by having a narrow tortuous path from the inner surface of the membrane to the anode, although this may also lead to problems of ohmic drop between cathode and anode. Another possibility is to use an ion-exchange membrane as the electrolyte in the cell [20]. This allows good ionic contact between cathode and anode, but minimises contamination of the anode because ion-exchange membranes generally have low permeabilities for gases.

A third possibility is deliberately to use a contaminated electrolyte in the detector, thus starting off with a poisoned anode. An example of such a detector would be one with a gold cathode, a sulphide-containing electrolyte and an Ag/Ag_2S anode [21]. This detector can be used in H_2S-contaminated environments: as has been shown here, the gold cathode is unaffected by contact with a sulphide-containing electrolyte, while $Ag/Ag_2S/S^{2-}$ forms the reference electrode [22]. The only problem with such a detector is the tendency of the sulphide in the electrolyte to oxidise to polysulphides [23] which can then contaminate the cathode, but this effect can be minimised by keeping an applied negative voltage on the cathode so that there is little oxygen in the vicinity to bring about sulphide oxidation. Also, of course, such a detector is only strictly preconditioned against contamination in H_2S-containing environments. In prolonged contact with environments containing other gaseous contaminants, there may still be an effect on the anode.

REFERENCES

1 V. Spiehler, Bibliography of Application Areas for Beckman Polarographic Oxygen Analyzers, Beckman Technical Report No. 545.
2 F. Kreuzer, Oxygen Pressure Recording in Gases, Fluids and Tissues, S. Karger, Basel, 1969.
3 M. Kessler (Ed.), Oxygen Supply, Urban and Schwarzenberg, Munich, 1973.
4 H. Degn, I. Balslev and R. Brook (Eds.), Measurement of Oxygen, Elsevier, Amsterdam, 1976.
5 I. Fatt, Polarographic Oxygen Sensors, CRC Press, Cleveland, 1976.
6 M. L. Hitchman, Measurement of Dissolved Oxygen, Wiley-Interscience, New York, 1978.
7 M. Schmid and K. H. Mancy, Chimia, 23 (1969) 398.
8 R. N. Adams, Electrochemistry at Solid Electrodes, Marcel Dekker, New York, 1969, p. 104.
9 J. M. Hale and M. L. Hitchman, J. Electroanal. Chem., 107 (1980) 281.
10 D. T. Sawyer and J. L. Roberts, Experimental Electrochemistry for Chemists, Wiley-Interscience, New York, 1974, p. 256.
11 W. H. Kibbel, C. W. Raleigh and J. A. Shepherd, Eng. Bull. Purdue Univ., 141 (1972) 824.
12 M. A. Amerine and E. B. Roessler, Wines: Their Sensory Evaluation, W. H. Freeman, San Francisco, 1976, p. 202.
13 J. W. Clark, W. Viessman and M. J. Hammer, Water Supply and Pollution Control (3rd edn.), Harper and Row, New York, 1977, p. 452.

14 T. R. Camp and R. L. Meserve, Water and its Impurities (2nd edn.), Dowden, Hutchinson and Ross, Pennsylvania, 1974, p. 69.
15 W. J. Albery, Electrode Kinetics, Clarendon Press, Oxford, 1975, p. 58.
16 A. A. Frost and R. G. Pearson, Kinetics and Mechanism (2nd edn.), Wiley, New York, 1961, p. 163.
17 W. J. Albery and M. L. Hitchman, Ring-Disc Electrodes, Clarendon Press, Oxford, 1971, p. 84.
18 M. L. Hitchman, W. Mehl and J. P. Millot, U. S. Patent 3, 785, 948, Jan. 15, 1974.
19 A. K. M. S. Huq and A. J. Rosenberg, J. Electrochem. Soc., 111 (1964) 270.
20 L. W. Niedrach and W. H. Stoddard, U. S. Patent 3,703,457, Nov. 21, 1972.
21 J. M. Hale, in E. Gnaiger and H. Forstner (Eds.), Handbook of Polarographic Oxygen Sensors, Springer, Berlin, 1982.
22 D. J. G. Ives and G. J. Janz, Reference Electrodes, Academic Press, 1961, p. 381.
23 K. Y. Chen and J. C. Morris, Environ. Sci. Technol., 6 (1972) 529.

Analytica Chimica Acta, 143 (1982) 143—151
Elsevier Scientific Publishing Company, Amsterdam — Printed in The Netherlands

POTENTIOMETRIC TITRATION OF ORGANIC CATIONS WITH SODIUM TETRAPHENYLBORATE AND A LIQUID-MEMBRANE TETRAPHENYLBORATE ION-SELECTIVE ELECTRODE

T. K. CHRISTOPOULOS, E. P. DIAMANDIS and T. P. HADJIIOANNOU*
Laboratory of Analytical Chemistry, University of Athens, Athens (Greece)
(Received 4th May 1982)

SUMMARY

Simple potentiometric titrations are described for the determination of various organic cations (usually 5—25 μmol) with 0.01 M sodium tetraphenylborate. A liquid-membrane electrode with tetrapentylammonium tetraphenylborate dissolved in 4-nitro-*m*-xylene as liquid ion-exchanger is used successfully in the semi-automatic titration of quaternary ammonium compounds, cationic surfactants, alkaloids and other substances of pharmaceutical importance which are precipitated by tetraphenylborate. Analysis of pharmaceutical preparations gave satisfactory results.

Sodium tetraphenylborate has been used extensively for the determination of univalent cations, various alkaloids, cationic surfactants, quaternary ammonium compounds and amines. These methods are based on the formation of sparingly soluble tetraphenylborate salts. Classically, gravimetric and titrimetric methods were used. In some methods, an excess of sodium tetraphenylborate solution is added to the sample solution, and the excess of reagent in the filtrate is titrated with silver nitrate or cetylpyridinium chloride using adsorption indicators [1, 2]. Organic cations precipitated by tetraphenylborate can also be determined by two-phase titration using various dyes as indicators; the dye moves from one phase to the other at the end-point [3—5].

Ion-selective electrodes have been applied successfully to various titrations in which tetraphenylborate served as titrant [6—14]; early work in this area has been reviewed by Vytras [15].

In this paper, a liquid-membrane electrode which can be used in potentiometric precipitation titrations with sodium tetraphenylborate is described. The liquid ion-exchanger is tetrapentylammonium tetraphenylborate dissolved in 4-nitro-*m*-xylene. This electrode exhibits near-Nernstian response to the tetraphenylborate anion in the range 5×10^{-6}—3×10^{-4} M. It can be used in the semi-automatic potentiometric titration of a large number of organic cations (including quaternary ammonium compounds, cationic surfactants, alkaloids and other substances of pharmaceutical importance) which are precipitated by tetraphenylborate(TPB^-). The proposed methods

0003-2670/82/0000-0000/$02.75

are simple, accurate and sensitive. Satisfactory results were obtained for several organic cations in pharmaceutical preparations.

EXPERIMENTAL

Apparatus

The tetraphenylborate-sensitive electrode was used with a double-junction silver—silver chloride reference electrode (Orion Model 90-02-00). The outer chamber of the reference electrode was filled weekly with a 10% (w/v) sodium nitrate solution. E.m.f. values were measured with a Corning Model 12 Research pH/mV meter. The cell potential was recorded with a Heath-Schlumberger system, which consisted of a pH/pIon electrometer (EU-200-30), a potentiometric amplifier (EU-200-01), a d.c. offset module (EU-200-02) and a strip-chart recorder (EU-205-11). The titrant was added with a multi-speed constant-rate burette (Radiometer Model ABU12). Titration rates were kept constant at 0.36 ml min^{-1}. pH values were measured with a Metrohm pH meter (Model E350B). All solutions were titrated at ambient temperature (22 ± 2°C) with constant magnetic stirring.

Reagents

All solutions were prepared with deionized distilled water from reagent-grade materials.

Standard 0.010 M sodium tetraphenylborate solution. Dissolve 3.422 g of sodium tetraphenylborate (Merck) in water and dilute exactly to 1 l with water. Let the solution stand for 24 h and filter through Whatman No. 42 paper. This solution is standardized by potentiometric titration with tetraphenylarsonium chloride as described below.

Standard 0.001000 M tetraphenylarsonium chloride solution. Dissolve 0.4188 g of anhydrous tetraphenylarsonium chloride (Merck) in water and dilute exactly to 1 l with water. The purity of the dry substance is checked by gravimetry [16].

Standard solutions of organic cations. The organic cationic compounds used were of the highest purity available and were used without further purification. Generally, 0.00100 M solutions were prepared, by dissolving the appropriate amount of substance, or its hydrochloric, phosphate or sulfate salt, in water. Organic bases were dissolved by the addition of small amounts of hydrochloric acid (brucine, cinchonine) or sulfuric acid (quinaldine). In some cases 0.0100 M solutions of organic cations were used (for amphetamine sulfate).

Tetrapentylammonium bromide and tetraheptylammonium bromide were purchased from Eastman Kodak Co., and tetraphenylphosphonium bromide, 4-nitro-*m*-xylene, *o*-nitrotoluene, nitrobenzene, tri-n-butyl phosphate and gelatine from Merck.

Acetate buffers (0.10 M, pH 3.3 or 5.0). Dissolve 6.0 g of anhydrous acetic acid in about 800 ml of water, adjust the pH to 3.3 or 5.0 with 6 M NaOH solution and dilute to 1 l with water.

Phosphate buffers (0.10 M, pH 7.0 or 10.2). Dissolve 13.8 g of sodium dihydrogenphosphate monohydrate in about 800 ml of water, adjust the pH to 7.0 or 10.2 with 6 M NaOH solution and dilute to 1 l with water.

Preparation of the liquid ion-exchanger. Precipitate tetrapentylammonium tetraphenylborate by mixing 10.0 ml of 0.010 M sodium tetraphenylborate solution with 1.0 ml of 0.10 M tetrapentylammonium bromide solution. Extract the salt with 10.0 ml of 4-nitro-*m*-xylene and wash the organic phase three times with water. Filter the organic phase through a filter paper, Whatman No. 42, containing 1—2 g of anhydrous sodium sulfate, to remove traces of water. The filtrate should be clear and yellow. This solution is approximately 0.010 M in tetrapentylammonium tetraphenylborate. It is stored in a dry glass bottle.

Procedures

Construction of the electrode. An Orion liquid-membrane electrode body (Model 92) was used as the electrode assembly with a Millipore LCWPO-1300 teflon membrane; the teflon membranes were cut to the appropriate size and a stack of four was used to avoid any leakage of the liquid ion-exchanger.

After the body has been assembled in the usual way, inject the internal solution and the liquid ion-exchanger through the appropriate ports in the electrode body. The internal aqueous reference solution is 0.010 M sodium tetraphenylborate—0.10 M NaCl. Condition the electrode by soaking in a stirred 0.01 M sodium tetraphenylborate solution for 1 h before use. When not in use, store the electrode in a 10^{-3} M sodium tetraphenylborate solution. The operative life of the electrode is about 3—4 months.

Preparation of the calibration curve. Pipet 30.00 ml of water into the measurement cell (a 50-ml beaker), immerse the electrodes into the solution, start stirring at the maximum speed at which air bubbles are not formed, and add 1.00 μl of 0.010 M sodium tetraphenylborate solution. Read the e.m.f. when it has stabilized to ± 0.1 mV (0.5—2 min). Continue with new additions of sodium tetraphenylborate solution to cover the concentration range 3.3×10^{-7}—5×10^{-3} M. Record the e.m.f. after stabilization in each case and plot E (mV) vs. log [TPB^-].

Standardization of the 0.01 M sodium tetraphenylborate solution. Pipet into a 50-ml beaker a 25.00-ml aliquot of the 0.001000 M tetraphenylarsonium chloride standard solution, start the stirrer, and after the potential has stabilized ($\approx$1 min), start simultaneously the burette and the recorder to obtain the titration curve. Calculate the titer of the sodium tetraphenylborate solution, preferably using the mean result from four titrations. The titer of the sodium tetraphenylborate solution should be checked weekly.

Titration of organic cations with standard 0.01 M sodium tetraphenylborate solution. For Method 1, pipet into a 50-ml beaker a 25.00-ml aliquot of the sample in the following concentration ranges: 4.00×10^{-5}—1.00×10^{-3} M for papaverine hydrochloride; 2.00×10^{-4}—1.00×10^{-3} M for tetraphenylarsonium chloride, tetrabutylammonium bromide, cetyltrime-

thylammonium bromide, cetylpyridinium bromide, trimethylphenylammonium bromide, tetraphenylphosphonium bromide, atropine sulfate, cocaine hydrochloride, cinchonine hydrochloride, brucine hydrochloride or novatropine; 4.00×10^{-4}—1.00×10^{-3} M for codeine phosphate and quinaldine sulfate; 6.00×10^{-4}—1.00×10^{-3} M for thiamine hydrochloride; 8.00×10^{-4}—1.00×10^{-3} M for morphine hydrochloride; 2.00×10^{-4}—6.00×10^{-4} M for quinine sulfate; and 1.00×10^{-3} M for acetylcholine hydrochloride. Adjust the volume to 30.00 ml by adding 5.00 ml of the appropriate buffer solution (see Tables) or water and add 3 ml of 0.02% (w/v) gelatine solution if required. Continue as in the procedure for the standardization of the sodium tetraphenylborate solution from the point of starting the stirrer.

For Method 2, pipet into a 25-ml beaker a 3.00-ml aliquot of amphetamine sulfate (2.00×10^{-3}—1.00×10^{-2} M), adjust the volume to 5.00 ml by adding 2.00 ml of the appropriate buffer solution or water, and titrate as described above.

RESULTS AND DISCUSSION

Membrane material and optimal pH range

For the construction of the tetraphenylborate electrode, the liquid ion-exchangers examined were the tetraphenylborate salts of tetrapentylammonium, tetraheptylammonium and tetraphenylphosphonium, dissolved in 4-nitro-*m*-xylene, *o*-nitrotoluene, nitrobenzene or tri-n-butyl phosphate. The results indicated that the best combination was tetrapentylammonium tetraphenylborate dissolved in 4-nitro-*m*-xylene.

To check the pH dependence of the electrode potential, potential-pH curves at various tetraphenylborate concentrations were constructed. The pH of the initial solution was altered by addition of very small volumes of 18 M NaOH or 12 M HCl solution. The results showed that the potential is practically unaffected by pH in the range 3—12. Thus, the constructed electrode can be used in potentiometric titrations over this wide pH range.

Characteristics of the electrode

Calibration curve. A typical calibration curve for the tetraphenylborate electrode is shown in Fig. 1. The response is linear in the range 5.0×10^{-6}—3.0×10^{-4} M with a slope of about 51 mV/concentration decade, at 20°C. The slope of the calibration curve is stable during the operative lifetime of the electrode. The deviation from linearity at high tetraphenylborate concentrations may be due to micellar association.

Response time and stability. The electrode provides stable potential readings (±0.1 mV) within 3—10 s provided that the concentration of the measured solution is within the linear response range. In this range, the day-to-day reproducibility is within ±5 mV. Electrode stability is not a critical factor when the electrode is applied in potentiometric titrations only.

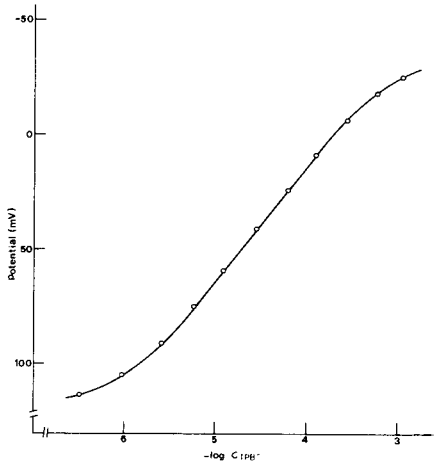

Fig. 1. Calibration curve for the tetraphenylborate-sensitive liquid membrane electrode in aqueous solutions.

Potentiometric titrations

Selig [8] and Vytras et al. [10] recommend the use of thallium(I) for the standardization of sodium tetraphenylborate solutions. Tetraphenylarsonium chloride was preferred here because it is commercially available in a very pure form, its purity can be checked by gravimetry [16] and its potentiometric titration with sodium tetraphenylborate yields large and sharp potentiometric breaks ($\approx$430 mV) as shown in Fig. 2. The precision of such a titration is about 0.3%.

Results are presented in Table 1 for the potentiometric titration of aqueous solutions of various cations with sodium tetraphenylborate. In most cases the precision of the method is better than 1%. It is well known that in potentiometric semi-automatic precipitation titrations, there is frequently a blank which depends, among other factors, on the concentration of the sample and the titrant, the stirring rate, the titration rate, the adsorption of the titrant on the precipitate, and the reaction rate. All these factors can be kept constant except for adsorption and reaction rate, which depend on the individual compound. The blank effect can be eliminated by subtracting the appropriate blank volume from the end-point volume for each titration. This blank volume is estimated under constant experimental conditions, by titrating standard solutions of the compound of interest.

The optimum pH for each titration was found from tests with solutions buffered in the pH range 3—10 and with unbuffered solutions. The optimum pH value was chosen so as to achieve accuracy and precision, small blanks and steep potentiometric breaks near the equivalence point. For the quaternary ammonium, arsonium or phosphonium compounds, the pH dependence of the results was negligible. For the organic bases, the optimum pH was generally calculated from the expression $pH \leqslant 12 - pK_b$, where K_b is the dis-

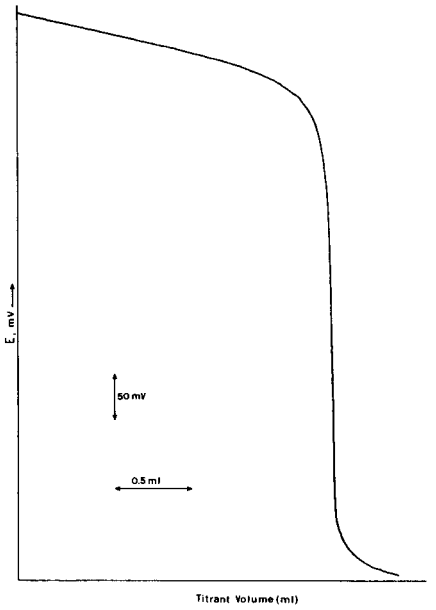

Fig. 2. Titration curve of 20.00 ml of 1.0×10^{-3} M tetraphenylarsonium chloride with 1.0×10^{-2} M sodium tetraphenylborate (other conditions as under Procedure).

sociation constant of the base, because at this pH value the base is quantitatively protonated. The optimum pH for the organic bases was always checked experimentally.

The optimum pH for thiamine is 7.0 (phosphate buffer); at pH 3—5 or in unbuffered solutions large positive errors occur (40—65%) and at pH 10 no titration curve is obtained. The titration of quinine at pH <5 yields large positive errors and unsatisfactory curves. Papaverine can be titrated at pH values <3.3; at pH 5, large positive errors occur (60%) because of the slow formation of papaverine tetraphenylborate and adsorption of the titrant on the precipitate. The titration of weak organic bases with sodium tetraphenylborate at pH values less than 2.5 is not feasible because the electrode is not useful in such acidic solutions and the titrant decomposes.

During the titration of mephentermine sulfate (see below), the precipitate formed affected the electrode, resulting in noisy response and erratic recording of titration curves. This difficulty was overcome by adding a small amount of a 0.02% (w/v) gelatine solution to the reaction mixture (see Procedures). Such quantities of gelatine do not affect the accuracy of the titration and help in obtaining a noise-free, steep titration curve.

Stirring rate is crucial in precipitation titrations. For best results, the maximum speed at which air bubbles are not formed must be used. In some cases, after a titration, the electrode exhibits sluggish response because of adherence of the precipitate to the membrane. In such cases, the membrane is rinsed thoroughly with water and cleaned with soft tissues.

TABLE 1

Results for the potentiometric titration of aqueous solutions of various cations with sodium tetraphenylborate [a]

Compound	Optimum pH	Amount of sample (μmol)	Av. error (%)	R.s.d. (%)	Av. potential break (mV)
Tetraphenylarsonium chloride	Unbuffered	5—20	1.3	0.3 (n=4)	400
Tetrabutylammonium bromide	Unbuffered	7—25	—	0.6 (n=3)	170
Cetyltrimethylammonium bromide	Unbuffered	5—20	0.9	0.6 (n=4)	380
Cetylpyridinium bromide	Unbuffered	10—20	1.0	1.3 (n=3)	470
Trimethylphenylammonium bromide	Unbuffered	10—20	1.6	0.4 (n=3)	80
Acetylcholine chloride	Unbuffered	25	1.6	0.4 (n=3)	65
Tetraphenylphosphonium bromide	Unbuffered	5—20	3.2	0.5 (n=3)	400
Atropine sulfate	3—7	5—25	1.5	1.3 (n=5)	55
Papaverine hydrochloride	3.3	5—25	1.6	1.3 (n=3)	150
Morphine hydrochloride	3—5	25	1.6	0.7 (n=4)	50
Codeine phosphate	3—7	25	—	0.6 (n=9)	65
Cocaine hydrochloride	3—5	5—25	2.0	0.4 (n=6)	120
Cinchonine hydrochloride	7	5—25	0.7	1.0 (n=7)	80
Brucine hydrochloride	2—7	5—25	2.1	0.6 (n=3)	120
Novatropine	3—7	5—25	2.2	0.3 (n=4)	120
Quinine sulfate	7	5—15	3.0	0.5 (n=3)	100
Quinaldine sulfate	2.7	12—31	1.7	1.0 (n=3)	65
Thiamine hydrochloride	7	15—25	1.5	0.4 (n=3)	80
Amphetamine sulfate	7	30	3.3	1.0 (n=3)	70

[a] All compounds except amphetamine sulfate were titrated by Method 1.

As is usual with liquid-membrane electrodes, some pre-conditioning is necessary before the first titrations of the day or in changing from one compound to another. For the present systems, one titration of a relatively concentrated sample proved to be sufficient for conditioning. For titrations of dilute solutions of substances which give small potentiometric breaks, 2—3 pre-titrations are needed for conditioning.

Generally, the potentiometric breaks and the steepness of the titration curve increase with increasing concentration of the substance titrated, with the exception of papaverine hydrochloride and cocaine hydrochloride. Representative curves are shown in Fig. 3. The titration curves for tetraphenylphosphonium bromide, tetrabutylammonium bromide, cetyltrimethylammonium bromide, cetylpyridinium bromide, papaverine hydrochloride, cocaine hydrochloride, and novatropine were similar to the sigmoidal curves obtained for tetraphenylarsonium chloride. The titration curves for morphine hydrochloride, codeine phosphate, cinchonine hydrochloride, brucine hydrochloride, quinine sulfate, thiamine hydrochloride and quinaldine sulfate were similar to those obtained for atropine sulfate (Fig. 3a). The titration curves for trimethylphenylammonium bromide were similar to those obtained for acetylcholine chloride (Fig. 3b).

In the titration curves for atropine sulfate (and for compounds with similar titration curves) and for amphetamine sulfate, the electrode potential drops initially because the tetraphenylborate added is not precipitated instantaneously; as the titration proceeds, the sigmoidal shape is regained.

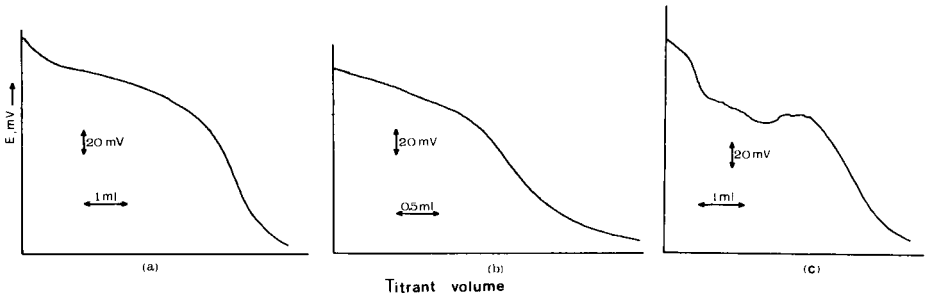

Fig. 3. Titration curves of organic cations with 1.0×10^{-2} M sodium tetraphenylborate: (a) 25.00 ml of 1.0×10^{-3} M atropine sulfate; (b) 25.00 ml of 1.0×10^{-3} M acetylcholine chloride; (c) 2.00 ml of 1.0×10^{-2} M amphetamine sulfate (other conditions as under Procedure).

Analysis of pharmaceutical preparations

Several pharmaceutical preparations which contain active substances precipitated by sodium tetraphenylborate were analyzed.

Mephentermine sulfate injection. The solution (6.00 ml) is diluted to exactly 50 ml with water, and 2.00-ml aliquots are titrated after addition of 3.00 ml of 0.02% (w/v) gelatine solution.

Thiamine hydrochloride tablets. Twenty tablets are powdered and dissolved in water, and the solution is adjusted to exactly 1 l. Aliquots (25.00 ml) of this solution are diluted to exactly 500 ml. Then 20.00-ml aliquots of this solution are mixed with 5.00 ml of buffer pH 7 for titration.

Atropine sulfate eye drops. A 4.00-ml portion of the solution is diluted to exactly 100 ml, and 20.00-ml aliquots are mixed with 5.00 ml of buffer pH 5 for titration.

Cetylpyridinium chloride in lozenges. Fifteen lozenges are powdered, 60 ml of water is added and the mixture is boiled for 5 min. The hot solution is filtered through a sintered glass crucible (G4) under suction, cooled and diluted to exactly 100 ml. For titration, 5.00-ml aliquots of this solution are diluted with 15.00 ml of water.

Amantadine hydrochloride capsules. Two capsules are added to 10 ml of water, and the mixture is heated to boiling until the capsules have completely melted. After cooling and dilution to exactly 50 ml, 2.00-ml aliquots of this solution are mixed with 6.00 ml of water and titrated.

Domiphen bromide in gargle solution. A 10.00-ml portion of the solution is diluted to exactly 250 ml with water, and 20.00-ml aliquots of this solution are titrated.

Results for the determination of organic compounds precipitated by tetraphenylborate in pharmaceutical preparations are shown in Table 2. There is fairly good agreement between the nominal values and the amounts of substance calculated from the titrimetric method. The titration curves for domiphen bromide were similar to those obtained for tetraphenylarsonium

TABLE 2

Potentiometric titration of organic compounds in pharmaceutical preparations with sodium tetraphenylborate

Compound	Content (mg)[a]		R.s.d. (%)	Potential break (mV)
	Nominal	Found		
Mephentermine sulfate injection	15[b]	15.3	0.7 (n=7)	110
Thiamine hydrochloride tablets	300	307.7	0.5 (n=6)	80
Atropine sulfate eye-drops	10	9.2	1.0 (n=6)	55
Cetylpyridinium chloride lozenges	2.5	2.3	1.0 (n=6)	470
Amantadine hydrochloride capsules	100	110	1.5 (n=4)	85
Domiphen bromide gargle solution	10	10.4	0.8 (n=4)	520

[a]Contents are given as mg ml^{-1} for liquid preparations, otherwise as mg per tablet, lozenge or capsule. [b]Expressed as base.

chloride. The titration curves of amantadine hydrochloride and mephendermine sulfate were similar to those obtained for atropine sulfate.

Conclusions

The tetraphenylborate-sensitive electrode described here is very easily constructed and is a useful sensor for the titration of many organic cations or bases with sodium tetraphenylborate. The proposed procedures are simple, accurate, precise and sensitive. The application of the electrode in the titration of active substances precipitated by tetraphenylborate in pharmaceutical preparations gave satisfactory results. It should be possible to extend the use of the electrode in titrations of drugs of major pharmaceutical importance such as phenothiazines, tricyclic antidepressants, etc.

REFERENCES

1 C. A. Johnson and R. E. King, J. Pharm. Pharmacol., 14 (1962) 77T.
2 British Pharmaceutical Codex 1973, The Pharmaceutical Press, London, p. 892.
3 J. T. Cross, Analyst, 90 (1965) 315.
4 G. F. Longman, Talanta, 22 (1975) 621.
5 T. Sakai, M. Tsubouchi, M. Nakagawa and M. Tanaka, Anal. Chim. Acta, 93 (1977) 357.
6 S. Pinzauti and E. La Porta, Analyst, 102 (1977) 938.
7 W. Selig, Talanta, 27 (1980) 914.
8 W. Selig, Mikrochim. Acta, (1980 II) 133.
9 E. P. Diamandis and T. P. Hadjiioannou, Anal. Lett., 13 (B15) (1980) 1317.
10 K. Vytras, M. Dajkova and V. Mach, Anal. Chim. Acta, 127 (1981) 165.
11 A. Gur'ev, G. M. Lizunova, I. M. Korenman and O. N. Medvedeva, Zh. Anal. Khim., 36 (1981) 130.
12 E. P. Diamandis, E. Athanasiou-Malaki, D. S. Papastathopoulos and T. P. Hadjiioannou, Anal. Chim. Acta, 128 (1981) 239.
13 C. E. Efstathiou, E. P. Diamandis and T. P. Hadjiioannou, Anal. Chim. Acta, 127 (1981) 173.
14 W. Selig, Frezenius Z. Anal. Chem., 308 (1981) 21.
15 K. Vytras, Int. Lab., 9 (1979) No. 2, 35.
16 D. Glover and J. M. Rosen, Anal. Chem., 37 (1965) 306.

Analytica Chimica Acta, 143 (1982) 153—161
Elsevier Scientific Publishing Company, Amsterdam — Printed in The Netherlands

COMPLEX FORMATION OF URANYL IONS WITH POLYAMINOPOLYCARBOXYLIC ACIDS

PER A. OVERVOLL and WALTER LUND*
Department of Chemistry, University of Oslo, Box 1033, Blindern, Oslo 3 (Norway)
(Received 28th June 1982)

SUMMARY

The complex formation of uranyl ions with ethylenediaminetetraacetic acid, diethylenetriaminepentaacetic acid and triethylenetetraminehexaacetic acid has been studied by pH titrations, with computer evaluation of the titration data. For each ligand, the formation constants of a series of mono- and di-nuclear complexes were determined in 0.1 M KNO_3 at 25.0°C. The hydrolysis constants for uranyl ions and the dissociation constants of the ligands were also calculated. A novel approach was used to obtain realistic estimates of the uncertainties in the respective constants. Certain likely structures of the complexes are suggested.

Studies of the complex formation of uranyl ions with EDTA have revealed a pronounced tendency to form dinuclear complexes [1, 2] which is rather unusual, considering that EDTA shows a strong preference to form mononuclear complexes with most other metals. The linear O—U—O configuration of the uranyl ion allows the EDTA to coordinate this metal only in the equatorial plane, which probably results in decreased stability of the mononuclear complexes. To obtain a clearer picture of the complex formation of uranyl ions with polyaminopolycarboxylic acids, the behavior of a series of these ligands was studied. The ligands were ethylenediaminetetraacetic acid (EDTA), diethylenetriaminepentaacetic acid (DTPA) and triethylenetetraminehexaacetic acid (TTHA). Few quantitative data have been published for the uranyl complexes of the larger ligands in this series. The complex formation was studied by potentiometric pH titrations, with computer evaluation of the data obtained. On the basis of the results, certain conclusions could be drawn regarding the structures of the different complexes.

EXPERIMENTAL

Apparatus and reagents

A Beckman Research pH meter was used with Orion glass and reference electrodes (910100/9001). The pH meter was standardized against 0.05 mol kg^{-1} potassium hydrogenphthalate and 0.01 mol kg^{-1} borax buffers. The titrations were done in a closed double-walled glass cell, which was thermo-

0003-2670/82/0000-0000/$02.75

statted at 25.0 ± 0.1°C. An argon atmosphere was maintained within the cell, and the sample was stirred with a magnetic stirrer. A Metrohm Multiburette E485 (10 ml) was used for adding standard acid and base.

The stock uranyl solution was prepared from uranyl nitrate, and standardized by gravimetry [3, 4]. The amount of free acid in the solution was determined as described previously [5]. Ethylenediaminetetraacetic acid disodium salt (EDTA; Merck, Germany) was dried at 80°C for 4 h. Diethylenetriaminepentaacetic acid (DTPA; Geigy, Switzerland) and triethylenetetraminehexaacetic acid (TTHA; Geigy, Switzerland) were recrystallized twice and thrice, respectively, from water, and dried at 100°C for 2 h. The stock solutions of these ligands were standardized by titration with alkali, after addition of nickel(II) nitrate in slight excess. For TTHA a two-fold excess of nickel was employed.

A standard acid solution was prepared from nitric acid, and standardized against sodium hydroxide. The carbonate-free sodium hydroxide solution was prepared in an argon atmosphere, from sodium metal which was cut under petroleum and rinsed with ether. The solution was standardized against potassium hydrogen-iodate. All solutions were made 0.1 M in potassium nitrate. The pH of the carbon dioxide-free stock solution of the latter salt was adjusted to 6.9—7.1.

Determination of $[H^+]$ and $[OH^-]$

The activity coefficient of the hydrogen ion (f_H) was determined by measuring pH in nitric acid solutions of known strength and using the equation $f_H = 10^{-pH}/[H^+]$. It was found to be 0.83 ± 0.02 in 0.1 M KNO_3 at 25.0°C. The ionic product $[H^+][OH^-]$ was determined by measuring pH in sodium hydroxide solutions of known strength and using the equation $[H^+][OH^-] = [OH^-]\ 10^{-pH}/f_H$. Log$[H^+][OH^-]$ was found to be −13.80 ± 0.02 in 0.1 M KNO_3 at 25.0°C.

These constants were then used to calculate the concentrations of H^+ and OH^- from the measured pH values.

Dissociation constants of the ligands

The dissociation constants are defined by the general equation (the charge is omitted): $H_nL \rightleftharpoons H^+ + H_{n-1}L$. The maximum value of n was 4, 5 and 6 for EDTA, DTPA and TTHA, respectively; K_1 represented the dissociation of the last proton. The constants were calculated by a procedure similar to that used for the complex constants (see below). The two basic equations accounted for the total amounts of ligand and hydrogen ions, respectively. The calculations covered the pH region 3—11.

Hydrolysis constants of uranyl ions

The constants are defined according to the general equation:

$$mUO_2^{2+} + nH_2O \rightleftharpoons (UO_2)_m\,(OH)_n^{2m-n} + nH^+$$

The constants were calculated by a procedure similar to that used for the complex constants. The two basic equations accounted for the total amounts of uranyl and hydroxide ions, respectively. The calculations covered the pH region 3—5; at higher pH values, precipitation signalled the formation of poorly soluble species.

Determination of the complex constants

The following complexes were considered: M_2H_2L, M_2HL, M_2L, M_2OHL, $M_2(OH)_2L$, MH_4L, MH_3L, MH_2L, MHL, ML, MOHL and $M(OH)_2L$ (where M represents UO_2^{2+} and the charges are omitted). In addition, various complexes involving more than one ligand molecule per species were considered, but no such complexes were found.

The formation constants of the complexes were defined according to the equations:

$$aM + H_bL \rightleftharpoons M_aH_bL \text{ and } aM + cOH + L \rightleftharpoons M_a(OH)_cL$$

where a and c can have the values 1 or 2, and b may be 4, 3, 2, 1 or 0 (2, 1 or 0 for the binuclear species).

Titration curves were recorded for (2 + 1), (1.5 + 1) and (1 + 1) mixtures of uranyl and the ligand. The concentration of the ligand was usually ca. 5×10^{-4} M. A total of eight curves were recorded for each mixture and each ligand. Normally, the mean pH values obtained from the eight curves were used in the calculations, which covered the pH region 3—7; at higher pH values, precipitation signalled the formation of poorly soluble species.

For each pH value, a theoretical value of a, the number of moles of alkali added per mole of ligand, was calculated. The calculations were based on three equations, which accounted for the total amounts of metal, ligand and hydrogen ions, respectively [6, 7]. Approximate values were introduced for the complex constants, and a_{cal} was calculated numerically. The initial set of constants was refined by an iterative process, which involved a systematic variation of the complex constants, until the minimum in the equation

$$D = \sum_{i=1}^{n} [a_{cal}(i) - a_{exp}(i)]^2 \qquad (1)$$

was found. Alternatively, the method of least squares [6, 7] was employed; in both cases one constant was treated at a time.

The calculation of the formation constants was started by considering only the most likely species. Then additional complexes were introduced, one at a time. Only those complexes which did decrease the quadratic expression D (Eqn. 1) or contributed significantly to a better fit between the experimental and calculated titration curves within a given pH region, were finally accepted. In these calculations, the hydrolysis constants of the uranyl ion and the dissociation constants of the ligand were kept constant.

RESULTS AND DISCUSSION

Dissociation constants of EDTA, DTPA and TTHA

The dissociation constants calculated in this work for the three polyaminopolycarboxylic acids are given in Table 1; K_1 represents the dissociation of the last proton. The values agree well with those reported by other workers [7—11].

Hydrolysis of uranyl ions

The calculations indicated the presence of a series of polynuclear species: $(UO_2)_2OH^{3+}$, $(UO_2)_2(OH)_2^{2+}$, $(UO_2)_3(OH)_4^{2+}$ and $(UO_2)_3(OH)_5^{+}$. The respective pK values were found to be 4.5 ± 0.6, 5.95 ± 0.04, 12.5 ± 0.2 and 16.54 ± 0.08, in 0.1 M KNO_3 at 25.0°C. The principal species in the pH region 4—5 were $(UO_2)_2(OH)_2^{2+}$ and $(UO_2)_3(OH)_5^{+}$, whereas $(UO_2)_3(OH)_4^{2+}$ was found in minor amounts around pH 5. Precipitation was observed at pH values above 5. The inclusion of $(UO_2)_2OH^{3+}$ improved the theoretical curve at pH values below 4, but the existence of this species is somewhat questionable. The presence of other species, e.g., UO_2OH^{+} and $(UO_2)_2(OH)_3^{+}$, was not confirmed in this study. The values given above agree well with those reported by other workers [8, 12—16] although most of the literature values refer to an ionic strength higher than 0.1.

Uranyl—EDTA complexes

The (1 + 1) titration curve showed an inflexion at a = 1, indicating the complex UO_2HL^{-} (the disodium salt of EDTA was used). The (2 + 1) curve had inflexions at a = 2 and a = 4, corresponding to the complexes $(UO_2)_2L$ and $(UO_2)_2(OH)_2L^{2-}$. Precipitation was observed above pH 7.0. The computer calculations indicated the presence of three dinuclear and two mononuclear complexes, which are shown in Table 2 with their respective formation constants. In the (1 + 1) mixture the main species were UO_2HL^{-} and $(UO_2)_2L$ below pH 6, and $UO_2OH{\cdot}HL^{2-}$ (or UO_2L^{2-}) and $(UO_2)_2(OH)_2L^{2-}$ above pH 6. In the (2 + 1) mixture the $(UO_2)_2L$ species predominated below pH 6, while $(UO_2)_2(OH)_2L^{2-}$ was the principal species above pH 6. The formation constants of $(UO_2)_2L$, UO_2HL^{-} and UO_2L^{2-} agree reasonably well with those reported by other workers [1, 2, 17, 18]. There appear to be no values published for $(UO_2)_2OHL^{-}$ and $(UO_2)_2(OH)_2L^{2-}$.

TABLE 1

Dissociation constants of EDTA, DTPA and TTHA in 0.1 M KNO_3 at 25.0°C

	pK_6	pK_5	pK_4	pK_3	pK_2	pK_1
EDTA	—	—	—[a]	2.64 ± 0.02	6.14 ± 0.02	10.26 ± 0.02
DTPA	—	1.8 ± 0.1	2.62 ± 0.03	4.32 ± 0.02	8.51 ± 0.03	10.40 ± 0.04
TTHA	2.43 ± 0.04	2.73 ± 0.03	4.08 ± 0.02	6.10 ± 0.03	9.42 ± 0.03	10.55 ± 0.05

[a]Constant not determined.

TABLE 2

Log K values for UO_2^{2+} complexes of EDTA, DTPA and TTHA in 0.1 M KNO_3 at 25.0°C

Formula[a]	EDTA	DTPA	TTHA
$(UO_2)_2H_2L$	—	—	11.8 ± 0.2
$(UO_2)_2HL$	—	13.4 ± 0.3	17.4 ± 0.3
$(UO_2)_2L$	17.8 ± 0.3	19.0 ± 0.4	—
$(UO_2)_2OH \cdot HL$[b]	—	—	22.4 ± 0.3
$(UO_2)_2OHL$	26.2 ± 0.3	27.3 ± 0.5	—
$(UO_2)_2(OH)_2HL$[b]	—	—	30.4 ± 0.3
$(UO_2)_2(OH)_2L$	34.4 ± 0.4	35.1 ± 0.4	—
UO_2H_4L	—	—	4.4 ± 0.4
UO_2H_3L	—	—	5.5 ± 0.1
UO_2H_2L	—	4.8 ± 0.3	7.6 ± 0.1
UO_2HL	6.9 ± 0.3	8.8 ± 0.2	—
$UO_2OH \cdot HL$[b]	11.4 ± 0.3	—	—

[a]The charge is omitted. [b]Probable formula, see text.

Uranyl—DTPA complexes

The (1 + 1) and (2 + 1) titration curves both showed a slight inflexion at $a = 4$, and in addition the curves had inflexions at $a = 5$ and $a = 7$, respectively. Precipitation occurred above pH 7.5. The calculations indicated the presence of four dinuclear and two mononuclear complexes, which are shown in Table 2 with their respective formation constants. At pH values below 4 the complex $UO_2H_2L^-$ predominated and at pH values above 6 the principal species was $(UO_2)_2(OH)_2L^{3-}$. In the intermediate pH region, UO_2HL^{2-} was the main species in the (1 + 1) mixture, whereas in the (2 + 1) mixture $(UO_2)_2HL$, $(UO_2)_2L^-$ and $(UO_2)_2OHL^{2-}$ each predominated in a certain part of the pH range. These results are somewhat at variance with previous polarographic and spectrophotometric evidence, which indicated the predominance of a dinuclear complex below pH 6, and a mononuclear complex at higher pH values [19—21].

Uranyl—TTHA complexes

For the titrations, a ligand concentration of 2.5×10^{-4} M was chosen because precipitation was observed even in acidic solution at higher TTHA concentrations. The (1 + 1) curve showed an inflexion at $a = 4$, and the (2 + 1) curve had a slight inflexion at $a = 5$, and a more pronounced inflexion at $a = 7$. Precipitation occurred above pH 7.5. The calculations indicated the presence of four dinuclear and three mononuclear complexes, which are shown in Table 2 with their respective formation constants. At pH values below 4 the complex $UO_2H_3L^-$ predominated, and at pH values above 6 the principal species was $(UO_2)_2(OH)_2HL^{3-}$ (or $(UO_2)_2OHL^{3-}$). In the intermediate pH range, $UO_2H_2L^{2-}$ predominated in the (1 + 1) mixture, whereas $(UO_2)_2HL^-$ was the main complex in the (2 + 1) mixture. The existence of

$(UO_2)_2H_2L$ and UO_2H_4L is somewhat questionable. They were only found in minor amounts, and introduced separately they did not improve the value of D significantly (Eqn. 1). However, in combination they improved the D value and the agreement between the experimental and theoretical curves below pH 4.

Structure of the complexes

The relative concentrations of the mono- and di-nuclear species indicate that the complex formation of uranyl ions with polyaminopolycarboxylic acids is somewhat different from that of most other metals. For uranyl, the tendency to form dinuclear complexes decreases in the sequence EDTA > DTPA > TTHA, the predominance of the dinuclear complexes over mononuclear species is more pronounced in alkaline solution than in acidic solution, and the number of dinuclear complexes is greater than the number of mononuclear complexes. For most metals precisely the opposite trends are observed, suggesting that certain characteristics of the uranyl ion may be responsible for the unusual behavior. The most likely cause is the steric hindrance from the O—U—O axis, which forces the ligands to coordinate only equatorially, in a maximum of four positions. This results in a decreased stability of the mononuclear complexes, while the formation of the dinuclear complexes is favored. To achieve four-coordination, one aminodicarboxyl group may coordinate a uranyl ion in three positions, while the fourth position in the equatorial plane is occupied by water, or by a hydroxide ion, or by one of the other carboxyl groups of the ligand. The protolytic equilibria of the ligand are probably not much affected, unless the respective groups are directly engaged in coordination of the uranyl ion.

In the mononuclear EDTA complex UO_2HL^-, only one aminodicarboxyl group can be expected to coordinate the uranyl ion, owing to the relatively small size of the EDTA molecule. This leaves one position in the equatorial plane of the uranyl ion for coordination of water. The dissociation of a proton from this water molecule leads to the formation of the complex $UO_2OH \cdot HL^{2-}$ [1, 2]. This reaction, which takes place above pH 5, is more likely than the dissociation of the last proton, on account of the high pK_1 value of EDTA.

For the mononuclear complexes of DTPA, complete four-coordination involving both ends of the ligand molecule is possible on account of its greater size, compared to EDTA. This should improve the stability of the mononuclear complexes, as was also observed experimentally. Further, this structure prevents the formation of mononuclear hydroxo species. The transition from $UO_2H_2L^-$ to UO_2HL^{2-} predominance occurred at pH 4.6, indicating that this corresponded to the dissociation of the K_3 proton of DTPA.

The coordination of the mononuclear complexes of TTHA is probably similar to that of DTPA. Four-coordination of the uranyl ion can be achieved by engaging both ends of the TTHA molecule. The transition from $UO_2H_3L^-$ to $UO_2H_2L^{2-}$ predominance occurred at pH 4.2, indicating that the K_4 proton of the ligand was involved in the process.

In the dinuclear complexes, the two uranyl ions are probably coordinated by the end aminodicarboxyl groups of each ligand, leaving one position per uranyl ion for coordination of water. The species may therefore be written as $(UO_2 \cdot H_2O)_2H_bL$ rather than $(UO_2)_2H_bL$ (where b is 0, 1 or 2). When the pH is increased, the dissociation of protons from the coordinated water molecules results in the formation of mono- and di-hydroxo complexes. Further, polymeric species may be formed through the formation of hydroxo bridges, as discussed by Frausto da Silva and Simoes [2] and Åberg [22].

For EDTA no protonated dinuclear complex is expected. For DTPA the transition from $(UO_2)_2HL$ to $(UO_2)_2L^-$ predominance occurred at pH 4.7, indicating that this reaction corresponded to the dissociation of the K_3 proton of DTPA. For TTHA the transition from $(UO_2)_2H_2L$ to $(UO_2)_2HL^-$ occurred at pH 3.7, which indicated that the K_4 proton of TTHA was involved. At higher pH values the formation of mono- and di-hydroxo complexes appears much more likely than the dissociation of the last proton of TTHA, leading to the complexes $(UO_2)_2OH \cdot HL^{2-}$ and $(UO_2)_2(OH)_2 \cdot HL^{3-}$.

Uncertainty of the constants

The uncertainties in the different complex constants are given in Table 2. These values were calculated in the following way. After a final set of constants had been established, the value of each experimental parameter was increased, one by one, by an amount equal to its estimated uncertainty, and the corresponding new sets of constants were calculated. For each complex the changes in the $\log K$ value for all parameters were squared, added, and the square root of this sum was finally taken as a measure of the total uncertainty in that particular $\log K$ value.

The results are shown in Table 3, for two complexes of each ligand. Of the twelve parameters studied, only the ligand dissociation constants gave $\Delta \log K$ values which varied significantly from one complex to another; here the values were within the range 0.09—0.18 for EDTA, 0.02—0.22 for DTPA and 0.02—0.16 for TTHA.

The uncertainties in the experimental parameters were estimated in different ways, depending on the parameter in question. For the concentrations of titrant, ligand and uranyl ions, the values used were 0.2, 0.3 and 0.3%, respectively. For the activity coefficient of H^+, the ionic product of water, the hydrolysis constants of uranyl and the dissociation constants of the ligands, the uncertainties given in the respective paragraphs in this text were used. The kinetic effects were estimated by comparing the constants obtained from normal titration curves with those obtained from reverse titrations with acid. Dilution effects were similarly estimated from titration curves with decreasing concentrations of reactants. The uncertainty in calculating the minimum in D (Eqn. 1) was linked to a 0.1% change in D. The determinate error in pH, which depends on the liquid junction potential of the reference electrode, was assumed to be 0.01 pH unit. Finally, the indeterminate errors of the titrations were estimated from the highest and lowest pH values observed for each a value.

TABLE 3

Estimates of the uncertainty in the formation constants for $(UO_2)_2L$ (I) and $(UO_2)_2OHL$ (II)[a]

Experimental parameter	Change in log K					
	EDTA		DTPA		TTHA	
	I	II	I	II	I	II
Titrant concentration	0	0.01	0.01	0.01	0.01	0.03
Ligand concentration	0	0	0.02	0.03	0.01	0.02
Uranyl concentration	0	0.01	0	0	0	0
Activity coefficient of H^+	0.08	0.08	0.08	0.10	0.03	0.03
Ionic product of water	0.01	0.04	0	0.05	0.02	0.03
Hydrolysis constants of uranyl	0	0	0.01	0.01	0	0
Dissociation constants of ligand	0.11	0.09	0.22	0.22	0.02	0.02
Kinetic effects	0.07	0.09	0.07	0.09	0.07	0.08
Dilution effects	0.02	0.04	—	—	—	—
Calculation of minimum in D	0.01	0	0.04	0.05	0.15	0.15
pH, determinate error	0.26	0.28	0.27	0.36	0.20	0.20
Indeterminate errors	0.02	0.04	0.05	0.06	0.01	0.02
Total uncertainty	0.30	0.32	0.36	0.45	0.26	0.27

[a]For TTHA, the formulae are $(UO_2)_2OH \cdot HL$ and $(UO_2)_2(OH)_2 \cdot HL$.

From Table 3 it can be seen that the determinate error of the pH measurement contributes the most to the uncertainty in the K values. The influence of the mathematical uncertainty in D increases from EDTA to TTHA, because the total number of complex species increases. The values for indeterminate errors shown in Table 3 correspond to the uncertainty normally obtained by the method of least squares. Obviously, the indeterminate errors account for only a small part of the total uncertainty in the K values. The latter values probably represent more realistic estimates of the true uncertainty in the complex constants.

We thank Professor E. Jacobsen, University of Oslo, for initiating the present investigation.

REFERENCES

1 T. R. Bhat and M. Krishnamurthy, J. Inorg. Nucl. Chem., 26 (1964) 587.
2 J. J. R. Frausto da Silva and M. L. S. Simoes, Talanta, 15 (1968) 609.
3 A. I. Vogel, Quantitative Inorganic Analysis, 2nd edn., Longmans, London, 1951, p. 470.
4 C. Duval, Inorganic Thermogravimetric Analysis, Elsevier, Amsterdam, 1953, p. 502.
5 P. A. Overvoll and W. Lund, Anal. Chim. Acta, 102 (1978) 211.
6 W. Lund, Anal. Chim. Acta, 45 (1969) 109.
7 W. Lund, Anal. Chim. Acta, 53 (1971) 295.

8 L. G. Sillén and A. E. Martell, Stability Constants of Metal—Ion Complexes, Spec. Publ. No. 17, The Chemical Society, London, 1964; Suppl. No. 1, Spec. Publ. No. 25, 1971.
9 G. Schwarzenbach and H. Ackermann, Helv. Chim. Acta, 30 (1947) 1798.
10 A. E. Frost, Nature, 178 (1956) 322.
11 T. A. Bohigian and A. E. Martell, Inorg. Chem., 4 (1965) 1264.
12 C. F. Baes, Jr. and N. J. Meyer, Inorg. Chem., 1 (1962) 780.
13 R. M. Rush, J. S. Johnson and K. A. Kraus, Inorg. Chem., 1 (1962) 378.
14 R. M. Rush and J. S. Johnson, J. Phys. Chem., 67 (1963) 821.
15 H. S. Dunsmore, S. Hietanen and L. G. Sillén, Acta Chem. Scand., 17 (1963) 2644.
16 C. F. Baes, Jr. and R. E. Mesmer, The Hydrolysis of Cations, Wiley, New York, 1976, p. 174.
17 A. G. Kozlov and N. N. Krot, Russ. J. Inorg. Chem., 5 (1960) 954.
18 J. Starý and J. Prášilová, J. Inorg. Nucl. Chem., 17 (1961) 361.
19 T. T. Lai and C. S. Wen, J. Electrochem. Soc., 117 (1970) 1122.
20 E. Jacobsen, G. O. Kalland and O. Lykkjen, Anal. Chim. Acta, 58 (1972) 193.
21 K. K. Kamble, V. S. Jatkar, S. S. Tamhankar, G. D. Shahapure and V. Damodaran, J. Inorg. Nucl. Chem., 42 (1980) 1067.
22 M. Åberg, Acta Chem. Scand., 24 (1970) 2901.

Analytica Chimica Acta, 143 (1982) 163—176
Elsevier Scientific Publishing Company, Amsterdam — Printed in The Netherlands

SOME ASPECTS OF THE SCOPE AND LIMITATIONS OF DERIVATIVE SPECTROSCOPY

TREVOR R. GRIFFITHS*, KEITH KING and HUGH V. St. A. HUBBARD

Department of Inorganic and Structural Chemistry, The University, Leeds LS2 9JT (Gt. Britain)

MARIE-JOSÉ SCHWING-WEILL and JEAN MEULLEMEESTRE

Laboratoire de Chimie-Physique, E.R.A. 166, E.N.S.C.S., Université Louis Pasteur, 67000 Strasbourg (France)

(Received 7th April 1982)

SUMMARY

Synthesised spectra are used to illustrate discussion of some relationships between recorded absorption profiles and their second and fourth derivative spectra. Limitations arising from the fortuitous overlap of a derivative peak with a neighbouring wing, and the possibilities of resolving spectra into their overlapping bands are also considered. The combined use of second and fourth derivative spectra to ascertain the correct number of bands within an observed profile is described. It is suggested that the practice of computing a least-squares fit of overlapping bands to a spectral profile be changed, because the minimisation achieved often produces a result involving excessive or negative absorbances: the spectral profile should be regarded as a boundary limit and any unaccounted (positive) absorbance then assessed as possible evidence for an additional band. An example is given, concerning the resolution of the spectrum of a thin, single crystal of uranium(IV) oxide at 77 K superimposed on an absorption edge. A comparison of the difference between the observed spectrum and the sum of its resolution into twelve overlapping bands, plus a similar comparison of their fourth derivative spectra, reveals a thirteenth band.

The initial proposal that derivative methods could be applied with advantage to experimental data was made by Sir Ernest Rutherford, who suggested [1] that the sensitivity of mass spectroscopy would be increased on applying the first derivative technique. Derivative data are now utilised in most spectroscopic techniques as well as in gas chromatography and polarography. Derivative methods were first applied to u.v.—visible and infrared spectroscopy in 1953 [2—4], but at that time only a few workers became interested [5—7]. The deconvolution of absorption spectra by least-squares fitting was introduced in 1960 [8], but it was another decade before derivative spectroscopy became widely used. Butler and Hopkins [9] calculated up to the fourth derivative spectra of photosynthetic processes, and Green and O'Haver [10] determined the fundamental features of the derivative method in luminescence spectroscopy and other areas. Since then derivative techniques have been widely applied: a representative list is given in a review by Talsky

0003-2670/82/0000-0000/$02.75

et al. [11]. Derivative techniques have not been without their problems; in early work, the main problem was in the direct encoding of data via mechanical devices. Many recent instruments are computer-compatible and are often supplied with a microprocessor, permitting the direct presentation of first, second or higher derivative spectra.

Several applications in u.v.—visible and infrared spectroscopy have been developed recently for the assay of polynuclear aromatic hydrocarbons and other pollutants [12, 13], drugs [14], biological materials [15, 16] and plastics [17]. These methods illustrate in a general fashion various features of the derivative technique, including enhanced information content, discrimination against background noise and greater selectivity in quantitative analysis. The analytical procedures are self-consistent and reasonably accurate, provided that a suitable calibration process is employed.

The approach made in earlier papers from this laboratory [18—23] has been to conduct fundamental and developmental studies, which are absolute, rather than relative. The second derivative plot of, say, an absorption spectrum can be obtained mathematically in numerous ways and not all derivative spectra so obtained are identical. Also, when a spectrum is deconvoluted into its constituent bands, different computer programs do not produce identical resolutions. Even recent commercial spectrophotometers offer the user little opportunity to vary the mathematical parameters involved in calculating a derivative spectrum, and hence to check whether an observed feature is real, or an artefact of the program being used and the profile under examination. This paper examines how derivative spectra may best be obtained and interpreted, and the limitations that apply. Finally, consideration is given to how a complicated spectrum may be unambiguously deconvoluted by the combined use of derivative spectra and computer resolution techniques.

GENERAL CONSIDERATIONS

Derivative spectroscopy is an excellent way of determining the number of peaks within a profile and also their positions, because even-order derivative spectra narrow the band widths of the composite bands, and increase the relative contributions of minor bands. Several authors have noted that, when synthesised spectral profiles are differentiated, the component peak maxima thereby determined are displaced from the original positions [24—26]. Allen and McMeeking [26], for example, differentiated and deconvoluted composite curves of two equal Gaussian functions, and also considered the case where one band was double the intensity of the other. (However, they did not differentiate their very different experimental profile, the reflectance spectrum of $Ag(II)SnF_6$, which would probably have simplified the deconvolution problems.)

The present work is mainly concerned with second and fourth derivative spectra, because they are the most useful, displaying bands as minima and

maxima, respectively. It is again apparent that the peak positions obtained in this way are not necessarily the true positions; in even-order derivative spectra overlap of a lobe of the derivative of one band into the region of the main component of an adjacent band may lead to a marked shift from the true position of this contiguous band. Further, as the even order of the differential spectra increases, the magnitude of the positive and negative components in the wings of each differentiated component band increases. The increase may be such that it cancels out the peak of a neighbouring band.

The present calculations provide insight into the magnitudes of these effects, because the derivative of a profile is equivalent to the sum of the derivatives of its component bands. Thus the differences between band maxima determined from derivative spectra and those of the original component bands may be appreciated, as well as the reasons why an expected maximum (or minimum) in a derivative curve is not found. Unfortunately, it is not possible to derive a general relationship, because each combination of bands and the extent of their overlap will be unique, but selected examples will indicate the principles and the pitfalls. The second and fourth derivatives of a synthesised spectrum of two Gaussian bands, and their precision in locating the band maxima from the summed profile are discussed, and the approach is extended to more realistic systems. The calculations are limited to Gaussian bands, but the principles are equally applicable to any smooth band.

OVERLAPPING GAUSSIAN BANDS

The standard Gaussian function is $y = y_o \exp(-\ln 2[2(x - x_o)/\Delta x]^2)$, where y_o is the band height at its maximum x_o, and Δx is the band width at half-height. A "standard" Gaussian equation is obtained when $y_o = 1, x_o = 0$, and $\Delta x = 2(\ln 2)^{1/2} = 1.665$, i.e., $y = \exp(-x^2)$. The derivatives are $dy/dx = 2xy$; $d^2y/dx^2 = 4x^2y - 2y$; $d^3y/dy^3 = 12xy - 8x^3y$; and $d^4y/dx^4 = 12y - 48x^2y + 16x^4y$.

For the other Gaussian bands, the situations when height, half-width and position are varied are examined relative to the standard Gaussian band.

Case 1: Overlap of two identical Gaussian bands

Allen and McMeeking [26] have discussed the use of the second derivative method to estimate the positions of component bands for Gaussian and Lorentzian doublets. Here, the fourth derivative, determined by using a programmable calculator (Texas Instruments TI58) is considered. The peak maximum of the standard Gaussian, band A, is separated from that of band B by p. The derivatives were calculated for each band for various values of p and summed to produce the envelope of the pair. The observed peak positions were obtained, and compared with the true positions. Here the summed spectra were symmetrical and hence the shift was the same for each band.

As p varies, the observed maxima can shift inwards or outwards, as already noted with second derivative spectra [26]. The convention adopted is that shifts towards the centre of gravity of the pair are designated negative. It is also useful to discuss the shifts and separations in terms of the half-widths (Δx) as well as x units; the relationship for this example is $\Delta x = 1.665x$. Thus when distances are quoted in x units they will be followed, in parentheses, by the equivalent value in half-width units.

Some typical plots of the summed fourth derivatives are shown in Fig. 1, which shows that for a separation of 3 x units (1.8 half-widths) the shift is small, 0.007 (0.004). As p decreases, the shift increases to a small negative maximum of —0.017 (—0.010) at $p = 2.4$, reverses direction to become zero at 2.03 (1.22), and exhibits a positive maximum of 0.123 (0.074) at 1.2 (0.72). Further reduction in band separation leads to another zero shift at 0.97 (0.54), and at the resolution limit the shift is —0.28 (—0.17). This limiting value is the point at which the saddle in the summation of the two bands just disappears, and it is identified precisely by the numerical process at 0.88 (0.53). It was expected that the displacement of observed peak position from true peak position would be proportional to the fifth derivative of the underlying tail, because the shift will depend on the slope of the added curve, and this is so, as the plot of d^5y/dx^5 in Fig. 1 shows.

The above account follows the general observations made for second derivative spectra [26], but more detailed calculations done here (Fig. 2) show that the shifts again follow the slope of the underlying tail (here the third

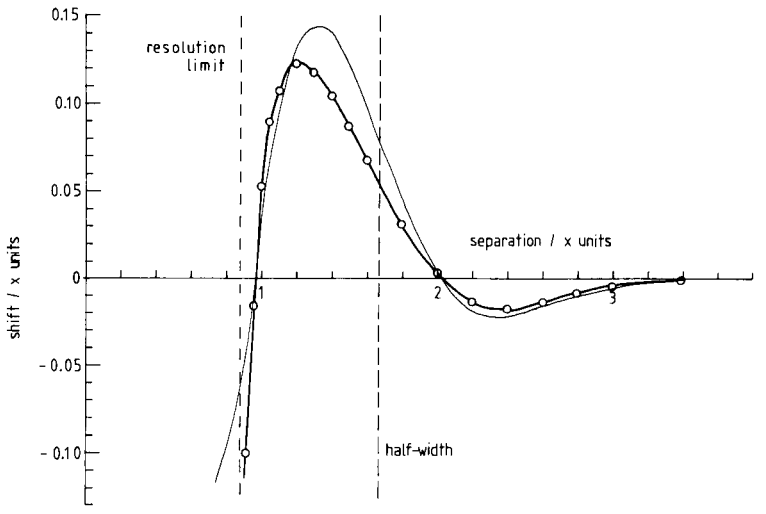

Fig. 1. Variation of the shift from the true peak position of the calculated peak position obtained from the fourth derivative as a function of the true peak maxima separation, for a pair of identical Gaussian bands. (○) Shift; the thinner line indicates the fifth derivative (appropriate scale).

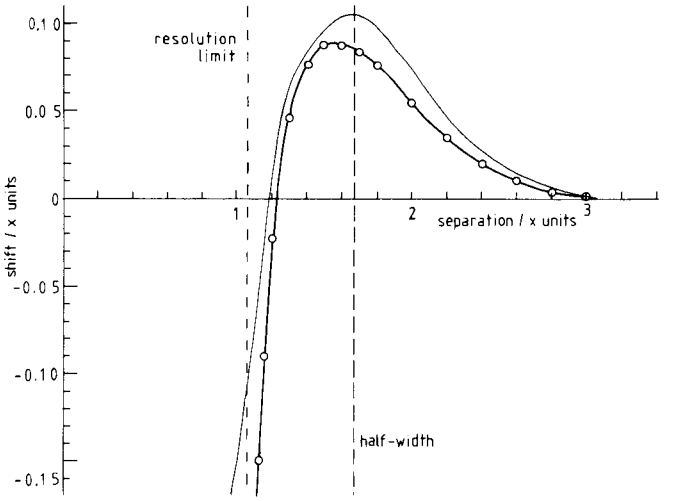

Fig. 2. Variation of the shift from the true peak position of the calculated peak position obtained from the second derivative as a function of the true peak maxima separation, for a pair of identical Gaussian bands. (○) Shift; the thinner line indicates the third derivative (appropriate scale).

differential), and a similar pattern as p is reduced. The resolution limit of 1.05 (0.63) is now not as small as that for the fourth derivative.

Case 2: Overlap of two non-equivalent Gaussian bands

Although the resultant profile from the summation of Gaussian bands of unequal heights and widths as a function of peak separation, and its resolution, have been investigated [25, 26], detailed studies on the derivative spectra of such systems have not been made. Here, the system with band A, $y \exp(-x^2)$, and band B having half the height and half the width of A, was investigated at various separations p.

Most obvious is that the originally bigger band A is swamped by the now larger band B when the second or fourth derivatives are summed (Fig. 3). This arises from the inverse dependence of derivative peak heights (y_o) on band width at half-height (Δx): it may readily be shown that $(d^2y/dx^2)_{x=x_o}$ is proportional to $-y_o/(\Delta x)^2$ and $(d^4y/dx^4)_{x=x_o}$ to $y_o/(\Delta x)^4$.

For this example, separations are again expressed in x units, but now a mean half-width of the two bands, Δx, must be used, the relationship being $\Delta x = 1.248x$. For the second derivative (Fig. 3a) at separations less than 1.2 (0.96), the peak observed near band A is due to the tail of the second derivative of band B, because the apparent shift becomes linear. The shift observed for band B is not spurious, and reaches −0.037 (−0.03) at a peak separation of approximately 0.4 (0.32). Similar behaviour was observed with the fourth derivative (Fig. 3b): with separations of 1.55 (1.24) or less, the variation of the shift with p also became linear. The shift of band B reached

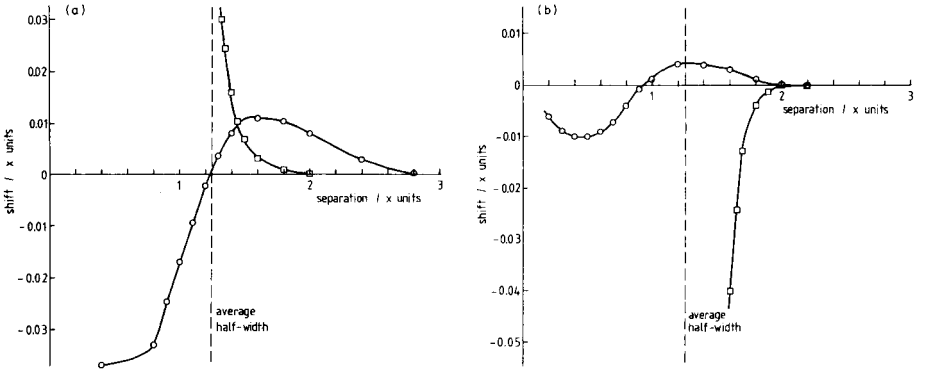

Fig. 3. Variation of the shift from the true peak positions of the calculated peak positions obtained from the second and fourth derivatives as a function of the true peak maxima separation, for a pair of non-equivalent Gaussians. In the original spectrum band B is half the height and half the width of band A. (a) Second derivative; (b) fourth derivative. (□) Shift of band A; (○) shift of band B.

its maximum positive value, 0.004 (0.0032), at a separation of 1.3 (1.04), and the maximum negative value of —0.01 (—0.008) is at a separation of 0.5 (0.4).

Vandeginste and de Galan [25] have derived expressions for the theoretical limit of the resolution of a pair of unequal Gaussian or Lorentzian bands, from their first three derivatives. They defined a shoulder limit as that separation between the two peaks for which the minimum between them just disappears (cf. Westerberg [27]): this occurs when the inner inflection point of the smaller band coincides with the disappearing minimum, i.e., $dy/dx = d^2y/dx^2 = 0$. This is illustrated in Fig. 4 for a pair of Gaussian bands having the same half-width, but with band B twice the height of A. As the bands are brought closer than the shoulder limit separation, the first derivative fails to intersect the zero axis at a point between them.

Using the second and third derivatives, Vandeginste and de Galan also defined a detection limit, when the separation between the bands is such that the inflection points defining a visually detectable peak just merge into the same point, i.e., the condition $d^2y/dx^2 = d^3y/dx^3 = 0$. The pair of Gaussian bands is shown at the detection limit separation in Fig. 5. A further reduction in p would result in the second derivative (as opposed to the first for the shoulder limit) failing to cut the zero axis between the bands. This principle may be extended to any nth and $(n + 1)$th derivative pair [28]. Hence for $n = 3$, $d^3y/dx^3 = d^4y/dx^4 = 0$. This may be regarded as the shoulder limit on the second derivative, i.e., the maximum just disappears between the two (inverted) peaks of the second differential. Similarly, for $n = 4$, their suggested detection limit is available on the second derivative. Vanderginste and de Galan [25] considered that no resolution is possible if the second derivative does not intersect the zero axis between the bands. In practice,

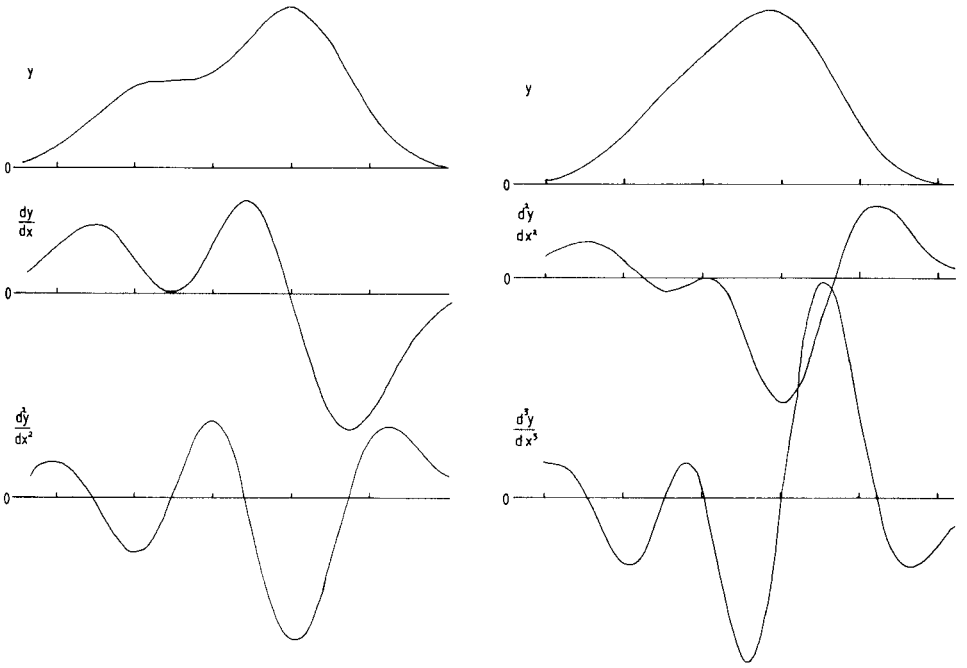

Fig. 4. Envelope and first two derivatives for a pair of Gaussian bands at the shoulder limit. The original bands have identical half-widths, but one is half the height of the other.

Fig. 5. Envelope, second and third derivatives for a pair of Gaussian bands at the resolution limit. The original bands have identical half-widths, but one is half the height of the other.

this is not so: in Fig. 5, it is still possible to identify two bands from the second derivative as long as there is a maximum between them. This is, of course, the above shoulder limit on the second derivative, and it is not necessary to resort to determining the fourth derivative in order to prove that the original spectrum consists of just two bands.

Case 3: Effect of differentiating four overlapping bands

The profile chosen as example is typical of many u.v. and visible spectra (Fig. 6a). It is necessary to establish if three or four bands are present. Two peaks and a shoulder are obvious, but the asymmetry of the main band around $x = 1$ may be due to a fourth band. Initial reaction to this profile (Fig. 6a) would be to place two strong bands close to the two observed peaks, and a third small band under the shoulder, and then to bring in a fourth small band between the two main bands if the asymmetry was not satisfied by slight variations in the mixing of the three bands. However, the profile comprises four Gaussian bands, two of which (A and D) are identical (Fig. 6b). That the main band B is not located close to the main band in the profile, and the other resolved band is due to the smallest band is certainly surprising.

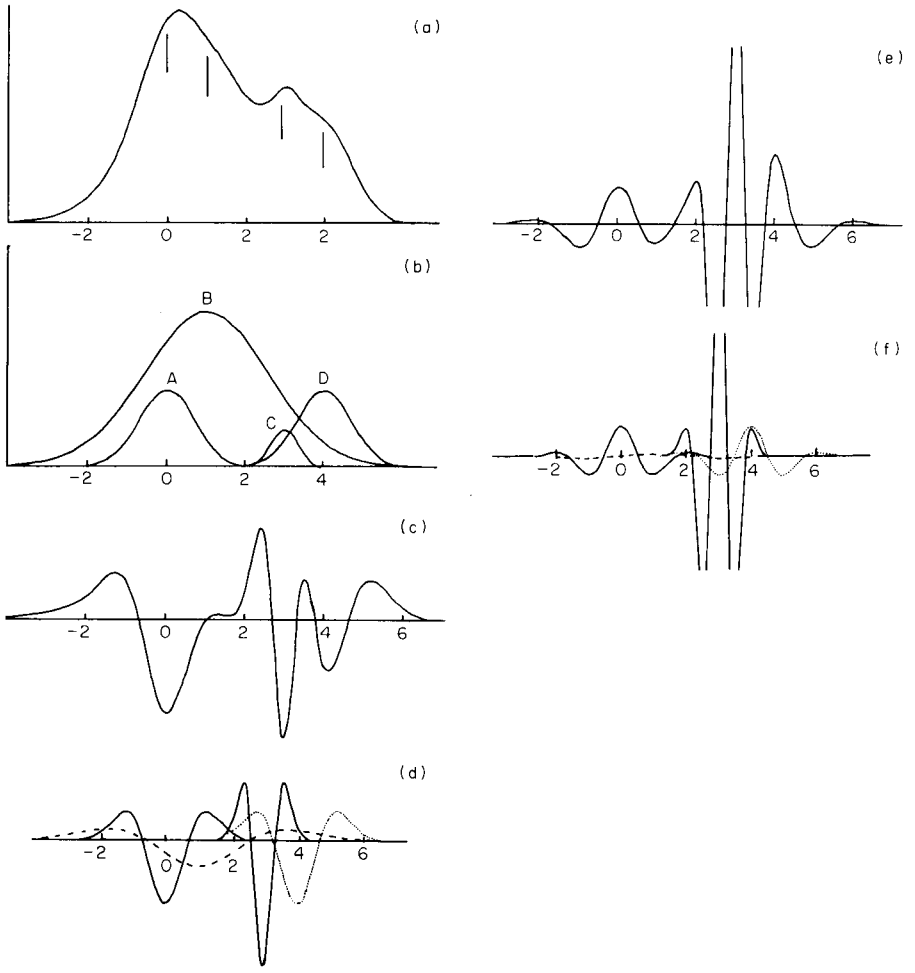

Fig. 6. (a) Profile of the sum of four Gaussian bands; vertical lines show the positions of the individual band maxima at 0, 1, 3 and 4. (b) The four individual Gaussian bands; the bands with maxima at 0 and 4 are half the height and half the half-width of the band at 1, and twice the height and half-width of the band at 3. (c) Second derivative of (a). (d) Second derivative of (b) for the separate bands. (e) Fourth derivative of (a). (f) Fourth derivative of (b).

The equations of the bands are: $y = \exp(-x^2)$ (A); $y = 2\exp[-0.2(x-1)^2]$ (B); $y = 0.5\exp[-4(x-3)^2]$ (C); and $y = \exp[-(x-4)^2]$ (D). The peak maxima are, respectively, at $x = 0$, 1, 3 and 4, and their heights at $y = 1, 2, 0.5$ and 1.

Figure 6(c) shows the second derivative of the profile in Fig. 6(a). There are three minima, corresponding to, but not identical with, the maxima at $x = 0$, 3 and 4. A shoulder around $x = 1.7$ shows the presence of the fourth band. Figure 6(d) shows the second derivative of each of the four individual

bands, and the missing maximum may now be explained. The minimum of B is almost exactly cancelled by the positive portion of the wing of A. In the zero-order spectrum, it is smaller and narrower than B, but on differentiating it becomes larger than the derivative of B. The positive portions of the wings of C and D combine to give the shoulder around $x = 1.7$.

Taking the next higher even-order derivative (the fourth) of the profile in Fig. 6(a) does not necessarily clarify or eliminate this difficulty. There are now (Fig. 6e) four clearly resolved maxima, close to $x = 0$, 2, 3 and 4. The small maxima at $x = -2$ and 6 are neglected as obvious wings of main bands. But the maxima at $x = 2$ and 4 must now be questioned. The difference in their heights, and the minimum around $x = 5$, suggest a band at around $x = 4$. Thus only three bands can be identified from the fourth derivative spectrum, the maximum at $x = 2$ perforce being one of the wings of the now intense band C. Of band B there is now no sign, even though it was only double the height and width of bands A and D. Figure 6(f) shows the fourth derivatives of each of the four bands. Obviously, band B has been essentially eliminated upon fourth differentiation, and the maximum of D almost coincides with a wing of C.

While it is true that increasing the order of differentiation sharpens the small maxima in the original spectrum [11], the wings of the bands broaden. The second derivative spectrum of, say, band C (Fig. 6d) has a minimum at the original peak maximum and two positive wings. Its fourth derivative (Fig. 6f) has a maximum at the original peak maximum, two negative wings, and two positive wings. Thus although the maxima and minima of the wings are at x values of 2.4 and 3.6 for the second derivative, and 2.5 and 3.5 for the fourth, implying narrowing, the additional maxima of the fourth derivative are at 2.0 and 4.0, and the original band has essentially zero absorbance at these x values. Thus sharpening a band by differentiation does not produce overall narrowing. Further, if two bands overlap originally, as do C and D, then differentiating will reveal their peak maxima to within a few per cent, provided that they are of approximately equal width and intensity, and that they occur under a bigger band. However, the extent of overlap of the wings of their original bands will not be reduced, and care must be taken to avoid concluding the presence of a third (spurious) band between them, seen in fourth and higher-order derivative spectra, and arising from the fortuitous coincidence of the two wing maxima between these two bands.

Some general rules and suggestions

From the above examples, it can be concluded that derivative spectroscopy does not necessarily reveal the number and peak maxima of all the bands within a profile. Commonly, it identifies the presence and position of all bar one of the bands present, the one "lost" being the biggest and broadest band. Its presence, but not always its peak maximum, can usually be determined from derivative spectra of orders less than four.

Obviously, if a profile is to be resolved into its component bands (the mathematical expression that best fits them being known) the correct number of bands within the profile and their approximate peak positions can be determined from a careful study of second and fourth derivative spectra. Band widths and band heights may in principle also be determined from derivative spectra [24], but only for very simple systems. The example above readily shows how cancelling of overlapping peaks and wings can make this information almost impossible to obtain. Thus a resolving computer program can only be given information on the number of bands present, and reasonable estimates of the positions of all except the largest band, but merely crude estimates of their heights and half-widths from derivative spectra: the estimates required for the main band may be obtained from measurements made on the original spectrum. The accuracy with which the computer then fits the bands to the profile depends on a number of parameters. On the above data, there would be little difficulty as there is no noise present in the data. With signal noise, the resolution achieved will depend on the sophistication of the computer program. In the past the practice has been to examine the standard deviation of the fit, and other statistical functions, and compare the sum of the resolved bands with the original profile for "goodness of fit". Experience is then the criterion to confirm that the best possible resolution has been obtained. However, in many published resolutions of spectra, the summation of the resolved bands in certain wavelength regions exceeds the recorded absorbance values, and in other regions the reverse is true. It is sometimes implied that the resolution is "appropriate" or "correct" because the excessive absorbance balances the unaccounted-for negative absorbance, and that this minor mismatch is simply due to the mathematical function used to describe the bands. However, mismatches between observed and calculated profiles could equally be due to the overlooked presence of a small additional band. Accordingly, in resolving spectra, computer programs should be constrained not to exit when the excess and dearth between the observed and computed profiles is a minimum. Instead, no excessive or negative absorbances (above the noise level) should be permitted (because these are known experimentally not to occur). Instead, the deficit absorbance that cannot be accounted for under the experimental profile should be minimised. This will help to identify any overlooked bands. At this point, any necessary or subsequent modifications to the mathematical description of the component bands becomes appropriate.

An alternative approach, which has the merit of not laying stress on prior knowledge of the precise mathematical shapes of the individual bands, is to take the derivatives of the original spectrum and of the resolved bands (determined if possible using the above provisos), and compare the former with the sum of the latter. Poor resolutions and any missing or additional bands will be readily apparent. The power of this approach is illustrated below, in determining the number of bands under the complex spectrum of a thin section of a single crystal of uranium(IV) oxide, and in resolving this spectrum into its composite bands.

Differentiating and smoothing recorded spectra

The spectrum examined is shown in Fig. 7(a) and was digitised at 0.5-nm intervals. Differentiation was done by using the method of Savitsky and Golay [29] as amended by Steinier et al. [30] and Anderson [31]. This method can also be used, separately or simultaneously, to smooth the data. Alternatively, instead of using every point, every second, third, etc., point can be taken; this may be termed a stepping process. This approach is employed in some modern spectrophotometers. It is inefficient, because it effectively discards small weak bands, and the derivative spectra obtained as the size of the step is increased are not identical. The process does appear to remove some of the noise within the derivative spectrum, but in practice, information within the original profile is concealed: the spectrum must be smoothed before or during the differentiation process. The process of smoothing and differentiating by using convolution coefficients is an exact, least-squares fitted procedure. The improvement in the original signal-to-noise ratio is approximately the square root of the number of data points n used in the calculation. Increasing the size of the step does not affect the signal-to-noise ratio; the apparent smoothing achieved is rather a degradation of the optimum derivative spectrum. Thus if the original data were first properly smoothed, less noisy and more accurate derivative spectra would be obtained using the smallest possible step size.

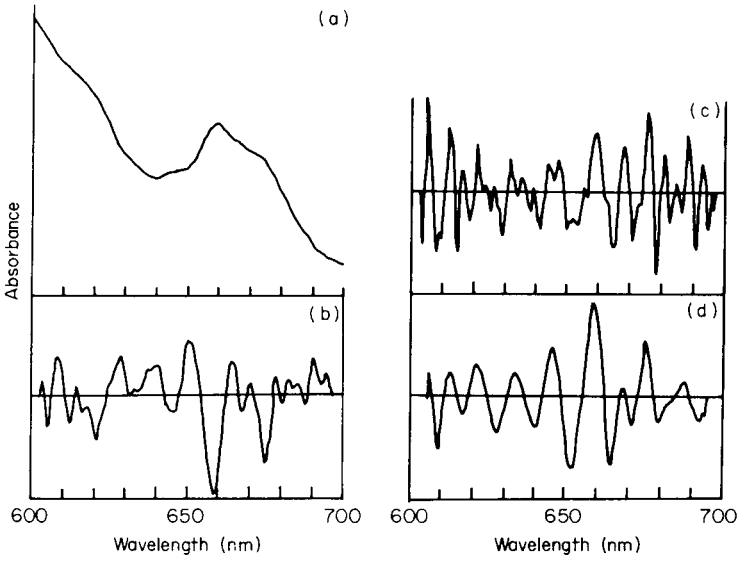

Fig. 7. (a) Absorption spectrum of a thin single crystal of UO_2 at room temperature. (b) Second derivative calculated using a 15-point convolute. (c) Fourth derivative calculated using a 15-point convolute. (d) Fourth derivative calculated using a 25-point convolute.

The need for appropriate mathematical smoothing before or during differentiation is emphasised by the fact that the absorbance of a second derivative minimum is about one hundredth of the corresponding peak in the original spectrum, and for fourth derivative maxima the ratio is about one thousandth. Currently, spectrophotometer options are not sufficiently flexible and do not effect the smoothing needed for reliable fourth derivative spectra.

Determining the optimum parameters

The best combination of the number of convolution coefficients and the order of the fitted polynomial must be determined by experiment, to distinguish genuine small bands from noise. The use of a 15-point quadratic convolute on a 15-point quadratic smooth to determine the second derivative of the spectrum of a section from a uranium(IV) oxide single crystal yields the data in Fig. 7(b) and (c). Both procedures achieve a noise reduction of nearly four, and the combined effect is around a six-fold reduction. There is general correspondence between the minima of the second derivative (Fig. 7b) and the maxima of the fourth derivative (Fig. 7c). Differences between the derivatives are clearly seen, and are greater when fourth derivative spectra are compared. The size of the convolute is thus too small (the extent of smoothing is effectively independent of the order of derivative calculated). For the spectra in this system, the best procedure was found to be smoothing with a 25-point quartic function, differentiating similarly, and using all the data points (a step of unity), (Fig. 7d). Most of the noise has now been removed, and yet the same basic maxima are still identified. These spectra were used to give the number of bands present, and their positions. The remaining parameters required for computer resolution of the spectrum were estimated, and refined as follows.

The programmable calculator was used to calculate the summed profile, and this was compared with the original. It was assumed that there were no underlying broad bands, (none had been identified earlier), and that the only other contribution to the observed absorbance was an exponential edge. This was determined from the absorbance values at 560 and 575 nm on the rapidly rising absorbance, the derivative spectra having shown the absence of small bands in this region. The band parameters were changed one at a time until a reasonable fit between the observed and calculated spectrum was obtained. Most parameters were adjusted no more than three times. These improved estimates were then entered interactively into a modified curve-fitting computer program; the program converged and the resolution shown in Fig. 8 was obtained.

After convergence had been reached by using the 12 bands (B—N) and exponential edge A, the original profile and the sum of the resolved bands were compared. The difference tended to zero, except in the 17 200 cm^{-1} region. The difference was recognisable as a band, as the bands appearing in this region would have been minimised as far as possible to remove this anomaly. The fourth derivative of the original spectrum and of the synthesised

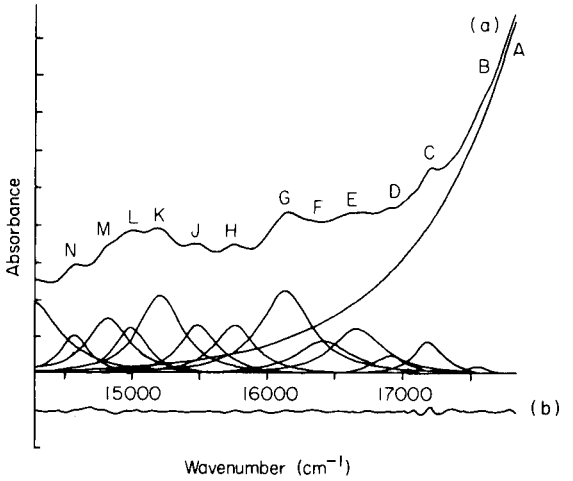

Fig. 8. (a) Absorbance spectrum of a thin single crystal of UO_2 at 77 K and its resolution into 12 Gaussian bands and an exponential edge. (b) Difference between the observed profile and the sum of the resolved bands and absorption edge, using the same absorbance scale.

spectrum were then examined and a marked difference was seen in this region. The band originally labelled D (Fig. 8) did not therefore fully represent this spectral region: the data now suggested that another band was present in this region. Putting the extra band into the computer program produced a very satisfactory resolution and no significant deviations from zero as a function of wavelength between the observed and calculated profiles.

Finally, attention is drawn to two recent reviews on the computer resolution of overlapping electronic absorption bands [32, 33]. Both mention differentiation of spectra, but give little indication of the care necessary in obtaining and interpreting such spectra. A careful study of variously calculated fourth derivative spectra, before any attempt is made to resolve into individual bands, would eliminate many of the problems concerning the determination of the correct number of bands within a profile, and the appropriate mathematical function for the band shape. It is also suggested that curve resolutions should be rejected if the sum of the resolved bands, in any wavelength region, exceeds significantly the measured absorbance.

We thank the North Atlantic Treaty Organisation for a Research Grant (No. 1974) to T.R.G. and M.-J.S. K.K. thanks the Science and Engineering Research Council for a CASE Studentship Award with the Central Electricity Generating Board (N.E. Region), and H.V.St.A.H. thanks the Council for a CASE Award with the U.K.A.E.A., Harwell (Materials Development Division). The provision by the Council of the Cary 14 H spectrophotometer, and of the digitising apparatus by Harwell (EMR 1913), is gratefully acknowledged. We also thank Dr. P. Gans for valued and helpful discussions.

REFERENCES

1 E. G. Dymond, Proc. Cambridge Philos. Soc., 22 (1923–25) 405.
2 V. J. Hammond and W. C. Price, J. Opt. Soc. Am., 43 (1953) 924.
3 E. Tannenbauer, P. B. Merkel and W. H. Hamill, J. Phys. Chem., 21 (1953) 311.
4 J. D. Morrison, J. Chem. Phys., 21 (1953) 1767.
5 A. T. Giese and C. S. French, Appl. Spectrosc., 9 (1955) 78.
6 G. L. Collier and F. Singleton, J. Appl. Chem., 6 (1956) 495.
7 A. E. Martin, Nature, 180 (1957) 231.
8 T. R. Griffiths and M. C. R. Symons, Trans. Faraday Soc., 56 (1960) 1125.
9 W. L. Butler and D. W. Hopkins, Photochem. Photobiol., 12 (1970) 439, 451.
10 G. L. Green and T. C. O'Haver, Anal. Chem., 46 (1974) 2191; 48 (1976) 312.
11 G. Talsky, L. Mayring and H. Kreuzer, Angew. Chem., Int. Ed. Engl., 17 (1978) 785.
12 A. R. Hawthorne and J. H. Thorngate, Appl. Spectrosc., 33 (1979) 301.
13 J. Reid, B. K. Garside, J. Shewchun, M. El-Sherbiny and E. A. Ballik, Appl. Opt., 17 (1978) 1806.
14 A. F. Fell, Proc. Anal. Div. Chem. Soc., 15 (1978) 260.
15 C. Balestrieri, G. Colonna, A. Giovane, G. Irace and L. Servillo, Eur. J. Biochem., 90 (1978) 433.
16 A. F. Fell, UV Spectrom. Group Bull., 7 (1979) 5.
17 W. Pump and D. Voltjes, Kunststoffe, 69 (1979) 317.
18 T. R. Griffiths and R. H. Wijayanayake, J. Chem. Soc. Faraday Trans. 1, 69 (1973) 1899.
19 J. R. Dickinson, T. R. Griffiths and P. J. Potts, J. Inorg. Nucl. Chem., 37 (1975) 511.
20 T. R. Griffiths and P. J. Potts, J. Inorg. Nucl. Chem., 37 (1975) 521.
21 T. R. Griffiths and R. A. Anderson, Inorg. Nucl. Chem. Lett., 15 (1979) 41; J. Chem. Soc. Chem. Commun., (1979) 61; Inorg. Chem., 18 (1979) 2506.
22 T. R. Griffiths and D. C. Pugh, J. Solution Chem., 8 (1979) 247.
23 T. R. Griffiths and R. A. Anderson, J. Chem. Soc. Faraday Trans. 2, 75 (1979) 957; J. Chem. Soc. Dalton Trans., (1980) 205, 209.
24 J. R. Morrey, Anal. Chem., 40 (1968) 905.
25 G. M. Vandeginste and L. de Galen, Anal. Chem., 47 (1975) 2124.
26 G. C. Allen and R. F. McMeeking, Anal. Chim. Acta, 103 (1978) 73.
27 A. W. Westerberg, Anal. Chem., 41 (1969) 1770.
28 P. Gans, private communication, 1982.
29 A. Savitzky and M. J. E. Golay, Anal. Chem., 36 (1964) 1627.
30 J. Steinier, Y. Termonia and J. Deltour, Anal. Chem., 44 (1972) 1906.
31 R. A. Anderson, Ph. D. Thesis, University of Leeds, 1974.
32 B. E. Barker and M. F. Fox, Chem. Soc. Rev., 9 (1980) 143.
33 W. F. Maddams, Appl. Spectrosc., 34 (1980) 245.

Analytica Chimica Acta, 143 (1982) 177—184
Elsevier Scientific Publishing Company, Amsterdam — Printed in The Netherlands

CATALYTIC-KINETIC ABSORPTIOSTAT TECHNIQUE WITH THE INDIGO CARMINE—HYDROGEN PEROXIDE REACTION AS THE INDICATOR REACTION

HERBERT WEISZ*, SIEGBERT PANTEL and GOTTFRIED MARQUARDT

Institut für Analytische Chemie, Chemisches Laboratorium der Universität, D-7800 Freiburg i.Br. (Federal Republic of Germany)

(Received 28th June 1982)

SUMMARY

The absorptiostat method previously described is used for the catalytic-kinetic determination of sulphur compounds (sulphide, thioacetamide, thiourea and thiosulphate) in the micromolar range by means of their catalytic action for the indigo carmine—hydrogen peroxide indicator reaction. The thiosulphate catalyst is activated by iron(III) or aluminium(III); aluminium(III) is deactivated by fluoride. On this basis, iron(III) is determined in the ng range, and aluminium(III) and fluoride in the μg range.

The principle of Stat methods was first described by Møller [1]; they are classed as open systems and are an important tool for measurements in the so-called initial state. In this region, the indicator reaction, $A + B \overset{K}{\rightleftharpoons} x + y$, follows a rate law of quasi-zero order, and the concentrations of the reactants A and B can be regarded as constant. This is achieved, for example, by adding the reactant in deficit at the same speed as it is consumed in the catalyzed reaction. The speed of addition, extrapolated as tan α_K from a suitable recorder trace (see Fig. 1), is a measure of the catalyst concentration. This principle can be used to determine catalysts as well as substances that react with them [2—5].

In the absorptiostat technique [6], the concentration of a coloured reactant A is kept constant by adding it to the measuring cell at the rate at which it is consumed by the catalyzed oxidation with B to yield a colourless product.

In the present paper, the oxidation of indigo carmine (deep blue, λ_{max} = 610 nm) by hydrogen peroxide to give a colourless product is chosen as the indicator reaction. This indicator system was used in the 19th century for examination of the "peroxidatic" properties of blood, platinum black, colloidal platinum and iron(II) sulphate [7, 8]. The system has also been used for the kinetic determination of peroxidases [9—11]; both inorganic and organic substances can catalyze the reaction in homogeneous and heterogeneous media [12—21]. Unfortunately, the papers of Krause et al. [12—20] give little practical information; only the decolorization times were measured, and in some cases their dependence on temperature was examined.

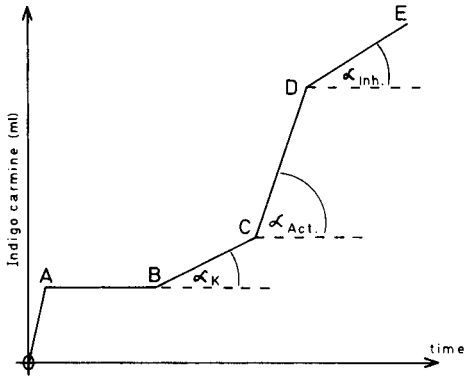

Fig. 1. Schematic recorder plot for the determination of catalysts, activators and deactivators.

It seemed of special interest that the indigo carmine—hydrogen peroxide reaction is catalyzed by thiosulphate [16], the latter being activated by aluminium(III) and iron(III). Therefore, this system was re-investigated with the aid of the absorptiostat method; it was found that sulphide, cysteine, thioacetamide and thiourea also catalyze the reaction to different degrees.

To characterize the relation of the catalytic activities of certain substances, a "relative molar coefficient of catalytic activity" F was introduced [22]: F is the quotient of the molar concentrations of a reference catalyst (in this case, sulphide) and the compound X considered, which have exactly the same catalytic activity under identical conditions: $F = C_{S^{2-}}/C_X$. The F values for the sulphur compounds mentioned above are given in Table 1. Cystine, colloidal sulphur, sulphite and tetrathionate do not show any measurable catalytic activity in the indicator system. In this paper, the absorptiostat method is used to determine sulphide, thioacetamide, thiourea and thiosulphate in the micromolar range.

TABLE 1

Catalytic activities of sulphur compounds and metal ions compared to sulphide with the indigo carmine—hydrogen peroxide as indicator reaction
(The F values are determined for $\tan \alpha_K = 0.4$.)

Compound	F value	Compound	F value
Sulphide	1.00	Fe(III)	0.63
Cysteine	0.40	Th(IV)	0.17
Thioacetamide	0.17	Cr(III)	0.026
Thiosulphate	0.048	Zr(IV)	0.016
Thiourea	0.045	Ti(IV)	0.012
		Cu(II)	0.005
		Co(II)	0.0015

The indigo carmine—hydrogen peroxide reaction is catalyzed not only by sulphur compounds, but, under identical conditions, also by metal ions (see Table 1). Manganese(II) shows only a weak activity; it is noteworthy, however, that it can be determined in carbonate buffer solution with good selectivity and sensitivity [21].

Thiosulphate as catalyst for the indicator reaction used here is strongly activated by iron(III) and to a smaller extent by aluminium(III); iron(III) can thus be determined in the nanogram range, and Al(III) in the microgram range. Thiosulphate is also activated by other metal ions to different degrees. In this case the relative molar coefficient of activation, F', defined as $F' = C_{Fe^{3+}}/C_{M^{n+}}$, is the quotient of the molar concentrations of iron(III) as reference substance and the respective metal ion that give the same activation under identical conditions; the F' values are given in Table 2. Fluoride acts as a deactivator for aluminium(III) and can also be determined in the microgram range.

EXPERIMENTAL

Apparatus

The apparatus used consists of a Combi-Titrator 3D (Metrohm, Herisau, Switzerland) and a Lightelectric Colorimeter Model J (Lange, Berlin, F.R.G.) operated in the "multiflex" mode. In this position, the photometer is internally compensated and adjustable to zero. The multiflex exit is fed to the input of an operational amplifier (Philbrick-Nexus Q200) and the amplified mV signal regulates the Combi-Titrator 3D. The circuitry is outlined in Fig. 2.

A round-bottomed 50-ml test tube (30 mm o.d.) is used as reaction vessel and photometric cuvette. It is mounted in a thermostatted cuvette holder. The capillary end of the burette (Mikrodosimat, 1-ml burette) is fitted through the plastic cover of the photometer; a 5-mm diameter hole in the cover is used to insert the tip of a 500-μl Eppendorf pipette. The reaction mixture is stirred by using a magnetic stirrer. The recorder speed was always

TABLE 2

Activating effect of metal ions on the thiosulphate-catalyzed oxidation of indigo carmine with hydrogen peroxide, compared to iron(III) as reference activator
(The F' values are determined for $\Delta \tan \alpha = (\tan \alpha_{Act} - \tan \alpha_K) = 1.2$ with 3 μmol of thiosulphate as catalyst in all cases.)

Metal ion	F' value	Metal ion	F' value	Metal ion	F' value
Fe(III)	1.00	Zn(II)	0.0059	Pb(II)	0.0028
Zr(IV)	0.026	Cu(II)	0.0053	Ti(IV)	0.0027
Hg(II)	0.0071	Cd(II)	0.0048	Al(III)	0.0018
Bi(III)	0.0071	Th(IV)	0.0032	Co(II)	0.0018
Ni(II)	0.0066				

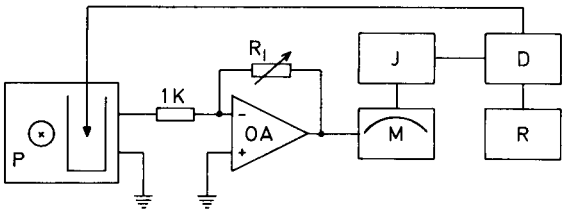

Fig. 2. Measuring circuit for the absorptiostat method. P, photometer; OA, operational amplifier (R_1 = 500 kohm); M, mV/pH meter (Metrohm E300B), J, comparator (Metrohm Impulsomat E473); D, automatic burette (Metrohm Mikrodosigraph E412); R, strip-chart recorder, mechanically driven from D.

1 cm min^{-1}, and the working temperature was 25.0 ± 0.2°C. The red filter used for the photometer had an absorption maximum of about 630 nm.

Optimization of the indicator reaction system

Tests were made by following the general procedure described below. The indicator reaction system was optimized by varying the pH value and the reagent concentrations. It was found [23] that the concentration of hydrogen peroxide must be high so that it can be regarded as constant in the reaction rate equation. The rate of the uncatalyzed reaction of indigo carmine with hydrogen peroxide increases with increasing pH value, and the difference between the rates of the catalyzed and uncatalyzed reactions becomes smaller with increasing pH. In addition, with increasing pH, the colour of the indigo carmine solution becomes paler. From these results, pH 4.0 was chosen for all measurements. At this value, the uncatalyzed reaction is immeasurably slow. Increasing amounts of buffer solution added increase the rate of the thiosulphate-catalyzed reaction, but the linear part of the recorder plot becomes shorter; 2 ml of 0.2 M sodium acetate buffer solution seemed to be best.

General procedure for the determination of catalysts

Into the cuvette are added 20 ml of hydrogen peroxide solution (unstabilized, 36 mg ml^{-1} H_2O_2) and 2 ml of sodium acetate buffer solution (pH 4.0, 0.2 M). The solution is thermostatted for 5 min, and the photometer is compensated to 0 and 100% transmittance as recommended in the instruction manual of the instrument. The zero point is again corrected at the mV meter if necessary. Then 300 µl of the indigo carmine solution (0.042 mg ml^{-1} in water) is added from the automatic burette. For this basic concentration (point A in Fig. 1), maintained through the whole measuring time, resistance R_1 is chosen so as to give a voltage rise of 200 mV on the mV meter M in Fig. 2 (working potential). Now the automatic addition of the indigo carmine solution from the Mikrodosimat is started and run for 2—3 min to give the addition plot for the uncatalyzed reaction (AB in Fig. 1). The catalyzed reaction is started at point B by the addition of

0.5 ml of the particular catalyst solution from an Eppendorf pipette; the addition plot is then recorded for a sufficient time (2—15 min; BC in Fig. 1) for the slope to be measured. A calibration graph is drawn by plotting the tan α_K values versus the catalyst concentration.

RESULTS AND DISCUSSION

Determination of sulphur compounds as catalysts

Sulphide. As can be seen from Table 1, sulphide has the highest catalytic activity among the sulphur compounds tested here. It can be determined in the range 0.5—5 μmol in the 0.5 ml of sample solution added by the procedure given above for the determination of catalysts. α_K is read from the linear parts of the addition plots; the calibration graph is almost linear in the determination range (tan α_K = 0.2—2.5). Some results for the determination of sulphide are given in Table 3.

Although cysteine gives linear addition plots in the section BC (Fig. 1), the calibration graph of concentration versus tan α_K is linear only between 0.5 and 2 μmol in the 0.5 ml of sample added and then quickly flattens; therefore the range for determination is unfavourable and results are not tabulated here.

Thioacetamide. The procedure given above is satisfactory for determinations of thioacetamide in the range 1—10 μmol in the 0.5 ml of sample added. The calibration graph is almost linear, but relatively insensitive (tan α_K = 0.3—1.2), so that errors are somewhat greater than for sulphide. Some results for the determination of thioacetamide are listed in Table 3.

TABLE 3

Determination of sulphur compounds as catalysts for the indigo carmine—hydrogen peroxide reaction

Sulphide (μmol/0.5 ml sample)										
Given	0.55	1.15	1.15	1.70	1.85	2.15	2.75	2.95	3.55	4.30
Found	0.60	1.20	1.25	1.60	1.95	2.10	2.95	3.15	3.75	3.65
Thioacetamide (μmol/0.5 ml sample)										
Given	1.3	2.0	3.1	3.7	4.1	5.5	7.0	7.9	9.4	9.7
Found	1.5	1.9	3.2	3.6	4.6	5.7	8.4	7.3	9.9	10.5
Thiourea (μmol/0.5 ml sample)										
Given	5.8	10.4	14.4	18.0	24.0	24.7	29.7	36.0	38.5	45.5
Found	6.5	10.0	14.0	18.5	24.0	24.0	29.5	33.5	39.5	45.5
Thiosulphate (μmol/0.5 ml sample)										
Given	2.7	2.9	5.1	7.8	9.1	10.1	13.2	14.4	20.4	22.4
Found	3.0	3.2	7.0	7.5	9.5	10.2	14.0	14.7	20.7	22.0

Thiourea. Thiourea can be determined by the same procedure in the range 5—50 μmol in the 0.5 ml of sample added. The addition plots on the recorder are sigmoidal; for the evaluation of α, the linear parts of these plots are used. The calibration graph is almost linear over the specified range (tan α_K = 0.3—2.3). Some results for the determination of thiourea are given in Table 3.

Thiosulphate. Thiosulphate can be determined between 2.5 and 25 μmol in the 0.5 ml of sample solution by the procedure described above. The addition plots on the recorder bend upwards for the first two minutes of the reaction and then become linear; α is extrapolated from these linear parts. The calibration graph is almost linear in the mole range specified (tan α_K = 0.2—2.9). Some results for the determination of thiosulphate are given in Table 3.

Activation of thiosulphate as catalyst

Several metal ions were investigated as activators for thiosulphate as catalyst in the indigo carmine—hydrogen peroxide reaction. The results are given in Table 2. The most effective activator proved to be iron(III); the respective values of tan α_{Act} are much higher than the sum of the values for the catalytic activities of the two species. A sensitive method for the determination of 15—300 ng of iron(III) could therefore be developed.

Determination of iron(III). The beginning of the procedure is analogous to the procedure described for the determination of catalysts, except that the same catalyst concentration is always used (0.1 ml of 30 μmol ml^{-1} sodium thiosulphate solution; Fig. 1, AC). The corresponding tan α_K value is about 0.23. After about 5 min, 0.5 ml of the activator solution (standard solution or unknown sample solution) is added from the Eppendorf pipette (Fig. 1, point C) and the recording is continued (Fig. 1, CD).

The calibration graph is drawn by plotting $\Delta\tan\alpha = \tan\alpha_{Act} - \tan\alpha_K$ on the ordinate versus activator concentration ($\Delta\tan\alpha$ = 0.3—2.4). The plot is linear within the specified range for iron(III), but cuts the ordinate because of a trace of iron(III) in the hydrochloric acid used to prepare the standard iron(III) solution. Some results for the determination of iron(III) are given in Table 4.

Determination of aluminium(III). With the same method, aluminium(III) can be determined as activator for thiosulphate in the range 10—100 μg in the 0.5 ml of sample added. The calibration graph is almost linear for the specified range ($\Delta\tan\alpha$ = 0.1—2.0). Some results for the determination of aluminium(III) are given in Table 4.

Determination of fluoride as deactivator for aluminium(III)

In the same way as it is possible to inhibit catalysts, activators can be deactivated. In most cases, inhibition is achieved by complex formation or precipitation. This has been used, for example, to determine fluoride with the aid of a catalytic-kinetic method [24] by inhibition of the zirconium

TABLE 4

Determination of activators for the thiosulphate catalyst in the indigo carmine—hydrogen peroxide reaction and determination of fluoride by its deactivation of aluminium(III)

Iron(III) (ng/0.5 ml sample)										
Given	25.0	34.5	62.5	87.0	90.0	120.0	147.0	232.5	242.5	266.0
Found	20.0	33.8	55.0	77.5	95.0	128.8	145.0	234.0	240.0	275.0
Aluminium(III) (μg/0.5 ml sample)										
Given	8.0	9.5	16.5	26.5	26.5	38.5	47.5	53.7	55.5	91.0
Found	7.0	7.0	15.0	32.5	26.0	40.5	45.0	51.0	59.0	100.0
Fluoride (μg/0.5 ml sample)										
Given	20.0	21.8	35.1	38.0	57.0	76.0	95.0	111.2	131.1	151.0
Found	15.2	22.8	32.3	60.8	64.6	91.2	110.2	115.9	130.2	152.0

catalyst. In the present work, the deactivation of aluminium proved best for the determination of fluoride, because aluminium is completely deactivated by a 1:2 molar ratio of Al:F. For the same effect, the ratio of iron(III) to fluoride must be about 1:10000.

The procedure begins in exactly the same way as the determination of aluminium as activator but the same amount of aluminium standard solution is always used (0.5 ml of a 200 μg Al(III) ml^{-1} solution). About 2 min after the addition of aluminium(III), 0.5 ml of the fluoride standard solutions (for preparing the calibration graph) or of the unknown sample solution is added and the recorder plot is continued (Fig. 1, DE).

For drawing a calibration graph, the best procedure seems to be to plot $\Delta \tan \alpha = \tan \alpha_{Act} - \tan \alpha_{Inh}$ (cf. Fig. 1) versus deactivator concentration. The graph is almost linear for the range 15—150 μg of fluoride in the 0.5 ml of sample added ($\Delta \tan \alpha = 1.5—0.4$).

Some results for the determination of fluoride are given in Table 4.

Conclusions

The indigo carmine—hydrogen peroxide reaction is catalyzed by sulphur-containing compounds as well as by metal ions and can be used to determine both. The catalytic activity of the sulphur compounds seems to depend on the presence of free SH groups or on the possibility of forming such groups by tautomerism. Therefore, the indigo carmine—hydrogen peroxide reaction may be a good supplement to the iodine—azide reaction.

Thiosulphate as catalyst is activated by iron(III) and aluminium(III), the latter being deactivated by fluoride; iron can be determined in the nanogram range, and aluminium and fluoride in the microgram range.

REFERENCES

1 K. M. Møller, Biochim. Biophys. Acta, 16 (1955) 162.
2 S. Pantel and H. Weisz, Anal. Chim. Acta, 109 (1979) 351, and literature cited therein.
3 B. Tan and J. K. Grime, Anal. Lett., 12B (1979) 1551.
4 J. K. Grime and K. R. Lockhart, Anal. Chim. Acta, 106 (1979) 251.
5 S. Pantel, Anal. Chim. Acta, 129 (1981) 231.
6 H. Weisz and K. Rothmaier, Anal. Chim. Acta, 75 (1975) 119.
7 G. Bredig, Anorganische Fermente, Leipzig, 1901.
8 C. F. Schönbein, J. Prakt. Chem., 75 (1858) 79.
9 B. Matkovics, E. Kovács and G. Buzás, Naturwissenschaften, 45 (1958) 491.
10 H. Herzmann, Naturwissenschaften, 46 (1959) 227.
11 G. Buzás, B. Matkovics and E. Kovács, Pharmazie, 14 (1959) 392.
12 A. Krause, Z. Anorg. Allg. Chem., 307 (1961) 229; Z. Naturforsch., Teil B, 20 (1965) 627.
13 A. Krause, E. Kukielka and J. Plura, Z. Phys. Chem. (Frankfurt am Main), 35 (1962) 289.
14 A. Krause and E. Nowakowski, Z. Naturforsch., Teil B, 19 (1964) 650; 20 (1965) 922; Sci. Pharm., 39 (1971) 39.
15 A. Krause and L. Lomozik, Z. Naturforsch., Teil B, 21 (1966) 86.
16 A. Krause and P. Meteniowski, Z. Naturforsch., Teil B, 21 (1966) 193.
17 A. Krause and T. Weimann, Z. Naturforsch., Teil B, 21 (1966) 288.
18 A. Krause and P. Meteniowski, Z. Naturforsch., Teil B, 21 (1966) 385.
19 A. Krause, St. Zielinski, J. Slawek, W. Skupin and W. Radecka, Z. Anorg. Allg. Chem., 357 (1968) 109.
20 A. Krause and J. Slawek, Fresenius Z. Anal. Chem., 244 (1969) 44.
21 A. Ya. Sychev, V. G. Isak and K. Pfanmeller, Zh. Anal. Khim., 33 (1978) 1355.
22 S. Pantel, Anal. Chim. Acta, 141 (1982) 353.
23 G. Marquardt, Diploma Thesis, Freiburg, 1981.
24 D. Klockow, H. Ludwig and M. A. Giraudo, Anal. Chem., 42 (1970) 1682.

Analytica Chimica Acta, 143 (1982) 185—190
Elsevier Scientific Publishing Company, Amsterdam — Printed in The Netherlands

EXTRACTION—SPECTROPHOTOMETRIC AND FLUORIMETRIC DETERMINATION OF THALLIUM WITH 2-(4-METHOXYPHENYL)-5,7-DIPHENYL-4*H*-1,3,4-THIADIAZOLO[3,2-*a*]PYRIDINIUM CHLORIDE

T. PÉREZ-RUIZ, C. SÁNCHEZ-PEDREÑO*, M. HERNÁNDEZ-CÓRDOBA and C. MARTINEZ-LOZANO

Department of Analytical Chemistry, University of Murcia (Spain)

P. MOLINA BUENDIA

Department of Organic Chemistry, University of Murcia (Spain)

(Received 24th May 1982)

SUMMARY

The synthesis, characteristics and applications of 2-(4-methoxyphenyl)-5,7-diphenyl-4H$^+$-1,3,4-thiadiazolo[3,2-*a*]pyridinium chloride (TDZP) as a reagent for the formation of ion-pair complexes is described. Tetrachlorothallate(III) can be extracted into isoamyl acetate as an ion-pair with TDZP. Thallium can be determined spectrophotometrically and fluorimetrically in the range 1—25 and 0.1—2 μg of thallium per 5 ml of organic layer, respectively. The molar absorptivity is 3.9×10^4 l mol^{-1} cm^{-1}. The quantum efficiency of the reagent is 0.42. The method is applicable to the determination of thallium in sphalerites and zinc or cadmium concentrates.

Thallium is usually present in lead, cadmium, indium or zinc metals as a trace constituent. Spectrophotometric methods for its determination are numerous, but the trend in recent years has been towards the formation of a complex of thallium(III) with a dyestuff that is extractable into an organic solvent for measurement. Xanthene dyes [1—4] and triphenylmethane dyes [5—8] among others have been used for this purpose; 2,4,6-triphenylpyrilium salts have been studied recently as ion-pair reagents for the determination of thallium(III) [9, 10], leading to sensitive and selective methods. 2,4,6-Triphenylpyridinium compounds behave similarly.

In this paper, a new reagent is introduced: 2-(4-methoxyphenyl)-5,7-diphenyl-4*H*-1,3,4-thiadiazolo[3,2-*a*]pyridium chloride, TDZP, is not only simple to synthesize but provides a high molar absorptivity and good fluorescent characteristics. Thallium in dilute hydrochloric acid forms an ion-pair complex with TDZP, which can be extracted into isoamyl acetate.

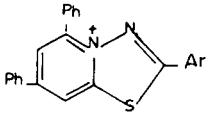

TDZP

Ar= 4-methoxyphenyl

0003-2670/82/0000-0000/$02.75

Spectrophotometric and fluorimetric procedures for thallium determinations are possible with this reagent.

EXPERIMENTAL

Apparatus

A Pye-Unicam SP8-200 spectrophotometer with 1-cm silica cells was used for recording spectra and absorbance measurements. Fluorescence spectra and spectrofluorimetric measurements were obtained with a Perkin-Elmer Model 3000 spectrofluorimeter, equipped with a quantum counter; excitation spectra were corrected, but emission spectra were not. A Perkin-Elmer Elemental Analyzer Model 240B, a Perkin-Elmer 177 grating infrared spectrophotometer, a Hewlett-Packard 5980A mass spectrometer, and a Varian FT-80 A nuclear magnetic resonance spectrometer were used for identification of the TDZP.

Reagents and solutions

All inorganic chemicals used were analytical-reagent grade. Ethyl benzoylacetate, *p*-methoxybenzonitrile (Aldrich) and isoamyl acetate (Merck) were used as received. Doubly-distilled water was used exclusively.

4,6-Diphenyl-2-pyridone (I) was synthesized from ethyl benzoylacetate by the procedure of Arndt and Eistert [11]. 4,6-Diphenylpyran-2-thione (II) was synthesized from (I) and phosphorus pentasulfide by the procedure of El-Kholy et al. [12]. 1-Amino-4,6-diphenylpyridine-2-thione was synthesized from (II) and hydrazine by the procedure of Molina et al. [13].

*Synthesis of 2-(4-methoxyphenyl)-5,7-diphenyl-4*H*-1,3,4-thiadiazolo[3,2-a]pyridinium chloride.* Pass a stream of dry hydrogen chloride through a solution of *p*-methoxybenzonitrile (5 mmol) in dry dioxane (20 ml) for 1 h, and then add 1-amino-4,6-diphenylpyridine-2-thione (5 mmol). Heat the solution at 50°C for 3 h. After cooling, separate the precipitated solid by filtration and recrystallize from ethanol. (Yield 96%, m.p. 297—300°C.) Elemental analysis: calculated 66.2% C, 3.7% H, 6.4% N; found 66.0% C, 3.5% H, 6.6% N. The purified product was dissolved in 50% (v/v) ethanol—water.

Thallium(III) standard solution (0.01 M). Dissolve thallium(III) chloride in 0.05 M hydrochloric acid and standardize by EDTA titration. Prepare working standards from this solution as required.

Procedures for determination of thallium(III)

Spectrophotometric method. To a volume of sample solution in a separating funnel containing up to 25 μg of thallium(III), add 2 ml of 3 M hydrochloric acid, 1 ml of 5×10^{-4} M TDZP solution, dilute to 25 ml with doubly-distilled water, and extract the mixture with 5 ml of isoamyl acetate. Shake the funnel vigorously for 2 min, allow the phases to separate for 5 min, then transfer the organic layer into a centrifuge tube, and centrifuge to give

an organic layer free from water. Measure the absorbance of the organic layer at 345 nm against a reagent blank prepared in a similar way, but without the thallium.

Prepare a calibration graph using different volumes of the standard solution of thallium(III) treated in the same way. Beer's law is obeyed over the concentration range 1—25 μg of thallium per 5 ml of organic extract.

Fluorimetric method. Treat the sample solution in the same way as described above, but use 1 ml of 5×10^{-5} M TDZP solution. Read the fluorescence of the complex at 475 nm with excitation at 340 nm. Under the recommended conditions, the calibration graph is linear over the range 0.1—2 μg of thallium.

RESULTS AND DISCUSSION

Spectra

Absorption spectra. Figure 1 shows the absorption spectra of a 8.7×10^{-6} M solution of TDZP in 50% (v/v) ethanol—water (curve 1) and of the isoamyl acetate extract (curve 2) of the ion-pair complex obtained by mixing thallium(III) solution (2.8×10^{-6} M) and TDZP solution (2×10^{-5} M) in 0.24 M hydrochloric acid. Curve 3 corresponds to the spectrum of TDZP in isoamyl acetate, showing the low extraction of the reagent by this solvent.

Fluorescence spectra. The excitation and emission spectra of the reagent (in 50% (v/v) ethanol—water) and the $TDZP^{+}TlCl_4^{-}$ (in isoamyl acetate) are shown in Fig. 2. The excitation spectra have maxima at 276 nm and 340 nm and the emission spectra have a maximum at 482 nm for the reagent and at 475 nm for the extracted ion-pair compound. The fluorescence quantum efficiency of TDZP in 50% (v/v) ethanol—water was determined by the Gains and Dawson method [14], and a value of 0.42 was obtained.

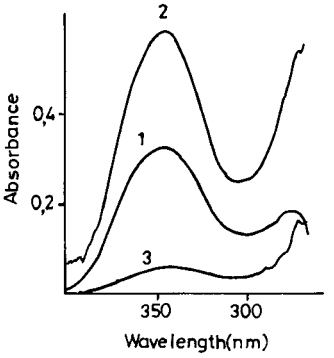

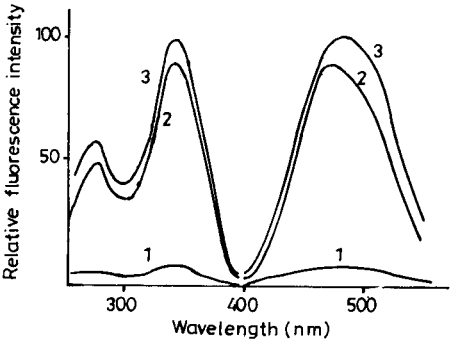

Fig. 1. Absorption spectra: (1) 8.7×10^{-6} M TDZP in 50% (v/v) ethanol—water; (2) 1.4×10^{-5} M thallium complex in isoamyl acetate; (3) reagent blank.

Fig. 2. Excitation and emission spectra: (1) reagent blank in isoamyl acetate; (2) thallium complex in the same solvent; (3) reagent in 50% (v/v) ethanol—water.

Effect of reaction variables and composition of the complex

The effect of the concentration of hydrochloric acid on the formation of the $TDZP^{+}TlCl_4^{-}$ complex and its extraction into isoamyl acetate was studied using fixed concentrations of thallium(III) (0.6 ppm) and TDZP (2×10^{-5} M) and varying the hydrochloric acid concentration from 10^{-2} to 1.5 M. The absorbance remained constant between 0.1 and 0.6 M in hydrochloric acid.

The influence of the chloride ion concentration was studied for 0.6 ppm of thallium(III) solution in 0.5 M sulphuric acid with sodium chloride concentrations ranging from 4×10^{-3} to 1.5 M. Maximum and constant absorbance values were obtained in isoamyl acetate extracts for chloride concentrations of 5×10^{-2} M and higher. Similar results were found when spectrofluorimetric techniques were used. Taking all these results into account, a 0.24 M hydrochloric acid medium was selected for both methods.

The effect of the concentration of the reagent was examined. A molar ratio [TDZP]/[Tl(III)] higher than 2 is necessary for the complete formation and extraction of the complex.

To establish the composition of the complex, the continuous variations and mole ratio methods were applied with spectrophotometric and spectrofluorimetric procedures in 0.24 M hydrochloric acid. The mole ratio of thallium to TDZP was found to be 1:1 by all methods. The apparent stability constant of the complex was calculated from the results of the mole-ratio and Job methods, and an average value of $\log K = 4.6 \pm 0.1$ was obtained.

Calibration graphs

Under the recommended conditions for the spectrophotometric method, the calibration graph was linear over the range 1—25 μg of thallium in 5 ml of isoamyl acetate. The molar absorptivity calculated from the slope of the graph is 3.9×10^4 l mol^{-1} cm^{-1} at 345 nm, and the Sandell sensitivity is 5.2×10^{-3} μg cm^{-2}. The coefficient of variation obtained from six measurements of 9.2 μg of thallium was 1.6%. The absorbance values of the complex extracted in isoamyl acetate remained constant for at least 8 h.

When the spectrofluorimetric procedure was used, the calibration graph was linear over the range 0.1—2 μg of thallium per 5 ml of isoamyl acetate. The coefficient of variation for six measurements of 0.69 μg of thallium was 2.4%. No significant changes in fluorescence values were observed in 2 h. The extraction efficiency calculated was higher than 99%.

Effect of diverse ions and application to zinc or cadmium concentrates and sphalerites

The effects of ions which interfere in the determination of 10.00 μg of thallium when present in <1000-fold amounts (by weight), are summarized in Table 1. Chloride and sulphate in at least 3000-fold amounts are without effect.

The positive interferences can be attributed to the fact that those elements also form ion-pair compounds with the reagent in hydrochloric acid and so

TABLE 1

Effect of diverse ions on the determination of 10.00 μg of thallium by the spectrophotometric procedure

Ion	Amount added (μg)	Tl found (μg)	Ion	Amount added (μg)	Tl found (μg)
Al	2700	9.98	In	500	10.02
	5000	10.30		800	10.10
Sb(V)	10	10.10	Fe(III)	5000	10.04
	20	10.45	Mn(II)	1500	9.97
As(V)	375	9.98		5000	10.05
	3000	9.50	Hg(II)	5	10.20
Bi	2	10.40	Mo(VI)	2500	9.98
Cd	2800	10.02	Sn(IV)	1000	9.97
	10 000	10.45		6000	10.30
Cr(III)	500	10.02	Zn	1500	9.99
	1250	10.40		5000	10.45
Cu(II)	1500	10.20	NO_3^-	100	10.17
Ga	300	10.15		300	10.50
	900	10.40	ClO_4^-	5	10.20
Au(III)	1	10.95			

are slightly extracted into the organic solvent. Bismuth, gold, mercury and perchlorate cause serious interference.

The method was applied satisfactorily to the determination of thallium in different materials. For the analysis of zinc concentrates, cadmium concentrates and sphalerites, the sample was dissolved in aqua regia, then sulphuric acid was added and the solution was boiled to white fumes twice with doubly-distilled water. The solution was then cooled and neutralized, and the hydrochloric acid concentration was adjusted to 1.4 M. The thallium was extracted with three successive 10-ml portions of ether, the combined ether extracts were evaporated to dryness and the residue was taken up in 0.24 M hydrochloric acid. The thallium was determined in such solutions by the recommended procedure. Some results are shown in Table 2.

TABLE 2

Determination of thallium in various materials

	Sphalerite	Zinc concentrate	Cadmium concentrate
Tl content (%)[a]	0.010	0.032	0.006
Tl found (%)	0.009	0.033	0.0054

[a]Values obtained by atomic absorption spectrometry.

REFERENCES

1 J. F. Wooley, Analyst, 83 (1958) 477.
2 R. L. Van Aman and J. H. Kanzelmeyer, Anal. Chem., 33 (1961) 1128.
3 M. M. Schneppe, Anal. Chim. Acta, 79 (1975) 101.
4 I. A. Bryum and N. A. Brushtein, Zh. Anal. Khim., 31 (1976) 1669.
5 M. Ariel and D. Bach, Analyst, 88 (1963) 30.
6 S. A. Lomonosov and F. Mil'shtein, Zavod. Lab., 33 (1967) 14.
7 C. Constantinescu and G. Constantinescu, Rev. Roum. Chim., 21 (1976) 571.
8 V. M. Tarayan, F. V. Mirzoyan, Zh. V. Sarkisyan and V. Zh. Artsruni, Zh. Anal. Khim., 32 (1977) 1456.
9 T. Pérez Ruiz, C. Sánchez-Pedreño, C. Martinez Lozano, M. Hernández Córdoba and P. Molina, An. Quim., 77 (1981) 397.
10 C. Sánchez-Pedreño, T. Pérez Ruiz, C. Martinez Lozano, M. Hernández Córdoba and P. Molina, An. Quim., 78 (1982) 60.
11 F. Arndt and E. Eistert, Chem. Ber., 58 (1925) 2318.
12 E. El-Kholy, F. Rafla and M. Mismrikey, J. Chem. Soc. C, (1970) 1578.
13 P. Molina, M. J. Vilaplana and A. Soler, An. Quim., 74 (1978) 1018.
14 N. Gains and A. P. Dawson, Analyst, 104 (1979) 481.

Analytica Chimica Acta, 143 (1982) 191—198
Elsevier Scientific Publishing Company, Amsterdam — Printed in The Netherlands

A COLLABORATIVE STUDY OF FOUR METHODS OF ASSAY OF BENZYLPENICILLIN

H. VANDERHAEGHE*
Rega Institute, Minderbroedersstraat, B-3000 Leuven (Belgium)
M. DUBOST
Centre de Recherches Rhône-Poulenc, F 94400 Vitry sur Seine (France)
M. FISCHLER
Astra Pharmaceuticals, S-15185 Södertalje (Sweden)
R. MALHERBE and C. VANDERVLIES
Gist-Brocades, Delft (The Netherlands)
(Received 21st May 1982)

SUMMARY

The assay of benzylpenicillin by iodimetric titration, spectrophotometry with a mercury(II) chloride—imidazole reagent, titration with mercury(II) nitrate in acetate buffer solution, and titration with mercury(II) perchlorate in aqueous pyridine solution, was examined in four laboratories. The first two methods were applied to two samples (the third one being the reference sample), the mercury(II) nitrate titration to three, and the mercury(II) perchlorate method to two samples. The four methods gave very similar results, but the purity obtained with the mercury(II) perchlorate method was slightly lower, and this procedure is less desirable because pyridine is used as solvent. There were no great differences in the relative standard deviations of the four methods. The titration with mercury(II) nitrate is preferred because it is an absolute method.

A great number of methods of assay of penicillins have been described. One of the first and still widely used methods is the iodimetric titration [1], which is based on the observation that penicillin does not react with iodine whereas penicilloic acid, formed by treatment with alkali, consumes iodine. The European Pharmacopoeia, Vol. II, describes this method for the assay of benzyl- and phenoxymethyl-penicillin, based on the modification of Örtenblad [2], in which iodine reacts in acetate buffer pH 4.6 rather than at pH 2 as mentioned in the original method [1].

The alkalimetric titration of penicillin is based on the formation of a new acid group with pK 5.3 (the imino group of the thiazolidine ring of penicilloic acid) during hydrolysis with alkali [3, 4]; potentiometric [5] or visual [6] end-points are suitable. The British Pharmacopoeia (1973) describes this method for the assay of carbenicillin, cloxacillin, phenethicillin and methicillin. With many penicillins, penicilloic acid can also be formed by the action of penicillinase, and the use of a pH-stat has been described for this purpose [7].

Penicillin reacts with hydroxylamine in alkaline medium to form a hydroxamic acid. The product forms a complex with iron(III) ions, that can be determined colorimetrically [8, 9]. This method is often used for the assay of dilute penicillin solutions. The Code of Federal Regulations describes it for the assay of pure penicillins and the British Pharmacopoeia (1973) for the assay of phenethicillin tablets.

Herriott [10] observed that benzylpenicillin could be converted into a product (penicillenic acid) with an absorption maximum at 322 nm under controlled conditions of pH, time and temperature. This reaction was studied in different laboratories and it was found that more reproducible results could be obtained by addition of copper or mercury salts. The optimal version uses mercury(II) chloride with imidazole [11, 12]. This method is described in the British Pharmacopoeia (1980) for ampicillin, amoxicillin, cloxacillin and phenethicillin.

A recently published titrimetric assay [13] is based on the reaction of mercury(II) nitrate with penicilloic acid, produced by the action of alkali or penicillinase on penicillin. The principle of this method had already been described [14, 15] and a similar titration can be done with mercury(II) perchlorate in aqueous pyridine [16]. The latter method is included in the Compendium Medicamentorum XI (1976) for ampicillin. The assay of several penicillins by high-performance liquid chromatography was described [17, 18] in the late stages of the present study. Although this method is selective and sufficiently accurate, a titrimetric assay seems to be preferable for pharmacopoeial purposes. Many modifications of other chemical and physical methods are mentioned in a recent review [19]. Microbiological and chromatographic methods are too numerous to be listed.

In order to select an assay method for the European Pharmacopoeia, it was decided to compare in several laboratories the mercury(II)—imidazole spectrophotometric method and the titrations with mercury(II) nitrate or perchlorate, with the classical iodimetric assay for a good and a poor quality sample of benzylpenicillin.

EXPERIMENTAL

Samples

The samples used were a potassium benzylpenicillin sample of good quality (Sample 5294), containing ~0.2% of penicilloic acid as determined from the blank of the iodimetric and mercurimetric titrations, and one of low quality (2476/3), containing ~4.5% of penicilloic acid. Sample 705-AN-52-1 was used as reference substance and was considered to have a purity of 100%; this was confirmed by the results of the assay with mercury(II) nitrate (see Table 1 and Discussion).

Equipment

A pH meter or a titrator must be fitted with the appropriate electrodes. Two laboratories used a platinum foil electrode and a mercury—mercury(I)

sulfate reference electrode, one laboratory a platinum foil electrode and an Orion 90-02 double-junction calomel electrode, and one laboratory a mercury electrode and a mercury—mercury(I) sulfate electrode. In one laboratory, the different electrodes were compared and no significant difference was observed. The results obtained in different laboratories (see Table 1) also show that all these electrodes give satisfactory results.

Reagents

All reagents were of analytical-reagent quality.

Acetate buffer pH 4.6. Dissolve 5.44 g of sodium acetate trihydrate in 25 ml of water, add 2.4 g of acetic acid and dilute to 100 ml with water.

Mercury(II) nitrate (0.02 M). Dissolve 6.85 g of mercury(II) nitrate monohydrate in 20 ml of 1 M nitric acid and dilute with water to 1 l. For standardisation, dissolve 15.0 mg of sodium chloride (primary standard quality) in 50 ml of water and titrate potentiometrically with the mercury(II) solution; omit the acetate buffer. (1 ml of 0.02 M $Hg(NO_3)_2 \equiv 2.338$ mg NaCl.) Potassium iodide can also be used (40.0 mg in 25 ml of water and 25 ml of acetate buffer); the potential jump at the end-point is greater than that with sodium chloride, but the titer must be corrected for the purity of potassium iodide used. One laboratory used disodium-EDTA solution diluted with acetate buffer for the standardisation.

Mercury(II) perchlorate (0.05 M). Dissolve 10.8 g of mercury(II) oxide in 10 ml of 1 M $HClO_4$ and 10 ml of water, and dilute with water to 1 l. For standardisation, dissolve 45.0 mg of sodium chloride in 25 ml of water and titrate potentiometrically with the mercury(II) solution.

Mercury(II)—imidazole reagent. Dissolve 8.25 g of recrystallised imidazole in 60 ml of water, and add 10 ml of 5 M hydrochloric acid. Add with stirring 10 ml of 0.25% mercury(II) chloride solution. If a cloudy solution results, discard and prepare a further solution, adding the mercury(II) chloride more slowly. Adjust to pH 6.80 ± 0.05 with 5 M hydrochloric acid (about 4 ml) and dilute with water to 100 ml.

Procedures

Iodimetric assay (Ph. Eur. II). To 10.0 ml of a solution containing 0.100 g of benzylpenicillin potassium in 100 ml of water, add 5 ml of 1 M NaOH. After reaction for 20 min, add 20 ml of acetate buffer pH 4.6, 5 ml of 1 M HCl and 25.0 ml of 0.02 N iodine (prepared as described in the European Pharmacopoeia). After reaction for 20 min, titrate the excess of iodine with 0.02 N sodium thiosulfate using starch as indicator. For the blank, add to 10.0 ml of the penicillin solution, 20 ml of acetate buffer and 25.0 ml of 0.02 N iodine solution. After 20 min, titrate the solution with sodium thiosulfate. The difference between the two titrations represents the volume of 0.02 N iodine consumed. Compare with a reference substance. The volumes of thiosulfate solution used were 10—11 ml in the assay and 20—22 ml for the blank.

Mercury(II)—imidazole method [11]. To 2.0 ml of a solution containing ca. 5.00 mg of benzylpenicillin potassium per 100 ml, add 10 ml of the mercury—imidazole reagent. After stoppering the tube, immerse in a water bath at 60°C with occasional swirling for 25 min and cool to 20°C. In another tube, mix 2.0 ml of the penicillin solution with 10 ml of the mercury—imidazole reagent. Without delay, measure the absorbances of both solutions at 325 nm. From the difference in absorbance of the two solutions and from the value obtained with the reference substance, calculate the potency. The absorbance readings were ca. 0.60.

Titration with mercury(II) nitrate [13]. Dissolve 100.0 mg of benzylpenicillin potassium in 50 ml of acetate buffer and titrate potentiometrically at room temperature with 0.02 M mercury(II) nitrate. To 10.0 ml of a solution containing 60.0 mg of the penicillin in 100 ml of water, add 2.5 ml of 2 M NaOH and allow to stand for 5 min. Add 2.5 ml of 2 M HNO_3 and 25 ml of acetate buffer. Titrate potentiometrically at 35—40°C with 0.02 M mercury(II) nitrate. Titrate slowly so that the titration takes about 15 min. Ignore any preliminary inflection of the titration curve. The volume of mercury(II) solution consumed was about 0.75 ml. After correcting for the blank, the amount of penicillin is calculated from the equation 1 ml of 0.02 M $Hg(NO_3)_2$ = 0.02 × 372.5 mg $C_{16}H_{17}N_2O_4SK$.

Titration with mercury(II) perchlorate [16]. Dissolve 0.450 g of benzylpenicillin potassium in 25 ml of water and 25 ml of pyridine, and titrate potentiometrically at room temperature with 0.05 M mercury(II) perchlorate. Dissolve 0.150 g of penicillin in 25 ml of 0.2 M NaOH and allow to stand for 10 min. Add 5 ml of 1 M $HClO_4$ and 25 ml of pyridine and titrate potentiometrically with mercuric perchlorate 0.05 M. Ignore any preliminary inflection on the titration curve. The volume of titrant consumed was 7—8 ml. After correcting for the blank, the amount of penicillin is calculated from the equation 1 ml of 0.05 M $Hg(ClO_4)_2$ = 0.05 × 372.5 mg $C_{16}H_{17}N_2O_4SK$.

RESULTS

The mercurimetric titration was done at about 35°C. If the reagent is added at room temperature, the addition should be very slow, otherwise high results may be obtained. These results are in agreement with the observations of Bird and Redrup [20]. The results of these authors for ampicillin, where the titration should be done at room temperature, were also confirmed.

The results obtained by the different methods are given in Table 1. In this table the average results for each sample in each laboratory obtained by each assay method are given together with two relative standard deviations. The first relative standard deviation (S_A), representing "the standard deviation of the method", is equal to the standard deviation of the mean of a duplicate analysis on one day. The standard deviation of the overall mean result (S_B) is $S_B = S_A\, n^{-1/2}$, where n is the number of days, on which assays were done. From these results and standard deviations, the 95% confidence intervals of the overall mean value for all samples and laboratories were calculated (Fig. 1).

TABLE 1

Assay of benzylpenicillin potassium samples[a]

Laboratory	Sample	Iodimetry			Mercury—imidazole			Mercury(II) nitrate			Mercury(II) perchlorate		
		%	S_A	S_B	%	S_A	S_B	%	S_A	S_B	%	S_A	S_B
I	5294	99.38	0.47	0.19	100.05	0.71	0.29	99.84			99.31	0.47	0.19
	2476/3	95.22			95.51			95.07	0.30	0.12	94.64		
	705-AN-52-1	Reference			Reference			99.90					
II	5294	100.13	0.29	0.12	100.00	0.69	0.28	99.92		0.14	99.83	0.39	0.16
	2476/3	95.57			95.59			94.76	0.34	0.14	94.55		
	705-AN-52-1	Reference			Reference			99.87		0.14			
III	5294	99.27	0.46	0.19	98.97	0.73	0.30	99.62		0.14	99.54	0.42	0.13
					(99.36)[b]	(0.58)[b]	(0.26)[b]						
	2476/3	95.57			95.06		0.30	95.03	0.35	0.14	94.76		0.12
	705-AN-52-1	Reference			Reference			99.80		0.18			
IV	5294	100.05	0.46	0.19	99.84	0.33	0.13	99.55	0.21	0.15	99.33	0.16	0.05
	2576/3	95.14			95.04			94.90			94.76		
	705-AN-52-1	Reference			Reference			99.95					
Mean	5294	99.71			99.72			99.73			99.52		
					(99.82)[b]								
	2476/3	95.38			95.30			94.90			94.69		
	705-AN-52-1	—			—			99.88			—		

[a] All assays, except those with mercury(II) perchlorate, for which only six results were obtained, were done in duplicate on six different days. In some laboratories, two analysts were involved in the work. [b] After elimination of one extreme day.

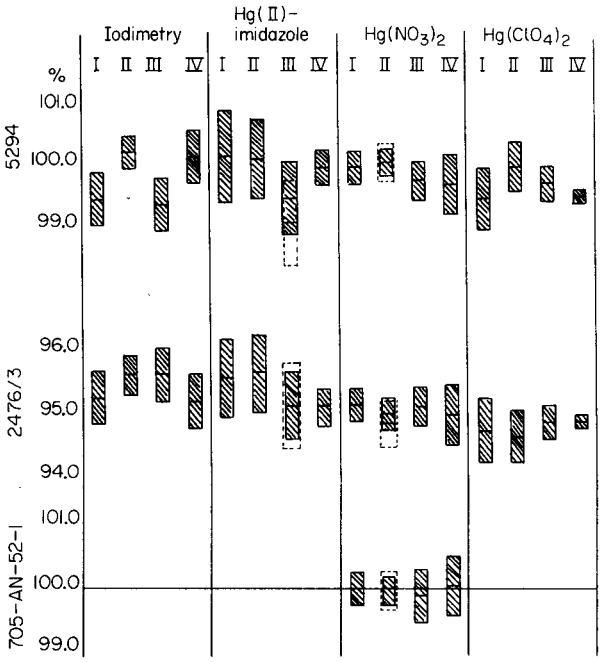

Fig. 1. Average assay results with 95% confidence limits. The boxes outlined with dotted lines show the results obtained when the one extreme day was included.

There is no great difference in the relative standard deviations of the methods (S_A). In most laboratories, the mercury—imidazole method showed the highest figures (0.6%), followed by the iodimetric assay (0.45%), the mercury(II) perchlorate assay (0.4%) and the mercury(II) nitrate assay (0.3%). Very few publications give adequate data on the precision of the various assay methods of penicillins. For the iodimetric assay, Örtenblad [2] found a standard deviation of 0.5% and Roksvaag et al. [21] a value of 1.32%. A standard deviation of 0.6% was mentioned for seven determinations by the mercury(II) perchlorate method [16]. It is the experience of one of the authors that when good automatic titration equipment is used, a standard deviation of 0.2—0.3% for the method can be obtained with the mercurimetric titration.

The assay with mercury(II) nitrate confirmed the assigned potency (99.9%) of the benzylpenicillin potassium reference substance (lot 705-AN-52-1) by all participating laboratories. The iodimetric assay of benzylpenicillin potassium (lot 5294) gave rather variable results between the four laboratories. The other methods gave more homogeneous results. It should be mentioned that the mercury(II)—imidazole assay of laboratory III and the mercury(II) nitrate assay of laboratory II were influenced by one extreme day. The overall potency of the benzylpenicillin potassium sample of high quality (5294) is about 99.7%. The mercury(II) perchlorate assay gives the lowest figure of about 99.5%.

The results of sample lot 2476/3 are reasonably homogeneous for all assay methods. The mean value for this sample is about 95.4% from the two relative assay methods, about 94.9% from the mercury(II) nitrate assay, and about 94.7% from the mercury(II) perchlorate assay.

The mercury(II) perchlorate method gave slightly lower values for both samples. This may be due to some decomposition of the penicillin in the pyridine solution during the blank assay. It has been suggested that the analysis should be done in an aqueous solution containing only 20% of pyridine. The relative assay methods (iodimetric and mercury(II)—imidazole) gave slightly higher values than the absolute mercurimetric methods in the case of the low-quality benzylpenicillin potassium, in contrast to the sample of high quality where almost identical results were obtained for all methods.

CONCLUSIONS

These data show that there are no great differences in the precision of the assay methods, but that the absolute mercurimetric titrations are slightly better than the relative iodimetric and mercury(II)—imidazole assays. The accuracy of the methods is the same for the high-quality benzylpenicillin potassium sample, whereas for the sample of poor quality the values from the mercurimetric titrations are a little lower, and probably more accurate, than the results of the two relative methods.

The selectivity (and the scope of application) of the different methods is very similar. The main advantage of the mercurimetric titration is that no reference substance is needed. It is also suitable for the assay of all kinds of penicillins not only as such but also in different dosage forms. Interference from excipients has not been found so far. Other titrations after hydrolysis with alkali or penicillinase are known but they lack the wide applicability just mentioned.

For routine use in the manufacturer's laboratory, the average time of an assay is of utmost importance. The time requirement can be reduced by automation as described for the iodimetric [22, 23] and hydroxamate [24] assays. The mercury(II)—imidazole method as described in the British Pharmacopoeia (1980) for several substances, can also easily be carried out by an AutoAnalyzer or similar equipment. However, although the results of all these relative methods may be similar as far as precision and even accuracy is concerned, they are not very suitable as reference methods. The proposed method of choice for inclusion in the European Pharamacopoeia is therefore the titration with mercury(II) nitrate in an aqueous buffer system to avoid the use of pyridine.

The authors thank J. Hoebus (Leuven), F. Bigeard and M. Tabillon (Vitry), B. Karlberg and B. Örtengren (Södertalje) and W. Plugge (Delft) for advice and help in the course of this study.

REFERENCES

1 J. F. Alicino, Ind. Eng. Chem., Anal. Ed., 18 (1946) 619.
2 B. Örtenblad, Acta Chem. Scand., 4 (1950) 518.
3 R. G. Benedict, W. H. Schmidt and R. D. Coghill, Arch. Biochem., 8 (1949) 377.
4 H. D. C. Rapson and A. E. Bird, J. Pharm. Pharmacol., 15 (1963) 222 T.
5 J. J. Murtaugh and G. B. Levy, J. Am. Chem. Soc., 67 (1945) 1042.
6 S. J. Patterson and W. B. Emery, Analyst, 73 (1948) 207.
7 J. P. Hou and J. W. Poole, J. Pharm. Sci., 61 (1972) 1594.
8 J. H. Ford, Anal. Chem., 19 (1947) 1004.
9 G. E. Boxer and P. M. Everett, Anal. Chem., 21 (1949) 670.
10 R. M. Herriott, J. Biol. Chem., 164 (1946) 725.
11 H. Bundgaard and K. Ilver, J. Pharm. Pharmacol., 24 (1972) 790.
12 H. Bundgaard, J. Pharm. Pharmacol., 26 (1974) 385.
13 B. Karlberg and U. Forsman, Anal. Chim. Acta, 83 (1976) 309.
14 J. Grafnetterova, Clin. Chim. Acta, 11 (1965) 128.
15 J. Körbl and V. Vanicek, Czech. Patent No. 132 991 (1969); Chem. Abstr., 73 (1970) 69934 g.
16 T. Paal and M. Molnar, Gyogyszereszet, 20 (1976) 8.
17 F. Nachtmann, Chromatographia, 12 (1979) 380.
18 F. Nachtmann and K. Gstrein, Acta Pharm. Technol., 26 (1980) 223.
19 D. W. Hughes, A. Vilim and W. L. Wilson, Can. J. Pharm. Sci., 11 (1976) 97.
20 A. E. Bird and C. E. Redrup, Proc. Anal. Div. Chem. Soc., 14 (1977) 285.
21 P. O. Roksvaag, H. I. Brummenaes and T. Waaler, Pharm. Acta Helv., 54 (1979) 180.
22 A. Ferrari, F. M. Russo-Alesi and J. M. Kelly, Anal. Chem., 31 (1959) 1710.
23 R. R. Goodall and R. Davies, Analyst, 86 (1961) 326.
24 A. O. Niedermayer, F. M. Russo-Alesi, C. A. Lendzian and J. M. Kelly, Anal. Chem., 32 (1960) 664.

Analytica Chimica Acta, 143 (1982) 199—207
Elsevier Scientific Publishing Company, Amsterdam — Printed in The Netherlands

MOLECULAR EMISSION CAVITY ANALYSIS
Part 24. Determination of Germanium, Gallium and Thallium

S. A. AL-TAMRAH[a] and A. Z. AL-ZAMIL[a]

Chemistry Department, University of Birmingham, P.O. Box 363, Birmingham B15 2TT (Gt. Britain)

ALAN TOWNSHEND*

Chemistry Department, University of Hull, Hull HU6 7RX (Gt. Britain)

(Received 12th June 1982)

SUMMARY

Germanium (10—500 ng) is determined by measuring its GeCl emission at 455 nm in a carbon cavity in a hydrogen—nitrogen—air flame. Similarly, gallium gives a violet GaI emission and a bluish white GaBr emission with maximum intensities at 391 and 350 nm, respectively. These emissions can be used for the determination of nanogram amounts of gallium or bromide, and microgram amounts of iodide. Thallium (20—2000 ng) is determined by measuring its atomic emission produced in an oxy-cavity at 377.5 nm. The effects of interferences on germanium, gallium and thallium emissions are described.

Molecular emission cavity analysis (m.e.c.a.) provides an environment conducive to the production of gaseous metal halide emissions [1—4]. The relatively cool surface and the sheltered nature of the cavity lead to decreased interaction with hydrogen flame radicals; this discourages the formation of metal oxides, hydroxides and hydrides and consequently promotes the production of metal halide molecules. Many halides such as those of indium [1], tin [4, 5] and copper [2] give rise to metal(I) halide band emissions within the cavity, enabling nanogram amounts of the metal or the halide (other than fluoride) to be determined. In this paper, traces of germanium and gallium are determined by measuring their halide emissions in the m.e.c.a. cavity.

Although m.e.c.a. has been developed mostly for measuring band emissions [6], atomic emissions from easily excited elements have also been observed in the m.e.c.a. cavity. Cadmium [7] and alkali metals [6, 8] have thus been determined. In this work thallium, which did not give any detectable halide emission, is determined by measuring its atomic emission in the oxy-cavity.

---

[a]Present address: Chemistry Department, College of Science, King Saud University, Riyadh, Saudi Arabia.

EXPERIMENTAL

Apparatus and reagents

A modified Evans Electroselenium (EEL) 240 atomic absorption spectrometer operating in the emission mode was used, as described previously [9]. The emission intensity was measured with an Oxford 3000 potentiometric recorder (response time 0.2 s for 90% full-scale deflection). The sample holder assembly used was that described by Belcher et al. [10]. A carbon cavity (4 mm deep, 4 mm diameter) was used for germanium and gallium measurements. The conventional steel Allen-screw cavity [9], modified to introduce a slow flow rate of oxygen through a hole in the side-wall of the cavity, was used for thallium determination.

All solutions were prepared with analytical-reagent grade chemicals, unless otherwise stated. Germanium stock solution (1 mg Ge ml^{-1}) was prepared by dissolving 0.36 g of germanium dioxide (99.999%, Koch-Light Laboratories Ltd.) in 15 ml of distilled water containing 1—2 pellets of sodium hydroxide. The solution was heated gently until the oxide dissolved and then diluted to 250 ml with distilled water. Thallium, gallium (each 1 mg ml^{-1}), iodide and bromide (0.1 M) stock solutions were prepared from thallium(I) acetate, gallium(III) nitrate, ammonium iodide and ammonium bromide, respectively, unless otherwise stated. The solutions of interfering ions were prepared mainly from their sodium or nitrate salts.

General procedure

In each experiment, 5 μl of sample solution was injected into the cavity fixed in position above the burner. The flame gases were switched on 10 s before ignition in order to have steady gas flow rates at the time of ignition. The flame was ignited immediately after the injection and the resulting emission was measured at the appropriate wavelength. After the flame had been switched off, the hot cavity was cooled to room temperature with an air blower. The results were obtained by measuring the height of the intensity—time peak.

Spectral measurements

The germanium and gallium m.e.c.a. emissions are fast (times for maximum emissions are 2.5 and ca. 4 s, respectively, after flame ignition) and cannot be sustained. Therefore, their emission spectra were obtained by injecting 5 μl of the sample solution, measuring the resulting emission at a given wavelength and repeating the process at different wavelengths. The thallium emission spectrum was scanned by injecting 10 μl of a 4 mg ml^{-1} solution of thallium(I) acetate. The yellowish green emission reached a maximum 15 s after ignition of the flame and remained stable for 10 min, during which the spectrum was continuously scanned.

RESULTS AND DISCUSSION

Optimization of conditions

The optimal conditions found for the determination of germanium, gallium and thallium are shown in Table 1. Greatest sensitivity for all three elements is achieved in a nitrogen-diluted fuel-rich hydrogen—air flame. When oxygen is introduced directly into the carbon cavity, germanium and gallium emissions are totally suppressed, because of the formation of stable, unexcited GeO and GaO at the expense of metal halide emitting species. In contrast, the introduction of oxygen into the Allen-screw cavity results in an increase in thallium atomic emission intensity, which is due partly to consequent restriction of the emission to within the cavity and partly to an increase in the flame temperature. The optimal oxygen flow rate into the cavity for thallium determination is 220 ml min^{-1}.

Determination of germanium

No visible emission is obtained when an aqueous sodium hydroxide solution containing 5 μg of germanium is injected into the Allen screw, the oxy-Allen screw or the carbon cavity. However, germanium solutions prepared in hydrochloric acid given an intense blue emission in the Allen-screw cavity but unfortunately the acid itself also gives an emission because metal chloride emitting species are formed from elements present in the stainless-steel. This very high background emission is almost eliminated when a high-purity carbon cavity is used (Fig. 1). The same blue emission is obtained from germanium solutions prepared in ammonium chloride, ammonium perchlorate or perchloric acid (Fig. 1), suggesting that the same emitting species (GeCl) is responsible [11, 12]. Further evidence for this assignment was recently obtained by El-Hag [13]. The emission obtained from germanium in ammonium perchlorate or perchloric acid is relatively very weak because these two compounds liberate oxygen, which decomposes the GeCl emitting species as mentioned above. In the presence of ammonium bromide, germanium

TABLE 1

Optimal conditions for the determination of germanium, gallium (GaI and GaBr) and thallium by m.e.c.a.

Element	Flow rates of flame gases (l min^{-1})			Cavity position in the flame (mm)	
	H_2	N_2	Air	Into the flame	Cavity-burner distance
Ge	4.1	6.1	4.2	Flame centre	20
Ga	4.1	5.3	2.7	3	13
Tl	8.0	4.5	2.4	6	25

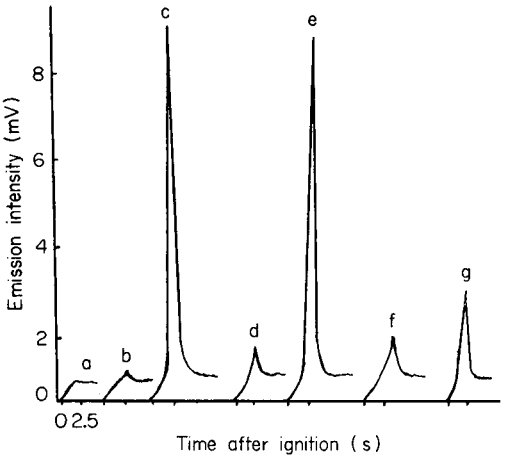

Fig. 1. Emission responses in a carbon cavity from 5 μl of various solutions: (a) Ge in NaOH; (b) 0.2 M HCl; (c) Ge in 0.2 M HCl; (d) 0.2 M NH_4Cl; (e) Ge in 0.2 M NH_4Cl; (f) Ge in 0.2 M NH_4ClO_4; (g) Ge in 0.2 M $HClO_4$. (Ge concentration, 0.1 $\mu g\ \mu l^{-1}$).

gives a very weak, irreproducible green emission which is inadequate for trace analysis, while in the presence of fluoride or iodide no emission is detected.

Hydrochloric acid is therefore used in the determination of germanium. The spectrum of the GeCl emission (Fig. 2) shows maximum intensity at 455 nm, and would appear to be similar to that obtained by Dagnall et al. [14]. For germanium solutions prepared in 0.2 M hydrochloric acid, measurements at 455 nm give a detection limit (signal = twice background noise) of 10 ng of germanium in 5 μl of solution. The calibration graph is linear up to 0.5 μg of germanium (Fig. 3) and the relative standard deviation for 8 replicate measurements of 150 ng of germanium is 1.2%. It is necessary that the concentration of hydrochloric acid does not exceed 0.2 M, otherwise the intensity will be decreased (Fig. 3). The GeCl emission cannot be used for the determination of traces of chloride because it is observed only when a large excess of chloride is present.

Determination of gallium

Gallium solutions give measurable emissions in the carbon cavity only if they contain an excess of iodide or bromide. These violet and bluish-white emissions are attributed to GaI and GaBr [15] and give maximum intensities at 391 and 350 nm, respectively. Emissions are not obtained from solutions containing gallium in the presence of chloride or fluoride. The GaI or GaBr emission increases with use of successive samples of the same solution. This probably occurs because increasing amounts of gallium remain in the cavity as gallium oxide, which interacts with the iodide in the next solution injected. This problem is solved by cleaning the carbon cavity with a tissue moistened with dilute hydrochloric acid after each measurement.

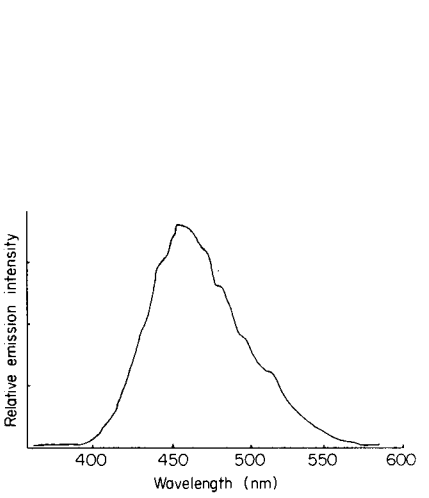

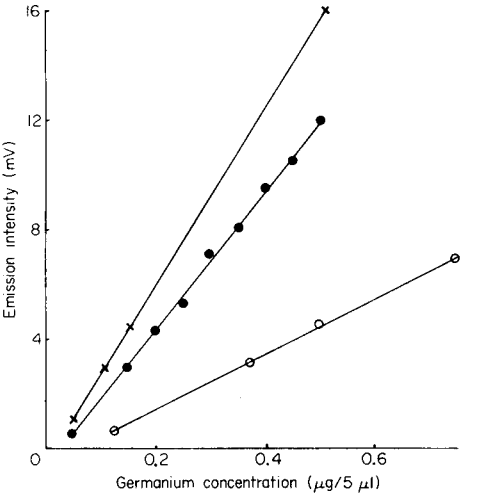

Fig. 2. Spectrum of GeCl emission obtained from germanium (0.1 $\mu g\ \mu l^{-1}$) in 0.5 M HCl.

Fig. 3. Calibration graphs for germanium in the presence of (•) 0.2 M HCl, and (○) 0.5 M HCl; (×) by the liquid—liquid extraction procedure.

For the determination of gallium, its solutions should be prepared either in 0.04 M ammonium iodide or 0.02 M ammonium bromide. Higher concentrations cause a decrease in the gallium halide intensity. The GaI emission is more sensitive than that from GaBr (Fig. 4); therefore, the former is recommended for the determination of traces of gallium. When the GaI emission is used, 5—50 ng of gallium can be determined (Fig. 4) with a detection limit of 0.5 ng of gallium in 5 μl of solution. The relative standard deviation for 10 replicate measurements of 0.1 μg of gallium in 5 μl is 2.5%.

Determination of iodide and bromide

The GaI emission at 391 nm and GaBr emission at 350 nm may also be used for the determination of iodide and bromide, respectively. When gallium is added in excess to iodide or bromide solutions, ca. 1—10 μg of the halide in 5 μl can be determined. The detection limits obtained for iodide and bromide are 0.25 and 0.6 μg, respectively. These values are much larger than those obtained for the corresponding indium halides [1], and agree with the observation of Dagnall et al. [15] that the gallium halides give less sensitive emission than those of indium.

The presence of iodide (5×10^{-3} M ammonium iodide) in the bromide solution considerably increases the GaBr emission intensity at 350 nm, making possible the determination of as little as 50 ng of bromide, with a detection limit of 10 ng in 5 μl of solution. This compares more favourably with the value of 2.5 ng of bromide obtained when indium is used [1]. A possible explanation of this effect is that a mixed halide such as GaI_2Br is formed which is more volatile than $GaBr_3$ and therefore is obtained more

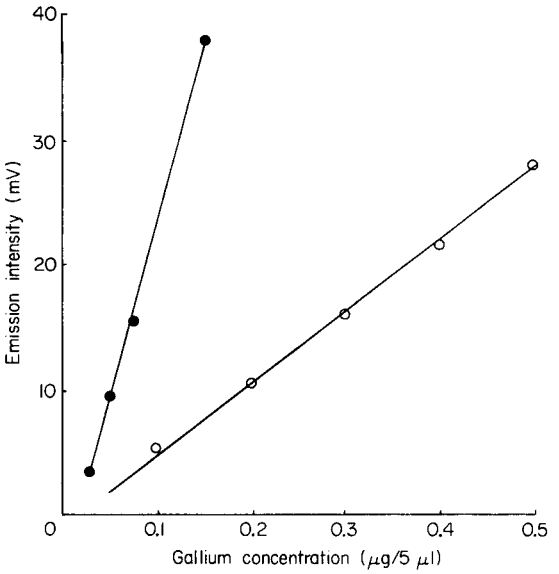

Fig. 4. Calibration graphs for the determination of gallium by measuring (•) GaI, and (○) GaBr emissions.

rapidly in the vapour phase. From bond energy considerations, it would appear that 5 kcal mol^{-1} less energy is required to break a GaI bond with formation of HI than to break a GaBr bond with formation of HBr [16]. This would be sufficient to ensure that nearly all the final product of reaction of GaI_2Br with hydrogen atoms in the flame would be GaBr.

Determination of thallium

When thallium solutions containing any halide are injected into the Allen screw or the oxy-Allen screw cavity, only an intense thallium atomic emission is observed. In the oxy-cavity the spectrum of this emission shows three atom lines in the following order of intensity 377.5 > 535.0 > 351.0 nm. Thallium (25—225 ng in 5 μl) is thus determined quite sensitively. The emission from thallium(I) acetate is more intense than that from thallium(I) carbonate (Fig. 5), probably because of a difference in bond strength and volatility of the thallium salts. The calibration is linear up to 2.0 μg and the detection limit is 5 ng of thallium as acetate in 5 μl of solution. The relative standard deviation for 7 replicate measurements of 0.5 μg of thallium is 5%.

Potassium was found to enhance thallium emission, perhaps by suppression of thallium ionization in the hot environment of the oxy-cavity. Therefore, it may be used as an ionization suppressor in the determination of thallium. When the thallium standard solutions are prepared with addition of 1 mg K ml^{-1} as potassium nitrate, the sensitivity for thallium is improved by 45% compared to that obtained in the absence of potassium (Fig. 5).

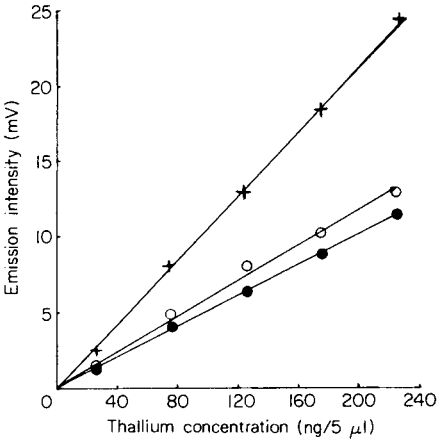

Fig. 5. Calibration graphs for thallium(I): (•) as its carbonate; (○) as its acetate; (×) as its acetate with addition of potassium nitrate.

Interferences

The effects of some cations and anions on the intensity of GeCl, GaI and Tl emissions were investigated. An interference is defined as significant if it causes a change in the emission intensity of more than two standard deviations. The results are shown in Table 2.

Several cations significantly depress the emissions from GeCl and GaI either by consuming the halide to form less volatile compounds (e.g. Ni, Cd, Zn) or themselves giving metal halide emissions (e.g. Cu(II), Co(II), Mn(II), Cr(III), Pb). Some anions, such as sulphate, phosphate and silicate, also suppress the emissions owing to the formation of less volatile germanium and gallium compounds. Selenium(IV) and tin(IV) give strong blue Se_2 and SnCl emissions that overlap the GeI emission. Iodide decreases the germanium emission, probably by forming the more stable GeI molecules. Likewise, the effect of bromide on gallium emission is due to the dissociation of the GaI molecules by the formation of the more stable GaBr molecules [16].

Of the many ions tested, only a few affect thallium atomic emission. The depressing effects from sulphate and phosphate are due to the formation of less volatile, more thermally stable thallium compounds. The suppressive effects of manganese(II) and gallium(III) could be due to formation of some less volatile material which occludes thallium, thus decreasing its emission intensity. These depressive effects can be eliminated by using a hotter flame and a cavity that heats up more quickly. Enhanced emissions are obtained in the presence of some other species. The effects of arsenic(III) and antimony(III) are due to their oxide emissions in the oxy-cavity [6] while the enhancement from potassium has been noted above. The maximum tolerable amounts of these interfering ions for the determination of 0.5 μg of thallium are 2.0 μg of Mn(II), Cu(II), Te(IV), SO_4^{2-} and PO_4^{3-}, 1.5 μg of As(III), Sb(III), Bi(III) and Ga, and 0.5 μg of K.

TABLE 2

The effect of some ions on the emissions obtained from 0.5 μg of germanium, 0.2 μg of gallium (in 0.04 M ammonium iodide) and 0.5 μg of thallium, in 5 μl solution

Added ion[a]	Change in intensity (%)			Added ion[a]	Change in intensity (%)		
	Ge	Ga	Tl		Ge	Ga	Tl
Na	0	−34	9	As(III)	—	—	35
K	—	−31	55	Sb(III)	—	—	36
Li	—	—	10	BO_3^{3-}	—	—	8
Ag	—	—	6	Ga	—	—	−20
Cu(II)	−53	−26	11	Sn(IV)	100	—	—
Cd	−69	—	−2	Te(IV)	—	—	16
Pb	−53	−42	1	Se(IV)	33	—	6
Ni	−93	−92	−3	Ge	—	−84	—
Co(II)	−53	−96	1	Cl^-	—	0	−2
Ca	—	0	—	Br^-	—	−59	−5
Ba	—	—	1	I^-	−44	—	7
Zn	−27	—	8	NO_3^-	−56	0	0
Mn(II)	−53	—	−15	Tartrate	−40	—	—
Bi	—	—	24	Acetate	—	0	0
Al	—	—	−5	Oxalate	—	[b]	—
Cr(III)	−76	—	−5	SO_4^{2-}	−25	−50	−11
Fe(III)	—	—	8	PO_4^{3-}	−39	−50	−17
In	—	—	0	SiO_4^{4-}	−100	[b]	—

[a] Amounts are 0.5 μg for Ge and Ga measurements and 5 μg for Tl measurements, except for the following: in Ge measurements, NO_3^-, SO_4^{2-}, PO_4^{3-} or tartrate = 0.25 μg and I^- = 0.75 μg, and in Ga measurements, Cl^-, NO_3^- or acetate = 5 μg.
[b] Almost complete suppression.

The effects of interfering ions can often be eliminated by selective liquid—liquid extraction of the element to be determined. For example, germanium tetrachloride may be extracted from hydrochloric acid into carbon tetrachloride [17] and the extract injected into the cavity. Although carbon tetrachloride itself gives a very weak bluish emission in the cavity, this procedure is slightly more sensitive than that in which aqueous solutions are applied (Fig. 3).

The authors thank (the late) Emeritus Professor R. Belcher and Dr. S. L. Bogdanski for their interest and advice. S. A. A. and I. Z. A. thank King Saud University for the provision of research scholarships.

REFERENCES

1 R. Belcher, S. L. Bogdanski, Z. M. Kassir, D. A. Stiles and A. Townshend, Anal. Lett., 7 (1974) 751.
2 R. Belcher, S. L. Bogdanski, S. A. Ghonaim and A. Townshend, Nature (London), 248 (1974) 326.

3 R. Belcher, S. L. Bogdanski, I. H. B. Rix and A. Townshend, Anal. Chim. Acta, 81 (1976) 325.
4 S. A. Ghonaim, Proc. Soc. Anal. Chem., 11 (1974) 167.
5 S. Liawruangrath, Ph.D. Thesis, Birmingham University, 1980.
6 M. Burguera, S. L. Bogdanski and A. Townshend, Crit. Rev. Anal. Chem., Vol. 10, December (1980) p. 185.
7 R. Belcher, S. L. Bogdanski, I. H. B. Rix and A. Townshend, Anal. Chim. Acta, 83 (1976) 119.
8 I. Z. Al-Zamil, Ph.D. Thesis, Birmingham University, 1978.
9 R. Belcher, S. L. Bogdanski and A. Townshend, Anal. Chim. Acta, 67 (1973) 1.
10 R. Belcher, S. L. Bogdanski and A. Townshend, Talanta, 19 (1972) 1049.
11 P. Deschampes, A. F. Robert and G. Pannetier, J. Chim. Phys., 65 (1968) 1084.
12 K. B. Rao and P. B. V. Haranath, J. Phys., B2 (1969) 1080.
13 I. H. El-Hag, Ph.D. Thesis, Birmingham University, 1982.
14 R. M. Dagnall, B. Fleet, T. H. Risby and D. R. Deans, Talanta, 18 (1971) 155.
15 R. M. Dagnall, K. C. Thompson and T. S. West, Analyst, 94 (1969) 643.
16 A. G. Gaydon, Dissociation Energies and Spectra of Diatomic Molecules, 3rd edn., Chapman and Hall, London, 1968, p. 110.
17 V. A. Nazarenko, Analytical Chemistry of Germanium, Wiley, New York, 1974, p. 82.

Analytica Chimica Acta, 143 (1982) 209—222
Elsevier Scientific Publishing Company, Amsterdam — Printed in The Netherlands

MICROLITER SAMPLE INTRODUCTION INTO AN INDUCTIVELY-COUPLED PLASMA BY ELECTROTHERMAL CARBON CUP VAPORIZATION

KIN C. NG and JOSEPH A. CARUSO*
Department of Chemistry, University of Cincinnati, Cincinnati, OH 45221 (U.S.A.)
(Received 3rd February 1982)

SUMMARY

An atomic emission spectrometric system is described for quantifying trace elements in microvolume samples. The system involves vaporizing the sample by electrothermal carbon cup vaporization followed by the atomization and excitation of the vapor cloud in an inductively coupled plasma (i.c.p.). The detection limits for 21 elements in 10-μl samples are at ng ml^{-1} and sub-ng ml^{-1} levels with linear dynamic ranges of over four orders of magnitude. Carbon cups coated with pyrolytic graphite are overcoated with tantalum carbide. These cups have resulted in improved detection levels (performances) for Al, As, Bi, Co, Cu and Sn relative to those not containing tantalum. However, cups not treated with tantalum are superior for Au, Cd, Ge, Hg, K, Li, Mg, Mn, Rb and Zn. Comparisons between the two types of carbon cups are presented and discussed. Results also are compared with literature values available for other electrothermal vaporization systems.

The inductively coupled plasma (i.c.p.) has been used increasingly as an excitation source for atomic emission spectrometry (a.e.s.). The i.c.p. allows the determination of elements at the ultratrace, trace, minor and major concentration levels with relative freedom from interferences [1]. When coupled with multichannel detection [1, 2], i.c.p.e.s. offers the advantage of multi-element determination [1—4]. The commonest sample introduction techniques used with the i.c.p. are solution nebulization [1, 2, 5]. Most standard instruments are equipped with pneumatic nebulizers which require sample input at the rate of ca. 1 ml min^{-1}. Other sample introduction techniques include the generation of elemental hydrides [6, 7] and cold mercury vapor [7]. Fassel [4] has described various modes of sample introduction into the i.c.p.

In many instances only limited sample is available so that microliter samples must be processed [8, 9]. Electrothermal graphite furnaces are capable of handling microliter samples. The samples are atomized in a graphite tube or cup and the free atoms are detected by atomic absorption spectrometry (a.a.s.) [9]. High sensitivity is obtained with this technique. However, the furnace method is subject to spectral background interferences, interelement interferences, nonspecific absorption or light scattering of the

0003-2670/82/0000-0000/$02.75

reference beam [10—13]. Generally, only single-element determinations are possible with the atomic absorption approach.

The combination of electrothermal vaporization into the i.c.p., coupled to a polychromator, should provide measurement of microliter samples on a simultaneous multi-element basis. In this system, the furnace is responsible for solvent removal, sample decomposition, and ultimately the vaporization of the sample, with the vaporized sample atomized and excited in the plasma. When the pneumatic nebulizer is used to convert sample solutions into aerosols, less than 10% of the aerosol reaches the plasma. In the plasma, considerable energy is spent in aerosol desolvation and chemical dissociation before the free atom or ion stage is reached. With the electrothermal sample vaporization/i.c.p. system, the samples are desolvated, removed from the matrix, and enter the plasma as a pulse of vapor. Therefore, the energy available from the plasma is more efficiently used in atomizing and exciting the sample. Detection limits approaching those of furnace a.a.s. are expected with this sample vaporization/i.c.p. system. Several workers have used electrothermal sample vaporization with various excitation cells for atomic fluorescence [14, 15] and atomic emission [16—23] spectrometry. Tantalum filaments have been used to vaporize samples into flames [16, 17], a microwave-induced plasma [18], and an i.c.p. [19]. Electrothermal graphite tubes [14] and graphite cups [15] have been used in conjunction with flames. Carbon cup [20] and carbon rod [21] furnaces have been used with the microwave-induced plasma. A graphite rod [22] has been used with the i.c.p.

The main disadvantage in using metals as the resistively heated element is that they become brittle after reacting with sample matrices [18] and with air [24]. At high temperatures, enough of the substrate metal vaporization may interfere with some of the analytical lines. Moreover, the metal filaments employed are relatively expensive. Therefore, graphite remains the preferred material for making vaporization cells. Graphite, however, has disadvantages such as porosity which can lead to the accumulation of analytes, formation of stable carbides, memory effects, and poor precision. To reduce the porosity and to minimize the formation of stable carbides for certain elements, the graphite surface can be coated with pyrolytic graphite [25—27]. Similar beneficial effects can be obtained by coating with stable metal carbides. The pyrolytic coating is readily removed at temperatures exceeding 2800°C and occasional recoating is necessary, whereas metal carbide coatings are more stable at high temperatures. Zatka [28] found improved useful life and greater long-term response stability for tantalum carbide-coated graphite tubes compared to simple pyrolytically coated tubes. Improved sensitivities were reported when metal carbide-coated tubes were used for Be, Cr, Mn, and Al [29], Sn [30—32]. Si [33], Pb [34], Y [35], Se and As [32]. The most popular metals used for the treatment of graphite tubes or cups to form refractory carbides are Ta [28, 30, 33, 35], Zr [29—32, 34, 35] and La [29, 35, 36].

This paper reports on the analytical utility of the electrothermal sample vaporization/i.c.p. system for 21 elements with treated carbon cups as electrothermal vaporization cells. The pyrolytically-coated carbon cups are overcoated with tantalum carbide. The performances of the pyrolytically-coated and tantalum-treated carbon cups are compared.

EXPERIMENTAL

Equipment

The i.c.p.e.s. equipment was the same as reported earlier [2]. The radio-frequency generator, impedance matching network, and torch enclosure are available commercially (Plasma-Therm Model HFP-2500D, Kresson, NJ). The load coil was 3 turns of 1.4-mm copper tubing. The external optic used was a 5-cm diameter concave mirror with a focal length of 7.5 cm. Emission radiation was focused onto the entrance slit of a 0.85-m Spex Model 1402 double monochromator (Spex Industries, Metuchen, NJ). Gratings were blazed at 300 nm and ruled at 1200 grooves/mm. The entrance and exit slits were set at 30 μm, and the intermediate slit was set at 250 μm. The output of the photomultiplier (RCA-4837) was taken by a laboratory-constructed d.c. amplifier. Signals were recorded by using either a Hewlett-Packard Model 7101B or OmniScribe Model B-5000 recorder.

The electrothermal vaporizer design was as described earlier [20], and is similar in design to that of Nixon et al. [19] and Gunn et al. [22], with electrode blocks resembling those of the Varian-Techtron atomizers [37]. Each electrode block was water-cooled independently. The top part of the pyrolytically-coated carbon cups (Ultra Carbon) were removed for more efficient heating [20]. The carbon cup was mounted between two carbon electrodes. The glass dome (inner volume $\approx$280 ml) was sealed to the aluminum base by using electrical tape. The electrothermal vaporizer assembly was positioned directly underneath the i.c.p. torch. The two were connected via 18 cm of teflon tubing (4.2 mm i.d.). The electrothermal vaporizer sample delivery port could be reached from the back of the torch enclosure. The vaporizer power supply was that of a Varian-Techtron Model 63 Carbon Rod Atomizer. Samples were delivered with disposable 10-μl capillary pipets (Drummond Wiretrol Micropipettes).

Reagents

Tantalum metal powder (Matheson Coleman and Bell) was capacitor grade. Other chemicals used were reagent grade. Most stock solutions were prepared by dissolving pure metals or reagent-grade salts in dilute acid or deionized distilled water. Other stock solutions were commercially available atomic absorption standards (Fisher Scientific Company). Working standard solutions were prepared by appropriate dilution of the stock solution.

Tantalum soaking solution. A 6% (w/v) tantalum solution was prepared as described by Zatka [28]. Tantalum powder (3 g) was placed in a 100-ml

PTFE beaker, and 10-ml of dilute hydrofluoric acid (51%) was added followed by 3 g of oxalic acid dihydrate and 1 ml of 30% hydrogen peroxide. The mixture was heated and more of the 30% hydrogen peroxide was added drop by drop until all the tantalum powder had dissolved. Then another 3 g of oxalic acid dihydrate and more distilled water were added. This soaking solution (50 ml) was stored in a polyethylene bottle.

Cup carbidization

The cup treatment procedures were similar to those described by Zatka [28]. The pyrolytically-coated carbon cups were soaked in the 6% tantalum solution for 24 h at atmospheric pressure. The cups were dried in air for 1 h, and then in an oven at 105°C for 1 h. Each cup was mounted between the electrodes of the vaporizer. With the argon carrier gas flowing, the dry, ash and atomize stages were set sequentially at 1.30, 3.69 and 10.08 V for 60, 30 and 10 s, respectively, followed by a repetition of the three stages at 1.3, 3.69 and 13.25 V for 60, 30 and 5 s, respectively. Then 20 μl of the 6% tantalum solution was deposited into the cup and the vaporizer power supply was again fired twice. The development of a gold-colored cup indicated the formation of a tantalum carbide surface [38].

Procedures

After the plasma was ignited, the coolant gas flow, carrier gas flow, power and viewing height were adjusted to the compromise conditions listed in Table 1. The dry, ash and atomize stages of the vaporizer power supply were then set as listed in Table 2. The appropriate wavelength for each element was selected by aspirating the solution containing the analyte and setting on maximum intensity in the wavelength region of interest. The pneumatic nebulizer was then disconnected from the plasma torch and replaced by the carbon cup vaporizer. Then 10 μl of sample solution was deposited into the cup and the firing sequence was initiated. The desolvated, vaporized sample was carried into the plasma by the argon carrier gas.

RESULTS AND DISCUSSION

Tantalum carbide treatment

Among the metals possible (Ta, Zr, La, Mo, V, W and Ti) for forming carbides, tantalum forms the most stable carbide. It has a melting temperature

TABLE 1

Compromise operating conditions

Parameter	Compromise condition
Generator forward power	1000 W
Reflected power	$\leqslant$ 5 W
Argon coolant flow	13 l min^{-1}
Carrier gas flow	0.4 l min^{-1}
Viewing height	18 mm

TABLE 2

Carbon cup vaporizer power supply settings[a] (Varian-Techtron CRA 63 Atomizer)

Element	Ash (10 s)		Atomize (1.5 s)	
	Setting[b]	Actual voltage (V)	Setting[b]	Actual voltage (V)
Ag	6	3.03	7.5	10.92
Al	6	3.03	10	13.25
As	6	3.03	9	13.21
Au	6	3.03	8	12.25
Bi	6	3.03	6.5	9.17
Cd	6	3.03	7.5	10.92
Co	7	3.69	10	13.25
Cr	7	3.69	10	13.25
Cu	6	3.03	8	12.25
Fe	6	3.03	9.5	13.21
Ge	6	3.03	9	13.21
Hg	0	0.38	4	5.98
K	0	0.38	7.5	10.92
Li	6	3.03	7.5	10.92
Mg	6	3.03	7.5	10.92
Mn	6	3.03	7.5	10.92
Ni	6	3.03	10	13.25
Pb	6	3.03	7.5	10.92
Rb	0	0.38	6	8.38
Sn	6	3.03	7.5	10.92
Tl	6	3.03	7.5	10.92
Zn	6	3.03	5.5	7.61

[a]The dry setting was chosen for the most efficient drying of sample. It varied from cup to cup. It was set at 4.5—5.5 (actual voltages 1.08—1.30 V) for 30—60 s. [b]The setting dial is incremented 0—10.

of 3983°C [38], is relatively chemically inert and is not decomposed by water [28]. The soaking solution contains a weak mixture of hydrofluoric acid and oxalic acid so that the carbon cups are not easily destroyed [28]. Vickrey et al. [32] have found that by using metal complexes such as zirconyl acetate, uniform coatings were obtainable. Alkaline molybdate or tungstate solutions, however, produced uneven coatings on the surfaces. Increased coating efficiencies were reported when molten metal chlorides were used [39], yet these coated surfaces degraded rapidly.

The chemical form of the tantalum in the present soaking solution may be a metal complex of tantalum oxalate and, therefore, a uniform coating using this tantalum soaking solution might be expected. In fact, after the cups have gone through the carbide-formation process, the surface became gold colored. This color has been attributed to tantalum carbide [38]. These treated cups appear to be stable in air indefinitely. The gold appearance of the cups becomes lighter as more atomizations are done. This is attributed to the progressive diffusion of the tantalum into the cups until the concentration is uniform. With a similar coating procedure, Vickrey et al. [32] and Wahab

and Chakrabarti [35] have shown by electron micrography, uniform tantalum concentration profiles across the tantalum-treated surfaces. Vickrey et al. [32] also found a decrease in zirconium concentration in the zirconium-treated cups after 62 firings, the loss being greater from the inside surfaces. They attributed this effect partially to the chemical attack of samples on the interior of the tubes. The coating procedures described here involve treating the entire cup with the 6% tantalum solution. Then 20 μl of the 6% tantalum solution was deposited inside the cup subjecting it to a second coating treatment. It is believed that the cup interior is more chemically resistive with this second coating. Wahab and Chakrabarti [35] have found greater effectiveness from the twice tantalum-treated surfaces. Zatka [28], using an optical pyrometer, found the temperatures achieved from tubes treated twice with tantalum carbide and the regular tubes to be essentially the same.

Operating parameters

The operating parameters investigated were the observation height in the plasma, carrier gas flow rate, drying, ashing and atomization settings. Compromise observation height and carrier gas flow rate were chosen for all experiments (Table 1). These operating conditions allow for potential simultaneous multi-element detection.

The setting of the drying stage of the vaporizer power supply was found to be critical. Care must be taken not to spatter the sample by boiling. The precision of the signals depends heavily on this parameter. It was found that the drying response varied from cup to cup. Drying settings at 1.08—1.30 V for 30—60 s were commonly used. For aqueous samples, the ashing setting should not be necessary. However, when this setting was used, a more reproducible atomization stage could be reached. The atomization setting was not critical. It was chosen to remove completely any analyte from the cup. Careful optimization of this setting was found to be unnecessary. Voltage settings higher than that chosen did not improve the signal intensity, yet tended to decrease the lifetime of the cup. Also, the cup separated more easily from the graphite supporting electrodes with longer atomization times and higher atomization voltages (12.25—13.25 V). The vaporizer operating conditions for the various elements are shown in Table 2. It can be seen that many elements yield optimal response at a single setting.

Background response profile

Figure 1 shows the complete response profile of a blank sample in the dry, ash and atomize steps. The background drop is caused by the temporary change of argon carrier gas flow as the cup temperature increases, causing expansion of the gas and inducing a higher argon flow rate. After the cup has cooled, the background signal level returns to its initial state.

The extent to which the background changes at point C (Fig. 1) depends on several parameters: carrier gas flow, observation height, atomization voltage and wavelength. With an increase of carrier gas flow or observation height, the change is lessened. An increase in the atomization voltage would extend the drop in signal. At the zinc (214 nm) and lithium (671 nm) wave-

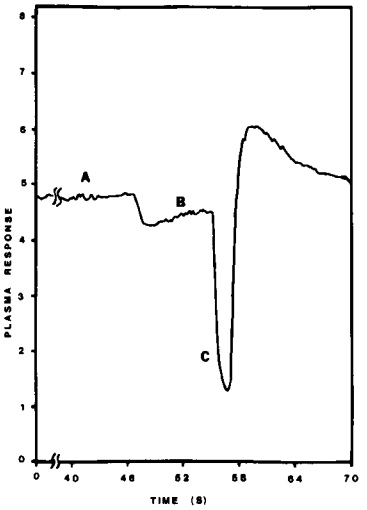

Fig. 1. Typical background response profile. A, Blank drying stage (30—60 s); B, Blank ashing stage (10 s); C, Blank atomizing stage (1.5 s). Response is given in arbitrary units.

lengths, no background intensity changes were seen, probably because the background signal decreased, on account of the lower sensitivity available in these regions from the grating blaze combined with the photomultiplier response.

Signal response profile

The emission signals produced by the elements investigated can be grouped into four different types (Fig. 2). The signal intensity is measured from the point where the vaporization starts to the tip of the peak. With type A, B and C blank signal regions, it is difficult to determine a meaningful noise level, which precludes detection limits in the usual 2 or 3σ fashion.

Changes of experimental parameters such as the carrier gas flow and observation height did not shift the analyte signal position whereas changes of the atomization voltage did. For example, if a lower atomization voltage was set for elements giving type A signals (Fig. 2), then the signal would change to resemble type B signals. Yet the signal intensities with the two different atomization voltage settings for the same sample were essentially the same and therefore no attempt was made to match signal positions. A single atomization voltage setting was chosen for many elements. Regardless of the analyte concentration, its signal appeared at the same position. Also, higher ashing settings shifted the signal position to the left by affecting the production of a deeper baseline well. It is apparent that even when the atomization voltage was kept constant, the change in the ashing setting changed the atomization temperature, i.e., the higher ashing settings result in higher atomization temperatures.

Comparison of cups with and without tantalum treatment

For most of the elements studied, the pyrolytically-coated carbon cups

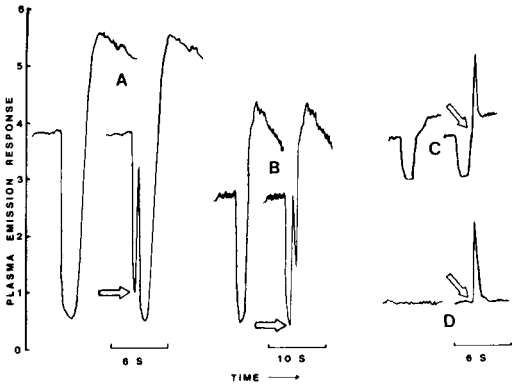

Fig. 2. Types of emission signal profiles compare to their blanks at the selected vaporization voltages (Table 2). Arrows point at vaporization starts. A, Signal type for Ag, As, Bi, Cd, Ge, Hg, K, Pb, Sn, Tl; B, Signal type for Au, Co, Cr, Cu, Fe, Mg, Mn, Rb; C, Signal type for Al, Ni; D, Signal type for Li, Zn. Response is given in arbitrary units.

TABLE 3

Comparison of pyrolytically-coated cups with and without tantalum treatment

Element	Ratio of signals from Ta-treated cup to untreated cup[a]	Comments	
		Ta-treated cup	Untreated cup
Ag	1.0		
Al	3.5		
As		Sharp single peak	Broad band, multiple peaks
Au	0.63		
Bi	1.5		
Cd	0.27		
Co	1.8	Memory[b]	No memory
Cr		Memory[c]	Memory[c]
Cu	0.51	No memory	Memory[c]
Fe	1.1		
Ge	0.088		
Hg	0.49		
K	0.17		
Li	0.037	Memory[c]	No memory
Mg	0.44		
Mn	0.23		
Ni	1.1		
Rb	0.33		
Sn	5.6		
Tl	1.0		
Zn	0.17		

[a]Mean of $\geqslant 5$ measurements. [b]Needs two decontamination firings. [c]Needs five decontamination firings.

without tantalum gave higher sensitivities. However, for As, Sn, Bi, Al and Co, the tantalum-treated cups gave higher emission signals (Table 3). Both kinds of cup had memory effects with some elements; this detracts from the application of the technique. For copper (Fig. 3), the cup without tantalum treatment shows severe memory effects and at least five decontamination firings are needed to reduce the signal to baseline; yet with the tantalum-treated cup, there is no memory. In contrast, for lithium (Fig. 4), a severe memory effect is shown by the tantalum-treated cup, possibly because a less volatile Ta—C—Li species is formed. At the highest atomization voltage (13.25 V), this lithium signal becomes a multiple peak but the memory effects remain. Cobalt exhibited a slight memory effect with the tantalum-treated cup but not with the plain pyrolytically-coated cup (Table 3). Severe memory for chromium resulted from both types of cup, but no memory effects were noted for any other element studied.

Peak heights were measured so that sharp signals were essential. For arsenic, the broad band peaks obtained from cups without tantalum (Fig. 5) were not improved by changing the atomization voltage, but signals were sharp with tantalum-treated cups. The tantalum carbide surface apparently prevents decomposition at lower temperatures. Millard et al. [23], using a graphite rod/i.c.p. system, found stabilization and enhancement of arsenic emission in the presence of chromium, whereas chromium depressed cadmium emission. In the present study, a four-fold depression of the cadmium emission intensity was noted in the presence of tantalum (Table 3). Toth [38] discussed the phenomena of compound formation between metal and transition metal carbides and stated that some of these compounds have stable crystal structures.

The data in Table 3 are consistent with those reported in the literature for aluminum [29], tin [30—32] and arsenic [32]. This suggests that metal

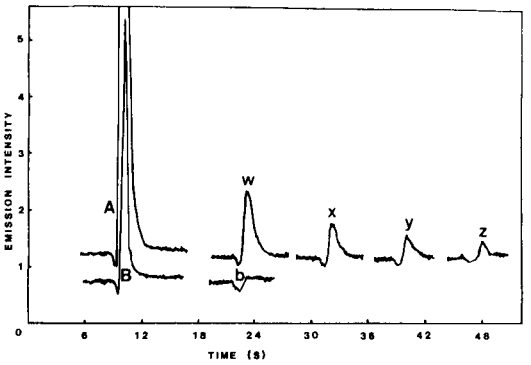

Fig. 3. Copper emission signals from 100 ng Cu. A, Signal obtained with a pyrolytically-coated carbon cup at an atomization voltage of 12.25 V, with the memory shown in subsequent decontamination firings: (w) 12.25 V; (x) 13.21 V; (y) 13.21 V; (z) 13.21 V. B, Signal obtained with a Ta-treated carbon cup at an atomization voltage of 12.25 V, with no memory effect in the decontamination firing b (12.25 V). Times given are relative and only to illustrate peak widths.

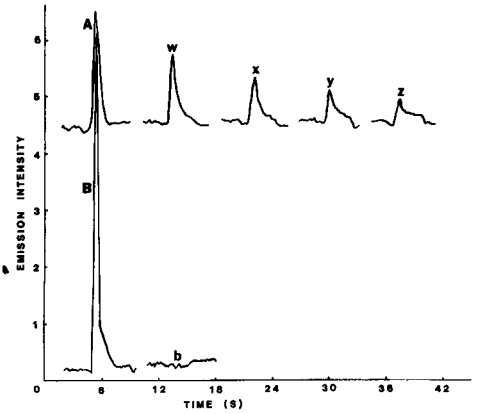

Fig. 4. Lithium emission signal. A, Signal for 10 ng Li obtained with a Ta-treated cup at an atomization voltage of 10.92 V, with the memory shown in subsequent decontamination firings: (w) 13.21 V; (x) 13.25 V; (y) 13.25 V; (z) 13.25 V. B, Signal for 1 ng Li obtained with a pyrolytically-coated cup at an atomization voltage of 10.92 V, with no memory effect in the decontamination firing b (10.92 V). Times given are relative and only to illustrate peak width.

carbide formation on graphite surfaces is useful for some elements in both the a.e.s. and a.a.s. techniques.

Element responses to the different cups

Both the tantalum-treated cups and the plain pyrolytically-coated cups show similar signal precision for most elements. Therefore, the cup surface porosity is probably not a major factor influencing atomization efficiency. The chemical composition of the cup surface, however, appears to be a

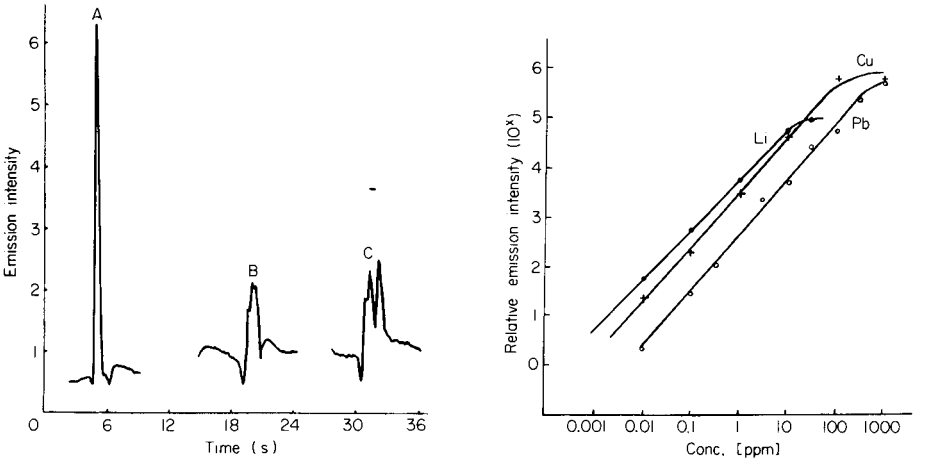

Fig. 5. Arsenic emission signals from 100 ng As. A, Ta-treated cup at scale expansion x; B and C, cups without Ta-treatment at scale expansion $2x$.

Fig. 6. Typical calibration curves covering over four orders of magnitude obtained by the proposed system.

primary contributor to the different responses from the elements. At the selected vaporization/atomization temperature (Table 2), vaporization (atomization), carbide formation and tantalum-carbide compound formation are competitive processes. When the pyrolytically-coated carbon cups are used, atomization and carbide formation are the competing processes. The tantalum-carbide surface restricts simple carbide formation with the element, but it may react with the sample elements to form ternary compounds. Vaporization and ternary compound formation are then the competitive processes.

Data from Table 3 give some indication concerning the processes operative for each element. In the cases of Al, Bi, Co, Cu, Sn and Cr, carbide formation is favored in the plain pyrolytically-coated cups. For Cu and Cr, compound formation is favored in the tantalum-treated cups. Ag, Fe, Ni and Tl do not form carbides nor compounds with Ta—C and are free to vaporize. For As, Au, Li, Cd, Ge, Hg, K, Mg, Mn, Rb and Zn, vaporization (atomization) is the dominant process in the pyrolytically-coated cups. However, when the tantalum-treated cups are used for these elements, compound formation predominates. The element vaporization efficiency in this process depends on the volatility of the generated Ta—C compounds.

Detection limits

As shown in Fig. 2, a single atomization voltage setting for many elements can result in four possible types of analyte signal, and it is difficult to associate a noise level with signals of type A, B and C, even at higher scale expansions. Therefore, the detection limit for metals giving such signals at the selected amplification settings is defined as the concentration of the element which gives a minimal detectable signal (1/4 of one chart paper block). Hence, these are subsequently referred to as lowest quantifiable levels. For the type D signals (Fig. 2), the detection limit is defined as the analyte concentration that gives a signal twice the standard deviation of the background noise.

The lowest quantifiable levels and detection limits for the present system are compared to those obtained by conventional continuous solution nebulization and non-flame atomic absorption in Table 4. Values obtained in this laboratory [2] with the same instrument and standards with continuous solution nebulization, are included to validate the comparisons. Overall, the present electrothermal sample vaporization/i.c.p. system gives superior lowest quantifiable levels and detection limits compared to continuous solution nebulization.

When compared to graphite-furnace a.a.s., the values are equal or somewhat worse. Of course, with graphite-furnace a.a.s., the analyte transport efficiency is considerably higher than with the electrothermal cup/i.c.p. system. In the latter, some of the vaporized analytes undoubtedly deposit on the inner surface of the glass dome, the connecting teflon tubing, as well as the injector tube of the plasma torch. Thus, a substantially smaller portion of analyte reaches the plasma.

TABLE 4

Detection limits

Element	Wavelength (nm)	Detection limits (ng ml^{-1})		
		I.c.p. carbon cup vaporization[a]	I.c.p. continuous solution nebulization	G.f.a.a.s. model 63 CRA[b]
Ag	328.1	0.3[c,e]	7[g]	0.04
Al	396.2	2[d,e]	28[g]	6.0
	236.7	—	83[h]	
As	228.8	20[d,e]	83[g]	20
Au	242.8	1[c,e]	17[g]	2.0
Bi	289.8	10[d,e]	330[g]	1.4
Cd	228.8	1[c,e]	3[h]	0.02
Co	238.9	3[c,e]	6[g]	1.2
Cu	324.8	1[d,e]	1[h]	1.4
Fe	372.0	3[c,e]	—	0.6
	259.9	—	4[h]	
Ge	303.9	1[c,e]	—	—
	209.4	—	40[g]	
Hg	253.7	1[c,e]	61[g]	20
K	404.7	300[c,e]	43000[g]	0.18
Li	670.8	0.6[c,f]	—	
	460.3	—	857[g]	1.0
Mg	285.2	0.01[c,e]	1.6[g]	0.012
	279.6	—	0.2[h]	
Mn	279.5	0.1[c,e]	—	0.1
	257.6	—	0.8[h]	
Ni	352.5	4[d,e]	45[g]	2.0
Pb	405.8	10[c,e]	272[g]	1.0
Rb	420.2	280[c,e]	38000[g]	1.2
Sn	317.5	5[d,e]	214[g]	12
Tl	377.6	5[c,e]	230[g]	0.6
Zn	213.9	0.3[c,f]	9[h]	0.016

[a]10-μl samples. [b]5-μl samples; no wavelength given [40]. [c]Pyrolytically-coated cups. [d]Ta-treated cups. [e]Lowest quantifiable level (see text for explanation). [f]Detection limit = 2σ of background noise. [g]Ref. 41. [h]Ref. 2.

The detection limits and lowest quantifiable levels are also compared to those obtained by similar techniques in Table 5. Overall, the present carbon cup vaporization/i.c.p. technique produces levels equal or superior to those of carbon cup vaporization/microwave-induced plasma [20], tantalum filament vaporization/i.c.p. [19] and graphite rod vaporization/i.c.p. [22].

Precision and linear range

Typical precisions in signal intensity measurements have 10% (or less) relative standard deviations whether or not the cups are treated with tantalum. For example, the relative standard deviations for ten consecutive runs were 6% for 0.1 ng Mn, 8% for 1 ng Sn, and 2% for 100 ng Pb. These figures represent the total uncertainty associated with sample deposition, vaporization temperatures, analyte transport and the stability of the plasma.

TABLE 5

Comparison of detection limits

Element	λ (nm)	Detection limits (pg)			
		Carbon cup-i.c.p.[a]	Carbon cup-m.i.p.[b]	Ta filament-i.c.p.[c]	Graphite rod-i.c.p.[d]
Ag	328.1	3[e]	—	10	1
Al	396.2	20[f]	—	—	—
As	228.8	200[f]	—	—	—
	193.7	—	200	1000	2000
Au	242.8	10[e]	—	—	—
	267.6	—	—	—	10
Bi	289.8	100[f]	—	—	—
	223.1	—	100	—	—
	306.8	—	—	200	—
Cd	228.8	10[e]	4	600	30
Co	238.9	30[e]	—	—	—
	240.7	—	70	—	—
Cu	324.8	10[f]	—	—	—
Fe	372.0	30[e]	—	—	—
Ge	303.9	10[e]	—	—	—
Hg	253.7	10[e]	—	200	60
K	404.7	3000[e]	—	—	—
Li	670.8	6[e,g]	—	—	4
Mg	285.2	0.1[e]	—	—	—
Mn	279.5	1[e]	—	—	—
	257.6	—	—	3	1
Ni	352.5	40[f]	—	—	—
	232.0	—	100	—	—
Pb	405.8	100[e]	80	300	100
Rb	420.2	2800[e]	—	—	—
Sn	317.5	50[f]	—	2000	—
	286.3	—	300	—	—
Tl	377.6	50[e]	—	—	—
	535.1	—	—	300	60
Zn	213.9	3[e,g]	5	—	20

[a]Present system. Unless otherwise noted, lowest quantifiable levels are listed. [b]Data from [20]. [c]Data from [19]. [d]Data from [22]. [e]Pyrolytically-coated cups. [f]Ta-treated cups. [g]Detection limit = 2σ of background noise.

Figure 6 illustrates typical calibration curves obtained by the present system. Linear ranges of over four orders of magnitude are attainable with this carbon cup/i.c.p. combination.

Conclusions

The electrothermal carbon cup sample vaporization/inductively coupled plasma combination is an efficient and sensitive technique for trace element determination of microliter sample volumes. A study of the influence of tantalum coating on the pyrolytically-coated cup surface for 21 elements showed that the vaporization efficiency depends on the dominant reaction process

between the analyte and the cup surface composition. With a proper choice between the tantalum-treated carbon cups and the plain pyrolytically-coated carbon cups, high sample vaporization efficiency is obtained for each of the elements investigated. Undesirable features for some elements such as memory effects and multiple peak/broad band formation can also be circumvented.

The authors are grateful to the National Institute of Occupational Safety and Health for support of this work through grant No. OH-00739.

REFERENCES

1 V. A. Fassel, Science, 202 (1978) 183.
2 J. P. McCarthy, M. E. Jackson, T. H. Ridgway and J. A. Caruso, Anal. Chem., 53 (1981) 1512.
3 P. W. J. M. Boumans, Science and Industry, No. 12 (1978) 1.
4 V. A. Fassel, Anal. Chem., 51 (1979) 1290A.
5 C. E. Taylor and T. L. Floyd, Appl. Spectrosc., 35 (1981) 408.
6 M. A. Eckhoff, J. P. McCarthy and J. A. Caruso, Anal. Chem., 54 (1982) 165.
7 A. F. Ward, 28th Pittsburgh Conference on Anal. Chem. and Appl. Spectrosc., Cleveland, OH, 1977, Abstract No. 310.
8 H. Uchida, Y. Nojiri, H. Haraguchi and K. Fuwa, Anal. Chim. Acta, 123 (1981) 57.
9 H. T. Delves, Prog. Anal. At. Spectrosc., 4 (1981) 1.
10 T. W. West, Pure Appl. Chem., 50 (1978) 837.
11 D. C. Manning, At. Absorpt. Newsl., 17 (1978) 107.
12 H. Massmann, Z. El Gohary and S. Gücer, Spectrochim. Acta, Part B, 31 (1976) 399.
13 W. K. Robbins, Am. Lab., August (1975) 23; September (1975) 38.
14 J. Ip, Y. Thomassen, L. R. P. Butler, B. Radziuk and J. C. Van Loon, Anal. Chim. Acta, 110 (1979) 1.
15 S. K. Hughes and R. C. Fry, Appl. Spectrosc., 35 (1981) 26.
16 M. R. McCullough and T. J. Vickers, Appl. Spectrosc., 48 (1976) 1006.
17 J. K. Grime and T. J. Vickers, Anal. Chem., 47 (1975) 432.
18 F. L. Fricke, O. Rose, Jr. and J. A. Caruso, Talanta, 23 (1976) 317.
19 D. E. Nixon, V. A. Fassel and R. N. Knisely, Anal. Chem., 46 (1974) 210.
20 F. L. Fricke, O. Rose, Jr. and J. A. Caruso, Anal. Chem., 47 (1975) 2018.
21 J. F. Alder and M. T. C. Da Cunha, Can. J. Spectrosc. 25 (1980) 32.
22 A. M. Gunn, D. L. Millard and G. F. Kirkbright, Analyst, 103 (1978) 1066.
23 D. L. Millard, H. C. Shan and G. F. Kirkbright, Analyst, 105 (1980) 502.
24 F. J. Langmyhr, Analyst, 104 (1979) 993.
25 D. D. Siemer, R. Woodriff and B. Watne, Appl. Spectrosc., 28 (1974) 582.
26 D. C. Manning and R. D. Ediger, At. Absorpt. Newsl., 15 (1976) 42.
27 F. J. Szydlowski, E. Peck and B. Bax, Appl. Spectrosc. 32 (1978) 402.
28 V. J. Zatka, Anal. Chem., 50 (1978) 538.
29 J. H. Runnels, R. Merryfield and H. B. Fisher, Anal. Chem., 47 (1975) 1258.
30 H. Fritzsche, W. Wegscheider, G. Knapp and H. M. Ortner, Talanta, 26 (1979) 219.
31 T. M. Vickrey, G. V. Harrison, G. J. Ramelow and J. C. Carver, Anal. Lett., 13 (1980) 781.
32 T. M. Vickrey, G. V. Harrison and G. J. Ramelow, Anal. Chem., 53 (1981) 1573.
33 D. J. Lythgoe, Analyst, 106 (1981) 743.
34 T. M. Vickrey, G. V. Harrison and G. J. Ramelow, Atom. Spectrosc., 1 (1980) 116.
35 H. S. Wahab and C. L. Chakrabarti, Spectrochim. Acta, Part B, 36 (1981) 463.
36 J. E. Poldoski, Anal. Chem., 52 (1980) 1147.
37 J. P. Matousek, Am. Lab. June (1971) 45.
38 L. E. Toth, Transition Metal Carbides and Nitrides (Refractory Materials, Vol. 7), Academic Press, New York, 1971.
39 M. C. Almeida and W. R. Seitz, Pittsburgh Conference on Anal. Chem. and Appl. Spectrosc., Atlantic City, NJ, March 1980, Abstract No. 590.
40 B. N. Noller, H. Bloom and A. P. Arnold, Prog. Anal. At. Spectrosc., 4 (1981) 81.
41 R. K. Winge, V. J. Peterson and V. Å. Fassel, Appl. Spectrosc., 33 (1979) 206.

Analytica Chimica Acta, 143 (1982) 223—228
Elsevier Scientific Publishing Company, Amsterdam — Printed in The Netherlands

ELECTROTHERMAL ATOMIC ABSORPTION SPECTROMETRIC DETERMINATION OF SELENIUM IN BLOOD SERUM AND SEMINAL FLUID AFTER PROTEIN PRECIPITATION WITH TRICHLOROACETIC ACID

KHALID SAEED and YNGVAR THOMASSEN*
Institute of Occupational Health, Gydas vei 8, Oslo 3 (Norway)
(Received 11th June 1982)

SUMMARY

The determination of selenium in body fluids by electrothermal atomic absorption spectrometry (e.a.a.s.) suffers from severe spectral interferences from phosphate which results in overcompensation when a continuum-source background corrector is used. The separation of selenium from phosphate by protein precipitation with trichloroacetic acid allows the determination of selenium in blood serum and seminal fluid by e.a.a.s. after thermal stabilization with silver, nickel or copper. The selenium concentration in seminal fluid from healthy, fertile Norwegian donors ranged from 0.09 to 1.30 μmol l^{-1} with a group average of 0.44 μmol l^{-1} (n = 15).

Direct determination of selenium in biological fluids by electrothermal atomic absorption spectrometry (e.a.a.s) is complicated because deuterium arc background correction is unable to compensate for structured non-specific absorption signals present at the 196.0-nm selenium resonance line. Uncorrectable signals are recorded from biological matrices containing iron and phosphates at wavelengths below 220 nm [1, 2]. If such interfering signals are not suppressed or eliminated, the possibility of introducing serious systematic errors is greatly increased. Recently, it has been demonstrated that overcompensation signals originating from calcium phosphate in blood serum are depressed in the presence of high concentrations of metals [2]. The direct e.a.a.s. procedure for determination of selenium in blood serum is not useful for matrices richer in phosphates, such as seminal fluid. Among others, Awwad et al. [3] showed that selenium in blood serum is protein-bound and that virtually all may be precipitated with trichloroacetic acid. This paper describes the separation of selenium by trichloroacetic acid protein precipitation from the interfering phosphate in human serum and seminal fluid with subsequent determination by e.a.a.s.

EXPERIMENTAL

Apparatus, reagents and standard solutions

A Perkin-Elmer model 5000 atomic absorption spectrometer equipped with selenium electrodeless and deuterium arc lamps, an HGA-500 graphite furnace, an AS-40 automatic sampler and a Perkin-Elmer model 56 recorder were used. The furnace was purged with argon. The γ-radiation was measured with a Packard Auto-Gamma scintillation spectrometer.

The reagents employed were of analytical-reagent grade. Commercially available 1000 ppm standard solutions (BDH) of copper (as nitrate), iron and selenium were used. Stock 1000 and 5000 ppm solutions of nickel and silver, respectively, were obtained by dissolving suitable amounts of the appropriate nitrate in distilled water. Stock solutions of trichloroacetic acid (50%), sodium hydroxide (58%), urea (48%), ammonia (10%) and guanidinium chloride (57%) were prepared in distilled water. Working solutions were prepared daily.

A ^{75}Se radionuclide in the form of sodium selenite (Radiochemical Centre, Amersham, Gt. Britain) was used to prepare the in-vivo labelled organoselenium compounds in whole blood as described elsewhere [4].

Procedures

Preparation of seminal fluid. After sampling, the semen was centrifuged for 10 min at 1000 rpm. The supernatant fluids were then kept frozen until required.

Distribution *of selenium in blood proteins.* To a test tube containing 2 ml of 10% trichloroacetic acid solution, 1 ml of rat blood labelled with ^{75}Se was added dropwise. The tube was shaken vigorously and the activity of the mixture was counted. The supernatant liquid was separated carefully from the denatured proteins by centrifugation at 3700 rpm for 10 min prior to counting their separate activities.

Separation and dissolution of serum and seminal fluid proteins. To a test tube (graduated at exactly 2 ml) containing 1 ml of 10% trichloroacetic acid solution, 0.2 ml of the sample was added dropwise. The protein precipitates were separated as described above and dissolved in one of the following ways.

(a) After addition of 2 ml of 65% nitric acid, the mixture was heated until the precipitate had completely dissolved. The solution was evaporated to a very small volume (but not to dryness), and the cooled sample was diluted to volume (2 ml) with distilled water.

(b) A 0.5-ml portion of 10% ammonia solution was added, and the mixture was shaken vigorously until the precipitate had completely dissolved. The sample was diluted to volume (2 ml) with distilled water.

(c) As (b), but with 58% guanidinium chloride.

Recommended procedure for selenium determination. A 0.2-ml portion of sample was dissolved as described in (b) above. Then 20 μl was injected into the furnace, followed by 30 μl of 0.1% silver nitrate solution, and the furnace program was run as given in Table 1. This was repeated for solutions to which standard additions of selenium had been made.

TABLE 1

Furnace program[a]

	Temp. (°C)	Ramp/hold (s)
Dry	110	5/60
	140	20/10
	170	10/5
Ash	800	5/15
		Baseline 5
Atomize	2200	0/5
	Recorder —6	Baseline —1
Clean out	2700	1/1

[a]Pyrolytically-coated tubes were used with an internal argon flow of 20 ml min^{-1} during atomization.

RESULTS AND DISCUSSION

Whole blood

As selenium in whole blood and serum is mainly bound to proteins [3, 5], a separation procedure which permits the determination of selenium in the protein fraction may eliminate the spectral interference from calcium phosphate described earlier [2]. Most proteins can be completely precipitated from aqueous solutions by the addition of certain acids, such as trichloroacetic and perchloric acids. The precipitation of eight aliquots of rat blood containing in-vivo ^{75}Se-labelled proteins with 10% trichloroacetic acid solution showed an average recovery of 97.4% of the total ^{75}Se (r.s.d. 1.5%). This shows that precipitation of selenium containing proteins with trichloroacetic acid is quantitative and reproducible and that selenium is bound to high-molecular-weight proteins.

A substantial amount of work was done in order to redissolve the precipitated proteins. Prime consideration was given to those procedures which involved simple but rapid dissolution. Considerable difficulties were encountered in the dissolution of whole-blood proteins when urea, guanidinium chloride, mercaptoethanol or ammonia was employed. Direct addition of these reagents to the precipitates resulted in only slight dissolution. When water (0.2 ml) was added with subsequent homogenization with a glass stirrer followed by addition of a few drops of one of the above dissolving reagents, dissolution was improved, but was still not quantitative. Complete dissolution of the proteins, however, was obtained after heating overnight at 50°C in 2 ml of 3 M sodium hydroxide. When 10-μl aliquots of this solution were atomized after charring at 1100°C in the absence of selenium-stabilizing agents, uncorrectable non-specific signals were recorded, because of evolution of excessive smoke which exceeded the capacity of the background corrector.

Owing to these difficulties, it was considered necessary to decompose the precipitate in a mixture of nitric and perchloric acids, which is most commonly employed for biological matrices. When aliquots of the acid-dissolved proteins were atomized in the absence of a matrix modifier, overcompensated signals were recorded at the 196.0-nm selenium line and slight uncorrectable non-specific positive signals were recorded at the 204.0-nm selenium line. These non-specific signals originated from the presence of iron and phosphorus in the matrix. The organic compounds of iron and phosphorus are converted into inorganic forms during acid dissolution. The presence of overcompensation effects from iron at the 196.0-nm line and poor sensitivity for selenium at the 204.0-nm line thus renders this protein separation technique unsuitable for determination of selenium in whole blood.

When aliquots of blood proteins, mineralized with nitric and perchloric acids were atomized (2200°C) after charring at 1150°C in the presence of copper, large positive non-selenium signals were recorded at 196.0 nm. The individual atomization of copper (0.1% solution) or (1 + 10) perchloric acid had no effect on the base-line at 196.0 nm, while a combination of both solutions in the graphite tube generated uncorrectable positive signals. This spectral interference is not present around the 204.0-nm selenium line. The above results were obtained at a spectral band-width of 2.0 nm. These signals were completely eliminated when a 0.07-nm spectral band-width was employed. Because the sensitivity of selenium is only slightly dependent on the spectral band-width, the background signals may be removed by employing this decreased band-width. However, this increased the detection limit for selenium by a factor of ten.

Blood serum

After the serum proteins had been precipitated as described for whole blood, they were dissolved in ammonia, guanidinium chloride or concentrated nitric acid. Best dissolution was achieved with sodium hydroxide, but this could not be used for the reasons given above. The instrumental parameters used to quantify selenium after the various dissolution procedures are described in Table 2. A two-step drying procedure is necessary when ammonia or guanidinium chloride has been used for dissolution. High-temperature ashing is not required when the proteins have been dissolved in nitric acid or ammonia, but the ashing temperature must be raised above 1000°C for guanidinium chloride in order to decrease the background. In contrast to the non-stabilization effect of copper on selenium in blood serum [4], the selenium present in redissolved precipitated serum proteins (in nitric acid or ammonia) is thermally stabilized by copper up to 700°C.

With regard to the choice of matrix modification and dissolution reagents, Table 3 shows that nitric acid dissolution, coupled with silver matrix modification and pyrolytically-coated tubes gave the best sensitivity. However, as dissolution of proteins in nitric acid is rather time-consuming, and the precision of the final measurement of selenium is poor, the ammonia—silver

TABLE 2

Instrumental parameters for quantifying selenium in dissolved proteins (sample volume 10 μl, alternative volume 10 μl)

Step		Dissolution reagent								
		Nitric acid			Guanidinium chloride			Ammonia		
		Temp. (°C)	Ramp (s)	Hold (s)	Temp. (°C)	Ramp (s)	Hold (s)	Temp. (°C)	Ramp (s)	Hold (s)
Drying	1	120	10	20	120	10	10	120	5	10
	2	—	—	—	140	5	20	140	2	10
Ashing	3	250	5	5	350	5	10	650	10	10
	4	650	10	20	450	5	5	—	—	—
	5	—	—	—	1050	10	10	—	—	—
Atomization	6	2200	0	6	2200	0	6	2200	0	6
Tube		Pyro-coated			Pyro-coated or standard			Pyro-coated or standard		
Matrix modifier		(0.1%) Cu, Ni, Ag			Ni, Ag			Cu, Ni, Ag		
Minimum gas flow (ml min^{-1})		10			30			10		

procedure is preferred; the recommended conditions are given in the Experimental section.

The same human serum samples were analyzed by the direct e.a.a.s. method [4] in addition to the proposed method. The results are listed in Table 4. The relative standard deviation of the method was calculated to be 3% for 10 determinations of 1.3 μmol Se l^{-1} and the detection limit was 0.012 μmol Se l^{-1}. The agreement between the two methods was satisfactory, and was not subject to any systematic error.

Seminal fluid

Instrumental neutron activation analysis for selenium in pooled seminal fluid showed that more than 95% of total selenium was bound to the pro-

TABLE 3

The influence of dissolution reagent, matrix modifier and type of graphite tube on sensitivity and precision (results are means of 10 determinations)

Matrix modifier	Standard tube		Pyro-coated tube	
	HNO_3	NH_3	HNO_3	NH_3
	Sensitivity (pg/0.004 absorbance)			
Silver	600	44	19	23
Copper	46	40	31	41
Nickel	67	200	30	100
	Relative standard deviation (%)			
Silver	6.1	2.6	7.2	2.4
Copper	2.6	3.0	5.2	3.0
Nickel	7.5	10.3	5.0	12.6

TABLE 4

Concentrations of selenium (μmol l^{-1}) found in human blood serum by the proposed method and by direct e.a.a.s.

Sample	Proposed method[a]	Direct e.a.a.s.	Sample	Proposed method[a]	Direct e.a.a.s.
1	1.19	1.29	10	1.50	1.35
2	1.19	1.09	11	1.15	1.41
3	0.90	0.80	12	1.24	1.25
4	1.49	1.39	13	1.76	1.73
5	1.39	1.39	14	1.47	1.42
6	1.60	1.60	15	1.38	1.36
7	1.71	1.77	16	1.51	1.24
8	1.35	1.40			
9	1.89	1.73			

[a]Ammonia dissolution.

teins after precipitation with trichloroacetic acid solution. Because of the high phosphate concentration in seminal fluid, it was not possible to determine selenium by the direct e.a.a.s. method. The interfering overcompensation signals were completely eliminated when selenium was determined by the proposed technique. The selenium concentration in seminal fluid from healthy Norwegian donors ranged from 0.09 to 1.30 μmol l^{-1} with a group average of 0.44 μmol l^{-1} (n = 15). Since chemical interactions of cadmium with selenoproteins are suggested by the demonstration that protein-bound selenium is found only in the cadmium-containing proteins present in seminal fluid [6], it may be of interest to determine selenium in this fluid for toxicological studies.

Conclusions

Deproteinization of biological fluids such as whole blood, serum and seminal plasma with trichloroacetic acid provides an opportunity to segregate selenium quantitatively from interfering electrolytes. This approach is suitable for determination of selenium in serum and seminal fluid by e.a.a.s. The protein precipitation with trichloroacetic acid may also be applicable in x-ray spectrometric and neutron activation analysis for selenium in body fluids.

REFERENCES

1 D. C. Manning, At. Absorpt. Newsl., 17 (1978) 107.
2 K. Saeed and Y. Thomassen, Anal. Chim. Acta, 130 (1981) 281.
3 H. K. Awwad, E. J. Potchen, S. J. Adelstein and J. B. Dealy, Metab. Clin. Exp., 15 (1966) 626.
4 K. Saeed, Y. Thomassen and F. J. Langmyhr, Anal. Chim. Acta, 110 (1979) 285.
5 K. R. Millar, N.Z. J. Agric. Res., 15 (1972) 547.
6 J. Alexander, J. Kofstad, K. Saeed, Y. Thomassen, S. Øvrebø and J. Aaseth, in P. Brätter and P. Schramel (Eds.), Trace Element Analytical Chemistry in Medicine and Biology, Walter de Gruyter, Berlin, 1982.

Analytica Chimica Acta, 143 (1982) 229—236
Elsevier Scientific Publishing Company, Amsterdam — Printed in The Netherlands

DETERMINATION OF LEAD BY CONTINUOUS-FLOW HYDRIDE GENERATION AND ATOMIC ABSORPTION SPECTROMETRY

Comparison of Malic Acid—Dichromate, Nitric Acid—Hydrogen Peroxide and Nitric Acid—Peroxodisulfate Reaction Matrices in Combination with Sodium Tetrahydroborate

KAZUO JIN*

Hokkaido Institute of Public Health, North 19, West 12, Kita-ku, Sapporo 060 (Japan)

MITSUHIKO TAGA

Department of Chemistry, Faculty of Science, Hokkaido University, North 12, West 8, Kita-ku, Sapporo 060 (Japan)

(Received 6th April 1982)

SUMMARY

A continuous-flow hydride generator is combined with a heated quartz tube atomizer—atomic absorption spectrometer system for the trace determination of lead. Malic acid—$K_2Cr_2O_7$, HNO_3—H_2O_2 and HNO_3—$(NH_4)_2S_2O_8$ are all effective for plumbane generation by means of sodium tetrahydroborate. The relative merits of these systems are investigated in terms of sensitivity, efficiency of plumbane generation and interferences. The sensitivities (0.0044 absorbance) obtained under the recommended conditions for the three systems are 3.2, 1.7 and 1.1 ng Pb ml^{-1}, respectively, whereas plumbane generation efficiencies are 33%, 47% and >80%, respectively, for 1 μg Pb ml^{-1}. Silver, Au, Cu and Cd interfere seriously in all reaction systems. A dithizone extraction and back-extraction method is utilized to eliminate interfering ions, followed by reduction of the resulting solution in the peroxodisulphate system. The proposed method is applied to water samples and NBS 1566 oyster tissue.

Atomic absorption spectrometry (a.a.s.) based on the atomization of volatile hydrides has been found to be very useful in the trace determination of As, Bi, Ge, Sb, Se, Sn, Te and Pb [1—9]. Sodium tetrahydroborate has been used most conveniently for the generation of the hydrides of these elements. However, the conditions that are effective for lead hydride generation by reaction with sodium tetrahydroborate are somewhat different from those for the other elements; the conversion efficiency of lead to plumbane is poor for straightforward reaction with an acidified sample solution and sodium tetrahydroborate [4]. Fleming and Ide [5] have shown the effectiveness of a tartaric acid—potassium dichromate matrix for plumbane generation with sodium tetrahydroborate, and they applied the method to the determination of lead in steels. Vijan and Wood [6] reported the effectiveness of nitric acid or perchloric acid—hydrogen peroxide matrices using a

0003-2670/82/0000-0000/$02.75

semi-automated hydride generator—a.a.s. system. Jin et al. [7] made a systematic study of effective reaction matrices for plumbane generation, and found that peroxodisulfate is as effective as dichromate and hydrogen peroxide. However, little has been reported about the relative merits of these reaction matrices [7, 10].

In this study, a continuous-flow hydride generator similar to that previously reported by Ikeda et al. [11, 12] was used in conjunction with a heated quartz tube atomizer—a.a.s. system for the determination of lead. Three reaction systems are compared in terms of sensitivity, efficiency of hydride generation and effect of foreign ions.

EXPERIMENTAL

Apparatus

A Varian-Techtron Model 175 atomic absorption spectrometer equipped with a lead hollow-cathode lamp and deuterium background corrector was used with a strip-chart recorder.

Figure 1 shows a schematic diagram of the manifold. A Technicon proportioning pump module was employed to control the flow rate of sample and reagents. Acidified sample solution was premixed with a solution from line 2, and the solution was mixed with sodium tetrahydroborate solution at the beginning of the reaction coil (6 mm i.d., 6 turns, water-cooled). Generated plumbane was purged by nitrogen which was introduced at the beginning of the reaction coil, and passed through two gas/liquid separators similar to that reported earlier [11, 12]. The plumbane was introduced into an open-ended quartz tube atomizer (14 mm i.d., 114 mm long) which was mounted on the air-acetylene burner head by metal clips.

Reagents

All the reagents were of analytical-reagent grade. Deionized water was distilled twice. A lead stock solution (1000 μg ml^{-1}) was made by dissolving lead (99.999%, Wako Chemicals, Tokyo) in 20 ml of 6 M nitric acid and

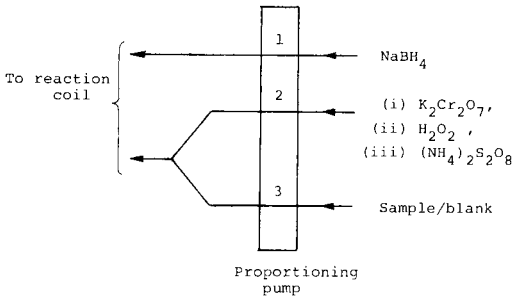

Fig. 1. Schematic diagram of the manifold. Solutions in line 3 acidified with (i) malic acid, (ii, iii) nitric acid. Flow rate is 3.9 ml min^{-1} in all lines.

diluted to 1 l with water. The solution was used after sequential dilution. Sodium tetrahydroborate solutions (1, 5 and 10% w/v) were prepared by dissolving sodium tetrahydroborate (powder, Aldrich Chemical Co.) in 0.3% sodium hydroxide, and the solutions were filtered through a 0.45-μm membrane filter. Ammonium peroxodisulfate solutions were prepared daily. An ammonium citrate solution was prepared by dissolving 105 g of ammonium dihydrogen citrate in 300 ml of water and adjusting to pH 9.0 with aqueous ammonia. A hydroxylamine solution was prepared by dissolving 60 g of hydroxylamine hydrochloride in 180 ml of water and adjusting to pH 9.0 with ammonia. A 10% potassium cyanide solution was prepared by dissolving the solid in water. A dithizone solution (0.01%) was prepared by dissolving 40 mg of dithizone in 400 ml of chloroform. The ammonium citrate, hydroxylamine and potassium cyanide solutions were shaken with the dithizone solution.

Procedure

The instrumental operating conditions were as follows: wavelength, 217.0 nm; spectral bandpass, 1.0 nm; lead lamp current, 5 mA; damping, "slow"; atomizer temperature, 900 ± 15° C at the center of the quartz tube.

The operating procedure for the continuous-flow hydride generator was as follows. After instrumental setting, the solutions were pumped as shown in Fig. 1 (blank solution in line 3) until the recorder indicated a stable base line. A sample solution (acidified with malic or nitric acid) was passed for 60 s, then a blank solution again for 90 s. The flow rate of each solution was 3.9 ml min^{-1} in all instances.

Sample preparation

Water samples. The acidity of water samples was adjusted by adding malic acid (0.3 M) or nitric acid (0.5 M), known amounts of lead were added and determined. For a sample to which this simple standard addition technique could not be applied because of severe interferences, the following dithizone—chloroform extraction and back-extraction was applied. The sample solution was transferred to a 100-ml separatory funnel, the volume was adjusted with water to about 25 ml; then 10 ml of ammonium citrate and 2 ml of hydroxylamine solutions were added, followed by a few drops of thymol blue as indicator. Aqueous ammonia was added until the solution just became green (pH 8.5—9.0), and 2 ml of potassium cyanide solution was added. A 5-ml portion of dithizone solution was added and the mixture shaken for 5 min (electric shaker). The phases were allowed to separate and the organic phase was transferred to another separatory funnel. The separation procedure was repeated, and the organic phases were combined. Exactly 10 ml of 0.1 M nitric acid was added to the organic phase and the mixture was shaken for 5 min. The resulting aqueous solution was measured by a.a.s. as described above.

Biological samples. The sample (0.5 g) was decomposed with 20 ml of nitric acid and 1 ml of perchloric acid in a 50-ml covered conical beaker. The beaker was heated until the perchloric acid began to fume. After cooling, 1 ml of nitric acid was added, the volume was made up to 20 ml with water, and the solution was measured for lead as described above.

RESULTS AND DISCUSSION

Optimization of operating conditions

The flow rate of nitrogen as purge gas affects the sensitivity; maximum sensitivity was obtained for 0.3—0.5 l min^{-1}; less than 0.3 l min^{-1} resulted in significant noise, and more than 0.5 l min^{-1} resulted in decreased sensitivity, e.g., 90% and 57% of the maximum sensitivity at 1 and 3 l min^{-1}, respectively. Therefore the flow rate was fixed at 0.5 l min^{-1}. Concentrations of tetrahydroborate solution greater than 10% (w/v) were not convenient, because hydrogen bubbles were easily produced in the transportation tube by decomposition of the reductant.

Comparison of reaction systems

Malic acid—dichromate—tetrahydroborate. In this system, only malic acid and tartaric acid were effective acidic components [7] and gave almost the same results. The concentrations of malic acid and dichromate were varied; the results are shown in Fig. 2. On the basis of these results, 0.3 M malic acid, 0.04 M potassium dichromate and 10% sodium tetrahydroborate are recommended for lead determinations.

Nitric acid—hydrogen peroxide—tetrahydroborate. The concentrations of nitric acid and hydrogen peroxide were varied; the results are shown in Fig. 3. Again, each dependence showed a maximum, as previously reported [6, 11]. Thus 0.5 M nitric acid, 10% w/v hydrogen peroxide and 10% sodium tetrahydroborate are recommended.

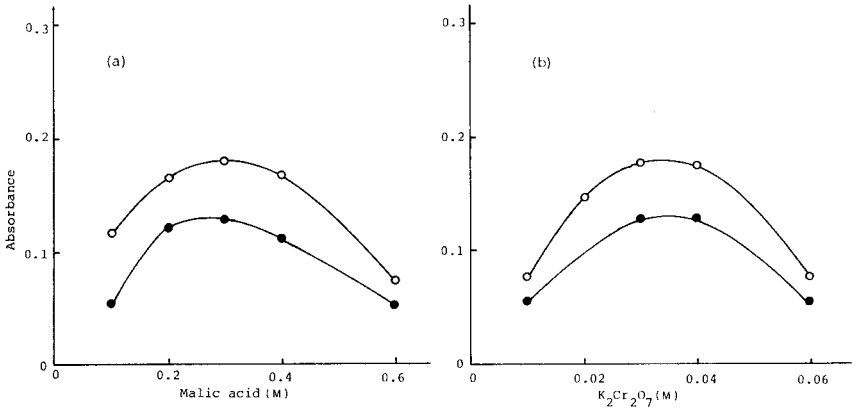

Fig. 2. Effect of (a) malic acid (0.04 M $K_2Cr_2O_7$); (b) potassium dichromate (0.3 M malic acid) on the absorbance for lead (0.1 μg ml^{-1}); (•) 5% $NaBH_4$; (○) 10% $NaBH_4$.

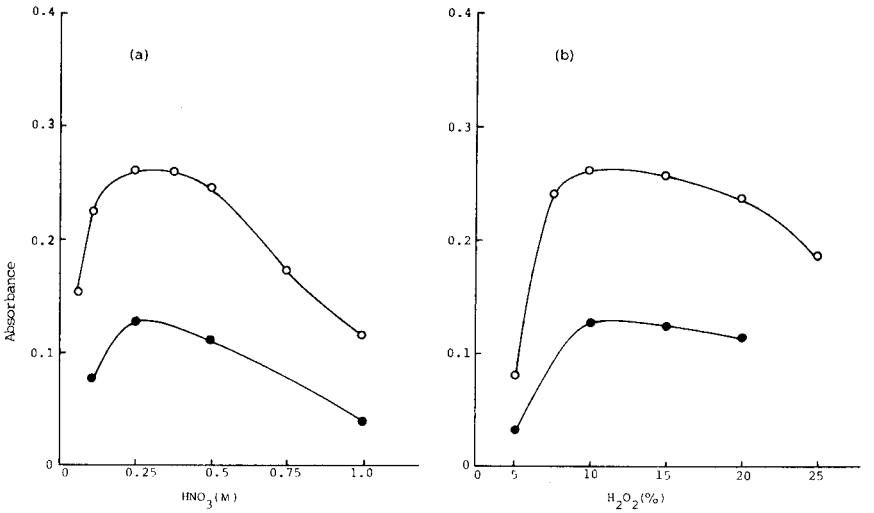

Fig. 3. Effect of (a) nitric acid (10% H_2O_2); (b) hydrogen peroxide (0.5 M HNO_3) on the absorbance for lead (0.1 μg ml^{-1}); (•) 5% $NaBH_4$; (○) 10% $NaBH_4$.

Nitric acid—ammonium peroxodisulfate—tetrahydroborate. The effects of variations of nitric acid and peroxodisulfate concentrations are shown in Fig. 4. The acidity which gives maximum absorbance increases with increasing tetrahydroborate concentration; maximum absorbance is obtained in 0.1 M,

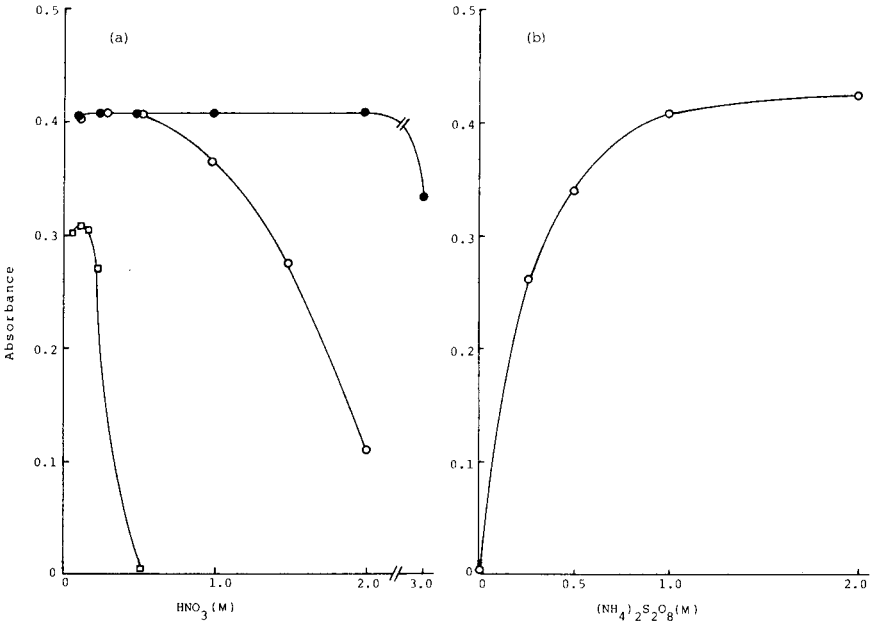

Fig. 4. Effect of (a) nitric acid (1 M $S_2O_8^{2-}$); (b) peroxodisulfate (0.2 M HNO_3) on the absorbance for lead (0.1 μg Pb ml^{-1}); (□) 1%; (○) 5%; (•) 10% $NaBH_4$.

0.1—0.5 M and 0.1—2 M nitric acid for, respectively, 1%, 5% and 10% sodium tetrahydroborate. The recommended conditions for this system are therefore 0.1—0.5 M nitric acid, 1 M ammonium peroxodisulfate and 5% sodium tetrahydroborate. When the sample solutions were prepared in 0.2—0.5 M hydrochloric acid, perchloric acid or phosphoric acid, the sensitivity fell to between 40 and 80% that for nitric acid.

Calibration, sensitivity and reduction efficiency

The calibration graphs for the three systems were linear up to 0.3 μg, 0.2 μg and 0.15 μg Pb ml^{-1} for the dichromate, peroxide and peroxodisulfate systems, respectively. The blank signal was equivalent to 11 ng Pb ml^{-1} in the peroxodisulfate system, but below 2 ng in the other reaction systems. The high blank originated mainly from the ammonium peroxodisulfate.

The sensitivities attained in the three reaction systems are summarized in Table 1. The detection limits are almost the same as the values of sensitivity. The nitric acid—peroxodisulfate system gives the greatest sensitivity.

The efficiency of plumbane generation was determined by collecting the waste water from the reaction coil in a measuring flask and measuring the residual lead concentration. Test solutions containing 1 or 100 μg Pb ml^{-1} were used for this purpose; a carbon-furnace a.a.s. system was used for the residual lead concentration in the former solution, and air—acetylene flame a.a.s. for the latter. The results are shown in Table 1. The reduction efficiency was less for the 100 μg Pb ml^{-1} solution. The reduction efficiency of 47% found for 1 μg Pb ml^{-1} in the peroxide system is somewhat smaller than the 64% reported by Ikeda et al. [11]. However, the reduction efficiency obtained with the peroxodisulfate system is the highest, as would be expected because it gives the highest sensitivity.

Effects of foreign ions and their elimination

The influence of various ions was studied by preparing a sample solution containing 0.1 μg Pb ml^{-1} and a known amount of the foreign ion, and using each of the three reaction systems. The changes of lead absorbance in the presence of these ions are listed in Table 2. Silver, gold, cadmium

TABLE 1

Sensitivity and efficiency of plumbane generation for the determination of lead

Reaction conditions[a]	Sensitivity[b] (ng ml^{-1})	Reduction efficiency (%)	
		1 μg Pb ml^{-1}	100 μg Pb ml^{-1}
0.3 M Malic acid, 0.04 M $K_2Cr_2O_7$	3.2	33	16
0.5 M HNO_3, 10% H_2O_2	1.7	47	25
0.2 M HNO_3, 1 M $(NH_4)_2S_2O_8$	1.1	>80	60

[a]The acidity is that of sample solution; in all cases 10% (w/v) $NaBH_4$ in 0.3% NaOH was used. [b]Concentration giving an absorbance change of 0.0044.

TABLE 2

Influence of foreign ions on lead absorbance (0.1 μg Pb ml^{-1})[a]

Ion	Amount (μg ml^{-1})	Change in absorbance (%)		
		Reaction system[b]		
		$K_2Cr_2O_7$	H_2O_2	$(NH_4)_2S_2O_8$
Se(IV)	0.1	0	−7	−76
	1	0	−47	−100
Te(IV)	1	0	−75	−90
Te(VI)	2	0	−30	−85
Ag(I)	1	−80	−40	−50
Au(III)	1	−43	−55	−48
Cd(II)	10	−20	−35	−67
Co(II)	1	0	−10	−38
Cu(II)	1	−60	−33	−75
Ni(II)	1	0	0	−50
	10	−20	−40	−100
Zn(II)	5	0	−25	0
Fe(III)	2	0	−65	0
	70	0	−100	−41
Al(III)	25	0	−36	0
	100	0	−83	−4

[a]The following ions had no effect up to 5 μg ml^{-1}: As(III, V), Bi(III), Ge(IV), Sn(IV), Sb(III), Mn(II, VII), Cr(III, VI), Mo(VI) and Ru(III); up to 100 μg ml^{-1}; PO_4^{3-}, SiO_3^{2-}; up to 500 μg ml^{-1}: BO_3^{3-}, SO_4^{2-}, ClO_4^-, IO_3^-, $C_2O_4^{2-}$, CH_3COO^-, Cl^- and Br^-. [b]The conditions were the same as shown in Table 1, except that 5% $NaBH_4$ was used.

and copper interfered seriously in all reaction systems. Hydride-forming elements such as arsenic, bismuth, germanium and tin showed no influence up to 5 μg ml^{-1} in each system, but selenium and tellurium showed severe suppression in the hydrogen peroxide and peroxodisulfate systems. Strong suppression was also observed for cobalt, zinc, aluminum and iron in the hydrogen peroxide system and nickel in the peroxodisulfate system.

As the malic acid—dichromate system exhibited the fewest interferences, malic acid, tartaric acid and acetic acid were tested instead of nitric acid in the other systems. However, no beneficial effects were observed.

The dithizone—chloroform extraction and back-extraction procedure was also applied; the resultant solution (0.1 M in nitric acid) can be treated by the peroxodisulfate system without any adjustment of acidity. None of the ions listed in Table 2 in amounts up to 100 μg affected the determination of 1 μg of lead, when a 1% sodium tetrahydroborate solution was used. Though the extraction and back-extraction technique is somewhat time-consuming, a batch of 20 samples can be prepared in ca. 90 min with the aid of an electric shaker; this is comparable to the co-precipitation technique [13].

TABLE 3

Comparison of results for lead in water samples[a] (ng Pb ml^{-1})

Sample	Reaction system[b]			Carbon furnace
	$K_2Cr_2O_7$	H_2O_2	$(NH_4)_2S_2O_8$[c]	
1	24	24	23	25
2	180	178	180	182
3	72	75	76	72
4	105	108	108	104
5	43	37	36	36
6	195	200	187	202
7	111	115	113	119
8	20	20	22	20
9	90	92	96	93
10	—	—	6	7
11	—	—	2	2
12	—	—	4	3

[a]Samples 1—9 were ore leachate solutions (these samples contained 20—720 ng Cu ml^{-1}, 600—9000 ng Mn ml^{-1}, 60—140 ng Zn ml^{-1}, 20—150 ng As ml^{-1} etc.), samples 10—12 were underground water. [b]Conditions as shown in Table 1. [c]Dithizone extraction used.

Application and accuracy of the method

Waste water samples were examined by the present method (all three reaction systems) and by a carbon-furnace a.a.s. method. The results are shown in Table 3; the peroxodisulfate system could not be applied directly to these samples because of the severe interferences, but it was applied after the dithizone extraction and back-extraction. The results obtained by all the procedures are in good agreement.

The accuracy of the method was studied by examining NBS 1566 oyster tissue. As the sample contained various interfering ions, the dithizone—chloroform extraction method was applied, and the resultant solution was treated by the peroxodisulfate system. The results of three separate determinations were 0.49, 0.49 and 0.48 μg Pb g^{-1}, respectively. These results are in good agreement with the certified value of 0.48 ± 0.04 μg Pb g^{-1}.

REFERENCES

1 W. Holak, Anal. Chem., 41 (1969) 1712.
2 R. S. Braman, L. L. Justen and C. C. Foreback, Anal. Chem., 44 (1972) 2195.
3 F. J. Fernandez, At. Absorpt. Newsl., 12 (1973) 93.
4 K. C. Thompson and D. R. Thomerson, Analyst, 99 (1974) 595.
5 H. D. Fleming and R. G. Ide, Anal. Chim. Acta, 83 (1976) 67.
6 P. N. Vijan and R. Wood, Analyst, 101 (1976) 966.
7 K. Jin, M. Taga, H. Yoshida and S. Hikime, Jpn. Anal., 27 (1978) 759.
8 W. B. Robbins and J. A. Caruso, Anal. Chem., 51 (1979) 889A.
9 R. G. Godden and D. R. Thomerson, Analyst, 105 (1980) 1137.
10 K. Jin and M. Taga, Jpn. Analyst, 29 (1980) 522.
11 M. Ikeda, J. Nishibe, S. Hamada and R. Tujino, Anal. Chim. Acta, 125 (1981) 109.
12 M. Ikeda, J. Nishibe and T. Nakahara, Jpn. Anal., 30 (1981) 368.
13 P. N. Vijan and R. S. Sadana, Talanta, 27 (1980) 321.

Analytica Chimica Acta, 143 (1982) 237—241
Elsevier Scientific Publishing Company, Amsterdam — Printed in The Netherlands

Short Communication

ELECTROLYTIC DETERMINATION OF TRACES OF IODIDE IN SOLUTION WITH A PIEZOELECTRIC QUARTZ CRYSTAL

T. NOMURA* and T. MIMATSU

Department of Chemistry, Faculty of Science, Shinshu University, Asahi, Matsumoto 390 (Japan)

(Received 26th May 1982)

Summary. The frequency of a piezoelectric quartz crystal is decreased when iodide is electrodeposited on the silver electrode of the crystal at —0.05 V vs. Ag/AgCl. From 3×10^{-7} M to 1×10^{-5} M iodide can be determined with few interferences, and a procedure for removal of interfering species is given. Iodide is removed from the electrode by electrolysis at —0.4 V after each determination.

A quartz crystal which adsorbs a substance on its electrode has a decreased piezoelectric frequency in proportion to the increase in weight [1]. A crystal which has the electrode on one side immersed in a solution also oscillates; the frequency depends on the density and conductivity of the solution [2]. If the properties of the solution are kept constant with a buffer, a change in weight of the electrode can be detected as a frequency change of the immersed crystal [2]. Cyanide [2] and iodide [3] can thus be determined by their deposition on a silver or copper electrode, respectively. Also copper(II) [4] and silver(I) [5] can be determined after electrodeposition, by using the electrode of the crystal as a working electrode.

In the work described here, reactions of anions in solution when a definite voltage was applied to the silver electrode of the crystal were investigated by using the frequency change of the crystal immersed in the solution. Iodide was deposited on the electrode as silver(I) iodide at —0.05 V vs. Ag/AgCl, and desorbed at —0.4 V. It was found that micromolar concentrations of iodide could be determined in this way with good reproducibility and few interferences. This method compares favourably with the determination of iodide using the copper electrode spontaneously to form copper(II) iodide on the electrode [3].

Experimental

Apparatus and reagents. The equipment used was as described previously [5], except that the AT-cut crystal had a silver-on-platinum-plated gold electrode (5 mm diameter) on each side. One silver-coated electrode was used as the cathode. The gold electrodes were first plated with platinum for

protection as described previously [5]. The frequency change caused by electrodeposition of platinum was ca. 100 kHz. The platinum-plated electrodes were plated with silver at 1.5 V for 2 min in alkaline 0.02 M potassium cyanoargentate(I) solution containing sodium carbonate. The frequency change caused by electrodeposition of silver was ca. 50 kHz. When the frequency of the quartz crystal became noisy because of roughness of the silver electrode surface caused by repeated electrolyses, silver was removed from the electrodes by electrolysis and the platinum-plated electrodes were replated with silver as described above. The frequency change was monitored by a digital counter (Takeda Riken TR-5104) and recorded (Rikadenki BC82001 recorder).

An iodide stock solution was prepared by dissolving 3.32 g of potassium iodide in 200 ml of water and was standardized by Volhard's method.

Determination of iodide (3×10^{-7}—1×10^{-5} M). Transfer the sample solution, which is 1×10^{-3} M in potassium chloride and adjusted to pH 9.8 with 1×10^{-3} M sodium borate—sodium hydroxide solution, and the reagent blank solution to their respective containers. Pass the reagent blank solution through the cell at 6.5 ml min^{-1} and apply —0.05 V vs. Ag/AgCl. When the frequency of the crystal has become constant (F_1), pass the sample solution for exactly 1 min (or 10 min for $\leq 1 \times 10^{-6}$ M iodide), and then pass the reagent blank solution through again until the frequency is constant (F_2). The frequency change $\Delta F = F_1 - F_2$ is proportional to the concentration of iodide, and a calibration graph may be constructed on this basis. Dissolve the iodide deposited on the electrode by electrolysis at —0.4 V in the flowing reagent blank solution, before starting the next determination.

Removal of interferences. Transfer the sample solution to a 100-ml dark-glass Erlenmeyer flask, dilute to ca. 50 ml with water, and add 10 ml of 0.1 M sodium sulfide, 2 ml of 1 M nitric acid and ca. 20 mg of zinc powder. Heat to just below boiling for 15 min and filter. Heat for 10 min after adding 20 ml of pH 9.8 buffer solution and filter. Heat again for 10 min after adding 5 ml of 3% hydrogen peroxide and cool to room temperature. Transfer the solution to a 200-ml volumetric flask, add 2 ml of 0.1 M potassium chloride, dilute to the mark with water and follow the recommended procedure.

Results and discussion

Electrodeposition of anions and selection of buffer solution. Electrodeposition potentials of anions in tartrate buffer (pH 3.0), phosphate buffer (pH 6.7), and sodium borate—sodium hydroxide buffer (pH 9.8) solutions were examined by scanning the voltage from —1.0 to +0.3 V (vs. Ag/AgCl) at 0.2 V min^{-1}. The frequency of the crystal shifted with the applied voltage in the reagent blank solution containing tartrate buffer. The rate of frequency shift was ca. +50 Hz per 0.2 V, although the frequency of the crystal returned to the original value when the initial voltage was re-applied. In the phosphate buffer solution, the frequency of the crystal in the reagent blank solution did not shift with the voltage so much as in the tartrate buffer, but repeated

scans gave different curves. In the borate—hydroxide buffer solution (pH 9.8), the frequency in the reagent blank solution shifted slightly with the voltage as shown in Fig. 1, and the original frequency was obtained when the initial voltage was re-applied. The decrease in frequency above +0.2 V was caused by the deposition of chloride, which was added as the supporting electrolyte for the silver—silver(I) chloride electrode. Above +0.4 V, the silver electrode of the crystal was dissolved, so that the frequency increased abruptly. The electrodeposition of anions in the borate—hydroxide buffer solution (Fig. 1) could be detected more clearly than in the other buffers because the blank (Fig. 1, curve a) was reproducible. In this buffer, iodide at micromolar levels could be determined with good selectivity by deposition of iodide at —0.05 V and dissolution at —0.4 V, as shown in Fig. 2.

Dependence of the frequency change on pH and flow rate. The frequency change of the crystal resulting from electrodeposition of iodide at —0.05 V only decreased very slightly (ca. 10%) and linearly with increasing pH over the pH range 7.8—11.0 examined. However, it increased with increasing flow rate, as shown in Fig.3. The plateau around 7 ml min^{-1} may be caused by turbulent flow in the cell. The frequency change was exactly proportional to the electrodeposition time. Large deposits of iodide resulted in poor reproducibility because some of the silver electrode also dissolved when the deposited iodide was dissolved at +0.4 V. Therefore, electrodeposition for 1 min was used for determination of micromolar concentrations, and 10 min only for smaller concentrations.

Calibration and reproducibility. The calibration graph of frequency change (ΔF) against iodide concentration [I^-] was linear over the range 1×10^{-6}—1×10^{-5} M, and is described by the equation $[I^-] = (\Delta F/14.1) \times 10^{-6}$ M, where ΔF is measured in Hz. The standard deviation was 2.51 Hz (3.3%) for 6 determinations of 5×10^{-6} M iodide. With electrodeposition for

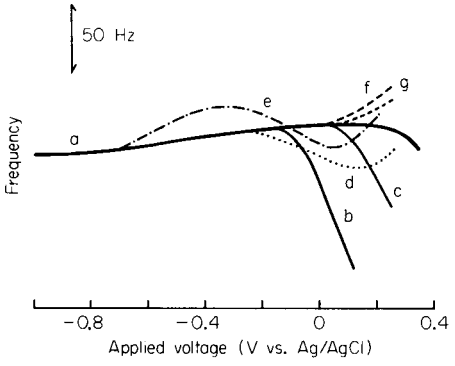

Fig. 1. Electrolytic potentials of 1×10^{-5} M anions in 1×10^{-3} M sodium borate—sodium hydroxide buffer (pH 9.8) containing 1×10^{-3} M KCl. Solution flow rate 4.2 ml min^{-1}; initial voltage —1.0 V; sweep rate + 0.2 V min^{-1}. (a) Reagent blank; (b) iodide; (c) bromide; (d) sulfide; (e) thiosulfate; (f) cyanide; (g) thiocyanate.

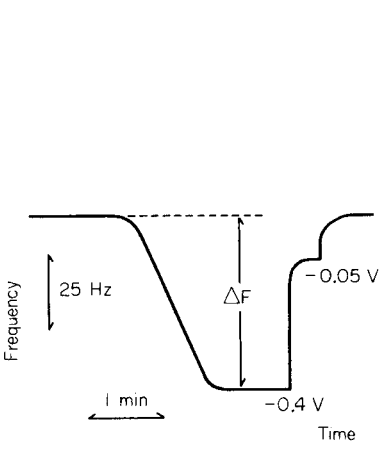

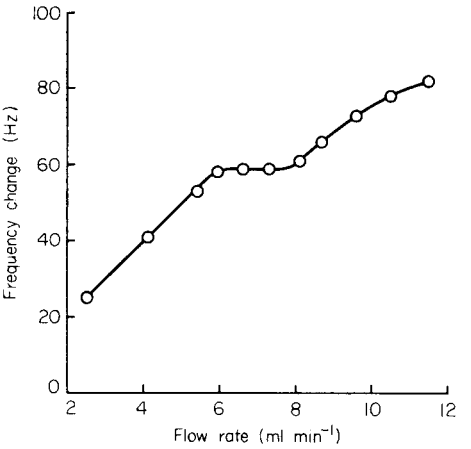

Fig. 2. Typical frequency change (ΔF) on electrolysis at −0.05 V vs. Ag/AgCl for 1 min of 4×10^{-6} M iodide in 1×10^{-3} M borate–hydroxide buffer (pH 9.8) containing 1×10^{-3} M KCl, followed by dissolution at −0.4 V, and recovery to the initial frequency by applying −0.05 V. Flow rate 6.5 ml min^{-1}.

Fig. 3. Dependence of frequency change on the flow rate for 4×10^{-6} M iodide in 1×10^{-3} M borate–hydroxide buffer (pH 9.8), 1×10^{-3} M in KCl, electrolyzed for 1 min at −0.05 V.

10 min under these same conditions, a linear graph having the same slope was obtained for 3×10^{-7}–1×10^{-6} M iodide. The calibration graph obtained after the procedure for the removal of interferences had been applied was linear having exactly the same slope but slightly poorer reproducibility. The system should be recalibrated when the quartz crystal has been re-plated with silver or completely replaced.

Effect of other ions. The effect of various ions on the determination of 8×10^{-6} M iodide was investigated; changes in the frequency of more than ±5% were considered to result from interferences. The tolerance limits for ions are shown in Table 1. Interferences of silver(I) and mercury(II) arose from the formation of iodide complexes, and those from lead(II) and iron(III) from the adsorption of hydroxides on the electrode resulting in high recoveries. Bromide and thiocyanate did not interfere, as is illustrated in Fig. 2. Sulfate, carbonate and chromate behaved as bromide, and phosphate or thiocyanate did not interfere because their electrolytic potentials were more positive than that of the iodide. These interferences (100-fold amounts) except for silver(I) and mercury(II) (10-fold each) could be eliminated by the method given above, in which sulfide, cyanide and thiosulfate were oxidized with hydrogen peroxide, whereas silver(I), and lead(II) and iron(III) were precipitated as sulfide and hydroxides, respectively, and mercury(II) was amalgamated by adding zinc powder.

TABLE 1

Tolerance limits for ions in the determination of 8×10^{-6} M iodide

Tolerance limit (ion:iodide mole ratio)	Ions
100	Cu(II), Co(II), Ni(II), Zn(II), Cd(II), Al(III), Bi(III)[a], NH_4^+, Cl^-, Br^-, SCN^-, SO_4^{2-}, CO_3^{2-}, PO_4^{3-}
10	Pb(II), Fe(III)
<1	Ag(I), Hg(II), CN^-, $S_2O_3^{2-}$, S^{2-}

[a]25-fold amounts of bismuth were limiting because of its solubility.

REFERENCES

1 W. H. King, Jr., Anal. Chem., 36 (1964) 1735.
2 T. Nomura and A. Minemura, Nippon Kagaku Kaishi, 1980 (1980) 1621.
3 T. Nomura and O. Hattori, Bunseki Kagaku, 31 (1982) 48.
4 T. Nomura, T. Nagamune, K. Izutsu and T. S. West, Bunseki Kagaku, 30 (1981) 494.
5 T. Nomura and M. Iijima, Anal. Chim. Acta, 131 (1981) 97.

Analytica Chimica Acta, 143 (1982) 243—247
Elsevier Scientific Publishing Company, Amsterdam — Printed in The Netherlands

Short Communication

DETERMINATION OF LEAD BY ADSORPTION OF THE EXTRACTED 8-QUINOLINOLATE ON THE ELECTRODES OF A PIEZOELECTRIC QUARTZ CRYSTAL

T. NOMURA* and T. YAMASHITA

Department of Chemistry, Faculty of Science, Shinshu University, Asahi, Matsumoto 390 (Japan)

T. S. WEST

The Macaulay Institute for Soil Research, Craigiebuckler, Aberdeen, AB9 2QJ (Great Britain)

(Received 2nd July 1982)

Summary. Lead 8-quinolinolate extracted into chloroform is adsorbed on the electrodes of a piezoelectric quartz crystal. The change in frequency of the crystal is used to measure the lead concentration over the range 3×10^{-6}—5×10^{-5} M in aqueous solution. The interferences of Fe(III), Ni, Co(II), Zn, Cd and Ag(I) can be masked by L-ascorbic acid and cyanide.

The frequency of a piezoelectric quartz crystal changes with the mass of the electrodes when oscillating in a gaseous or a liquid medium. Thus cyanide [1] and silver [2] in solution have been determined by the change in frequency caused by reaction with, or electrodeposition on the electrode, respectively. Crystals immersed in chloroform solutions of metal 8-quinolinolates change frequency. The lead chelate gave the greatest change, as a result of adsorption of the solute. In this communication, a method is described for the determination of lead in aqueous solution by extraction of its 8-quinolinol chelate into chloroform, followed by piezoelectric determination.

Experimental

Apparatus and reagents. The piezoelectric detector was as described previously [2]. The crystal had platinum-plated gold electrodes (5 mm diameter). The crystal holder (brass wire) was plated with gold. The frequency change was monitored by a digital counter (Takeda Riken TR-5142G) and recorder (Toshin Electron TO 2NI-B). The chloroform used was special grade (Wako Pure Chemicals). Lead extractions were done on a shaker (Iwaki Co., KM-type). All experiments were done in a room thermostatted at 25 ± 1°C, and the frequency measurements were done with the oscillator in an air-bath thermostatted at 25 ± 0.5°C.

Procedures. A 5-ml sample of lead solution was adjusted to pH 11.0 with 10 ml of 0.05 M sodium tartrate—sodium hydroxide buffer, transferred to a 100-ml separating funnel, and diluted to 50 ml with water. A 10-ml portion of 1×10^{-3} M 8-quinolinol in chloroform was added, and the mixture was shaken for 2 min and allowed to stand for 5 min. The chloroform solution was transferred to a 10-ml beaker and a crystal plated with platinum was totally immersed in the solution. After 2 min, the frequency of the crystal was read on the frequency counter (F_1). The procedure was repeated with a reagent blank solution not containing lead (F_2). The concentration of lead in the sample solution was calculated from the difference in frequency ($F_1 - F_2$) by reference to a calibration curve prepared previously with standard lead solutions. After each measurement, the crystal was immersed in chloroform and then in 2 M acetic acid for about 1 min each, washed with water and acetone, and air-dried. At the end of each day, the crystal was immersed in 1 M nitric acid for a few minutes, washed with water and acetone, and dried.

Procedure for lead in the presence of interfering ions. To each lead sample solution (5 ml), 5 ml each of 2.5×10^{-2} M L-ascorbic acid and 5×10^{-2} M potassium cyanide were added, and the pH was adjusted to 11.0 with 10 ml of the tartrate buffer solution. The solution was transferred to a 100-ml separating funnel and diluted to 50 ml with water. The extraction and measurement procedures were followed as above.

Results and discussion

Behaviour of 8-quinolinol chelates. Different frequency changes of crystals immersed in chloroform containing metal chelates of 8-quinolinol, with ethanol as stabilizer, have been observed depending on the metal [3]. A larger frequency difference was observed when the solutions had been washed with water to remove ethanol. The biggest frequency change occurred with the lead chelate, the change being dependent on the concentration. As shown in Fig. 1 (curve a), the frequency change of a crystal, which was immersed in chloroform that had been shaken with water for 2 min and stood for 5 min, was the same as that of the same crystal immersed in an 8-quinolinol—chloroform blank solution prepared by the recommended procedure. Thus, the presence of 8-quinolinol in the chloroform did not affect the frequency. In contrast, the frequency change observed in chloroform extracts of lead quinolinolate decreased with time as shown in Fig. 1 (curve b).

It was thought possible that the frequency change might arise from electrodeposition of lead from the chloroform solution because the quartz crystal had a potential difference of about 1.5 V between the electrodes from the circuit of the oscillator. Figure 1 (curve c) is a plot of the frequency of the crystal in the lead 8-quinolinolate solution with frequency measurements every 2 min, the measuring circuit being switched on just before a reading to prevent electrodeposition during the standing period. This shows

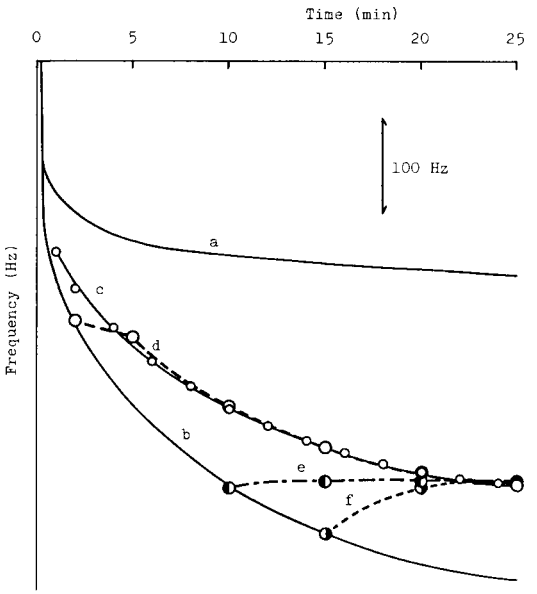

Fig. 1. Frequency changes of a crystal immersed in (a) chloroform washed with water or the reagent blank prepared as in the recommended procedure, and (b)—(f) lead 8-quinolinolate in chloroform prepared from 5×10^{-6} M lead nitrate solution as in the recommended procedure. Curves (a) and (b) were recorded with the oscillator continuously operational; (c) was obtained by taking a reading every 2 min by operating the detector only for a few seconds; (d), (e) and (f) are responses obtained after 2, 10 or 15 min of continuous operation of the oscillator and then monitored every 5 min as in (c).

that about 70% of the frequency change is due to physical adsorption and only 30% arises from electrostatic forces. This is confirmed by curves (d), (e) and (f) in Fig. 1, which show the frequency changes of the crystal immersed in a lead 8-quinolinolate solution in chloroform when 6 V was applied to the crystal and the voltage was cut off after 2, 10 or 15 min, and then the frequency was measured every 5 min as described above. Every response finally coincided with that of curve (c). The absence of lead electrodeposition was further confirmed by the observation that the crystal could easily be cleaned with dilute acetic acid so that the frequency returned to its original value. Had the lead been electrodeposited, such an easy removal would not have been observed. In these experiments, measurements of the frequency of the crystal were made 2 min after immersion because it decreased slowly thereafter and showed poor reproducibility because of evaporation of chloroform and changes in temperature during a longer run.

Dependence of chelate adsorption on pH. The effect of pH on the response from the extracted chelate was studied. The buffer solutions selected were sodium tartrate—sodium hydroxide and acetic acid—sodium acetate. The results are shown in Fig. 2. The cobalt(II), nickel, zinc and cadmium chelates

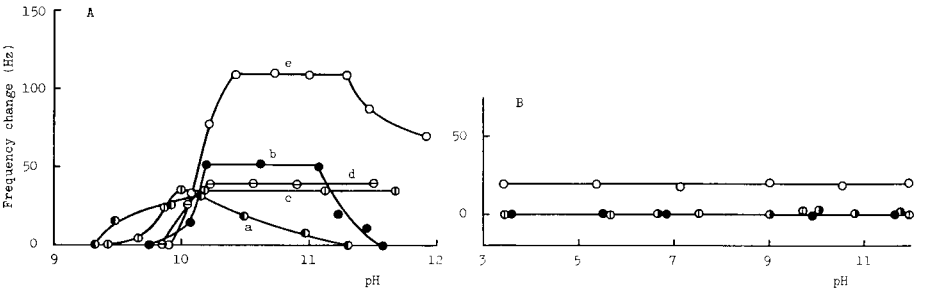

Fig. 2. Dependence of the frequency change on the pH of 5×10^{-6} M metal ion solutions extracted with chloroform by the recommended procedure. A, (a) Co(II); (b) Ni; (c) Zn; (d) Cd; (e) Pb. B, (●) Al; (◑) Mn(II); (○) Fe(III); (◐) Cu(II).

adsorbed on the crystal when they were extracted, but there were suspensions remaining in the aqueous phase. The manganese chelate was extracted from alkaline solution, but did not adsorb on the crystal. Iron(III) 8-quinolinate was slightly adsorbed, but the extracted copper(II) chelate exhibited no adsorption. Aluminium was not extracted over the pH range investigated. The extracted lead chelate adsorbed strongly on the crystal; the frequency change was not only much greater than that from the other metals, but was constant over the pH range 10.5—11.3.

Dependence of the frequency change on shaking and standing times. The effect of changing the shaking time from 30 s to 10 min on the response to lead was examined. The crystal immersed in the chloroform solution showed a constant frequency change after extraction times of 1 min. A 2-min shaking period is therefore recommended. The time required for phase separation was also investigated. The frequency change was constant for phase separation times between 3 and 30 min. A standing time of 5 min, therefore, should be allowed for separation of the chloroform phase.

Calibration, reproducibility and interferences. A calibration graph prepared by use of the recommended procedure was linear for $1—5 \times 10^{-6}$ M lead, with a slope of 20 Hz per 10^{-6} M, but showed a negative deviation above 5×10^{-6} M, and finally saturation occurred above 5×10^{-5} M. Lead in the range $1 \times 10^{-6}—3 \times 10^{-5}$ M may be determined reproducibly by the recommended procedure. The standard deviation was 5.83 Hz (5.8%) for five determinations of 5.0×10^{-6} M lead in the aqueous solution.

The effect of a number of other ions on the determination of 5.0×10^{-6} M lead was investigated; changes in frequency of more than ±8% were considered to constitute an interference. An equivalent concentration of sulphide and a 100-fold concentration of phosphate interfered by decreasing the extraction, but 100-fold concentrations of chloride, bromide, iodide, nitrate, perchlorate, cyanide, thiocyanate, thiosulphate, sulphate and carbonate did not interfere. Ten-fold concentrations of Mg, Ca, Al and Cu(II) and equivalent concentrations of Mn(II) and Ag did not interfere, but Fe(III), Co(II) Ni, Zn and Cd gave enhanced signals. Ten-fold concentrations of the

latter cations, except Mn(II), could be tolerated by using the masking procedure given above.

REFERENCES

1 T. Nomura and A. Minemura, Nippon Kagaku Kaishi, 1980 (1980) 1261.
2 T. Nomura and M. Iijima, Anal. Chim. Acta, 131 (1981) 97.
3 T. Nomura, M. Okuhara, K. Murata and O. Hattori, Bunseki Kagaku, 30 (1981) 417.

Analytica Chimica Acta, 143 (1982) 249—254
Elsevier Scientific Publishing Company, Amsterdam — Printed in The Netherlands

Short Communication

DETERMINATION OF METHYLMERCURY IN THE PRESENCE OF INORGANIC MERCURY BY ANODIC STRIPPING VOLTAMMETRY

J. IRELAND-RIPERT, A. BERMOND* and C. DUCAUZE

Laboratoire de Chimie Analytique, Institut National Agronomique, 16, rue Claude-Bernard, 75231 Paris Cedex 05 (France)

(Received 27th January 1982)

Summary. Methylmercury is determined in a non-complexing nitrate medium by differential pulse anodic stripping voltammetry at a gold film electrode, with a detection limit of 2×10^{-8} mol l^{-1} for 5-min plating times. A method of double standard additions is proposed for determining methylmercury in the presence of mercury(II) ions.

Voltammetric methods reported for the determination of mercury make use of carbon electrodes such as wax-impregnated graphite [1, 2], carbon paste [3] and glassy carbon [4]. However, the carbon electrodes do not provide satisfactory sensitivity for the determination of trace mercury because of the small affinity of the carbon electrode for mercury metal [5]. Recently, gold electrodes have received renewed attention for trace mercury determination because of the large solubility of mercury in gold. Gold electrodes [6], twin gold electrodes [7, 8] and gold film electrodes [9] have successfully been used for the determination of mercury(II) in water samples. Unfortunately, these analyses were made only for total mercury; no distinction was made between inorganic and organic mercury, the latter being considerably more toxic than the former. The aim of this study is to show the feasibility of electrochemical speciation of mercury in synthetic aqueous solution, by anodic stripping voltammetry on a gold film electrode.

Experimental

Apparatus. For voltammetric studies Tacussel equipment was used: a PRG5 polarograph was coupled with an ISIS 4000 voltmeter and an EPL2B potentiometric recorder; the EDI rotating glassy carbon disk working electrode (GCE) had a surface area of 7 mm^2. A silver—silver chloride electrode in a separate compartment with fritted glass junction was used as reference electrode and a platinum wire as counter electrode.

Reagents and solutions. The chemicals used were of analytical-reagent grade. Methylmercury(II) chloride was 98% pure; sodium gold(III) chloride was purified by plating on a GCE at +0.4 V, redissolving in the minimum volume of aqua regia, and diluting with water and nitric acid. Water was from

0003-2670/82/0000-0000/$02.75

a Milli-Q (Millipore S.A.) reagent-grade water system. The supporting electrolyte, unless otherwise stated, was 0.1 mol l^{-1} sodium nitrate containing 0.014 mol l^{-1} nitric acid. Standard 10^{-3} mol l^{-1} solutions of methylmercury were prepared daily by dissolving CH_3HgCl in 0.014 mol l^{-1} nitric acid. Before measurements, the 40-ml samples were purged with nitrogen for 15 min.

Gold film electrode. The potential of the GCE was scanned several times between —0.5 and +0.5 V in 0.014 mol l^{-1} nitric acid and the current recorded at —0.5 V. An aliquot of stock gold(III) solution was added to give a concentration of 5×10^{-6} mol l^{-1} and the solutions were allowed to mix. Gold was deposited at —0.5 V, and the quantity of gold electroplated at the GCE was calculated from the integral of the electrical current over the period plating time t_D. For bulk mercury concentrations of 10^{-7} mol l^{-1}, the best anodic stripping peaks were obtained with a thin gold film ($\simeq 2 \times 10^{14}$ atoms). If the deposit were uniform, this would be two monolayers of gold; this thickness was chosen for the present study. Between measurements, the gold film was freed of any trace of mercury by oxidation at +0.5 V in 0.1 mol l^{-1} nitric acid for 2 min.

Differential pulse anodic stripping voltammetry (d.p.a.s.v.). The operating conditions, unless otherwise stated, were: plating potential E_D = —0.5 V; plating time t_D = 5 min; electrode rotation, 1500 rpm (during plating only); electrode equilibration time (without stirring), 1 min; scan rate, 4 mV s^{-1}.

Results and discussion

Electrochemistry of methylmercury on gold. Figure 1 shows examples of reduction voltammograms of methylmercury at thick gold film electrodes for different pH values. As can be seen, two waves are present at pH 6, but only the first can be observed at pH 1 because of hydrogen discharge.

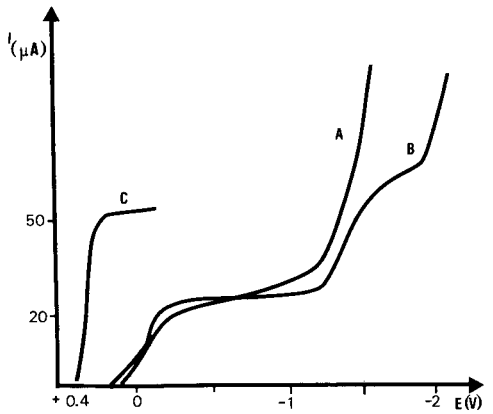

Fig. 1. D.c. voltammograms of mercury compounds at thick gold film electrodes (5×10^{16} atoms Au, scan rate 2 mV s^{-1}.) (A) CH_3HgCl (4×10^{-4} mol l^{-1}) in 0.14 mol l^{-1} HNO_3 (pH 1); (B) CH_3HgCl (4×10^{-4} mol l^{-1}) in 0.1 mol l^{-1} $NaNO_3$ (pH 6); (C) $HgCl_2$ (10^{-5} mol l^{-1}) in 0.1 mol l^{-1} $NaNO_3$—0.014 mol l^{-1} HNO_3 (pH = 2).

The half-wave potential of the first wave is more or less independent of pH between pH 1 and 6 and is ≈ -0.1 V; whereas at pH > 10 this wave is shifted cathodically at about 0.02 V pH^{-1}. The wave is distorted and there is a prewave; these irregularities can be attributed to subsequent chemical reactions and to interactions of methylmercury and its reduction products with gold. The wave for mercury(II) chloride is also shown in Fig. 1 for comparison.

The first wave appears to be diffusion-controlled as the dependence of the limiting current on the concentration of the electroactive species, as well as its variation with the square root of the electrode rotation speed, is linear. The number of electrons involved in the first step was determined by coulometry at —0.5 V; methylmercury was reduced, at a thick gold film bar electrode in a 1-electron reaction to mercury (formation of a grey deposit on the working electrode); this measurement was performed 5 times, with a relative standard deviation of 19%. The quantitative deposition of mercury on gold was investigated by comparing the amount of faradaic electricity consumed during mercury plating at —0.5 V (Q_1) with that consumed during anodic stripping (Q_2). The mean value for Q_2/Q_1 was found to be 0.86 (23 measurements, with a relative standard deviation of 8%). Thus the deposition is not quantitative and may vary with the gold film electrode surface.

These results indicate that the mechanism for reduction of methylmercury on gold may be similar to that proposed for methylmercury at the hanging mercury drop electrode [10, 11]

$$CH_3HgCl + e^- \rightleftharpoons CH_3Hg^{\bullet} + Cl^-$$

$$2CH_3Hg^{\bullet} \rightleftharpoons (CH_3Hg)_2$$

$$(CH_3Hg)_2 \rightleftharpoons (CH_3)_2Hg + Hg(0)$$

$$CH_3Hg^{\bullet} + H^+ + e^- \rightarrow CH_4 + Hg(0)$$

According to this mechanism, the reduction of methylmercury occurs in two 1-electron steps, the first of which results in the formation of a methylmercury(II) radical on the electrode surface. This step is considered reversible under voltammetric conditions, but the radical is involved in subsequent dimerisation and disproportionation reactions.

The reduction of methylmercury to mercury at the gold electrode has been found to be incomplete in an acidic medium (at —0.5 V). Nevertheless, this reduction wave has analytical utility, as the limiting current is linearly dependent on the concentration of methylmercury in solution. Differential pulse anodic stripping voltammograms at a gold film electrode, for different concentrations of methylmercury, are shown in Fig. 2. The relationship between the methylmercury concentration and the stripping peak height is linear; the detection limit, calculated from three times the standard deviation of the blank, for the determination of methylmercury under these experimental conditions is 2×10^{-8} mol l^{-1}.

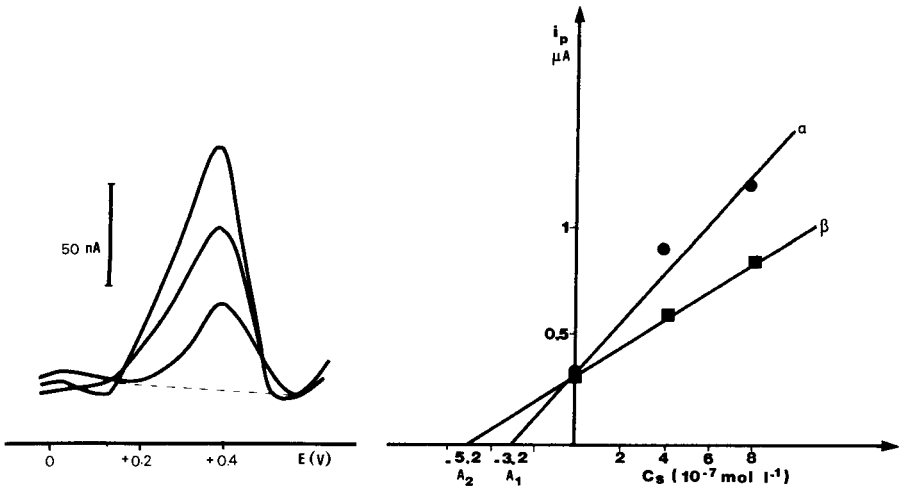

Fig. 2. Typical voltammograms obtained by d.p.a.s.v. (E_D = —0.5 V, t_D = 5 min, scan rate = 4 mV s^{-1}) at a gold film electrode, for bulk methylmercury concentrations of 2, 4 and 6 × 10^{-7} mol l^{-1}.

Fig. 3. Typical calibration graphs for double standard addition method of methylmercury determination by d.p.a.s.v. (E_D = —0.5 V, t_D = 5 min) at a gold film electrode: standard additions of (•) Hg^{2+}; (▪) CH_3Hg^+.

Determination of methylmercury in the presence of inorganic mercury(II). The normal standard addition method assumes that the analytical signal without additions is only due to the measured element and to no other compound in the sample. This is not the case for the determination by a.s.v. of methylmercury in the presence of inorganic mercury, as the stripping peak signal depends on the amount of both species. Thus, the normal standard addition method gives unsatisfactory results for this determination, whether the standard additions are of methylmercury or of mercury(II). Mercury formation is not quantitative for the first reduction step of methylmercury. Moreover, their diffusion coefficients may be different. For these reasons, standard additions of both species are necessary.

For the double standard addition procedures, $I_{p,\,n}$ is the height of the stripping peak for n standard additions, C_x is the unknown initial bulk concentration of Hg^{2+}, C_y is the unknown initial bulk concentration of CH_3Hg^+, C_s is the concentration of the standard addition, α and β are the slopes of the linear graphs of stripping peak height and the concentrations of Hg^{2+} and CH_3Hg^+, respectively (i.e., the slopes of the standard addition curves) and A_1 and A_2 are the intercepts of the two standard addition curves. The height of the mercury stripping peak is directly proportional to the bulk concentrations of Hg^{2+} and of CH_3Hg^+, i.e., $I_{p,\,o} = \alpha C_x + \beta C_y$. If the total volume remains constant (standard added by micropipette), standard addi-

tions of Hg^{2+} give $I_{p,n} = \alpha(C_x + nC_s) + \beta C_y$, and standard additions of CH_3Hg^+ give $I_{p,n} = \alpha C_x + \beta(C_y + nC_s)$. For standard additions of Hg^{2+}, α and A_1 can be calculated by linear extrapolation to zero current; then, β and A_2 can be calculated by standard additions of CH_3Hg^+. When C_x is already known, C_y can be determined from the two standard addition graphs shown in Fig. 3.

Table 1 summarizes the results of methylmercury determinations for an electrolyte solution spiked with 2×10^{-7} mol l^{-1} each of Hg^{2+} and CH_3Hg^+. Two standard additions of 2 or 4×10^{-7} mol l^{-1} Hg^{2+}, then CH_3Hg^+, were measured three times each and the plots obtained by linear regression. For each trial, the value of α/β is the result of two linear regressions (9 points each); the mean value was found to be 2.4. More precise results were obtained by calculating from standard additions of Hg^{2+} than of CH_3Hg^+, although both standard addition graphs were necessary to calculate the ratio α/β used in the calculation. The standard deviations are relatively large (Table 1), and may reflect the incomplete reduction of methylmercury to mercury metal and the influence of the gold electrode surface on the reduction of methylmercury.

Thus it is possible to determine methylmercury in the presence of inorganic mercury(II) ions in a non-complexing nitrate solution. This method may be extended to determine the two forms of mercury. In the media studied, their reduction potentials are sufficiently different (see Fig. 1) that inorganic mercury(II) could be determined by an initial deposition at 0.0 V followed by anodic stripping, and methylmercury by a second deposition at −0.5 V; it would be useful, for their simultaneous determination, to employ the double standard addition method, coupled with a multilinear regression analysis [12].

TABLE 1

Results for determination of 2.0×10^{-7} mol l^{-1} methylmercury with standard additions of Hg^{2+} (A_1) and CH_3Hg^+ (A_2) in nitrate solution (pH 2), by d.p.a.s.v. at gold film electrodes. ($E_D = -0.5$ V, $t_D = 5$ min; standard additions were of 2 or 4×10^{-7} mol l^{-1} mercury(II).)

Calculations from standard addition curves	Mean result[a]	R.s.d. (%)	Recovery (%)
$C_y = \alpha/\beta\ (A_1 - C_x)$	2.6×10^{-7} mol l^{-1}	20	130
$C_y = A_2 - \alpha/\beta\ C_x$	2.6×10^{-7} mol l^{-1}	45	130
α/β	2.4	24	—

[a]Mean of 5 determinations.

REFERENCES

1 S. P. Perone and W. J. Kretlow, Anal. Chem., 37 (1965) 968.
2 R. Fukai and L. Huynh-Ngoc, Anal. Chim. Acta, 83 (1976) 375.
3 P. Emmott, Talanta, 12 (1965) 651.
4 L. Luong and F. Vydra, J. Electroanal. Chem., 50 (1974) 379.
5 Z. Yoshida and S. Kihara, J. Electroanal. Chem., 95 (1979) 159.
6 R. W. Andrews, D. C. Johnson and J. H. Larochelle, Anal. Chem., 48 (1976) 212.
7 L. Sipos, H. W. Nürnberg, P. Valenta and M. Branica, Anal. Chim. Acta, 115 (1980) 25.
8 L. Sipos, J. Golimowski, P. Valenta and H. W. Nürnberg, Fresenius Z. Anal. Chem., 298 (1979) 1.
9 R. E. Allen and D. C. Johnson, Talanta, 20 (1973) 799.
10 R. C. Heaton and H. A. Laitinen, Anal. Chem., 46 (1974) 547.
11 C. Degrand and E. Laviron, Bull. Soc. Chim. Fr., 1968, No. 5, 2228.
12 B. E. H. Saxberg and B. R. Kowalski, Anal. Chem., 51 (1979) 1031.

Analytica Chimica Acta, 143 (1982) 255—260
Elsevier Scientific Publishing Company, Amsterdam — Printed in The Netherlands

Short Communication

DETERMINATION OF STABILITY CONSTANTS BY SEMI-INTEGRAL ANALYSIS OF VOLTAMMOGRAMS OBTAINED WITH A COMPUTERIZED ELECTROCHEMICAL SYSTEM

M. TKALČEC, B. S. GRABARIĆ* and I. FILIPOVIĆ

Laboratory of General and Inorganic Chemistry, Faculty of Technology, University of Zagreb, P.O.B. 179, 41000 Zagreb (Yugoslavia)

(Received 19th March 1982)

Summary. A versatile computerized electrochemical system is used for the determination of stability constants of lead(II) propanoate and 2-hydroxypropanoate complexes by semi-integral linear sweep voltammetry. Semi-integral voltammograms are analogous in characteristics to d.c. polarograms, and the half-wave potentials ($E_{1/2}$) and limiting currents (i_l) for a depolarizer can be obtained by nonlinear least-squares fitting of semi-integrally transformed voltammograms. An advantage of the proposed method is that $E_{1/2}$ and i_l values are obtained from a single mercury drop (hanging or dropping mercury electrode); working time is reduced while accuracy and precision are maintained. The computer-controlled system provides automated reagent addition, signal generation, response measurement and sampling, data evaluation, etc. The results agree well with those obtained by the usual d.c. polarographic method.

Linear sweep voltammetry is a very useful technique for qualitative investigations of electrode reaction mechanisms [1]. For quantitative evaluation of the thermodynamic and kinetic characteristics of electrode reactions, this technique has been less used mainly because of its poor quantitative reproducibility compared to d.c., a.c., pulse and differential pulse voltammetry. This poor reproducibility can be ascribed in part to the solid indicator electrodes used, which are sensitive to deposited electrode reaction products and to their previous treatment, and in part to the problems of quantitative evaluation of the characteristic current—potential curves obtained. Compared to some other electroanalytical techniques, the greater sensitivity to ohmic drop within the electrochemical cell and the less favourable ratio of faradaic current to capacitive current are also contributing factors. The lack of commercially available computerized systems for accurate electrochemical data acquisition and flexible data evaluation also limits the broader quantitative application of linear sweep voltammetry. By careful design of the experiment and by using a computer-controlled electrochemical system, however, most of the above-mentioned limitations in obtaining better reproducibility can be eliminated or made negligible. Thus linear sweep voltammetry becomes a powerful technique for both qualitative investigation

of electrode reaction mechanisms and quantitative study of thermodynamic and kinetic features of electrode reactions.

A significant improvement in classical linear sweep voltammetry, especially with respect to quantitative evaluation of electrode kinetics, was made by Oldham and co-workers [2—7] and by Saveant and co-workers [8—12], who proposed mathematical models for transforming classical voltammograms into more convenient curves, as well as efficient methods for evaluation of voltammograms. These workers also provided extensive experimental verification of the theory for different mechanisms of electrode reactions. Oldham transforms are known as semi-integral electroanalysis, Goto and Ishii [6] proposed semidifferential electroanalysis, while Saveant called the technique convolution potential sweep voltammetry. Semi-integral transform and convolution of the voltammogram give a sigmoidal curve of the transformed current vs. potential relation, while semidifferential transform gives a peak-shaped curve.

In the work reported here, the semi-integral transform was combined with on-line computerized measurement and data processing. A hanging or dropping mercury electrode was selected so that a clean electrode surface would always be available to improve reproducibility. Another advantage of semi-integral technique is its ability to correct for uncompensated ohmic drop within the electrochemical cell during data processing. This technique of correction for ohmic drop has been applied to reversible systems by Whitson et al. [13] and Imbeaux and Saveant [9], and to quasi-reversible systems by VandenBorn and Evans [14].

The semi-integral transforms were calculated from the current data using a series discussed by Nicholson and Shain [15]:

$$m(t) = 2(\delta/\pi)^{1/2} \left\{ i(1)N^{1/2} + \sum_{j=1}^{N-1} (N-j)^{1/2} \left[i(j+1) - i(j) \right] \right\} \qquad (1)$$

where $m(t)$ is the semi-integral value, $i(j)$ is the current at point j, and δ is the time between data points. The semi-integral transforms can be corrected for sphericity effects as proposed by Imbeaux and Saveant [9].

Once the semi-integral transform has been obtained, a nonlinear least-squares regression analysis can be applied, in order to extract the half-wave potential ($E_{1/2}$), the limiting value of the semi-integral ($m(t)_l$), and the transfer coefficient (α) from the relationship [16]

$$m(t) = m(t)_l / \{1 + \exp [(\alpha nF/RT)(E - E_{1/2})]\} \qquad (2)$$

where all other symbols have their usual meaning.

In investigations of complex formation equilibria by d.c. polarography with increasing ligand concentration, at constant metal ion concentration, ionic strength and temperature, the features observed are the shift of $E_{1/2}$ values of the electroactive species (metal ion complexes) towards more negative potentials and the changes in diffusion current. The same will hold for semi-integral transforms. Therefore, if the electrode reaction is reversible [17], the F_0 polynomials can be obtained from

$$F_0 = \exp(nF/RT)(E^s_{1/2} - E^c_{1/2}) + \ln[m(t)^s_l / m(t)^c_l] \quad (3)$$

where superscripts s and c denote the corresponding parameters obtained from a solution of metal ion without and with the ligand present, respectively. These polynomials also correspond [18] to

$$F_0 = 1 + \sum_{j=1}^{k} \beta_j [L]^j \quad (4)$$

where k is the number of complex species present in the solution, β_j are cumulative stability constants, and $[L]$ is the free ligand concentration. By nonlinear least-squares fitting of Eqn. (4), it is possible to obtain the cumulative stability constants and their standard errors.

Experimental

Chemicals and solutions. Lead(II) perchlorate was prepared from lead(II) oxide and perchloric acid and was recrystallized three times. Sodium propanoate and 2-hydroxypropanoate were prepared from the corresponding acids and sodium hydroxide and were also recrystallized three times. All chemicals were of p.a. grade. The ionic strength of all aqueous solutions was kept constant (I = 2 mol dm^{-3}) by adding sodium perchlorate. All measurements were made in buffered solution with a constant initial concentration (10^{-2} mol dm^{-3}) of propanoic or 2-hydroxypropanoic acid to avoid hydroxy complex formation. The concentration of metal ion was also constant (5×10^{-4} mol dm^{-3}). All solutions were thermostated at 298.2 ± 0.1 K.

Apparatus. The electrochemical computerized system consisted of a PDP-8/E (Digital Equipment Corp.) OS-8/10 system, a home-made potentiostat, interface, peripherals and recording devices. The drop detacher, microburette and valve for gas purging, all computer-controlled, were also part of the system. A three-electrode cell was used; the indicator electrode was a hanging or dropping mercury electrode. The system was largely as described in detail previously [19]. The block diagram shown in Fig. 1 illustrates the differences from the previously described system which were necessary for semi-integral linear sweep voltammetry.

Computer programs. All subroutines for control of devices connected to the computer were written in SABR assembler language. The main program which connects all the assembler subroutines and performs all the data processing was written in the extended version of FORTRAN II.

Results and discussion

An example of a linear sweep voltammogram and its semi-integral transform obtained at a hanging mercury drop electrode (HMDE) in a solution of lead(II) propanoate complexes is shown in Fig. 2. Resistance compensation and correction for sphericity were done as suggested in the literature [9, 13]. When the dropping mercury electrode (DME) was used, a correction for drop growth was also applied.

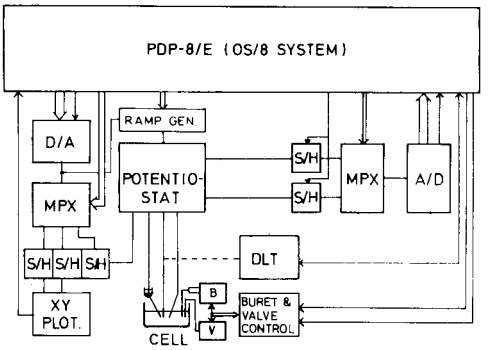

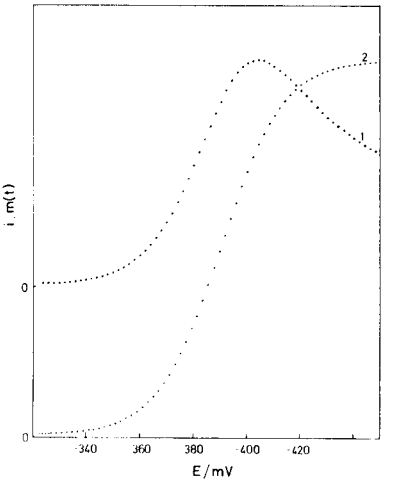

Fig. 1. Block diagram of the computerized electrochemical system. D/A, D/A converter; MPX, multiplexer; S/H, sample and hold amplifiers; XY PLOT, XY recorder; RAMP GEN, perturbation signal generation; A/D, A/D converter; DLT, drop life timer; B, burette; V, gas valve.

Fig. 2. An example of a voltammogram (1) and its semi-integral transform (2) obtained at the HDME. T = 298.2 ± 0.1 K; I = 2 mol dm^{-3} ($NaClO_4$); 5 × 10^{-4} mol dm^{-3} lead perchlorate; 0.1 mol dm^{-3} propanoate. Current is given in arbitrary units.

Plots of $\Delta E_{1/2}$ against free ligand concentration for the lead(II) propanoate and 2-hydroxypropanoate complexes are given in Fig. 3. Logarithmic values of the cumulative stability constants with their standard errors obtained at the HMDE and the DME are listed in Table 1. The stability constants for the same systems, under same solution conditions but obtained by d.c.

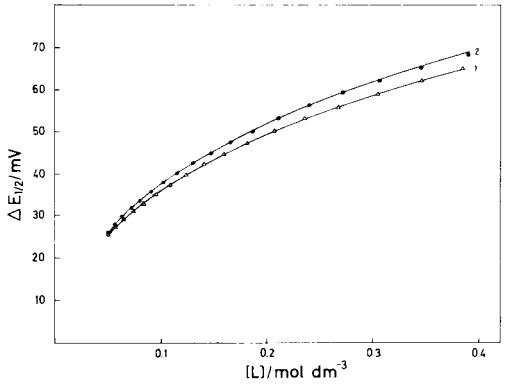

Fig. 3. Plot of $E_{1/2}$ vs. [L] for the lead(II) propanoate (2) and 2-hydroxypropanoate (1) complexes.

TABLE 1

Stability constants of lead(II) propanoate and 2-hydroxypropanoate complexes obtained at $T = 298.2 \pm 0.1$ K and $I = 2$ mol dm^{-3}

Method[a]	Ligand	log K_1	log β_2	log β_3	Ref.
s.l.s.v./HDME	Prop	2.17 ± 0.01	3.21 ± 0.01	3.42 ± 0.03	This work
	2—OH—prop	2.06 ± 0.01	3.05 ± 0.01	3.24 ± 0.02	
s.l.s.v./DME	Prop	2.19 ± 0.02	3.20 ± 0.03	3.44 ± 0.03	This work
	2—OH—prop	2.03 ± 0.02	3.07 ± 0.02	3.26 ± 0.03	
D.c. polarography	Prop	2.17 ± 0.01	3.22 ± 0.01	3.45 ± 0.02	[19]
	2—OH—prop	2.05 ± 0.01	3.04 ± 0.01	3.26 ± 0.02	

[a]s.l.s.v., semi-integral linear sweep voltammetry.

polarography [19] are given for comparison. The values obtained with different electrodes by semi-integral linear sweep voltammetry and those obtained by d.c. polarography are in good agreement. The accuracy and reproducibility are similar for all three methods, while significant working time is saved when the semi-integral linear sweep technique is used, especially with the DME. All the statements made earlier about the stability of the investigated complexes [19] were confirmed in this work.

The proposed method permits fast determination of stability constants, retaining the same reproducibility as in d.c. polarography. The computerized system is almost mandatory for this purpose.

This work was supported by the National Bureau of Standards, Washington, U.S.A., and by the Self-management Community for Chemical Research of the Federal Republic of Croatia, Zagreb, Yugoslavia, through the U.S.—Yugoslav Joint Board on Scientific and Technological Cooperation. The authors are indebted to both Agencies.

REFERENCES

1 R. N. Adams, Electrochemistry at Solid Electrodes, Marcel Dekker, New York, 1969.
2 K. B. Oldham, Anal. Chem., 41 (1969) 1904; 44 (1972) 196; 45 (1973) 39.
3 K. B. Oldham and J. Spanier, J. Electroanal. Chem., 26 (1970) 331.
4 M. Grenness and K. B. Oldham, Anal. Chem., 44 (1972) 1121.
5 M. Goto and K. B. Oldham, Anal. Chem., 45 (1973) 2043; 46 (1974) 1522.
6 M. Goto and D. Ishii, J. Electroanal. Chem., 61 (1975) 361.
7 K. B. Oldham, J. Electroanal. Chem., 72 (1976) 371.
8 C. P. Andrieux, L. Nadjo and J. M. Saveant, J. Electroanal. Chem., 26 (1970) 147.
9 J. C. Imbeaux and J. M. Saveant, J. Electroanal. Chem., 44 (1973) 169.
10 F. Ammar and J. M. Saveant, J. Electroanal. Chem., 47 (1973) 215.
11 L. Nadjo, J. M. Saveant and D. Tessier, J. Electroanal. Chem., 52 (1974) 403.
12 J. M. Saveant and D. Tessier, J. Electroanal. Chem., 61 (1975) 251.
13 P. E. Whitson, H. W. VandenBorn and D. H. Evans, Anal. Chem., 45 (1973) 1298.
14 H. W. VandenBorn and D. H. Evans, Anal. Chem., 46 (1974) 643.

15 R. S. Nicholson and I. Shain, Anal. Chem., 36 (1964) 706.
16 A. M. Bond and B. S. Grabarić, Anal. Chim. Acta, 101 (1978) 309.
17 D. D. DeFord and D. N. Hume, J. Am. Chem. Soc., 73 (1951) 5321.
18 I. Leden, Z. Phys. Chem., Leipzig, Abt. A, 188 (1940) 160.
19 M. Tkalčec, B. S. Grabarić, I. Filipović and I. Piljac, Anal. Chim. Acta, 122 (1980) 395.

Analytica Chimica Acta, 143 (1982) 261—264
Elsevier Scientific Publishing Company, Amsterdam — Printed in The Netherlands

Short Communication

THE DETERMINATION OF LEAD IN PETROL BY ATOMIC ABSORPTION SPECTROMETRY

I. J. FRIGERIO*, M. J. McCORMICK and R. K. SYMONS

Laboratory Services Branch, Environment Protection Authority, 240 Victoria Parade, East Melbourne, Victoria 3002 (Australia)

(Received 2nd June 1982)

Summary. The lead compounds are extracted into aqueous iodine monochloride, converted to lead nitrate by digestion with nitric acid, and determined by atomic absorption spectrometry against aqueous lead nitrate standards. The procedure is accurate, precise and rapid.

Several methods have been reported for the determination of the total lead content of petrol: volumetric and gravimetric [1], titrimetric [1, 2] and colorimetric [3] procedures have been applied. These methods are time-consuming and do not exploit the benefits of instrumentation currently available for determinations of heavy metals. The determination of the lead content of petrol by atomic absorption spectrometry (a.a.s.) has often been reported since the pioneering work of Robinson [4]. Early determinations were based on dilution of the petrol sample with a suitable organic solvent [4—6] before aspiration into the flame. These procedures required calibration against alkyllead standards carried through the entire procedure to alleviate the effects of differing extraction efficiencies and response factors. The main problem is that different lead alkyls yield different responses [7, 8]. The sensitivity for tetramethyllead has been reported [7] to be 2.5-fold greater than that for tetraethyllead. It was necessary, therefore, to prepare standards which closely matched the composition of the sample being analysed. Some authors claimed that this problem could be minimized by careful selection of solvent [5—7, 9], burner height [6, 8], and dilution ratios and aspiration rates [7]. McCorriston and Ritchie [10] reported the use of a total consumption burner in the analysis of low-lead petrols diluted with iso-octane-acetone but with no chemical pretreatment. Kashiki et al. [9] overcame the problem by the addition of iodine to petrol samples diluted in methyl isobutyl ketone (MIBK), permitting calibration against a single alkyllead standard measured in an air—acetylene flame. Robbins [11] found that this iodine procedure also overcame the different alkyllead responses when carbon-rod a.a.s. was used.

The iodine—MIBK method was modified [12] by the addition of tricaprylmethylammonium chloride (Aliquat 336), which was found to improve the

response and increase the stability of the alkyllead iodide complex. With minor modification this method was adopted as the standard method for the determination of lead in gasoline by the American Society for Testing and Materials [13]. Water has been used as the diluent to obtain an oil—water emulsion with a variety of emulsifiers [14—16], thus avoiding the use of large amounts of organic solvents. The emulsion was considered sufficiently homogeneous to aspirate directly into an air—acetylene flame.

Moss and Campbell [2] showed that mixed lead alkyls in petrol could be efficiently extracted with aqueous iodine monochloride solution and determined by direct titration with EDTA to a xylenol orange end-point after buffering to dimethyl yellow. Tetraalkyllead compounds reacted with the iodine monochloride and were extracted into the aqueous phase as the dialkyllead compounds. Organic matter was destroyed by oxidation with nitric acid, which also converted the dialkyllead compounds to lead nitrate. This procedure was accepted by the Institute of Petroleum [17] as a standard method. While this procedure overcame the problems of differing responses, the titration is time-consuming. However, as the digestion produces lead nitrate, it is apparent that the lead can also be determined accurately by a.a.s. by using aqueous lead nitrate as calibrant. The results of the investigation of such a possibility are reported here.

Experimental

Apparatus. A Perkin-Elmer Model 400 atomic absorption spectrometer was used with a Perkin-Elmer lead electrodeless discharge lamp containing argon, operated at 10 W. The 283.3-nm resonance line was used with a spectral slitwidth of 0.7 nm. A standard 10-cm air—acetylene burner was positioned ca. 5 mm below the centre of the beam image. No background correction was used.

All glassware was presoaked consecutively for 24 h in (1 + 1) nitric acid and 24 h in (1 + 9) nitric acid, and then rinsed with (1 + 99) nitric acid prior to use.

Reagents. Reagent-grade petroleum spirit (80—100°C boiling range) and laboratory-distilled reagent-grade nitric acid (69.5—71.5% w/w) were employed. Iodine monochloride reagent (1.0 M) was prepared as described by Moss and Campbell [2]. All dilutions were done with a (1 + 99) mixture of sub-boiling point distilled nitric acid and distilled water passed through a Millipore Milli-Q reagent-grade water system.

Standards. A stock lead solution (1000 mg Pb l^{-1}) was prepared by diluting an aqueous 1.000 ± 0.002 g Pb solution ($Pb(NO_3)_2$, Merck Titrisol) with (1 + 99) nitric acid. This stock solution may be stored indefinitely in an acid-washed polyethylene container. Calibration solutions (0—20 mg Pb l^{-1}) were prepared by diluting the stock solution in prewashed 100-ml volumetric flasks. (These solutions gave a linear calibration graph.)

Procedure. A 10.0-ml sample of petrol was pipetted into a 250-ml separating funnel, and 30 ml of petroleum spirit (80—100°C) and 15 ml of

iodine monochloride reagent were added. The funnel was stoppered and shaken thoroughly for 60 s. After the phases had separated (some minutes), the lower aqueous phase was collected in a 150-ml conical flask. The extraction was repeated with a further 10 ml of iodine monochloride reagent and then with two separate 30-ml aliquots of water. All aqueous phases were added to the conical flask. Several boiling chips were placed in the flask and the contents were mixed by swirling. The mouth of the flask was covered with a small watch-glass and the flask placed on a hot plate. The contents were boiled until 15—20 ml of solution remained; 10 ml of concentrated nitric acid was then added carefully down the inside of the flask. The contents were again evaporated to about 10 ml and the nitric acid treatment was repeated. If organic matter was still present at this stage, 2 ml of 29—32% (w/w) hydrogen peroxide was added carefully and heating continued. The flask was finally removed from the hot plate and allowed to cool. The contents were quantitatively transferred to a 500-ml volumetric flask and diluted to volume with the (1 + 99) nitric acid. Samples (and standards) were then measured by a.a.s. using the conditions described above.

Results and discussion

The mean result of 18 determinations of lead in the National Bureau of Standards Lead in Reference Fuel (SRM 1638, 91-octane fuel containing 0.512 g Pb l^{-1} at 22°C) was 0.51 g Pb l^{-1}, with a standard deviation of 0.01 g l^{-1}. These determinations were done routinely at 22°C during runs of real samples. Of the 18 determinations, only four gave results that differed from the actual concentration by more than 0.01 g Pb l^{-1} (1 standard deviation). The mean error (lead found — lead present) was —0.002 g Pb l^{-1} and the greatest error in an individual determination was ±0.02 g Pb l^{-1}, indicating very satisfactory accuracy and precision.

A slight modification was made to the extraction procedure of Moss and Campbell [2]. Instead of a single (25-ml) iodine monochloride extraction, two aliquots of 15 ml and 10 ml were used. The mean results of triplicate determinations using the one and two extraction procedures were 0.50 and 0.51 g Pb l^{-1}, respectively, for SRM 1638, indicating a slight improvement in recovery by using two extractions.

The SRM 1638 reference fuel is a mixture of 91% (v/v) 2,2,4-trimethylpentane and 9% (v/v) *n*-heptane. Lead is added as a mixture of tetramethyllead and tetraethyllead in an unstated ratio. The results indicate that all lead species are converted to lead nitrate after the oxidation of organic material, permitting calibration with aqueous lead nitrate solution. The iodine monochloride a.a.s. procedure therefore has the advantage of not requiring standards which closely match the viscosity and composition of the samples, a common problem with previous a.a.s. determinations [7, 9]. Consequently, there is a large saving in procedural time, and the need to use toxic tetramethyllead and tetraethyllead standard solutions is obviated.

The NBS standards do not contain the dyes that are routinely added to

real petrol samples. The NBS standard was analysed as a quality-control measure each time a number of real petrol samples was to be monitored for lead. The results for 41 determinations carried out on these real samples were 0.44 g Pb l^{-1}, with a standard deviation of 0.01 g l^{-1}. The legal lead content in Victoria for 97-octane petrol is currently 0.45 g Pb l^{-1}. The dyes contained in both the super and standard grade petrols were found to be partially extracted, but were completely digested during the nitric acid oxidation and caused no interference.

The time taken for a single determination is <1 h, comparable to the EDTA titration [2]. Routinely, twelve samples may be processed simultaneously, and the speed of measurement by a.a.s. is such that these samples may be analysed in just over 1 h whereas titrations would take considerably longer.

REFERENCES

1 Annual Book of ASTM Standards, Parts 23, 24 and 25, Petroleum Products and Lubricants, American Society for Testing and Materials, Philadelphia, PA, 1981.
2 R. Moss and K. Campbell, J. Inst. Pet. London, 53 (1967) 89; Chem. Abstr., 66 (1967) 97169k.
3 K. Campbell and R. Moss, J. Inst. Pet. London, 53 (1967) 194; Chem. Abstr., 67 (1967) 45720j.
4 J. W. Robinson, Anal. Chim. Acta, 24 (1961) 451.
5 H. W. Wilson, Anal. Chem., 38 (1966) 920.
6 R. M. Dagnall and T. S. West, Talanta, 11 (1964) 1553.
7 D. J. Trent, At. Absorpt. News, 4 (1965) 348.
8 B. E. Buell, Anal. Chem., 34 (1962) 635.
9 M. Kashiki, S. Yamazoe and S. Oshima, Anal. Chim. Acta, 53 (1971) 95.
10 L. L. McCorriston and R. K. Ritchie, Anal. Chem., 47 (1975) 1137.
11 W. K. Robbins, Anal. Chim. Acta, 65 (1973) 285.
12 E. Lindemanis, Direct Determination of Lead in Gasoline by Atomic Absorption, Analytical Method No. M113-71, E. I. du Pont de Nemours and Co., Wilmington, DE, 1971.
13 Lead in Gasoline by Atomic Absorption Spectrometry, D3237-79, American Society for Testing and Materials, Philadelphia, PA, 1979.
14 R. J. Lukasiewicz, P. H. Berens and B. E. Buell, Anal. Chem., 47 (1975) 1045.
15 V. Berenguer, J. L. Guinon and M. de la Guardia, Fresenius Z. Anal. Chem., 294 (1979) 416.
16 L. Polo-Diez, J. Hernandez-Mendez and F. Pedroz-Penolva, Analyst, 105 (1980) 37.
17 Total Lead in Gasoline, Iodine Monochloride Method, IP Standards for Petroleum and its Products, Part 1, Heyden, London, IP 270/70, 1974.

Analytica Chimica Acta, 143 (1982) 265—268
Elsevier Scientific Publishing Company, Amsterdam — Printed in The Netherlands

Short Communication

THE DETERMINATION OF LEAD IN TAPWATER BY RESIN PRE-CONCENTRATION FOLLOWED BY FLAME ATOMIC ABSORPTION SPECTROMETRY

A. G. ROWLEY*, I. A. LAW and F. M. HUSBAND

Department of Chemistry, University of Edinburgh, West Mains Road, Edinburgh EH9 3JJ (Gt. Britain)

(Received 3rd June 1982)

Summary. The preparation and use of a polystyrene-supported poly(maleic anhydride) resin for the preconcentration of lead from tapwater samples is described. After elution with dilute nitric acid, lead is determined by flame atomic absorption spectrometry down to levels well below the 50 ng cm^{-3} E.E.C. limit.

The directive of the Council of the European Communities [1], which relates to the quality of water for human consumption, specifies an upper limit of 50 ng cm^{-3} for lead in tapwater drawn from lead pipes. The routine monitoring of this limit is ideally carried out by flame atomic absorption spectrometry (a.a.s.) which is well able to cope with the rapid throughput of samples required. This limit, however, is below the practical detection limit for flame a.a.s. so that it is usual to preconcentrate the lead before completing the determination. Several procedures are available, notably liquid—liquid extraction [2] and, most commonly in the routine laboratory, simple evaporation of water samples to small bulk. The last method, although crude, is widely used because it requires no expensive reagents and little active participation by an operator, but it is very slow if high concentration factors are required.

The system described here for the preconcentration of lead is based on an easily prepared resin of polystyrene-supported poly(maleic anhydride) prepared by initiation of the polymerisation of maleic anhydride by polystyryl(ethylpyridine).

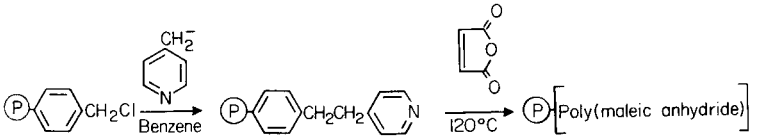

0003-2670/82/0000-0000/$02.75

The structure of poly(maleic anhydride) is unknown but its similarity to fulvic acid [3], a natural chelator of metals, has been pointed out and it has been reported [4] that polystyrene-supported poly(maleic anhydride) is a selective and efficient, water-insoluble, lead adsorber.

Experimental

Preparation of the resin. Wash Amberlite XAD-2 (B.D.H.) with deionised water until the washings are chloride-free ($AgNO_3$) and then with acetone and methanol before drying at 40°C and 0.6 mm Hg overnight. Chloromethylate the purified resin by treatment with chloromethylmethyl ether in the presence of tin(IV) chloride as described by Merrifield [5] to obtain a resin that on analysis for chlorine contains 1.60 mmol chloromethyl residues g^{-1}. Add powdered sodamide (3.12 g, 80 mmol) to 4-picoline (29.8 g, 320 mmol distilled from barium oxide) and sodium-dried benzene (75 cm^3) under dry nitrogen. Stir for 0.5 h and then add chloromethylated Amberlite XAD-2 (5 g, 8 mmol chloromethyl residues). Continue stirring for a further 18 h. Pour the residue into 100 cm^3 of cold water with rapid stirring and filter off the polymer. Wash well with acetone, benzene and methanol before drying as described above. Analysis for chlorine and nitrogen showed that replacement of the chlorine by ethylpyridine residues was quantitative.

Stir polystyryl(ethylpyridine) (20 g, prepared as above) with molten maleic anhydride (150 g) under nitrogen at 120°C for 5 h. After cooling to ca. 50°C, add acetone (250 cm^3), and after stirring for 0.5 h, filter off the polymer and purify by treatment in a Soxhlet extractor with acetone, water, and acetone until the extract is colourless at each stage. Dry at 40°C and 1 mm Hg overnight to give 25.6 g of brown polymer beads.

Reagents. Standard solutions were prepared using analytical-reagent grade lead nitrate or from a commercial standard solution (1 mg cm^{-3}) of lead nitrate (B.D.H.). Nitric acid was Aristar grade. All dilution water was deionised and then glass-distilled.

Apparatus. A Pye SP9-800 atomic absorption spectrometer was used with an air—acetylene flame. Samples and standards were stored in polypropylene bottles.

Procedure. The resin was held by glass wool in a vertical tube of flexible PVC (8-mm i.d.). Normally the columns contained 1 g of the resin and the natural flow rate through the resin bed (ca. 1000 cm^3 h^{-1}) was used, under which conditions adsorption of lead was quantitative and the column could be left to run unattended. Control of the flow rate by a screw clip at the base of the column was required only during stripping (see below). Although the flow through the column decreased slightly as the resin packed down in use, it never fell below 700 cm^3 h^{-1}.

Add the sample solution, normally 1 l contained in a polypropylene bottle, to the resin column by inverting the sample bottle into a 100-mm i.d. polyethylene funnel on top of the column and leave the sample to drain through under gravity over 1 h. Then close the clip at the bottom of the

column and pipette 15 cm^3 of 2 M nitric acid onto the column, whilst temporarily opening the clip slightly to allow the column to become fully wetted with the acid. Close the clip completely. Collect any acid escaping from the bottom of the column in a 25-cm^3 volumetric flask. After soaking for 2 min, drain the acid from the column into the flask. Finally, wash the column with 8 cm^3 of the distilled water, collecting the washings in the same flask. Dilute the solution to the mark before determination of the lead by a.a.s. at 217 nm.

Prepare the column for re-use by washing with water until the washings are neutral; normally ca. 50 cm^3 of water is required.

Results and discussion

A 5-l sample of lead nitrate solution (50 ng Pb cm^{-3}) was prepared and split into five 1-l samples, each of which was concentrated as described above; the lead level in each concentrate was measured by ten replicate a.a.s. measurements. The results from the ten replicates in five subsets were pooled to obtain a standard deviation. The expected lead level in the concentrate was 2.00 μg cm^{-3}. The mean measured concentration was 2.00 μg cm^{-3} with a standard deviation of 40 ng cm^{-3}. This is equivalent to 50 ± 1 ng cm^{-3} in the original sample. Reagent blank determinations on 1 l of the distilled water used gave no detectable lead in the concentrate (<40 ng cm^{-3}). A similar study in which a solution of 5 ng Pb cm^{-3} was used gave a value for the concentrate of 0.21 ± 0.02 μg Pb cm^{-3} (expected value 0.20 μg cm^{-3}).

The pH of the sample was not a critical factor, but the performance of the polymer deteriorated below pH 5 and above pH 9. The pH of the samples, therefore, was adjusted to 6.0—6.5 with nitric acid or ammonia.

One column was subjected to ten cycles of lead uptake and stripping. There was no detectable change in performance. Furthermore, a batch of columns has been in routine daily use for three months without any deterioration in performance.

The method was used in the analysis of samples of tapwater kindly supplied by Lothian Region Water Supply Services Laboratory and the precision was found to be as good as that quoted above for the laboratory-prepared water samples, at similar concentrations.

Conclusions

The method developed for the determination of lead in tapwater is applicable at levels below the E.E.C. limit. Determinations down to 10% of this limit can be done with ease and high precision by flame a.a.s. The simplicity and cheapness of the preconcentration apparatus and the ease of preparation of the resin from economical starting materials makes it possible to have a large number of columns in use simultaneously, with little demand on the operator.

The authors thank SERC for a studentship for F. M. H. and Mr. N. Michie of Lothian Region Water Supply Services Laboratory for the provision of samples and helpful discussions.

REFERENCES

1 Official Journal of the European Communities, 23 (1980). No L229/11 (80/778/EEC).
2 S. E. Allen, H. M. Grimshaw, J. A. Parkinson and C. Quarmby, Chemical Analysis of Ecological Materials, Blackwell, Oxford, 1974, p. 319 and p. 163; M. S. Cresser, Solvent Extraction in Flame Spectroscopic Analysis, Butterworths, London, 1978.
3 H. A. Anderson and J. D. Russell, Nature, (London), 290 (1976), 597.
4 F. M. Husband and A. G. Rowley, Chem. Ind. (London), (1982) 164.
5 R. B. Merrifield, J. Am. Chem. Soc., 85 (1963) 2149.

Analytica Chimica Acta, 143 (1982) 269—272
Elsevier Scientific Publishing Company, Amsterdam — Printed in The Netherlands

Short Communication

DETERMINATION OF ARSENIC AND ANTIMONY IN NIOBIUM BY RADIOCHEMICAL NEUTRON ACTIVATION—γ-SPECTROMETRY

R. CALETKA and V. KRIVAN*

Sektion Analytik und Höchstreinigung, University Ulm, D-7900 Ulm-Donau (Federal Republic of Germany)

(Received 8th June 1982)

Summary. A method for the determination of arsenic and antimony in niobium, with simultaneous determinations of Au, Cu and Mo, is described. The samples are irradiated for 12 h in a thermal neutron flux of 8×10^{13} n cm^{-2} s^{-1} and then dissolved in hydrofluoric—nitric acid. After addition of various masking agents, and reduction with potassium iodide, As(III) and Sb(III) are extracted with diethylammoniumdiethyldithiocarbamate in chloroform. Before reduction, Au, Cu and Mo can be extracted as dithiocarbamates and determined. For samples of about 100 mg, the limits of detection are 10 pg g^{-1} for As, 20 pg g^{-1} for Sb, 0.8 pg g^{-1} for Au, 10 pg g^{-1} for Cu and 25 ng g^{-1} for Mo. Results are given for niobium samples of different grades of purity.

Considerable progress has been achieved in trace characterization of niobium in recent years [1, 2], but little attention has been given to the determination of arsenic and antimony in this matrix. Nazarenko et al. [3] determined arsenic at the 0.1 μg g^{-1} level in niobium and some other metals; separation of arsenic as AsH_3 was followed by photometric determination as molybdenum blue. Direct optical emission spectrography enables antimony ($\geqslant$10 μg g^{-1}) to be determined in niobium or tantalum [4, 5].

The radiochemical neutron activation technique described below allows arsenic and antimony to be determined down to 10 pg g^{-1} levels. Of the various possibilities for the separation of these two elements solvent extraction was chosen because it provides good selectivity and greater convenience for routine work than the distillation procedures [6, 7].

Experimental

Chemicals. All reagents were of "pro analysi" grade. The radiotracers used for development of the separation procedure (^{76}As, ^{198}Au, ^{64}Cu, ^{99}Mo and $^{122,124}Sb$) were prepared by irradiation of the respective metals or oxides in a reactor; their radioactive purity was checked by γ-ray spectrometry.

Irradiation. Samples (50—100 mg of niobium) and standards for irradiation were prepared as described earlier [2]. Irradiations were done in the FR-2 reactor, Kernforschungszentrum Karlsruhe, at a thermal neutron flux of 8×10^{13} n cm^{-2} s^{-1} for 12 h. The cooling time was about 6 h.

0003-2670/82/0000-0000/$02.75

The fractions obtained after the separation were counted with a high-resolution γ-ray spectrometer consisting of an Ortec Ge(Li) detector and a Canberra multichannel analyzer. The system had an energy resolution of 1.9 keV FWHM at 1.332 MeV and an efficiency of 20% relative to a 3 × 3-in. NaI(Tl) detector.

Separation procedure. The surface contamination was removed by etching in a (9 + 1) mixture of concentrated hydrofluoric and nitric acids, and the irradiated sample was transferred to a 20-ml plastic syringe [8] which was then closed with the piston. Another 5-ml syringe was fitted to the top of the first one by means of a short plastic tube and 0.5 ml of 48% HF was added. By manipulating the pistons this volume was drawn into the first syringe. Similarly, 0.2—0.3 ml of 65% (w/w) HNO_3 was added to achieve complete dissolution of the sample. Then the carriers (100 μg for each element), 2 ml of 36% (w/w) HCl, two portions of 0.5 ml of 20% (w/v) urea solution (to eliminate nitrous acid), and 5 ml of a saturated solution of boric acid (to mask fluoride) were added. This mixture was shaken with two 5-ml portions of 0.024 M diethylammoniumdiethyldithiocarbamate (DDTC) in chloroform for about 1 min each, and washed with 5 ml of chloroform. For withdrawal and addition of the liquid, a narrow polyethylene tube (7—10 cm long) with a Luer—Lok adapter was used. The collected organic phase was washed with 2 M HCl and used for counting ^{198}Au, ^{63}Cu and ^{99}Mo.

To the aqueous phase, 1 ml of 20% tartaric acid (to mask niobium) and 0.5 ml of iodide—ascorbic acid solution (15% (w/v) KI/2.5% (w/v) ascorbic acid) were added. The syringe was closed with a Luer—Lok stopper and heated on a water bath for 20—30 min at 80° C. After cooling, 0.1 ml of 15% (w/v) ascorbic acid was added and the above-described extraction with DDTC solution in chloroform was repeated. Finally, the collected organic phase was washed with 2 M HCl and the indicator radionuclides ^{76}As and ^{122}Sb were counted at the 0.559-MeV and 0.564-MeV peaks, respectively (see below).

Results and discussion

Dissolution of the sample. Arsenic can be lost almost completely during dissolution of niobium in an open beaker and/or during evaporation of the solution [9]. These losses can be avoided by dissolving the sample in a closed system. If sample dissolution and extraction are done in plastic disposable syringes [8], losses are negligible.

Extraction with diethyldithiocarbamate. The extraction of arsenic(III) and antimony(III) with diethylammoniumdiethyldithiocarbamate (DDTC) in chloroform is simple and highly selective from hydrochloric or sulphuric acid media [6]. In a general study of the extraction of elements with DDTC from hydrofluoric acid solutions [9], it was found to be impossible to reduce arsenic(V) and antimony(V) to the trivalent extractable states in these media. In this work, it was confirmed that the nitrous acid formed and hydrofluoric acid required in the dissolution of niobium can be masked with

TABLE 1

Chemical yields and limits of detection

Element	Yield (%)	Limit of detection ($ng\ g^{-1}$)
Au	99.5 ± 0.5	0.0008
As	92.8 ± 1.8	0.01
Cu	99.2 ± 0.3	0.01
Mo	96.8 ± 2.1	25
Sb	93.6 ± 3.2	0.02

urea and boric acid, respectively. After addition of hydrochloric acid, Au, Cu and Mo are extracted with DDTC in chloroform. Then tartaric acid is added and arsenic and antimony are reduced with iodide at 80°C for extraction with DDTC.

The procedure developed was free of interference from other elements. The decontamination factors for Nb (matrix), Ta and W was $>10^6$. The recoveries (chemical yields) obtained when radiotracers were added to inactive niobium are listed in Table 1. In addition to As and Sb, recoveries are given also for Au, Cu and Mo which can be determined simultaneously.

Determination of arsenic and antimony in niobium. The procedure developed was applied to niobium samples with different grades of purity. The results are given in Table 2. As the lines of ^{76}As (0.559 MeV) and ^{122}Sb (0.564 MeV) form a double peak in the γ-spectrum, more accurate results would be obtained if the two radionuclides were chemically separated, e.g., by extraction of antimony with cupferron [10]. This would be essential for cases in which the difference between the activities of the two radionuclides is large.

TABLE 2

Contents of trace elements found in niobium with different grades of purity (contents are given in $\mu g\ g^{-1}$, $ng\ g^{-1}$ or $pg\ g^{-1}$. Results in parentheses were obtained by an independent radiochemical neutron activation technique [2])

Element	Nb—P[a]	Nb—ES[a]	Nb—WCT[a]	Nb—R—1[b]	Nb—R—2[b]
Au	35 ± 4 ng	3.8 ± 1.2 ng	3.9 ± 0.7 pg	28 ± 10 pg	<1 pg
	(29 ± 7)	(3.2 ± 0.3)	(4.6 ± 1.3)	(22 ± 6)	(<0.2)
As	0.4 ± 0.1 μg	1.5 ± 0.1 ng	0.34 ± 0.1 ng	<0.15 ng	<50 pg
Cu	0.61 ± 0.12 μg	0.48 ± 0.05 μg	68 ± 15 ng	25 ± 6 ng	6 ± 3 ng
	(0.54 ± 0.06)	(0.43 ± 0.03)	(55 ± 11)	(12 ± 2)	(4 ± 2)
Mo	176 ± 12 μg	26 ± 4 μg	3.2 ± 0.3 μg	0.21 ± 0.07 μg	52 ± 12 ng
	(191 ± 5)	(19.3 ± 3.8)	(2.4 ± 0.4)	(0.73 ± 0.15)	(39 ± 15)
Sb	13 ± 2 ng	0.2 ± 0.05 ng	0.2 ± 0.05 ng	<0.1 ng	<50 pg

[a]Commercially available materials. [b]High-purity niobium obtained from MPI für Metallforschung, Laboratorium für Reinststoffe, Stuttgart.

The contents of copper, gold and molybdenum were determined simultaneously. As can be seen in Table 2, good agreement with results of a different activation technique was achieved.

The limits of detection attainable after the separation are summarized in Table 1. They were estimated for Nb-WCT as a material of good purity.

REFERENCES

1 V. Krivan, Pure Appl. Chem., 54 (1982) 787.
2 R. Caletka, W. G. Faix and V. Krivan, J. Radioanal. Chem., 72 (1982) 109.
3 V. A. Nazarenko, G. V. Flyntikova and N. V. Lebedeva, Zavod. Lab., 23 (1957) 891.
4 Sh. G. Melamed and A. M. Saltykova, Zavod. Lab., 23 (1957) 573.
5 N. N. Kuznetsova and L. S. Kranz, Zh. Anal. Khim., 18 (1963) 1090.
6 O. G. Koch and G. A. Koch-Dedic, Handbuch für Spurenanalyse, Part 1, Springer-Verlag, Berlin, 1974, pp. 265 and 308.
7 W. Kiesel, Fresenius Z. Anal. Chem., 227 (1967) 13.
8 R. Caletka, Fresenius Z. Anal. Chem., 311 (1982) 124.
9 R. Caletka and V. Krivan, Fresenius Z. Anal. Chem., 311 (1982) 177.
10 J. Růžička, J. Stary and A. Zeman, Talanta, 11 (1964) 1151.

Analytica Chimica Acta, 143 (1982) 273—276
Elsevier Scientific Publishing Company, Amsterdam — Printed in The Netherlands

Short Communication

EXTRACTIVE SPECTROPHOTOMETRIC DETERMINATION OF NITRITE IN POLLUTED WATERS

ABHA CHAUBE, ANIL K. BAVEJA and V. K. GUPTA*
Department of Chemistry, Ravishankar University, Raipur 492010 (India)
(Received 16th March 1982)

Summary. Nitrite is diazotised with *p*-nitroaniline in hydrochloric acid and coupled with 8-quinolinol in alkaline medium to give a purple azo dye (λ_{max} = 550 nm, $\epsilon = 3.88 \times 10^4$ l mol^{-1} cm^{-1}). Extraction of the dye into 3-methyl-1-butanol shifts the absorption maximum to 570 nm and improves the apparent molar absorptivity to 5.852×10^4 l mol^{-1} cm^{-1}. Beer's law is obeyed for 0.01—0.06 ppm nitrite. The Sandell sensitivity is 0.00078 μg cm^{-2}. The method is applicable to polluted waters.

Nitrite can induce methemoglobinemia and form carcinogenic nitrosomines when present with secondary or tertiary amines and amides [1]. The maximum permissible limit specified by the U. S. Public Health Service for nitrite in potable water is 0.06 ppm. Methods based on the Griess diazotisation reaction are most popular for the spectrophotometric determination of nitrite in water and wastewater [2, 3]. Solvent extraction has often been used [4—9] to enhance the sensitivity of the method.

The present communication describes a highly sensitive method for the extractive spectrophotometric determination of nitrite at ppb levels with *p*-nitroaniline (as diazotisation reagent) and 8-quinolinol (as coupling reagent). The purple dye formed in alkaline medium is measured spectrophotometrically. This reagent couple was proposed earlier [10], but extraction of the product to increase sensitivity has not been investigated previously. The proposed extraction increases the sensitivity to 1.5-fold.

Experimental

Apparatus. An ECIL spectrophotometer model GS865 and a Zeiss Spekol spectrophotometer were used with 1-cm matched glass cells. An ECIL digital meter type pH5651 was used to measure pH.

Reagents. Standard nitrite solutions, 1×10^{-3} M *p*-nitroaniline solution, 0.2% (w/v) 8-quinolinol solution, 3 M sodium hydroxide solution and 10% (w/v) EDTA solution were prepared as reported earlier [10].

Procedure. An aliquot (about 100 ml) of sample containing 1—6 μg of nitrite (0.01—0.06 ppm) was mixed in a 250-ml separatory funnel with 1 ml of *p*-nitroaniline reagent, and the acidity was adjusted to 0.5 M with hydrochloric acid. After 5 min of occasional shaking, 1 ml of EDTA solution

(masking agent) and 2 ml of 8-quinolinol solution were added. The solution was shaken for 1 min and then made alkaline (ca. pH 11.0) with sodium hydroxide. The purple dye formed was extracted with two 5-ml portions of isoamyl alcohol (3-methyl-1-butanol). The organic phase was dried over anhydrous sodium sulphate and then diluted to 10 ml in a volumetric flask. The absorbance was measured at 570 nm, against a reagent blank. The calibration curve was prepared in a similar manner. Samples with high concentrations of nitrite were diluted appropriately before reaction.

Results and discussion

All spectral studies were made with 100 ml of distilled water containing the required amount of nitrite. The spectral characteristics of the dye in various solvents are listed in Table 1. 3-Methyl-1-butanol provided the greatest sensitivity, with maximum absorption at 570 nm. The dye showed no change in absorbance in 24 h and in 36 h the change in absorbance was within ±2%. The absorbance remained constant from 15 to 40°C. These tests were done at about pH 11.0; at lower pH values, the dye was unstable in all solvents, causing low results [10].

At least 0.05 M hydrochloric acid was found to be necessary for complete diazotisation. Constant absorbances were obtained within the range 0.05—2 M hydrochloric acid. Times for diazotisation and coupling, the pH for full colour development and effect of varying molar ratios of *p*-nitroaniline and 8-quinolinol were, of course, the same as reported earlier [10]. The pH of the alkaline solution extracted was 10.4 ± 0.3.

Beer's Law and reproducibility. Beer's Law was obeyed for the concentration range 1—6 μg of nitrite per 100 ml (0.01—0.06 ppm); for the calibration plot, the regression coefficient was 0.12 with a correlation coefficient of 0.99 and zero intercept. The molar absorptivity and the Sandell sensitivity were 5.852×10^4 l mol^{-1} cm^{-1} and 0.00078 μg cm^{-2}, respectively, for the 3-methyl-1-butanol extract. The standard deviation on the absorbance in 7 measurements of 0.04 ppm nitrite was found to be 0.004 (relative standard deviation 0.57%), showing that the method is reproducible.

Effect of diverse ions. To study the effect of various ions, known amounts

TABLE 1

Spectral characteristics of the azo dye in various higher alcohols[a]

Solvent	λ (nm)	Molar absorptivity (10^4 l mol^{-1} cm^{-1})	Solvent	λ (nm)	Molar absorptivity (10^4 l mol^{-1} cm^{-1})
Water	550	3.88	3-Methyl-1-butanol[b]	570	5.85
1-Pentanol	570	5.76	1-Octanol	565	4.82
1-Hexanol	570	5.27			

[a]A 100-ml aliquot of 0.04 ppm nitrite solution was used for extraction. [b]1-Butanol itself was too miscible with water to provide clean solutions.

of ions normally present in effluents were added to 100-ml aliquots of 0.04 ppm nitrite solution before the recommended procedure was applied. Interferences of metal ions forming hydrated oxides in alkaline medium were masked with EDTA. Iron(III) and bismuth(III) were masked with tartrate while sulphite was oxidized with hydrogen peroxide. Iron(II), chromium(II) and sulphide ions interfere. Copper(II) interferes seriously in spectrophotometric methods based on the Griess reaction but can be tolerated upto 100 ppm if masked with EDTA. The results (Table 2) indicate that the extraction process increases the tolerance limits.

Application of the method to river water. Samples of river water were taken upstream and downstream from a source of industrial effluent, in wide-mouthed plastic vessels. Mercury(II) chloride (4 mg/100 ml of sample) was added to preserve the samples, which were then stored at 0° C. Samples were filtered before measurement through Whatman no. 41 paper.

The validity of the method for nitrite in river water was checked as follows. First, different volumes of sample solution were diluted to constant volume with deionised water. For all the samples, the linear plots obtained could be extrapolated to the same point obtained with deionised water, which is a clear indication that the procedure for nitrite in river water was quantitative. Secondly, various amounts of nitrite were added to a sample and the recovery of nitrite was checked; the results were linear and the slope was identical to that of a calibration graph obtained with deionised water. Potable water having a negligible amount of nitrite was also spiked with nitrite (1—6 μg/100 ml); the recoveries of added nitrite were in the range 98—100%.

Comparison with the conventional sulphanilamide—N(1-naphthyl)-ethylenediamine dihydrochloride method. A comparison of the values obtained by the conventional method [11] with those obtained by the proposed method is shown in Table 3. The correlation coefficient for the

TABLE 2

Effect of diverse ions[a]

Tolerance limit[b] (ppm)	Diverse ion
800	SO_4^{2-}
200	NO_3^-, PO_4^{3-}, HCO_3^-, SiO_3^{2-}
100	Li^+, Be^{2+}, Mg^{2+}[c], Ca^{2+}[c], Sr^{2+}[c], Ba^{2+}[c], Zr^{4+}, Cr(VI), Mo(VI), W(VI), Co^{2+}[c], Ni^{2+}[c], Cu^{2+}[c], Zn^{2+}[c], Cd^{2+}[c], Hg^{2+}[c], Pb^{2+}[c], Sb^{3+}, Bi^{3+}[d], Se(IV), Te(IV), F^-, Br^-.
50	Fe^{3+}[d], SO_3^{2-}[e]
25	I^-, aniline, HCHO, phenol.

[a]For 100 ml of 0.04 ppm nitrite solution. [b]Concentration causing an error ⩽2%. [c]Masked with 1 ml of 10% EDTA. [d]Masked with 1 ml of 10% solution potassium tartrate. [e]H_2O_2 added.

TABLE 3

Determination of nitrite in river water[a]

Nitrite found (ppm)			
Proposed method[b]	Standard method[c]	Proposed method[b]	Standard method[c]
0.34	0.31	0.71	0.71
0.37	0.36	0.75	0.74
0.41	0.39	0.66	0.69
0.47	0.47	0.81	0.79
0.52	0.52	0.83	0.81
0.65	0.63	0.88	0.91

[a]Kharoon river water was sampled: six samples were taken upstream and six downstream from the source of effluent on 17:8:81. Each value is the mean of 5 replicate determinations. [b]5 ml of sample was diluted to 100 ml. [c]Volume of 3-methyl-1-butanol used per determination was 10 ml.

two methods was 0.995 in the determination of nitrite in 12 samples from the Kharoon River. Thus it can be concluded that the proposed method is satisfactory for practical analysis of river water. The method is rapid, selective and more sensitive than other extractive methods reported for nitrites in water [4—8].

The authors are grateful to the Head of the Department of Chemistry for providing laboratory facilities. A.C. and A.K.B. thank the UGC, New Dehli, and CSIR, New Delhi, for providing fellowships.

REFERENCES

1 F. A. Patty, Industrial Hygiene and Toxicology, Vol. II, Interscience, New York, 1963.
2 C. A. Steruli and P. R. Averall, The Analytical Chemistry of Nitrogen and its Compounds, Part I, Wiley—Interscience, New York, 1970.
3 A. K. Babko and A. T. Pilipenko, Photometric Analysis—Methods of Determining Non-Metals, translated from Russian by A. Rosinkin, Mir Publishers, Moscow, 1976.
4 H. D. Zeller, Analyst, 80 (1955) 1.
5 M. Nishimura, K. Matsunga and K. Matsuda, Bunseki Kagaku, 19 (1970) 1096.
6 A. Foris and T. R. Sweet, Anal. Chem., 37 (1965) 701.
7 K. Tôei and T. Kiyose, Anal. Chim. Acta, 88 (1977) 125.
8 M. Nakamura and A. Murata, Analyst, 104 (1979) 985.
9 A. K. Baveja, J. Nair and V. K. Gupta, Analyst, 106 (1981) 955.
10 J. Nair and V. K. Gupta, Anal. Chim. Acta, 111 (1979) 311.
11 Standard Methods for the Examination of Water, Sewage and Industrial Waste, American Public Health Association, New York, 14th edn., 1975, p. 434.

Analytica Chimica Acta, 143 (1982) 277—281
Elsevier Scientific Publishing Company, Amsterdam — Printed in The Netherlands

Short Communication

KINETIC SPECTROPHOTOMETRIC DETERMINATION OF ANTIMONY(III) BASED ON INDUCED OXIDATION OF TRIS(1,10-PHENANTHROLINE)IRON(II) BY CHROMIUM(VI)

NORINOBU YONEHARA*, YASUYUKI NISHIMOTO and MASAAKIRA KAMADA

Department of Chemistry, Faculty of Science, Kagoshima University, Korimoto, Kagoshima 890 (Japan)

(Received 26th May 1982)

Summary. The method involves the measurement of the extent of the induced reaction, which ceases a few seconds after initiation. Antimony(III) can be determined in the range 0.4—10 μg ml^{-1}. The standard deviation is ±0.25 μg. The method is applied to marine sediments.

Very few kinetic methods have been reported for the determination of antimony. Dutt and Mottola [1] proposed a method involving initial rate measurements for the determination of arsenic(III), vanadium(IV) and oxalic acid by their accelerating effects on the oxidation of tris(1,10-phenanthroline)iron(II) by chromium(VI). Since antimony(III) interfered seriously in the method, they suggested the possibility of developing a kinetic method for determining antimony(III), but this possibility has not been investigated previously. The present communication describes such a procedure. The resulting method is rapid, simple and reasonably sensitive.

Experimental

Reagents. Deionized, distilled water was used throughout. Antimony(III) stock solution (100 mg l^{-1}) was prepared by dissolving 100 mg of pure antimony metal in 25 ml of concentrated sulfuric acid with strong heating, and diluting the solution to exactly 1 l with 2.6 M sulfuric acid. The concentration of acid in this solution was determined titrimetrically with sodium carbonate. A 20 mg l^{-1} working solution of antimony(III) was prepared by taking 20 ml of the stock solution, adding just sufficient sodium carbonate to neutralize the acid and diluting to 100 ml with water. More dilute working solutions were prepared by simple dilution. The ferroin stock solution (1.4×10^{-3} M) contained 0.170 g of 1,10-phenanthroline and 0.080 g of iron(II) sulfate heptahydrate dissolved in and diluted to 200 ml with water. Working solutions were prepared by suitable dilution. All chemicals used were of analytical-reagent grade.

Apparatus. A Hitachi Model-200-20 double-beam spectrophotometer was used with a thermostated (±0.1°C) cell-holder coupled with a Hitachi

Model-200 recorder. Temperature was controlled with a Taiyo Model CL-15 circulating thermostated bath. For the reaction, 1-cm glass cells were used. The reaction was initiated by injection of potassium dichromate solution from a Gilson Pipetman Model P-200. For mixing, a remotely controlled magnetic Acrobat stirrer (MS Instruments, Osaka, Japan) was installed at the side of the cell holder in the spectrophotometer. The stirring performance of this device was checked by manually injecting 0.10 ml of 4.7×10^{-4} M ferroin in 2.0 ml of 1.35 M sulfuric acid and recording the absorbance change at 510 nm. The mixing time required for the absorbance to become constant was 2 s.

Recommended procedure. To a sample solution (<1.5 ml) containing up to 20 μg of antimony(III) in a 1-cm glass cell, 0.30 ml of 9.0 M sulfuric acid and 0.20 ml of 4.7×10^{-4} M ferroin were added. Adjustment to a final volume of 2.0 ml was done with water. The cell was placed in the holder at 25°C and injected with 0.10 ml of aqueous 2.0×10^{-3} M potassium dichromate. The decrease in absorbance of ferroin at 510 nm was recorded for about 1 min, against a distilled water reference. The absorbances were then measured at 10, 20 and 30 s and Log (absorbance) vs. reaction time was plotted. This gave a linear relationship, and the intercept on the absorbance axis was calculated by the least-squares method. The value of the intercept vs. antimony concentration was plotted as a calibration graph.

Determination of antimony in marine sediments. A sample was fused with 1.5 g of potassium pyrosulfate and the cake was dissolved in 10 ml of 3 M sulfuric acid. The resulting suspension was centrifuged and the supernatant solution neutralized with 1 M sodium carbonate, diluted to 100 ml with water, and the above procedure was applied to a suitable aliquot.

Results and discussion

Effect of antimony(III) on the ferroin—chromium(VI) reaction. In sulfuric acid, chromium(VI) oxidizes ferroin to the iron(III) complex, ferrin. The reaction can be followed by measuring the decrease in absorbance of ferroin at 510 nm. Antimony(III) greatly accelerates the very early stages of this reaction. The reaction appears to be induced by antimony(III). The oxidation of ferroin by chromium(VI) is greatly accelerated by the simultaneous oxidation of antimony(III) by chromium(VI), which proceeds very rapidly. Once the effect of the antimony(III) has been exhausted, the reaction proceeds more slowly and the larger the amount of antimony(III) originally present, the slower the reaction. This is because more chromium(VI) has been consumed by the fast reaction with antimony(III) and ferroin, so that the concentrations of unreacted chromium(VI) and ferroin and hence the later reaction rate decrease.

Figure 1 shows the first-order plots for the ferroin—dichromate reaction in the presence and absence of antimony(III). The earlier part of the reaction, which deviates from first-order behavior with respect to ferroin, is the region in which the antimony(III) affects the rate of the reaction. The intercepts on

the ordinate, obtained by extrapolation to zero reaction time, become lower as the concentration of antimony(III) increases. As can be seen in Fig. 1, the effect of the antimony(III) has ceased after the first 6 s. As the mixing time in the reaction cell is about 2 s, the antimony(III)-induced reaction must proceed to some extent before mixing is complete. However, the intercept was found to be reproducible enough as a parameter for the determination of antimony(III).

Effect of reaction parameters. The influence of temperature on the reactions in the presence and absence of antimony(III) was studied in the range 20—40°C, under conditions otherwise as in the recommended procedure. The rate of the ferroin—chromium(VI) reaction increases with an increase in temperature. The intercept is lowered gradually with increasing temperature, but 25°C gives a linear calibration graph with better reproducibility than at higher temperatures.

Figure 2 shows the effect of ferroin concentration. For the reaction both in the presence of antimony(III) and in its absence, the intercept rises with an increase in the concentration of ferroin, while the difference in the intercepts slightly decreases. A ferroin concentration of 4.5×10^{-5} M was selected because it gave rise to a linear calibration graph, although a wider range of antimony concentrations can be measured at higher concentration of ferroin.

Figure 3(a) shows the effect of dichromate concentration. Although the blank remains constant, the intercept for the reaction in the presence of antimony(III) falls with increasing dichromate concentration. The results are not reproducible at 2.0×10^{-4} M dichromate, thus a dichromate concen-

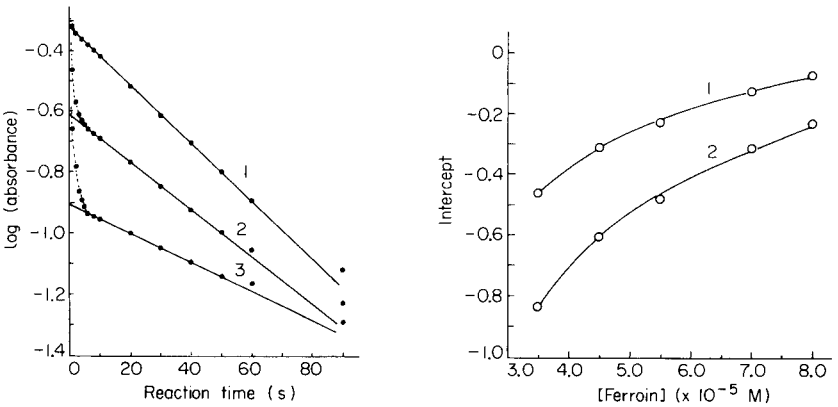

Fig. 1. First-order plots for the ferroin—dichromate reaction. Antimony(III) added: (1) 0 μg; (2) 8.4 μg; (3) 16.8 μg (4.5×10^{-5} M ferroin; 1.0×10^{-4} M potassium dichromate; 1.3 M sulfuric acid; 25°C).

Fig. 2. Effect of ferroin concentration. (1) Reagent blank; (2) 8.4 μg of antimony(III) per 2.1 ml (other conditions as in Fig. 1).

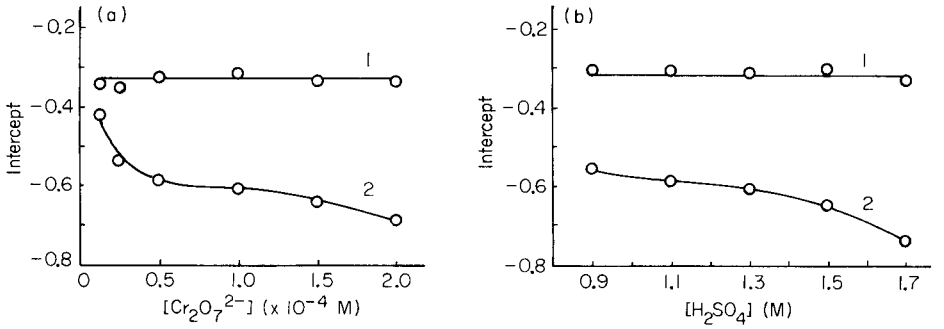

Fig. 3. Effect of (a) dichromate concentration and (b) sulfuric acid concentration: (1) reagent blank; (2) 8.4 μg antimony(III) per 2.1 ml (other conditions as in Fig. 1).

tration of 1.0×10^{-4} M is recommended for better sensitivity and reproducibility.

The effect of sulfuric acid concentration (Fig. 3b) is quite similar to that of dichromate. The results are less reproducible at higher acidities, so a concentration of 1.3 M sulfuric acid has been chosen as optimal.

Calibration. The calibration graph obtained by the recommended procedure was linear over the range 0—20 μg of antimony(III) per 2.1 ml of the reaction solution. The standard deviation for 11 replicate determinations of 8.40 μg of antimony(III) was 0.25 μg. The smallest amount that could be determined was 0.4 μg Sb ml^{-1}.

Interferences. The effect of diverse ions on the determination of 8.40 μg of antimony(III) was examined for the recommended procedure. No interferences were found up to at least the following concentrations: 24 mg of NO_3^-; 10 mg of ClO_4^-; 5 mg of SO_4^{2-}; 7 mg of K, NH_4^+; 2 mg of Na; 200 μg of Mg, Zn, Cd, Co(II), Ni, Al, Cr(III), Nb, As(V), PO_4^{3-}; 20 μg of Ag, Ca, Pb, Fe(III), Sn(IV), Ti(IV), W(VI), F^-, Cl^-. A precipitate was formed when 200 μg of calcium was present. The supernatant liquid, which was obtained by centrifuging the precipitate, gave a slightly low result. Similar behavior was observed in the presence of 200 μg of lead. Interfering ions are listed in Table 1. Ions which are known to participate in several induced reactions as an inductor, acceptor, actor or suppressor [2], cause serious interferences.

In order to check the analytical applicability of this method, the procedure described above was applied to the determination of antimony in marine sediments, which were taken at the sea bottom quite near the submarine fumaroles of the Sakurajima volcano in Japan and may contain various interfering ions. The results are shown in Table 2, together with those obtained by a standard addition procedure, using the same reaction. The values directly obtained from a calibration graph show excessive recoveries of added antimony. The results obtained by the standard addition method, however, are in good agreement with those obtained by the rhodamine-B extraction method [3].

TABLE 1

Effect of interfering ions on the determination of 8.40 μg of antimony(III) by the recommended procedure

Ion added	Amount added (μg)	Sb(III) found (μg)	Ion added	Amount added (μg)	Sb(III) found (μg)
Cu(II)	20	10.1	Mo(VI)	20	4.2
Mn(II)	20	10.7	V(IV)	2	6.5
Hg(II)	20	6.5	V(V)	2	7.1
Fe(II)	2	14.5	Br^-	20	5.9
As(III)	2	10.3	S^{2-}	2	5.9
Ce(III)	2	12.2	Oxalate	2	9.7
Ce(IV)	2	12.8	Acetate	20	9.9

TABLE 2

Determination of antimony in marine sediments

Sample	Aliquot (ml)	Sb added (μg)	Calibration graph		Standard addition		Rhodamine-B method [3]
			Sb found (μg)	Recovery (%)	Sb found (μg)	Sb in sample (μg mg^{-1})	Sb in sample (μg mg^{-1})
I[a]	0.30	0	6.1	—	3.6	11	15
		2.1	9.2	148			11
		4.2	13.4	174			16
	0.15	0	2.7	—	1.9	12	
		2.1	5.9	152			
		4.2	9.0	150			
						av. 12	av. 14
II[b]	1.30	0	3.6	—	2.7	1.0	
		2.1	6.7	148			1.1
		4.2	10.1	155			1.1
	1.00	0	3.2	—	2.1	1.0	1.0
		2.1	5.7	119			
		4.2	9.0	138			
						av. 1.0	av. 1.1

[a]Prepared by treating 109 mg of marine sediment I.
[b]Prepared by treating 205 mg of marine sediment II.

REFERENCES

1 V. V. S. E. Dutt and H. A. Mottola, Anal. Chem., 46 (1974) 1090.
2 A. I. Medalia, Anal. Chem., 27 (1955) 1678.
3 Japanese Industrial standard Method (JIS) K-0102-1971.

Analytica Chimica Acta, 143 (1982) 283—287
Elsevier Scientific Publishing Company, Amsterdam — Printed in The Netherlands

Short Communication

EXTRACTION—SPECTROPHOTOMETRIC DETERMINATION OF BORON WITH NAPHTHALENE-2,3-DIOL AND CRYSTAL VIOLET

SHIGEYA SATO and SUMIO UCHIKAWA*

Faculty of Education, Kumamoto University, 2-40-1 Kurokami, Kumamoto 860 (Japan)

(Received 20th January 1982)

Summary. Boron reacts with naphthalene-2,3-diol to form a complex anion extractable into benzene with crystal violet and is determined indirectly by measuring the absorbance of the crystal violet in the extract at 610 nm. The calibration graph is linear for boron over the range 8.0×10^{-7}—8.0×10^{-6} mol l^{-1}; the apparent molar absorptivity is 8.8×10^4 l mol^{-1} cm^{-1}. The method is applied to the determination of boron in natural waters.

The analytical chemistry of boron is very important in the fields of nuclear energy, pharmacy and agriculture. Several spectrophotometric methods for boron have been reported; the methods based on extraction of tetrafluoroborate with methylene blue [1—3] and curcumin [4—8] are very sensitive. However, in the former method, ordinary glassware cannot be used and the conditions needed for the complete formation of tetrafluoroborate are time-consuming and troublesome. Recently, Kuwada et al. [9] reported a sensitive method based on extraction of ion-pairs formed between boron complex anions and colored large cations; glassware can be used, but evaporation to dryness must be done to form the complex. For such reasons, a simpler and more sensitive method for the determination of boron is desirable.

In 1976 Vlacil and Drbal [10] reported that boron was extracted into butanol with naphthalene-2,3-diol and a diphenylguanizium salt. In the work described here, it was found that the boron—naphthalene-2,3-diol complex anion can be extracted into benzene with the crystal violet cation and that the color of the organic phase is very stable. The extraction—spectrophotometric procedure for boron based on these phenomena and its application to the determination of boron in natural waters are reported below. The procedure does not require evaporation to dryness, and common glassware can be used, because boron reacts immediately with naphthalene-2,3-diol in neutral or weakly acidic medium at room temperature to form a complex anion.

Experimental

Apparatus. Hitachi Model 100-10 and Model 624 digital spectrophotometers were used with 10-mm glass cells. A Taiyo incubator M-1N mixer, an

Iwaki Model V-DN Type KM shaker and a Hitachi centrifuge 03P were also used. The pH values were measured with a Hitachi-Horiba M-3 pH meter.

Reagents. A 1.0×10^{-2} mol l^{-1} crystal violet solution was prepared in deionized water. A boron stock solution (2.0×10^{-2} mol l^{-1}) was prepared by dissolving boric acid in water; working solutions were prepared by suitable dilution. The buffer solution (pH 4.7) was prepared from sodium acetate (0.1 M) and anhydrous acetic acid (0.1 M). A benzene solution containing 2.0×10^{-2} mol l^{-1} naphthalene-2,3-diol was used as extraction solvent. Deionized water was used throughout.

All other reagents were of analytical-reagent grade and were used as received.

Standard procedure. Mix an aliquot of standard boron solution (2.0×10^{-5} mol l^{-1}) with 5 ml of acetate buffer (pH 4.7) and 1 ml of crystal violet solution (1.0×10^{-2} mol l^{-1}), and dilute to exactly 25 ml with deionized water. Pipette 10 ml of this solution into a stoppered conical flask. Shake the solution with 10 ml of benzene containing naphthalene-2,3-diol (2.0×10^{-2} mol l^{-1}) for 30 min. After phase separation, transfer 5 ml of the organic phase to a separatory funnel and shake for 10 min with 5 ml of 1 M sodium hydroxide in order to remove the excess of crystal violet co-extracted into benzene. Transfer the organic phase to a centrifuge tube and centrifuge for 5 min. Measure the absorbance of the organic phase at 610 nm length against benzene as reference.

Results and discussion

Absorption spectra. The absorption spectra of the reagent blank and the ion-pair formed between the boron complex and crystal violet in benzene are shown in Fig. 1. Crystal violet chloride itself was not extracted into benzene when the diol was absent. The wavelength of maximum absorption of each spectrum occurs at 610 nm.

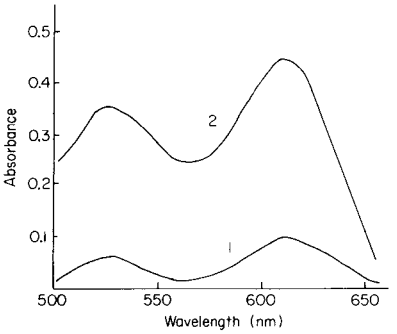

Fig. 1. Absorption spectra: (1) reagent blank; (2) 4.0×10^{-6} M H_3BO_3. Conditions: 4.0×10^{-4} M crystal violet, 2.0×10^{-2} M naphthalene-2,3-diol in benzene, pH 4.7, benzene reference.

Effect of reaction variables. A study of the effect of pH on the extraction of the ion-pair between crystal violet and the boron complex showed that there was maximum constant absorbance in the organic phase over the pH range 3—6, when the reagent blank solution served as reference. Outside this pH range, the absorbance decreased rapidly. When the standard procedure was applied to a constant concentration of boron (4.0×10^{-6} mol l^{-1}) but with varying concentrations of crystal violet, it was found that constant maximum absorbance was achieved when the crystal violet concentration exceeded 3.0×10^{-4} mol l^{-1} in the 25 ml of solution. The reagent blank increased only by 15% as the crystal violet concentration was changed from 2.0 to 6.0×10^{-4} mol l^{-1}. The concentration of crystal violet was fixed finally at 4.0×10^{-4} mol l^{-1}. Maximum constant extraction was obtained when the naphthalene-2,3-diol concentration in benzene was greater than 1.6×10^{-2} mol l^{-1}; the blank was also constant under these conditions. For routine work, the concentration of the diol in benzene was fixed at 2.0×10^{-2} mol l^{-1}. An extraction time of about 20 min was necessary to attain constant absorbance; for security, 30 min was allowed.

Washing the organic phase after extraction is necessary to remove the large excess of crystal violet co-extracted into benzene. This removal was done effectively by washing the organic phase with sodium hydroxide solution (Fig. 2). The optimal conditions were 1 mol l^{-1} sodium hydroxide and a shaking time of 10 min.

Various other solvents were tested for the extraction. Dichloromethane, 1,2-dichloroethane and chloroform were very good extractants for crystal violet chloride itself, whether or not naphthalene-2,3-diol was present. Cyclohexane and carbon tetrachloride containing the diol did not extract the boron-containing ion-pair. Chlorobenzene and toluene were as useful as benzene, but for chlorobenzene the absorbance of the reagent blank was high and for toluene the apparent molar absorptivity was small.

Calibration curve. A linear calibration graph was obtained for 8.0×10^{-7}—

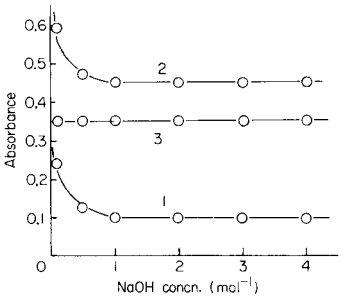

Fig. 2. Effect of alkali concentration on back-washing: (1) reagent blank (benzene reference); (2) 4.0×10^{-6} M H_3BO_3 (benzene reference); (3) net (reagent blank as reference). Other conditions as in the recommended procedure.

8.0×10^{-6} mol l^{-1} boron. The apparent molar absorptivity calculated from the slope of the graph was 8.8×10^4 l mol^{-1} cm^{-1}. The absorbance of the reagent blank was 0.10 against benzene as reference and the coefficient of variation was 2.8% in absorbance for ten runs at 4.0×10^{-6} mol l^{-1} boron.

Effect of diverse ions. Table 1 shows the recovery of boron in a series of solutions containing 4.0×10^{-6} mol l^{-1} boron and a foreign ion. Most of the anions did not interfere, but large ratios of perchlorate or thiocyanate interfered (Table 1). Fluoride did not interfere even when present in 1000-fold amounts of boron. Iron (III) and aluminum(III) interfered when present in 50-fold amounts compared to boron, but were tolerated up to about 500-fold amounts when EDTA was added to the sample solution at a level of 2.0×10^{-2} mol l^{-1}.

Application to the determination of boron in river and sea waters. As described above, most of the ions normally present in natural waters do not interfere with the determination of boron. Thus the proposed method was applied to the determination of boron in river and sea waters in Kumamoto Prefecture, Japan. Samples were filtered, and 10 ml of river water or 0.2 ml of seawater was used for the standard procedure. The results obtained are shown in Table 2, together with the data obtained by a well known methylene blue method [3]. The values obtained by the two methods are in good agreement with those obtained by the methylene blue method. Recoveries of boron checked by standard addition are also good.

In conclusion, the proposed method is simple, yet shows adequate sensitivity and selectivity for application to natural waters.

TABLE 1

Effect of foreign ions on the recovery of 4.0×10^{-6} mol l^{-1} boric acid

Ion	Added as	Mole ratio	Recovery (%)	Ion	Added as	Mole ratio	Recovery (%)
F^-	KF	1000	99.0				
Cl^-	NaCl	5000	99.4	Ca^{2+}	$CaCl_2$	5000	101.5
Br^-	NaBr	5000	97.0	Mg^{2+}	$MgCl_2$	5000	100.8
I^-	NaI	500	94.4	Cd^{2+}	$CdSO_4$	5000	99.6
ClO_4^-	$NaClO_4$	250	99.0	Fe^{3+}	Fe alum	50	88.5
		500	133.0			500	99.4[a]
SCN^-	KSCN	50	97.8	Al^{3+}	Al alum	50	—[b]
		100	91.9			500	100.8[a]
NO_3^-	$NaNO_3$	500	101.0				
SO_4^{2-}	Na_2SO_4	5000	99.2				

[a] In the presence of 2.0×10^{-2} mol l^{-1} EDTA. [b] Not measurable.

TABLE 2

Determination of boron in sea and river water from Kumamoto Prefecture and recovery of boron

Sample[a]	B found[b] (ppb)	Recovery test			Comparative B value[d] (ppb)
		B in aliquot taken[c] (μg)	B found (μg)	Recovery (%)	
Seawater					
Seashore					
at Ushibuka	3030	0.61	1.71	102	3060
at Misumi	4040	0.81	1.91	102	4000
at Oda	4190	0.87	1.96	101	4220
River water					
Shirakawa	91	0.91	1.94	95	86
Midorikawa	79	0.79	1.84	97	

[a] 0.2 ml of seawater or 10 ml of river water was taken.
[b] Mean of five determinations.
[c] 1.08 μg of boron was added to each aliquot.
[d] By the methylene blue method [3].

REFERENCES

1 L. Ducret, Anal. Chim. Acta, 17 (1957) 213.
2 S. Utsumi, S. Ito and A. Isozaki, Nippon Kagaku Zasshi, 86 (1965) 921.
3 L. Pasztor, J. D. Bode and Q. Fernando, Anal. Chem., 32 (1960) 277.
4 M. E. Schlumberger, Bull. Soc. Chim., 5 (1866) 194.
5 C. E. Cassel and H. Gerrans, Chem. News, 87 (1903) 27.
6 G. S. Spicer and J. D. H. Strickland, Anal. Chim. Acta, 18 (1958) 231.
7 J. A. Naftel, Ind. Eng. Chem., Anal. Ed., 11 (1939) 407.
8 R. Greenhalgh and J. P. Riley, Analyst, 87 (1962) 970.
9 K. Kuwada, S. Motomizu and K. Tôei, Anal. Chem., 50 (1978) 1788.
10 F. Vlacil and K. Drbal, Collect. Czech. Chem. Commun., 41 (1976) 1169.

Analytica Chimica Acta, 143 (1982) 289—292
Elsevier Scientific Publishing Company, Amsterdam — Printed in The Netherlands

Short Communication

SPECTROPHOTOMETRIC DETERMINATION OF MICROGRAM AMOUNTS OF AROMATIC ALDOXIMES WITH CHLORANIL

T. S. AL-GHABSHA*, A. S. AZZOUZ and Y. I. HASSAN

Department of Chemistry and Biology, College of Education, University of Mosul, Mosul (Iraq)

(Received 9th July 1982)

Summary. Benzaldoxime and its *p*-hydroxy, methyl, chloro and nitro derivatives (50—500 μg) are determined by using chloranil as a π-acceptor at pH 9. The method is simple, precise (r.s.d. < 3%) and accurate (±2%).

Charge-transfer complexes formed between molecules usually have characteristic absorption spectra and high molar absorptivities [1]. These attributes have been utilized for the spectrophotometric determination of sulphur dioxide [2], nitrate [3] and oxygen [4], by complexation with *o*-xylene, toluene and *N,N*-dimethylaniline, respectively. In particular, the charge-transfer complexes formed by the reaction of amines [5—8], and amino acids and related compounds [9—13] with chloranil have been used for the determination of traces of these species. This communication describes an investigation of the reaction of chloranil with some aromatic aldoximes; a simple, rapid, relatively sensitive and accurate method for the determination of these compounds is proposed.

Experimental

Apparatus. All mass measurements were carried out using an AEI MS902 mass spectrometer fitted with a direct insertion probe. Samples were admitted in pyrex glass tubes 27 mm long and 1 mm internal diameter which were fitted to the end of the probe and discarded after use. Into the tubes, 1—7 μl of solutions of the compounds under investigation were injected by means of a Hamilton syringe. A Perkin-Elmer 180 infrared spectrophotometer was used for measuring the i.r. spectra of the aromatic aldoximes in a potassium bromide disc. All absorbance measurements were made on a Shimadzu UV-210A double-beam spectrophotometer, supplied with a digital printer DP80Z; matched 1-cm silica cells were used.

Synthesis of aromatic aldoximes. Benzaldoxime and its *p*-nitro, *p*-chloro, *p*-hydroxy and *p*-methyl derivatives were prepared by the following procedure. In a 50-ml round-bottomed flask, attached to a reflux condenser, 2.5 g of hydroxylammonium chloride, 10 ml of 10% (w/v) sodium hydroxide solution and 1 g of aldehyde were mixed to dissolve. If the aldehyde

0003-2670/82/0000-0000/$02.75

was not soluble, sufficient methanol was added to give a clear solution. The mixture was heated under reflux for 10—15 min and cooled in ice. If crystals separated, the product was filtered and recrystallised from methanol. If not, the methanol was removed under reduced pressure (water pump), and the mixture diluted with 2—3 times its volume of water, followed by cooling, filtration and recrystallisation of the product from methanol. Table 1 summarises some of the properties of these compounds.

Reagents. Chloranil was used as a saturated (1×10^{-3} M) solution in ethanol. Absolute (99—100%) ethanol was used. A borate buffer solution of pH 9 (5×10^{-2} M sodium tetraborate) was used. Aqueous solutions (100 ml, 100 ppm) of each aldoxime were prepared; a little ethanol was added to increase the solubility.

Recommended procedure. For calibration, add 0—5-ml aliquots of the appropriate aqueous 100 ppm aldoxime solution (0—4 ml for benzaldoxime) to a series of 25-ml volumetric flasks, and add exactly 3 ml of chloranil solution and 2 ml of pH 9 borate buffer. Dilute to volume with distilled water, and leave the solution for 45 min at room temperature (25°C). Measure the absorbance against the blank solution at 338 nm. Plot the absorbance vs. oxime concentration. For sample determinations, take an approximately aqueous sample ($\leqslant$20 ml) through the above procedure. Read the concentration from the calibration graph.

Results and discussion

When chloranil solution was added to *p*-hydroxybenzaldoxime in alkaline solution (pH 9), a colour developed which was stable for about 2 h after developing slowly for 45 min at room temperature. Maximum absorbance occurred at 338 nm, at which wavelength the blank had negligible absorbance. This wavelength was used in all subsequent experiments.

TABLE 1

Physical and spectroscopic properties of some aromatic aldoximes

Oxime	M.p. (°C)		Characteristic i.r. peaks (cm^{-1})[a]	Molecular formula[b]
	Lit. [14, 15]	Found		
Benzaldoxime	35	35	3340(sh), 1631(s), 952(s)	C_7H_7NO
p-Nitrobenzaldoxime	133	115—116	3322(m), 3020(w), 1605(s), 1530(s), 1350(w), 940(s)	$C_7H_6N_2O_3$
p-Chlorobenzaldoxime	107	103—104	3300(m), 3000(m), 1650(m), 1600(s) 952(s)	C_7H_6NOCl
p-Hydroxybenzaldoxime	117	94	3360(m), 3000(vw), 1638(w), 1608(s), 952(s)	$C_7H_7NO_2$
p-Methylbenzaldoxime	64—65	61—62	3305(b), 3000(w), 1604(s), 1104(m), 950(m)	$C_8H_9NO_2$

[a]Weak (w), broad (b), medium (m), strong (s), shoulder (sh), very weak (vw). [b]From precise mass measurements.

Sample solutions containing *p*-hydroxybenzaldoxime and the blank were treated identically with the reagent and buffer at temperatures ranging from 0 to 70°C. The complex was formed over the whole range but spectral interference from the blank was observed at 0°C and at ⩾30°C. However, a stable *p*-hydroxybenzaldoxime—chloranil complex was formed after the reaction mixture had stood for 45 min at room temperature (25°C), and there was no spectral interference from the blank. This temperature was also found to be suitable for the other aldoximes.

The effect of pH was investigated in the range 5—11. The results indicated that the *p*-hydroxybenzaldoxime complex was stable at pH 9—11, and pH 9 was selected for further study. The amount of pH 9 buffer solution added was not critical between 1 and 5 ml per 25 ml of final solution; 2 ml gave marginally the greatest absorbance.

Experiments showed that at least 2 ml of 1×10^{-3} M chloranil solution should be present in the reaction mixture; 3 ml was used to ensure quantitative results at the higher concentrations for calibration. The order of addition of reagents was of no consequence. Under the recommended conditions, linear calibration graphs were obtained up to the limits given in Table 2. Each graph had a slight negative intercept on the absorbance axis. The apparent molar absorptivity and the Sandell sensitivity are given in Table 2 for each oxime, together with the reproducibility. The accuracy was better than ±2%, as shown in Table 3.

Some interferences would be expected. Amino acids would give responses [10] as would amines [8]. Proteins and some other nitrogen-containing compounds also give sensitive responses [10, 12]. Other compounds such as urea do not give complexes, and ammonia and ammonium salts form only slightly absorbing species.

TABLE 2

Analytical parameters for the determination of aromatic aldoximes with chloranil at pH 9

Oxime	Molar absorptivity ($1\ mol^{-1}\ cm^{-1}$)[a]	Sandell index ($\mu g\ cm^{-2}$)	R.s.d.[b] (%)	Upper linear calibration limit (μg)
p-Hydroxybenzaldoxime	5000	0.0298	1.63	500
p-Methylbenzaldoxime	4000	0.0375	0.63	500
p-Chlorobenzaldoxime	3000	0.0536	0.76	600
p-Nitrobenzaldoxime	8000	0.0224	2.90	550
Benzaldoxime	4000	0.0310	1.01	450

[a]Calculated from the calibration graphs. [b]For 300 μg/25 ml (7 measurements).

TABLE 3

Determination of aromatic aldoximes

Oxime	Amount (μg/25 ml)		Error (%)
	Present	Found[a]	
p-Hydroxybenzaldoxime	50	51	+2
	250	247	−1.2
	350	345	−1.4
p-Methylbenzaldoxime	150	148	−1.3
	250	254	+1.6
	400	395	−1.3
p-Chlorobenzaldoxime	150	148	−1.3
	250	248	−0.8
	450	451	+0.2
p-Nitrobenzaldoxime	150	148	−1.3
	250	252	+0.8
	400	401	+0.3
Benzaldoxime	150	151	+0.7
	300	295	−1.7
	450	455	+1.1

[a]Mean of 3 determinations.

The authors thank Dr. J. R. Majer, Chemistry Department, University of Birmingham, Gt. Britain, for the precise mass measurements.

REFERENCES

1 A. Townshend, Proc. Soc. Anal. Chem., 10 (1973) 39 and references therein.
2 M. K. Bhatty and A. Townshend, Anal. Chim. Acta, 55 (1971) 401.
3 M. K. Bhatty and A. Townshend, Anal. Chim. Acta, 65 (1971) 55.
4 M. K. Bhatty and A. Townshend, Anal. Lett., 4 (1970) 357.
5 Y. Tashima, H. Hasegawa, H. Yuki and K. Takiura, Jpn. Anal., 19 (1970) 43.
6 J. P. Sharma and R. D. Tiwari, Microchem. J., 17 (1972) 151.
7 H. Yuki, S. Matsuda, Y. Tokuda and K. Takiura, Mikrochim. Acta, (1972) 132.
8 T. S. Al-Ghabsha, S. A. Rahim and A. Townshend, Anal. Chim. Acta, 85 (1976) 189.
9 J. B. Birks and M. A. Slifkin, Nature, 197 (1963) 42.
10 F. Al-Sulaimany and A. Townshend, Anal. Chim. Acta, 66 (1973) 195.
11 B. Y. Lin and K. L. Cheng, Anal. Chim. Acta, 120 (1980) 120.
12 T. S. Al-Ghabsha, M.Sc. Thesis, University of Mosul, 1975.
13 T. S. Al-Ghabsha, S. K. Ibrahim and M. Q. Al-Abachi, Microchem. J., in press.
14 A. I. Vogel, A Test Book of Practical Organic Chemistry, 3rd edn., Longman, London, 1967.
15 R. C. Weast, CRC Handbook of Chemistry and Physics, 59th edn., CRC Press, Boca Raton, Florida, 1978—1979.

ANALYTICA CHIMICA ACTA, Vol. 143 (1982)

AUTHOR INDEX

(*continued from outside cover*)

Short Communications

Elsevier Scientific Publishing Company, 1982

Printed in The Netherlands.

CONTENTS

(Abstracted/Indexed in: Anal. Abstr.; Biol. Abstr.; Chem. Abstr.; Curr. Contents Phys. Chem. Earth Sci.; Life Sci.; Index Med.; Mass. Spectrom. Bull.; Sci. Citatation Index; Excerpta Med.)

(continued on inside page of cover)